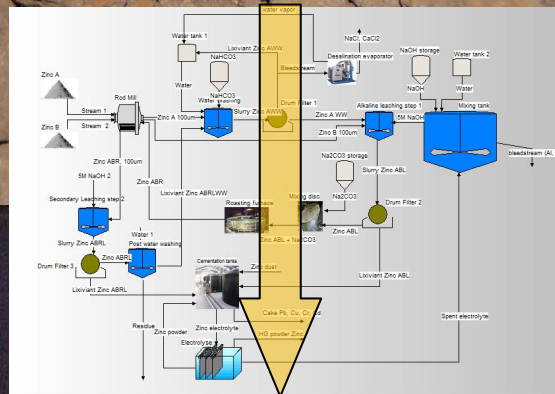


AES/RE/10-03

# Metallurgical processing of zinc-bearing residues



11-06-2010

Dennis Kemperman

 **TU Delft**



Title : Metallurgical processing of zinc-bearing residues

Author(s) : Dennis Kemperman

Date : June 2010

Supervisor(s) : Yongxiang Yang, Thilo Behrends

TA Report number : AES/RE/10-03

Postal Address : Section for Resource Engineering  
Department of Applied Earth Sciences  
Delft University of Technology  
P.O. Box 5028  
The Netherlands

Telephone : (31) 15 2781328 (secretary)

Telefax : (31) 15 2781189

Copyright ©2010 Section for Resource Engineering

*All rights reserved.*

*No parts of this publication may be reproduced,*

*Stored in a retrieval system, or transmitted,*

*In any form or by any means, electronic,*

*Mechanical, photocopying, recording, or otherwise,*

*Without the prior written permission of the*

*Section for Resource Engineering*

## Abstract

In this study metallurgical processing of two different kinds of zinc-bearing residues have been performed: Zinc A and Zinc B. These residues have been stored for over 15 years in Rotterdam Harbor.

The chemical compositions of the residues have been determined and showed that zinc ferrite is a major phase present. Zinc ferrite is not soluble under normal alkaline and acidic conditions and is not recovered by the Waelz-process, which is commonly employed for such zinc-bearing residues.

An innovative flowsheet for processing zinc ferrite-bearing residues has been developed during a pre-feasibility study, with goal to selectively recover zinc, including zinc from zinc ferrite. The innovative flowsheet consists of the following steps:

- (1) Water pre-washing: removing water soluble salts, in particular the chlorides in Zinc A (~9%).
- (2) 1<sup>st</sup> step alkaline leaching with caustic soda (NaOH): dissolving free ZnO into solution, for both water-washed Zinc A and original (unwashed) Zinc B.
- (3) Roasting of the first leach residue in the presence a suitable reagent: decomposing the zinc ferrite to free ZnO.
- (4) 2<sup>nd</sup> step alkaline leaching with NaOH: dissolving all free ZnO into solution.
- (5) Solution purification by cementation: removing impurities in particular lead and copper, by using zinc powder.
- (6) Electrowinning of zinc in NaOH solution: the purified zinc bearing solutions are subsequently precipitated to the final product of Zn metal.

Optimal operating conditions for the processes are deduced from a literature review in which similar residues are processed. Additionally, optimal operating conditions for the conversion of zinc ferrite into zinc oxide has been investigated using synthetic zinc ferrite with addition of  $\text{Mg}(\text{OH})_2$ ,  $\text{Ca}(\text{OH})_2$ , NaOH, or  $\text{Na}_2\text{CO}_3$ . Finally,  $\text{Na}_2\text{CO}_3$  has been chosen as reagent and used in experiments with real zinc-bearing residues.

Zinc A is water washed to remove the chlorides present. Then both the water washed residue of Zinc A, and Zinc B, are leached in an alkaline solution of 5M NaOH at 90°C for 1 hour. Both zinc and lead are selectively extracted, leaving iron oxides and zinc ferrite in the residue. The filtercake is fused with  $\text{Na}_2\text{CO}_3$  at 950°C for 2 hours to convert zinc ferrite into zinc oxide. The calcined product is leached in fresh alkaline solution of 5M NaOH to recover zinc. The final residue is then water washed to remove residual sodium. The filtrates from the first and second leaching step are purified, with use of zinc dust, or directly used for electrowinning experiments.

The removal efficiency of chloride, sodium and potassium during water washing of Zinc A were 62%, 41% and 71% respectively. Overall dissolution yields for Zinc A and Zinc B of zinc and lead were 82%, 80% and 64%, 78% respectively. Cementation of impurities (Pb, Cu, Cr) with zinc dust followed by an electrowinning step achieving a grade zinc deposit of 94%.

Finally, it can be concluded that the combined hydro -and pyrometallurgical flowsheet is technically feasible. Furthermore, results can be improved further by optimization of major operating steps.

# Table of Contents

Table of Contents .....	iv
List of Tables.....	vi
List of Figures .....	viii
List of symbols .....	x
List of abbreviations.....	x
1 Introduction .....	1
1.1 Zinc: Recources, production and market.....	1
1.2 Background of the research.....	2
1.3 Concept flowsheet design.....	2
1.4 Objective of the thesis .....	4
1.5 The structure of thesis .....	6
2. Zinc-bearing residues, metallurgical principles and operating conditions.....	7
2.1 Sources of zinc bearing residues .....	7
2.2 Steel making dusts.....	7
2.2.1 Blast furnace dust .....	8
2.2.2 Basic oxygen furnace dust.....	8
2.2.3 Electric arc furnace dust.....	8
2.3 Metallurgical principles.....	11
2.3.1 Alkaline leach process.....	11
2.3.2 Roasting.....	15
2.3.3 Cementation .....	16
2.3.4 Electrowinning .....	17
2.4 Operating conditions .....	19
3. Characterization of the raw materials.....	20
3.1 General characteristics for Zinc A and Zinc B.....	20
3.1.1 Zinc A.....	20
3.1.2 Zinc B .....	22
4. Experimental .....	24
4.1 Raw Materials .....	24
4.2 Experiments.....	25
4.2.1 Roasting of synthetic zinc ferrites .....	25
4.2.2 Water washing.....	25
4.2.3 First NaOH leaching.....	25
4.2.4 Roasting of first leached filter cake.....	26
4.2.5 Second NaOH leaching .....	26
4.2.6 Post water washing.....	26
4.2.7 Cementation .....	27
4.2.8 Electrowinning .....	27
5 Results and discussion.....	28
5.1 Zinc ferrite conversion .....	28
5.1.1 Zinc ferrite synthesis .....	28
5.1.2 Roasting of synthetic zinc ferrite .....	29
5.1.3 Leaching of roasted synthetic zinc ferrite .....	37
5.1.4 Conclusions .....	41
5.2 Water washing of Zinc A .....	41
5.3 First leaching step.....	44
5.3.1 First leaching step of water washed Zinc A .....	45
5.3.2 First leaching step of Zinc B .....	49

5.4 Roasting.....	52
5.4.1 Roasting of water washed and leached Zinc A .....	52
5.4.2 Roasting of leached Zinc B .....	55
5.4.3 Additional roasting experiments .....	57
5.5 Secondary leaching step .....	60
5.5.1 Leaching of water washed, leached and roasted Zinc A .....	61
5.5.2 Leaching of leached and roasted Zinc B .....	62
5.5.3 Leaching of water washed, leached and roasted Zinc A* and Zinc B* .....	63
5.6 Post water washing .....	66
5.6.1 Water washing of water washed, leached, roasted and leached Zinc A.....	67
5.6.2 Water washing of leached, roasted and leached Zinc B.....	68
5.7 Residue .....	70
5.7.1 Final residue of Zinc A.....	70
5.7.2 Final residue of Zinc B.....	70
5.8 Cementation .....	72
5.9 Electrowinning .....	73
5.9.1 Direct electrowinning .....	74
5.9.2 Electrowinning after cementation .....	75
6 Mass balance .....	78
6.1 Mass flow in the conceptual flowsheet .....	78
6.1.1 Water washing .....	78
6.1.2 First leaching .....	79
6.1.3 Roasting.....	79
6.1.4 Secondary leaching .....	79
6.1.5 Post water washing.....	80
6.1.6 Residue .....	80
6.1.7 Cementation .....	80
6.1.8 Electrowinning .....	80
7 Conclusions and recommendations .....	84
8 Acknowledgements .....	88
9 References .....	89
10 Appendices .....	92

## List of Tables

Table 1. World zinc production in tons ( <a href="http://minerals.er.usgs.gov/">http://minerals.er.usgs.gov/</a> ) .....	2
Table 2. Reported chemical composition of electric arc furnace dust in the literature (wt%).	10
Table 3. Mineralogical phase distribution of major elements present in EAFD. [7] .....	10
Table 4. Viscosity of aqueous solutions of NaOH, mPa.s ( <a href="http://www.solvaychemicals.com">www.solvaychemicals.com</a> ).....	15
Table 5. Approximate exchange current density ( $i_0$ ) for the hydrogen oxidation reaction on different metals at 25°C (1M H <sub>2</sub> SO <sub>4</sub> ).....	18
Table 6. Moisture content for 20kg as received Zinc A.....	20
Table 7. Particle size distribution of zinc A [43] .....	20
Table 8. Phases identified by XRPD analysis of Zinc A .....	20
Table 9. XRPD analysis [43].....	20
Table 10. Moisture content of as received Zinc B .....	23
Table 11. Particle size distribution of Zinc B [43] .....	23
Table 12. Phases identified by XRPD analysis of Zinc B from figure 12 and 13.....	23
Table 13. XRPD analysis of Zinc B [43] .....	23
Table 14. Operating conditions used during first water washing step for Zinc A and preliminary test of Zinc B. ....	25
Table 15. Operating conditions used during first leaching step for Zinc A and Zinc B. ....	26
Table 16. Operating conditions used for roasting of Zinc AL and Zinc BL. ....	26
Table 17. Operating conditions for post water washing of Zinc ARL and Zinc BRL. ....	27
Table 18. Operating condition of zinc dust cementation of impurities from Zinc P.....	27
Table 19. Reaction system Na <sub>2</sub> CO <sub>3</sub> in -and output at 25 -and 1000°C respectively (Kmol) ...	30
Table 20. Reaction system Ca(OH) <sub>2</sub> in -and output at 25 -and 1000°C respectively (Kmol)..	31
Table 21. Reaction system NaOH in -and output at 25 -and 1000°C respectively (Kmol) .....	32
Table 22. Reaction system Na <sub>2</sub> CO <sub>3</sub> in -and output at 25 -and 1000°C respectively (Kmol) ...	33
Table 23. Operating conditions for roasting of zinc ferrite for 2 hours. Stoichiometry additions are determined according to Eq. 5 and 6. ....	35
Table 24. Phases identified by XRPD analysis of synthetic zinc ferrite roasted with NaOH or Na <sub>2</sub> CO <sub>3</sub> .....	36
Table 25. Roasting conditions for NaOH and Na <sub>2</sub> CO <sub>3</sub> and final recoveries of zinc and iron after leaching .....	37
Table 26. Phases identified by XRPD analysis of synthetic zinc ferrite roasted with NaOH or Na <sub>2</sub> CO <sub>3</sub> after leaching for 1h with 10M NaOH at 90°C, L:S 10, 800 RPM. ....	40
Table 27. Water washing operating conditions for Zinc A and B.....	42
Table 28. Analysis of the filtrate (ICP), filter cake (XRF) and calculated removal efficiency after water washing of Zinc A.....	43
Table 29. Recovery of Zinc B-WW, based on ICP analysis .....	43
Table 30. Phases identified by XRPD analysis of water washed Zinc A (Zinc AL*) .....	45
Table 31. Phases identified by XRPD analysis of directly leached Zinc A (Zinc ALD) [2] ...	45
Table 32. Analysis of the filtrate, filter cake and calculated recovery after leaching of water washed Zinc A (Zinc AL) .....	45
Table 33. Analysis of the filtrate, filter cake and calculated recovery after leaching of Zinc BL .....	50
Table 34. Phases identified by XRPD analysis of Zinc BL* filter cake .....	51
Table 35. Phases identified by XRPD analysis of Zinc BLD filter cake .....	51
Table 36. Phases identified by XRPD analysis of Zinc AR.....	53
Table 37. Analysis of filter cake Zinc AL, calcine product Zinc AR and absolute weight difference.....	54
Table 38. Phases identified by XRPD analysis of Zinc BR .....	56

Table 39. Analysis of filter cake Zinc BL, calcine product Zinc BR and absolute weight difference.....	57
Table 40. Recovery of water washed and leached Zinc A* using XRF analysis of Zinc AWW and filter cake Zinc AL* .....	57
Table 41. Recovery of water washed and leached Zinc B* using XRF analysis of Zinc B and filter cake Zinc BL* .....	58
Table 42. Phases identified by XRPD analysis of Zinc AR* .....	60
Table 43. Phases identified by XRPD analysis of Zinc AR* .....	60
Table 44. Analysis of the filtrate, filter cake and recovery of Zinc ARL .....	61
Table 45. Analysis of the filtrate, filter cake and recovery of Zinc BRL.....	62
Table 46. Analysis of filtrate, filter cake and recovery of Zinc ARL* .....	64
Table 47. Analysis of filtrate, filter cake and recovery of Zinc BRL* .....	64
Table 48. Phases identified by XRPD analysis of Zinc ARL* .....	65
Table 49. Phases identified by XRPD analysis of Zinc BRL* .....	65
Table 50. Analysis of filtrate, filter cake and recovery of Zinc ARLWW .....	67
Table 51. Phases identified by XRPD analysis of Zinc ARLWW .....	68
Table 52. Analysis of filtrate, filter cake and recovery of Zinc BRLWW .....	69
Table 53. Phases identified by XRPD analysis of Zinc BRLWW .....	69
Table 54. XRF analysis of filter cake of Zinc ARLWW and Zinc BRLWW (wt%) .....	71
Table 55. Acid digestion ICP analysis of filter cake Zinc ARLWW and Zinc BRLWW (wt%) .....	71
Table 56. Recovery by cementation using zinc dust/Pb ratio of 1.7 (50°C, 2.5h) .....	72
Table 57. XRF analyses of cementation residue using zinc dust addition of 1.7 Zn/Pb ratio (50°C, 2.5h) .....	73
Table 58. Theoretical chemical composition of cementation product after removal of Na using water washing.....	73
Table 59. Typical direct electrowinning conditions for zinc .....	74
Table 60. Typical electrowinning conditions of 1.5L purified electrolyte for zinc. ....	75
Table 61. Description of zinc deposits obtained in unstirred alkaline solutions [41]. ....	77
Table 62. Estimated input of materials for processing Zinc A and Zinc B according to experimental results.....	81
Table 63. Estimated output of materials after processing Zinc A and Zinc B according to experimental results.....	81
Table 64. Total possible recovery of Zinc A and Zinc B .....	81
Table 65. Mass balance of conceptual flowsheet .....	82
Table 66. Criteria and sub-criteria to treat iron-making dusts via hydrometallurgical processes [9] .....	92
Table 67. Comparing hydrometallurgical technologies to treat iron-making dusts [9] .....	92
Table 68. Criteria and sub-criteria to treat iron-making dusts via pyrometallurgical processes [9] .....	93
Table 69. Comparing pyrometallurgical technologies to treat iron-making dusts [9] .....	94
Table 70. Weights of samples at start and end of their corresponding experiment .....	116
Table 71. Absolute weight differences in gram after roasting .....	127

## List of Figures

Figure 1. Main sources of zinc recycling (IZA, 1998).....	1
Figure 2. Zinc recycling circuit (IZA, 2009).....	1
Figure 3. World zinc production ( <a href="http://www.lme.co.uk/">http://www.lme.co.uk/</a> ) .....	2
Figure 4. Outline of general processing route [2] .....	3
Figure 5. Schematic representation of an Electric Arc Furnace [16]. .....	9
Figure 6. Solubility of ZnO as a function of pH, at 25°C. (a) Calculated with HSC 6.1, [28] (b) [21].....	13
Figure 7. Solubility of ferrous (a) and ferric (b) hydroxides as a function of pH, at 25°C. [21] .....	14
Figure 8. a) Activities of dissolved silica compounds in equilibrium with quartz, 25°C [29], b) Activities of dissolved aluminum compounds in equilibrium with gibbsite $[\text{Al}(\text{OH})_3]$ , 25°C. [29] .....	15
Figure 9. Calculations for half-cell potential of alkaline hydrogen evolution versus NHE based on an exact analysis of the relevant Nernst equation [31]. .....	18
Figure 10. Photo of as received Zinc A.....	20
Figure 11. Magnetic properties of Zinc A [2] .....	20
Figure 12. XRPD of Zinc A (Cu target).....	21
Figure 13. XRPD of Zinc A (Co target) [2] .....	22
Figure 14. As received Zinc B (EBS, 09-09-2007).....	22
Figure 15. Magnetic properties of Zinc B [2] .....	22
Figure 16. XRPD analysis of Zinc B (Cu target) .....	23
Figure 17. XRPD analysis of Zinc B (Co target) [2] .....	24
Figure 18. Electrowinning set-up: 1) Multimeter Volt, 2) Delta Electronica 3) Heater, 4) Electrolytic cell containing one cathode and two anodes. ....	27
Figure 19. XRPD of zinc ferrite synthesis .....	28
Figure 20. Blow-up of $\text{ZnFe}_2\text{O}_4$ -1.....	29
Figure 21. Calculated equilibrium compositions when roasting $\text{ZnFe}_2\text{O}_4$ with $\text{Mg}(\text{OH})_2$ in isobaric conditions over a temperature range of 25 to 1000°C [28].....	30
Figure 22. Calculated equilibrium compositions when roasting $\text{ZnFe}_2\text{O}_4$ with $\text{Ca}(\text{OH})_2$ in isobaric conditions over a temperature range of 25 to 1000°C [28].....	31
Figure 23. Calculated equilibrium compositions when roasting $\text{ZnFe}_2\text{O}_4$ with NaOH in isobaric conditions over a temperature range of 25 to 1000°C [28].....	32
Figure 24. Calculated equilibrium compositions when roasting $\text{ZnFe}_2\text{O}_4$ with $\text{Na}_2\text{CO}_3$ in isobaric conditions over a temperature range of 25 to 1000°C [28].....	33
Figure 25. Synthetic zinc ferrite roasted with NaOH (350°C, 2h, 2S).....	35
Figure 26. Synthetic zinc ferrite roasted with $\text{Na}_2\text{CO}_3$ (950°C, 2h, 2S) .....	35
Figure 27. XRPD analysis of synthetic zinc ferrite roasted with $\text{Na}_2\text{CO}_3$ .....	35
Figure 28. XRPD analysis of synthetic zinc ferrite roasted with NaOH.....	36
Figure 29. Roasting of syn- $\text{ZnFe}_2\text{O}_4$ with $\text{Na}_2\text{CO}_3$ for 2h at 950°C; “Theoretical” stands for the theoretical weightloss of carbon dioxide when sample reacted according to stoichiometry .....	36
Figure 30. Roasting of syn- $\text{ZnFe}_2\text{O}_4$ with NaOH for 2h at 350°C; “Theoretical” stands for the theoretical weightloss of water vapor when sample reacted according to stoichiometry .....	37
Figure 31. XRPD analysis of leached calcine product (a) NaOH-1, (b) NaOH-2, (c) $\text{Na}_2\text{CO}_3$ -1 and (d) $\text{Na}_2\text{CO}_3$ -2 .....	39
Figure 32. Zn recovery over time. (90°C, 5h, 800 RPM, L:S 10, 10M NaOH).....	40
Figure 33. Iron dissolution over time. (90°C, 5h, 800 RPM, L:S 10, 10M NaOH).....	40



Figure 34. Conductivity profile over time from water washing experiments, (normalized to 100g/L).....	43
Figure 35. “Zinc” film formation during water washing. ....	44
Figure 36. XRPD analysis of residue of leached Zinc AL* (5M NaOH, 50°C, 1h, L:S 5) .....	46
Figure 37. XRPD analysis of residue of direct leached Zinc ALD (10M NaOH, ~55°C, 3h, L:S 10) [2] .....	46
Figure 38. Concentration of elements in filtrate Zinc AL after 10 and 60 minutes of leaching. ....	48
Figure 39. Stability diagram of Zn, 0.38M at 25 and 90°C in 5M NaOH solution [28]. ....	49
Figure 40. XRPD analysis of residue of leached Zinc BL* (5M NaOH, 50°C, 1h, L:S 5).....	50
Figure 41. XRPD analysis of residue of leached Zinc BLD (10M NaOH, ~55°C, 3h, L:S 10) [2] .....	51
Figure 42. Concentration of elements in Zinc BL filtrate after 5 and 60 minutes of leaching	52
Figure 43. XRPD analysis of Zinc AR.....	53
Figure 44. Roasting products of water washed and leached Zinc A (left; hot, right; cold) .....	54
Figure 45. Corrosion effect of tray after roasting Zinc A with Na <sub>2</sub> CO <sub>3</sub> . ....	55
Figure 46. XRPD analysis of Zinc BR .....	56
Figure 47. Roasting products of Zinc BR .....	56
Figure 48. XRPD analyses of Zinc AR* .....	59
Figure 49. XRPD analyses of Zinc BR* .....	59
Figure 50. Roasting samples of Zinc AR* and Zinc BR* .....	60
Figure 51. Concentration of elements in Zinc ARL filtrate after 5 and 60 minutes of leaching .....	62
Figure 52. Concentration of elements in Zinc BRL filtrate after 15 and 60 minutes of leaching. ....	63
Figure 53. XRPD analyses of Zinc ARL* .....	64
Figure 54. XRPD analyses of Zinc BRL* .....	65
Figure 55. Equilibrium amount of products (1M NaFeO <sub>2</sub> /L) 25-100°C .....	66
Figure 56. Eh pH diagram of Na-Fe-O-H at a) 32°C b) 33°C .....	67
Figure 57. XRPD analysis of Zinc ARLWW .....	68
Figure 58. XRPD analysis of Zinc BRLWW .....	69
Figure 59. Decomposition voltage for Zn(OH) <sub>4</sub> <sup>2-</sup> /Zn. D.E.= direct electrolyte at 20°C, E.P = Electrolyte purified at 45°C .....	74
Figure 60. Microphotographs of zinc deposit after direct electrowinning. (750 Am-2, 1h, 40°C).....	74
Figure 61. XRPD analyses of Nr.1 zinc product from electrowinning .....	75
Figure 62. Microphotographs of zinc deposit of depletion electrowinning from purified electrolyte nr1, nr2 and nr3. (673 Am-2, 1h, 40°C) .....	76
Figure 63. Voltage change during electrolyse.....	77
Figure 64. Recommended conceptual flowsheet for metallurgical processing of zinc bearing residues.....	83

## List of symbols

$T$	<i>Temperature</i>
$\varepsilon_r$	<i>Relative permittivity or dielectric constant</i>
$M$	<i>Molality</i>
$n$	<i>Number of electrons</i>
$q$	<i>Charge of particle</i>
$\varepsilon_0$	<i>Vacuum permittivity</i>
$k_B$	<i>Boltzmann constant</i>
$a$	<i>Molal activity</i>
$E^0$	<i>Standard electrode potential</i>
$\Delta_r G^0$	<i>Gibbs free energy of reaction</i>
$K$	<i>Equilibrium constant</i>
$R$	<i>Gas constant</i>
$F$	<i>Faraday constant</i>

## List of abbreviations

<i>Zinc A</i>	<i>As received from ECB, denoted as Zinc A</i>
<i>Zinc AWW</i>	<i>The filter cake or filtrate after water washing of Zinc A</i>
<i>Zinc AL</i>	<i>The filter cake or filtrate after leaching the filter cake of Zinc AWW</i>
<i>Zinc AR</i>	<i>The calcined product after roasting the filter cake of Zinc AL</i>
<i>Zinc ARL</i>	<i>The filter cake or filtrate after leaching Zinc AR</i>
<i>Zinc ALRWW</i>	<i>The filter cake or filtrate after water washing the filter cake of Zinc ARL</i>
<i>Zinc B</i>	<i>As received from ECB, denoted as Zinc B</i>
<i>Zinc BWW</i>	<i>The filter cake or filtrate after water washing of Zinc B</i>
<i>Zinc BL</i>	<i>The filter cake or filtrate after leaching Zinc B</i>
<i>Zinc BR</i>	<i>The calcined product after roasting the filter cake of Zinc BL</i>
<i>Zinc BRL</i>	<i>The filter cake or filtrate after leaching Zinc BR</i>
<i>Zinc BLRWW</i>	<i>The filter cake or filtrate after water washing the filter cake of Zinc BRL</i>
<i>Zinc C</i>	<i>The equivolumetric mixed solution of Zinc AL, Zinc ARL, Zinc BL and Zinc BRL</i>
<i>Zinc P</i>	<i>The purified filtrate of Zinc C after cementation of impurities with zinc dust</i>
<i>Zinc CR</i>	<i>The filter cake of Zinc C after cementation of impurities with zinc dust.</i>
<i>Zinc AL*</i>	<i>The filter cake or filtrate after leaching the filter cake of Zinc AWW*</i>
<i>Zinc AR*</i>	<i>The calcined product after roasting the filter cake of Zinc AL*</i>
<i>Zinc ARL*</i>	<i>The filter cake or filtrate after leaching Zinc AR*</i>
<i>Zinc BL*</i>	<i>The filter cake or filtrate after leaching Zinc B</i>
<i>Zinc BR*</i>	<i>The calcined product after roasting the filter cake of Zinc BL*</i>
<i>Zinc BRL*</i>	<i>The filter cake or filtrate after leaching Zinc BR*</i>

# 1 Introduction

## 1.1 Zinc: Resources, production and market

According to the International Zinc Association approximately 11.5 million tons of zinc is being produced annually worldwide. Zinc is thereby the fourth most produced metal in the world. Approximately 70% of zinc produced worldwide is produced from mined ores.

Most zinc ore deposits are composed of a mixture of metal sulfides. The principal zinc ore mineral is sphalerite ( $\text{ZnS}$ ). The ore is grinded, crushed and concentrated by flotation processes. The zinc concentrate is then roasted in a fluidized bed at  $910^\circ\text{C}$  with oxygen to convert the sulfides to oxides; during this process zinc ferrites are also formed. The produced sulfur dioxide gas is converted to sulfuric acid, an important by-product. The oxidized zinc concentrates are then leached by dilute sulfuric acid at  $65^\circ\text{C}$  and filtrated. The residue is then leached by a hot sulfuric acid solution to recover zinc from zinc ferrites. Iron in solution is then removed by one of four processes; goethite, jarosite, hematite or ferric hydroxide precipitation. The zinc sulfate solution is then purified by addition of zinc dust in a two-stage process. Zinc is recovered from the purified solution by electrolysis.

The remaining 30% of worldwide zinc production is composed of recycled or secondary zinc resources. The main sources of zinc recycling are comprised of brass scrap and galvanizing residues (Figure 1). Approximately 6% is produced by the steel industry as filter dusts. Today, over 80% of the zinc available for recycling is indeed recycled and amount annually to 2.9Mt (Figure 2). This level of recycling is increased every year and is dictated by governmental directives and in pace with technological progress of zinc production and zinc recycling.

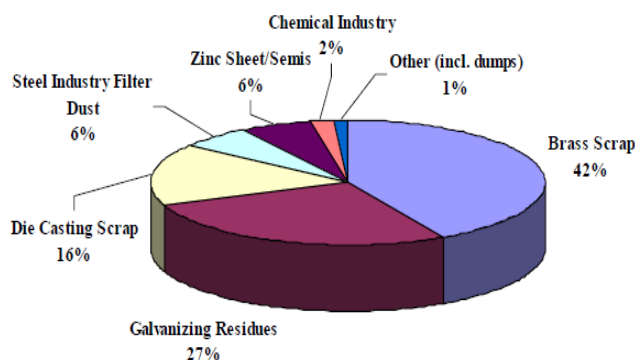


Figure 1. Main sources of zinc recycling (IZA, 1998)

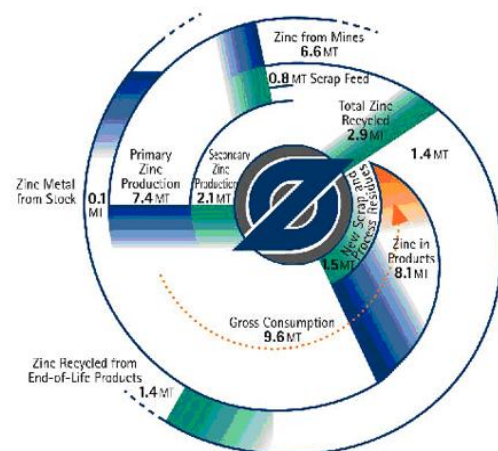


Figure 2. Zinc recycling circuit (IZA, 2009)

In 2008 it was predicted that the global zinc mine production would increase by 3.9%, which resulted in an increase of 5.1% in refined metal production. The total zinc production summed up to 11.9 million tons [1]. Offset against the consumption of 11.8 million tons, which increased by 3.8%, an excess remained. For 2009 a larger surplus is anticipated. Zinc prices have declined 70% from its peak value in 2006 to \$1,301 per metric ton in October 2008. This is aided by the remaining surplus on the market and credit crisis. On 22 December 2009 the value of zinc was \$2,407.50 per metric ton. Cutbacks and mine closings occurred as the prices fell below operating costs, particularly in Australia, Canada and the United States. The increased output is driven by expansions in Latin America, China and India. The decline in consumption within Europe and the U.S. has been offset by emerging markets of China,

Brazil and India. From Table 1 and Figure 3 the relation of world zinc production to the source per region can be quantified, showing that China and Europe were responsible for 77% of the total world zinc production in 2007.

**Table 1. World zinc production in tons**  
(<http://minerals.er.usgs.gov/>)

Zinc	2007
World mine production	10,900,000
World smelter production	11,500,000
Of which:	
primary	4,780,000
secondary	362,000
undifferentiated	6,310,000

**World zinc production**

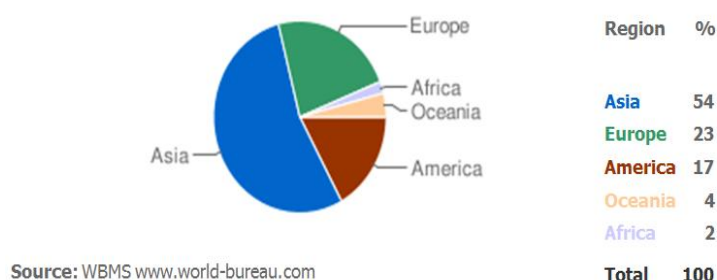


**Figure 3. World zinc production** (<http://www.lme.co.uk/>)

## 1.2 Background of the research

In Rotterdam Harbor 4700 tons of zinc bearing residues have been stored for more than 15 years at a company. This material can be classified, on chemical composition, as environmental hazardous waste and can be subdivided in two different fractions; Zinc A and Zinc B, 3000 and 1700 tons respectively. The zinc concentration of Zinc A is measured and found to be between 21-26 wt% and of Zinc B between 17-19 wt%.

The potential environmental and industrial problems arising from storing such residues have grasped the attention of the local and central government bodies and affiliated industrial companies. The Group of Metals production, Refining and Recycling at the Department of Materials Science and Engineering of TU Delft was therefore contacted to find an innovative technically – economically viable solution. A pre-feasibility study is conducted by Dr. Y. Yang on metallurgical processing of zinc bearing residues at Rotterdam Harbor [2] and economically evaluated in cooperation with Bridging Worlds, the DES Representative Benelux. From these studies a process flowsheet is developed (Figure 4).

## 1.3 Concept flowsheet design

In compliance with the low investment requirement and small capacities, for processing Zinc A and Zinc B, the flowsheet is based on hydrometallurgical methods [3]. In hydrometallurgy, the use of aqueous chemistry is employed to extract metals from ores, concentrates, and waste products.

It can be subdivided in three general steps:

- Firstly, a leaching process has to be applied to extract the valuable metal. An aqueous solution containing a leaching agent is used to selectively extract the desired metal. Type and concentration of the leaching agent is dependent on chemical composition of source material and mineral from which the metal has to be extracted. The most important parameters controlling the efficiency of the leaching process are; oxidation potential, concentration of lixiviant, temperature and pH.

- Secondly, filtration of the leachate is performed. Then the filtrate has to be cleared from undesirable metals in solution. This is called the purification process. Purification is achieved by crystallization, cementation, solvent extraction or ion exchange.
- Finally, from the purified filtrate the metal can be recovered by electrolysis, chemical reduction.

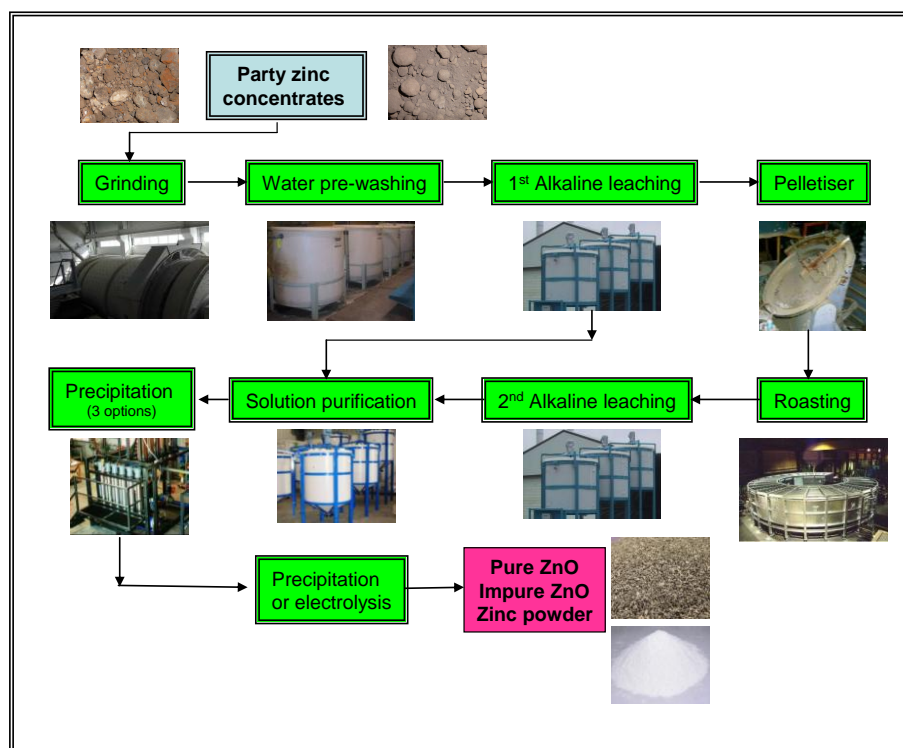


Figure 4. Outline of general processing route [2]

The conceptual flowsheet has been developed based on the state-of-the-art knowledge of the different processing steps. However, it is not known whether the flowsheet is technically feasible and what the efficiency of the various processing steps would be due to the complex mineralogical and chemical compositions of Zinc A and Zinc B.

Zinc A has particularly high chloride content. Presence of chlorides in the filtrate is detrimental for electrowinning operations and poses health risks due to formation of toxic chlorine gases. Chlorides are expected to be predominantly bound in halides and therefore a water washing step is included in the flowsheet. Presence of significant amounts of zinc, as zinc ferrites ( $\text{ZnFe}_2\text{O}_4$ ) in both Zinc A and B, a combined hydro-, and pyrometallurgical processing route is developed. Acidic or alkaline hydrometallurgical processes are not able to dissolve zinc ferrite. Therefore, a pyrometallurgical roasting step is used to convert zinc ferrite into soluble zinc oxides. Due to the high iron/zinc ratio, selective leaching of zinc is preferred using a suitable lixiviant such as caustic soda [4].

Additionally, it is beneficial that other heavy metals can be removed and hopefully recovered from the residues during leaching. Hopefully, a residue can be obtained which can be used as construction materials, served as feeding stock for steel industries or be suitable for disposal. After zinc is leached into the alkaline solution a purification process is conducted to remove other dissolved heavy metals such as lead, cadmium and copper by using zinc powder cementation. After purification zinc is recovered from solution by electrolysis.



Short description of the processing steps are as follows (Figure 4):

- (1) **Grinding:** Separate grinding and washing is preferred since Zinc A contains much more chloride than Zinc B. Grinding is done to achieve a particle size of about 100  $\mu\text{m}$ .
- (2) **Water washing:** Removal of chlorides and other water solvable salts, such as sulfates, to avoid product contamination and detrimental effects during electrolysis.
- (3) **First leaching step:** Zinc oxides and other soluble metals are dissolved.
- (4) **Roasting:** The filter cake is mixed with a suitable agent, such as soda ash ( $\text{Na}_2\text{CO}_3$ ) or caustic soda ( $\text{NaOH}$ ), and then roasted in a furnace to convert zinc ferrite into zinc oxides.
- (5) **Second leaching step:** The liberated zinc oxides from converted zinc ferrites are dissolved, leaving (sodium) iron oxides in the filter cake. Depending on the chemical composition of the residue it can be disposed of, sold or recycled.
- (6) **Solution purification:** Mixing of the first and second filtrate is followed by cementation with zinc dust. This is performed to precipitate undesirable metals in solution such as Cu, Pb and Cd. The cake could be sold as a semi-product, or further separation can be conducted to recover the metals separately.
- (7) **Electrowinning of Zinc:** Recovery of zinc from purified solution by electrolysis.

## 1.4 Objective of the thesis

The chemical composition of Zinc A and Zinc B are comparable with electric arc furnace dust from steel making industries. In general, disposal, treatment or storing of such residues has been a financial and environmental burden for the steel industry. The developed flowsheet and technology for Zinc A and Zinc B may be applied to process electric arc furnace dust or other steel industry filter dusts with minor adjustments.

The main objective of this MSc research is to evaluate the technical feasibility and efficiency of the proposed flowsheet for zinc recovery. As mentioned before, due to the composition of Zinc A and Zinc B, processing of these residues is difficult. These difficulties arise particularly from the following characteristics for Zinc A and Zinc B:

- Low zinc concentrations and presence of zinc ferrite
- Complex mineralogical composition
- High chloride content
- Presence of various heavy metals.

To evaluate the feasibility and efficiency of each processing step the following aims (A) and questions (Q) are determined:

### **Water washing**

A 1: Removal of chlorides from Zinc A by dissolution in water

- Q 1: What are the reported operating conditions in the literature?  
Q 2: What is the removal efficiency of chloride?  
Q 3: What are recommendations for future experiments?

### **First leaching step**

A 2: Selective recovery of zinc and other heavy metals from Zinc A and Zinc B by dissolution in an alkaline lixiviant.

- Q 4: What are the reported operating conditions in the literature?  
Q 5: What is the recovery of zinc and other heavy metals?  
Q 6: What are recommendations for future experiments?

### **Roasting**

A 3: Conversion of zinc ferrites into zinc oxides.

- Q 7: What are the reported operating conditions and reagents in the literature?  
Q 8: What is the most suitable reagent?  
Q 9: Is the conversion of zinc ferrite into zinc oxides complete?

### **Secondary leaching step**

A 4: Selective recovery of zinc and other heavy metals from Zinc A and Zinc B by dissolution in an alkaline lixiviant.

- Q 10: What is the recovery of zinc and of other heavy metals?  
Q 11: What are recommendations for future experiments?

### **Cementation**

A 5: Recovery of heavy metals from solution by precipitation by adding zinc powder.

- Q 12: What are the reported operating conditions in the literature?  
Q 13: Is the addition of zinc dust sufficient for cementation of heavy metals from solution?  
Q 14: What are recommendations for future experiments?

### **Electrowinning**

A 6: Recovery of zinc from strong alkaline solution through electrolysis.

- Q 15: What are the reported operating conditions in the literature?  
Q 16: What is the current efficiency and purity of zinc deposited during electrowinning?  
Q 17: What are recommendations for future experiments?

### **The following are additional objectives:**

#### **Residue**

A 7: Obtain a residue which can be used as aggregate in construction materials, serve as feeding stock for steel industries or be suitable for disposal.

- Q 18: Is the final residue after processing suitable as aggregate, feeding stock or for disposal?

#### **Mass balance**

A 7: Obtain a mass balance from processing experiments of Zinc A and Zinc B.

Q 19: What are the major in and outputs when processing Zinc A and Zinc B? Q 20: What are recommendations for future processes?
--

## 1.5 The structure of thesis

In *chapter 1* general structure, background and scientific questions of the thesis are described. The aims and questions are tackled in the following chapters. In *chapter 2.1 and 2.2*, zinc bearing residues which arise from steel making industries and coinciding treatment processes are shortly described. Their amounts involved, and general compositions are highlighted with extra focus on electric arc furnace dust. This is done to achieve a better understanding of the scope and link with this thesis. In *chapter 2.3* questions on reported operating conditions in the literature and metallurgical principles for each individual processing step are described and answered.

In *chapter 3*, the zinc-bearing residues (Zinc A and Zinc B) are characterized. In *chapter 4*, the methods for each processing step are described. In *chapter 5*, the results are described and discussed, answering most questions regarding feasibility and efficiency. In *chapter 6*, the mass balance has been calculated when processing Zinc A and Zinc B according to the proposed flowsheet. The major in-, and output are then determined. In *chapter 7*, the conclusions and recommendations for each process step are described.

## 2. Zinc-bearing residues, metallurgical principles and operating conditions

### 2.1 Sources of zinc bearing residues

In general, three major types of zinc-bearing secondary materials and wastes are determined (Figure 1)[2]:

1. **Zinc scrap of various forms:**

In this type of zinc-bearing materials, zinc exists in metallic form. Galvanized steel and brass are typical zinc-bearing scrap. The metallic zinc in the galvanized steel scrap is normally reported to flue dust during EAF steelmaking. The recycling of brass scrap is operated in secondary copper smelters either as new brass alloy for new scrap or pure copper for old scrap, the zinc in the latter operation will report to flue dust. Contaminated metallic zinc can be refined with liquation approach, and upon heating to just above the melting point of zinc the dissolved minor elements such as Pb and Fe can be removed to a large extent. If zinc is mixed with metals with higher melting point, zinc could be melted down and separated with the impurity metals with higher melting points.

2. **Galvanizing residues:**

These are zinc ash, drosses, skimmings and blowing secondary materials. They contain variable portions of metallic zinc and zinc oxide. They are normally treated with distillation where metallic zinc is vaporized and recovered as zinc oxide for further metal recovery.

3. **Zinc containing flue dust, slag and residues from pyro- and hydrometallurgical processes:**

The flue dust can originate from EAF steelmaking, from BOF steelmaking and blast furnace ironmaking (with much lower zinc content), and from treatment of brass scrap (Cu-Zn alloy). Zinc-bearing residues come often from the old neutral leaching process of hydrometallurgical processes.

### 2.2 Steel making dusts

In metallurgical processes there are numerous types of flue dust emitted with different chemical and mineralogical characteristics. Estimates for dust emission range between 1 and 2% per ton of steel produced [5-7]. Disposal, recycling or recovery of these dust emissions has been a major concern for the metallurgical industries. Due to increasing environmental regulations, land filling has become expensive and alternative processes are necessary. Recycling is limited due to accumulation of impurities such as, heavy metals, alkali and halides. An increasing effort is made, pressed by government directives, to develop processes that can recover this heavy metal fraction and produce a residue that can be disposed off, used as aggregate or recycled back to steelmaking industries.

In the iron and steel industry, dust is generally emitted by means of three different furnaces/processes:

- Blast Furnace (BF)
- Basic oxygen furnace (BOF)
- Electric arc furnace (EAF)

The 3 types of flue dust are shortly described below with emphasis on EAF dust. The treatment technologies for each type are tabulated in Appendix I and thoroughly described in Zinc college by Reuters and pre-feasability report from Yang[8-10].

### 2.2.1 Blast furnace dust

In Europe alone, 500 000 tons of blast furnace flue dust or sludges is produced by the steel industry. Typically blast furnace sludges (dry solid) contain 21-32% of Fe, 15-35% of C, 1.0-3.2% Zn and 0.3-1.2% Pb [11]. Recycling of the sludge is worthwhile due to high content of C and Fe. The input Zn concentrations should not exceed an average value of 120g/ton of pig iron [11]. The dry sludge however has an average zinc content of a few percent, which limits its direct recoverability because of the limitation of the Zn input of the blast furnace.

The primary aim is to remove zinc and lead, recycle the iron residue internally, and produce a saleable zinc-lead product [9]. Direct recycling or disposal of BFD is limited due to presence of zinc, lead, halides and alkali metals, which can cause operational difficulties in the blast furnace process. Direct recycling reduces sinter quality, strength, productivity and increases dust emissions [12, 13]. Recycling increases operating costs due to increased circulation load and built-up of impurities.

Technologies often used are shaft -or flame furnaces, e.g. a Cupola is a shaft furnace used by foundries to melt iron from scrap. The residence time in a cupola is very short and not sufficient for iron oxide reduction. Since Blast furnace dust contains finely divided particles of carbon and iron oxide, after briquetting the BF dust is reduced in the cupola, producing pig iron and zinc-rich flue dust which could be sold for ISP smelter to recover zinc metal.

### 2.2.2 Basic oxygen furnace dust

It is estimated that globally 5-7 Mt of basic oxygen furnace (BOF) sludge is generated each year [14]. Normally these sludges are disposed of by land filling. In general, basic oxygen furnace dust (BOFD) contains 30% iron oxide, 30% carbon and 1-3% zinc [14, 15].

Waelz Kiln Process is the most commonly used process to treat zinc-bearing flue dust and residues or slags. It uses the rotary kiln, a refractory lined cylindrical steel vessel with an inclination of about 2° rotating at a low speed, as the reactor. In the case of EAF dust, the dust is mixed with water, coal, limestone and other fluxes, and fed into the Waelz kiln. In the kiln the fed mixture is heated up to about 1100 – 1300°C to produce zinc vapor, iron-rich slag. The zinc vapor is oxidized in the flue gas system by leakage air and collected as zinc oxide which is much richer than the original EAF dust. The zinc-rich flue dust is collected in the bag filters. The iron-rich slag is sold as aggregate after cooling and crushing.

### 2.2.3 Electric arc furnace dust

EAF dust (EAFD) is generated during steelmaking from iron-containing steel scrap in an electric arc furnace (Figure 5). Increasing use of galvanized steel scrap (automotive industry) steadily increased dust emissions during production. About 1 to 2% of dust is emitted per ton steel produced by EAF processing [5-7]. In the U.S., the EAF steelmaking process produced 57 Mt/a of steel and accounted for 41.8% of total steelmaking. This totals approximately 0.85Mt/a in dust emissions (<http://minerals.er.usgs.gov/>). The production of EAFD in Europe is 1.2-1.3Mt/a. and the world production of EAFD is estimated to be around 7 Mt/a .



### **EAFD formation**

EAFD is high in zinc (15-25%), lead, and other heavy metals due to the use of large amounts of scrap metal in the process (Table 2). For that reason, EAFD is classified as hazardous waste. Guezennec et al. [16] concluded that EAFD is created by the following phenomena. First, emissions of particles from the steel bath occur. These particles are then transported by the gas flow in the fume extraction system in which the particles could agglomerate and undergo an in-flight physico-chemical transformation. Two mechanisms are responsible for up to 87% of the dust emission:

1. Projection of fine droplets by bursting of CO bubbles coming from the decarburization of the steel bath (60%).
2. Volatilization, especially localized at the hot spots in the arc zone and the jet zone, but taking place as well in the CO bubbles (27%).

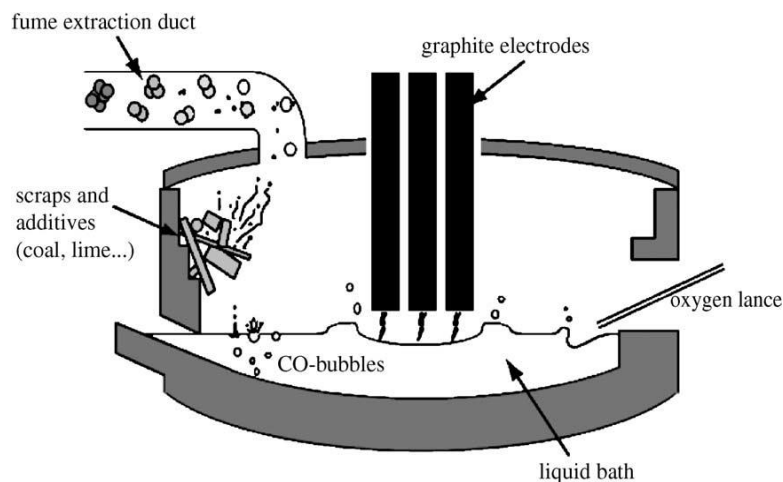


**Figure 5. Schematic representation of an Electric Arc Furnace [16].**

### **Particle size and its distribution**

In general, the mean particle diameter of EAFD depends on the agglomeration tendency of the particles. Individual particles tend to be very small and usually less than 10µm, but due to agglomeration effects larger particles are common [12, 16, 17]. These agglomeration tendencies are most likely caused by exposure to air moisture and consequent hydration reaction.

### **Chemical composition**

The chemical composition of EAFD varies widely (Table 2). It depends upon scrap use, operation conditions and procedures, and the type of steel being produced. No correlation is established between chemistry, arc furnace size, dust collection system or any other factors [3]. The wide range of composition in EAFD makes it necessary that accurate and precise analysis of each individual case is needed to optimize any recycling or recovery process. Flexibility for handling different source material for newly developed processes is therefore a necessity.

**Table 2. Reported chemical composition of electric arc furnace dust in the literature (wt%).**

Component	1 [18]	2 [19]	3 [7]	4 [5]	5 [4]	6 [12]	7 [20]	8 [21]	9 [6]
<b>Zn</b>	33	29	11,12-26,9	24.8	19.4	31.2	13.6	12.20	20.5
<b>Fe</b>	26	25	24,9-46,9	32	24.8	18.3	29.8	37.08	21
<b>Pb</b>	3.05	4	1,09-3,81	1.84	4.5	1.02	0.69	1.72	4
<b>SiO<sub>2</sub></b>	3.15	3	-	-	1.4	3.41	-	-	0.4
<b>Cu</b>	0.24	0.3	0,06-2,32	0.02	-	-	-	0.17	0.38
<b>Cd</b>	0.049	0.07	0,03-0,15	0.03	-	-	0.02	0.01	0.18
<b>Cr</b>	0.24	-	0,06-0,58	-	-	0.19	0.09	0.22	0.19
<b>Al</b>	0.6	-	-	-	-	0.68	-	0.41	0.6
<b>Mn</b>	1.83	3	2,46-4,60	3.31	-	2.2	-	-	2.25
<b>Ca</b>	2.9	-	1,85-10,0	4.08	-	15.6	-	-	12.5
<b>Na</b>	1.03	-	0,29-2,31	-	-	3.8	-	-	1
<b>K</b>	0.85	-	0,06-1,12	-	-	0.67	-	-	0.68
<b>Sn</b>	0.024	-	-	-	-	-	-	-	-
<b>Sb</b>	0.06	-	-	-	-	-	-	-	-
<b>Cl</b>	0.011	4	0,51-2,36	-	-	-	-	-	3.8
<b>F</b>	0.073	-	0,01-0,88	-	-	-	-	-	-

### **Mineralogical composition**

The average mineralogical composition is reported in Table 3. Some morphological aspects could aid physical separation processes: 1) concentration of ZnO increases in relation to spinel with decreasing particle size [3], and 2) the majority of zinc is associated with particles with a rougher surface and finer dust particles [21].

**Table 3. Mineralogical phase distribution of major elements present in EAFD. [7]**

Element	Phases containing element
<b>Fe</b>	Fe <sub>3</sub> O <sub>4</sub> is most prevalent phase. In this phase Fe cations are replaced to various degrees by Zn, Mg, Ca, Cr, Mn, etc. Some Fe occurs as a metal or as $\alpha$ -Fe <sub>2</sub> O <sub>3</sub>
<b>Zn</b>	50-80% as ZnO. Balance mainly associated with Fe in a mixed zinc iron ferrite spinel. Very small amounts of zinc may be as a sulphide, carbonate, silicate or aluminate
<b>Cd</b>	Distribution not well established, but possibly as for Zn considering the similarities in most properties of the two elements
<b>Pb</b>	Mostly as an oxide. PbSO <sub>4</sub> , PbCO <sub>3</sub> , and PbCl <sub>2</sub> are also present
<b>Cr, Ni</b>	Replace Fe in Fe <sub>3</sub> O <sub>4</sub> spinel phase. Some Cr could be as Cr <sub>2</sub> O <sub>3</sub>
<b>Ca</b>	As CaO and CaCO <sub>3</sub> mainly. The balance may occur as a fluoride, ferrite, or silicate
<b>Si</b>	Mainly present as quartz
<b>Halides</b>	Cl, Na, F, K, present as salts or chlorides.

### **Processing of EAFD**

For the treatment of EAFD, there are generally three types of approaches:

- (1) **Pyrometallurgical fuming process:** ZnO and other zinc-bearing compounds (e.g. franklinite or zinc ferrite) are reduced to zinc vapor and oxidized further in the off-gas system. The final product is zinc oxide containing 55-65% Zn, sold to zinc smelters for metal production. The pyrometallurgical fuming is dominated by the Waelz kiln process, where the coke particles and flux (silica sand) are mixed with the zinc-bearing residues and reduction of zinc oxide and zinc ferrite takes place at temperatures between 1150 and 1300°C. Zinc content must at least be >15-20% for economical processing [7].

- (2) **Hydrometallurgical process:** This is based on acid or alkaline leaching, followed by solution purification and electrowinning of zinc metal. Since zinc ferrite does not dissolve in alkaline solution, the leaching efficiency/recovery is very low if the raw material contains significant amount of zinc ferrite. Hot acid (H<sub>2</sub>SO<sub>4</sub>) can dissolve zinc ferrite, but dissolves iron oxides too. The subsequent separation of iron from zinc in the acid solution is a big financial and environmental burden. Alkaline leaching is more attractive than acid leaching, as no additional purification process for iron removal is necessary [21].
- (3) **Combined treatment of roasting and hydrometallurgical processing:** Roasting is used in particular to decompose the zinc ferrite before it can be leached into an alkaline solution. Both caustic soda (NaOH) and CaO or CaCO<sub>3</sub>, as well as soda ash (Na<sub>2</sub>CO<sub>3</sub>) have been studied for EAF dust [5, 12, 22, 23].

For a detailed review on metallurgical treatment methods for zinc-bearing secondary materials and wastes, please be referred to the following papers and book [9, 13, 24-26]. There are numerous technological alternatives for processing Zinc A and B. The difficult mineralogical and chemical composition, e.g. heavy metals, halides, alkalis and zinc ferrite, makes it, from a processing point of view, challenging to develop a process which includes both environmental and economical benefits:

- Reducing the energy required for mining and processing
- Reducing the volume of material that ends up on land filling
- Relieving environmental impacts on land and water
- Conserving zinc ores

## 2.3 Metallurgical principles

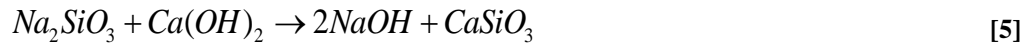
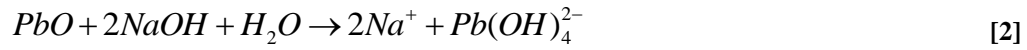
Based on the literature study the different steps of the proposed flowsheet will be reviewed. The goal is to derive optimal operating conditions for each processing step based on previous studies and theoretical considerations.

### 2.3.1 Alkaline leach process

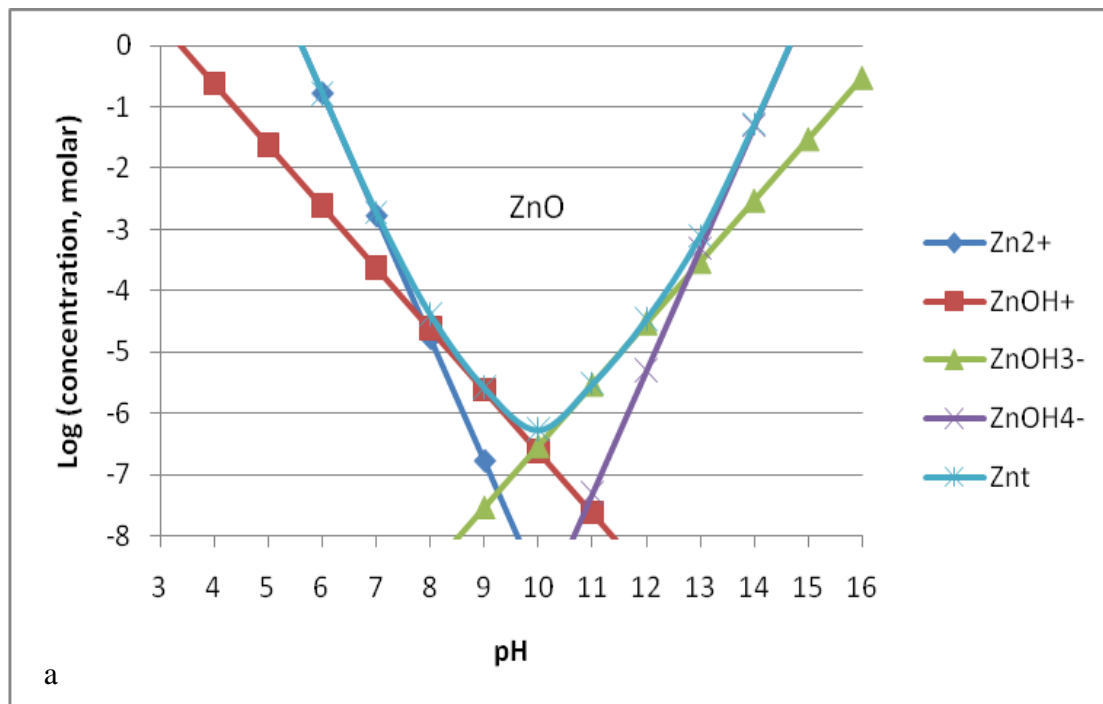
Caravaca et al. [4] compared acidic, alkaline and ammoniacal complexing lixiviates for leaching materials with similar chemical and mineralogical composition, such as Zinc A and Zinc B. From this study it can be concluded that alkaline leaching selectively dissolved zinc and not iron. This is depicted in equilibrium diagrams, which show that speciation and dissolution of iron hydroxide and zinc oxides are dependent on pH (Figure 6 a and b). At pH 14.5 it can be seen that the dissolution of zinc oxides exceed the dissolution of iron hydroxides (Figure 7a and b). Oxides of zinc and lead dissolved according to reaction 1 and 2. Aluminumhydroxide and silica are dissolved in basic solutions in a similar fashion (Figure 8 a and b, reactions 3 and 4).

Dissolution of silica and aluminum hydroxide caused problems during filtration due to formation of a gel like substance [27]. Dissolved silica compounds in alkaline solution can be precipitated as CaSiO<sub>3</sub> using Ca(OH)<sub>2</sub> (reaction 5). However, dissolution of aluminium hydroxide and its potential influence on the process or removal are not discussed. In primary hydrometallurgical production of zinc, Al is removed simultaneously during the Jarosite process by precipitation as gibbsite by pH adjustment.





In these calculations, effects of ionic strength have not been taken into consideration. Performing these calculations for concentrated NaOH requires the application of the Pitzer's equation. However, these calculations go beyond the scope of this study. Additionally, it must be taken into consideration that the viscosity of aqueous solutions changes at elevated solute concentrations and changes in viscosity has consequences for the diffusion rate of ions and the liquid/solid separation after leaching. The viscosity as function of temperature and concentration of NaOH can be determined from Table 4.



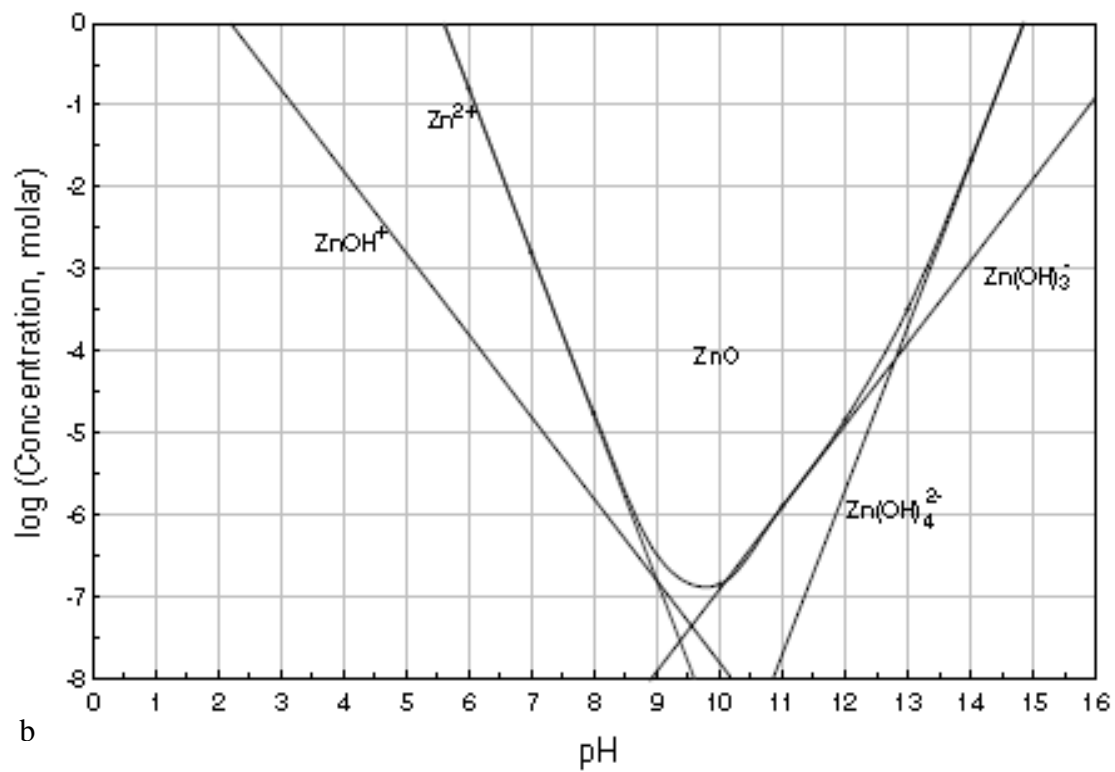
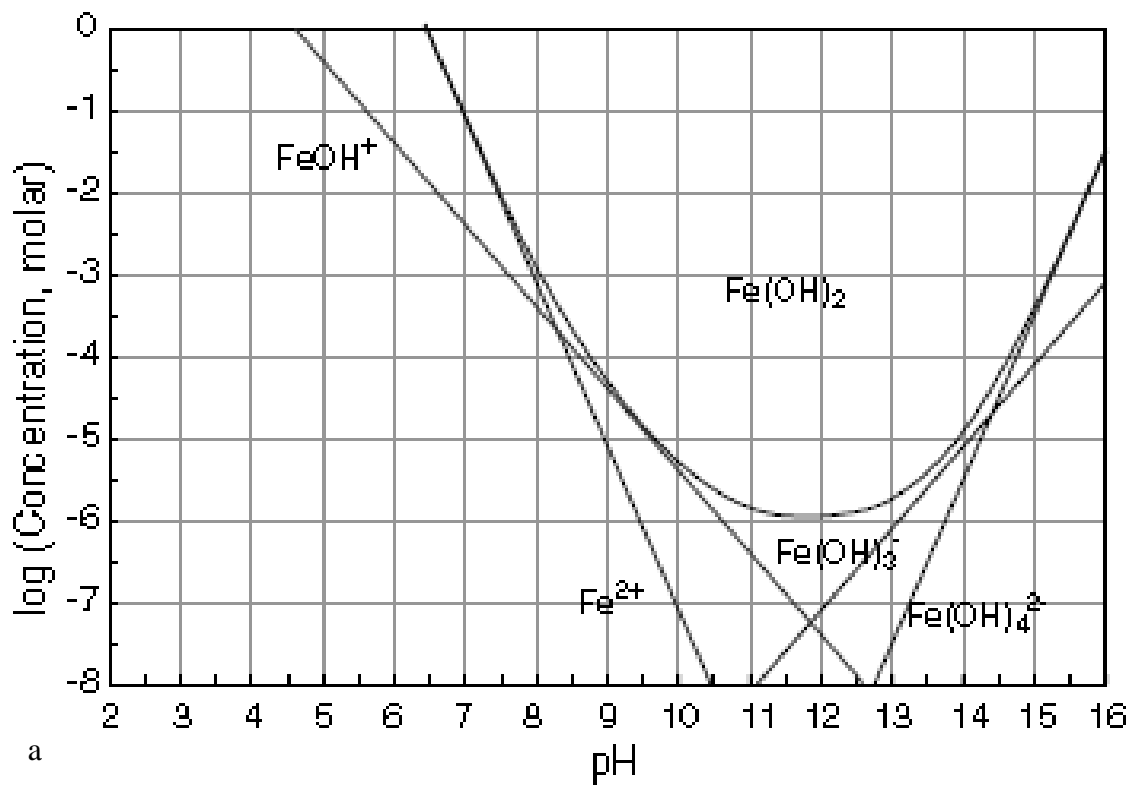


Figure 6. Solubility of ZnO as a function of pH, at 25°C. (a) Calculated with HSC 6.1, [28] (b) [21]





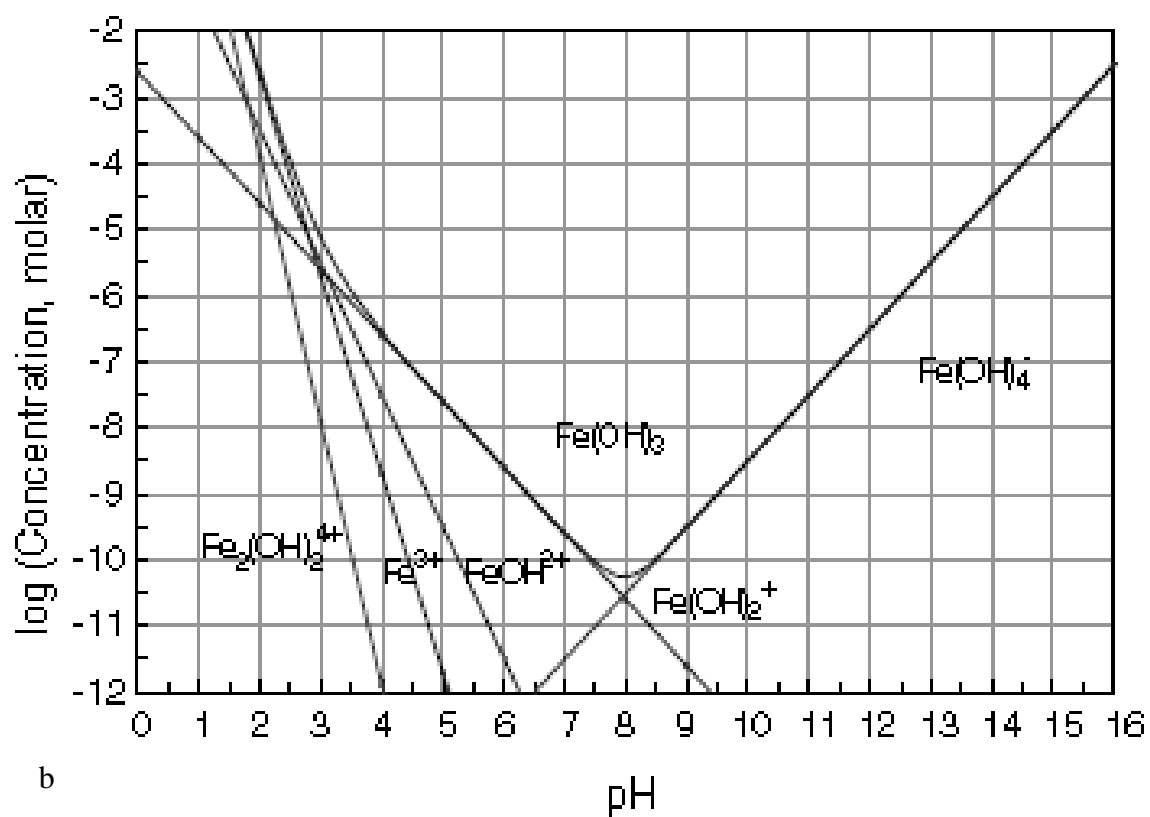
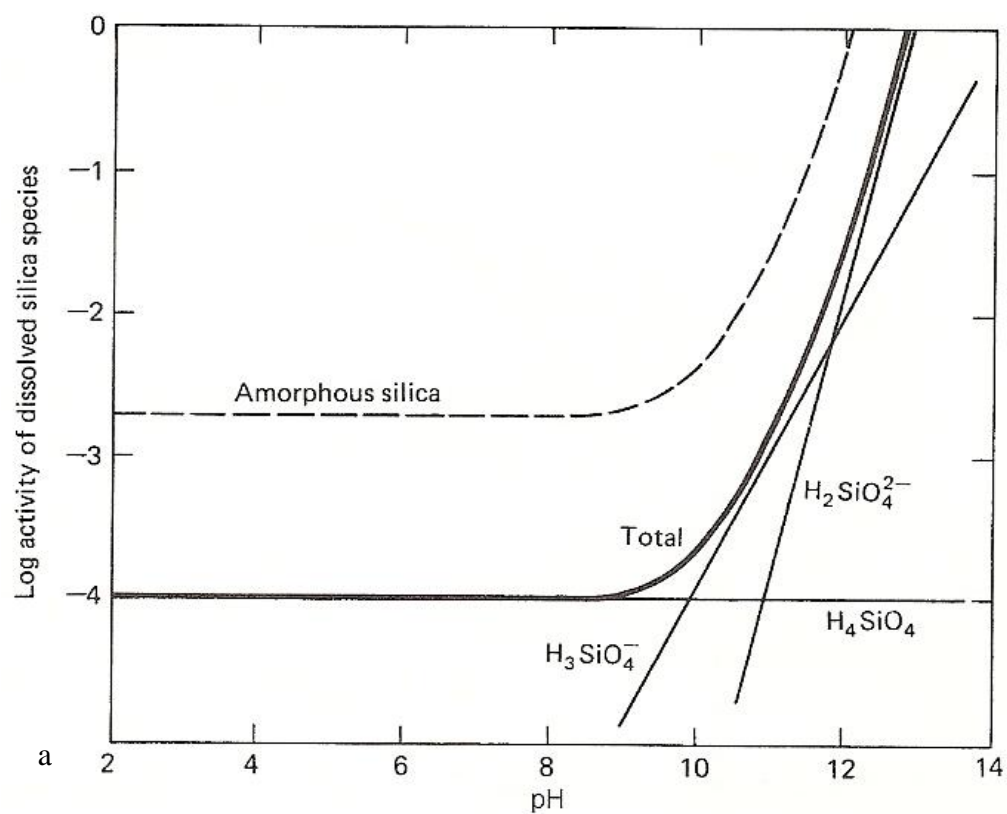


Figure 7. Solubility of ferrous (a) and ferric (b) hydroxides as a function of pH, at 25°C. [21]



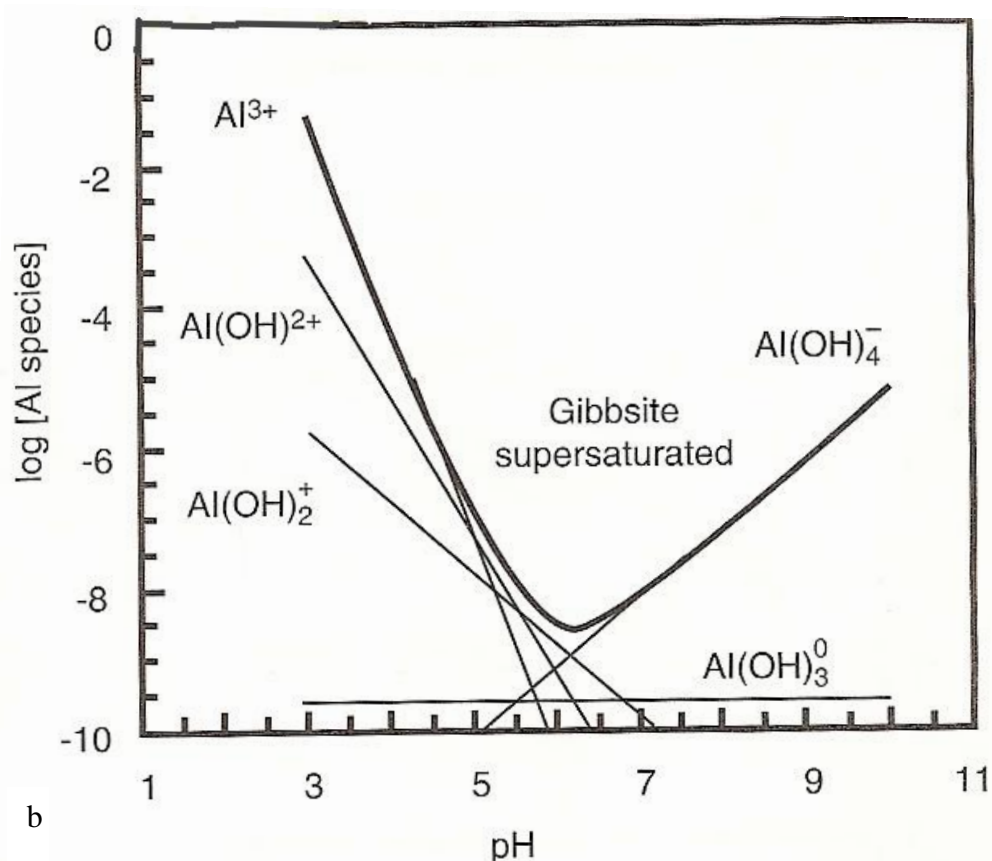


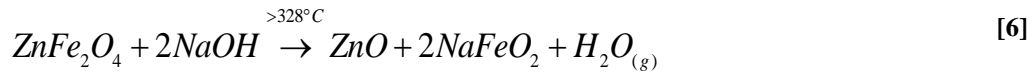
Figure 8. a) Activities of dissolved silica compounds in equilibrium with quartz, 25°C [29],  
b) Activities of dissolved aluminum compounds in equilibrium with gibbsite  $[\text{Al}(\text{OH})_3]$ , 25°C. [29]

Table 4. Viscosity of aqueous solutions of NaOH, mPa.s ([www.solvaychemicals.com](http://www.solvaychemicals.com))

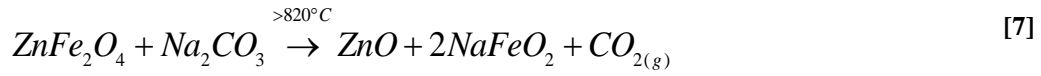
Concentration, kg NaOH/kg	Temperature, °C								
	20	30	40	50	60	70	80	90	100
0,00	0,97	0,78	0,64	0,54	0,46	0,4	0,35	0,315	0,28
0,05	1,31	1,03	0,83	0,69	0,58	0,5	0,43	0,375	0,33
0,10	1,86	1,43	1,14	0,93	0,78	0,66	0,55	0,47	0,4
0,15	2,78	2,07	1,62	1,31	1,08	0,9	0,73	0,62	0,51
0,20	4,43	3,17	2,43	1,93	1,57	1,26	1,03	0,84	0,68
0,25	7,45	5,15	3,76	2,87	2,26	1,8	1,44	1,16	0,94
0,30	12,6	8,43	5,99	4,38	3,28	2,55	2,02	1,62	1,28
0,35	21,6	13,4	9,23	6,41	4,71	3,57	2,79	2,2	1,75
0,40	38,1	21,8	13,5	9	6,36	4,76	3,69	2,89	2,29
0,45	68	32,8	18,9	12,1	8,37	6,13	4,62	3,63	2,85
0,50	120	47,7	25,5	15,8	10,4	7,6	5,6	4,36	3,41

### 2.3.2 Roasting

The recovery of zinc from Zinc A and Zinc B can be increased by converting zinc ferrites into soluble zinc oxides. The conversion of zinc ferrite into zinc oxide is supposed to occur in a roasting step. The conversion of zinc ferrite with additions of NaOH and  $\text{Na}_2\text{CO}_3$  is described to occur at 328°C and 820°C according to thermodynamic calculations (reactions 6 and 7) [12, 22, 30].



$$1000 \text{ kg} + 331.8 \text{ kg} \rightarrow 337.6 \text{ kg} + 919.4 \text{ kg} + 74.8 \text{ kg}$$



$$1000 \text{ kg} + 439.7 \text{ kg} \rightarrow 337.6 \text{ kg} + 919.4 \text{ kg} + 182.7 \text{ kg}$$

From reaction 6 and 7 it can be determined that 1 ton of  $ZnFe_2O_4$  can be decomposed by 439.6 kg  $Na_2CO_3$  or 331.8 kg  $NaOH$  respectively.

### 2.3.3 Cementation

Prior to electrolysis zinc cementation is applied to eliminate more noble metals from the zinc solution by addition of zinc dust (reaction 8). The spontaneity of the redox reaction, and feasibility of removal of other metals upon addition of  $Zn(s)$  can be determined based on electrode potential of reaction (equation 9). If Gibbs free energy of reaction is negative, the redox reaction occurs spontaneously, resulting in a positive electrode potential. A negative electrode potential denotes that the reverse reaction occurs.



$$E^\circ = \frac{RT \ln K}{nF} \quad \Delta_r G^\circ = -RT \ln K \quad [9]$$

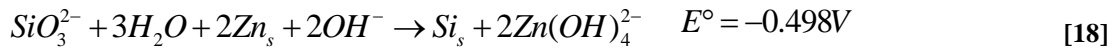
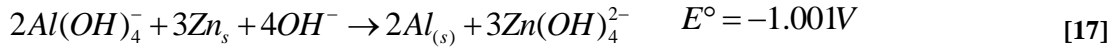
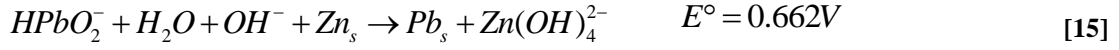
$E^\circ$  denotes the standard electrode potential,  $\Delta_r G^\circ$  is the Gibbs free energy of reaction,  $n$  denotes the number of electrons transferred and  $F$  is the Faraday constant ( $96485 \text{ C mol}^{-1}$ ).  $R$  is the gas constant ( $8.314 \text{ J K mol}^{-1}$ ),  $T$  temperature in Kelvin, and  $K$  is the equilibrium constant of the redox cell reaction.

Under basic conditions the following half cell reactions for  $Zn$ ,  $Cu$  and  $Pb$  occur (reaction 10-12). When reversing the half cell reaction, the electrode potential changes from negative to positive or vice versa. Thus, in basic solutions zinc dust ( $Zn_s$ ) dissolves spontaneously and the chemical energy is transformed into electrical energy which is used to reduce  $Pb$  and  $Cu$  in solution (reaction 15 and 16). Cementation of  $Si$  or  $Al$  with zinc dust showed a negative cell potential, meaning it does not occur spontaneously.





Total reactions:



For hydroxides of  $Fe(OH)_4^-$ ,  $Cr(OH)_4^-$  and  $Cd(OH)_4^{2-}$  total reaction with Zn powder have the following cell potential; 0.49V, 0.49V and 0.54V.

### 2.3.4 Electrowinning

In electrolysis, dissolved zinc from solution is recovered as solid zinc. This is achieved by applying an external source of electrical energy, which induces a chemical reaction. Electrowinning is the most important method by which zinc is produced, and 80% of the world's zinc production is obtained by this technology. In basic solution zinc can be precipitated by applying an electric potential of 1.6 V according to total reaction 21.

Cathode reaction:



Anode reaction:



Total reaction:



As the standard electrode potential of  $Zn(OH)_4^{2-}$  is -1.199V, a basic solution of zinc hydroxide should not deposit zinc on electrolysis: hydrogen should be liberated instead at -0.875V (Reaction 22 and Figure 9).



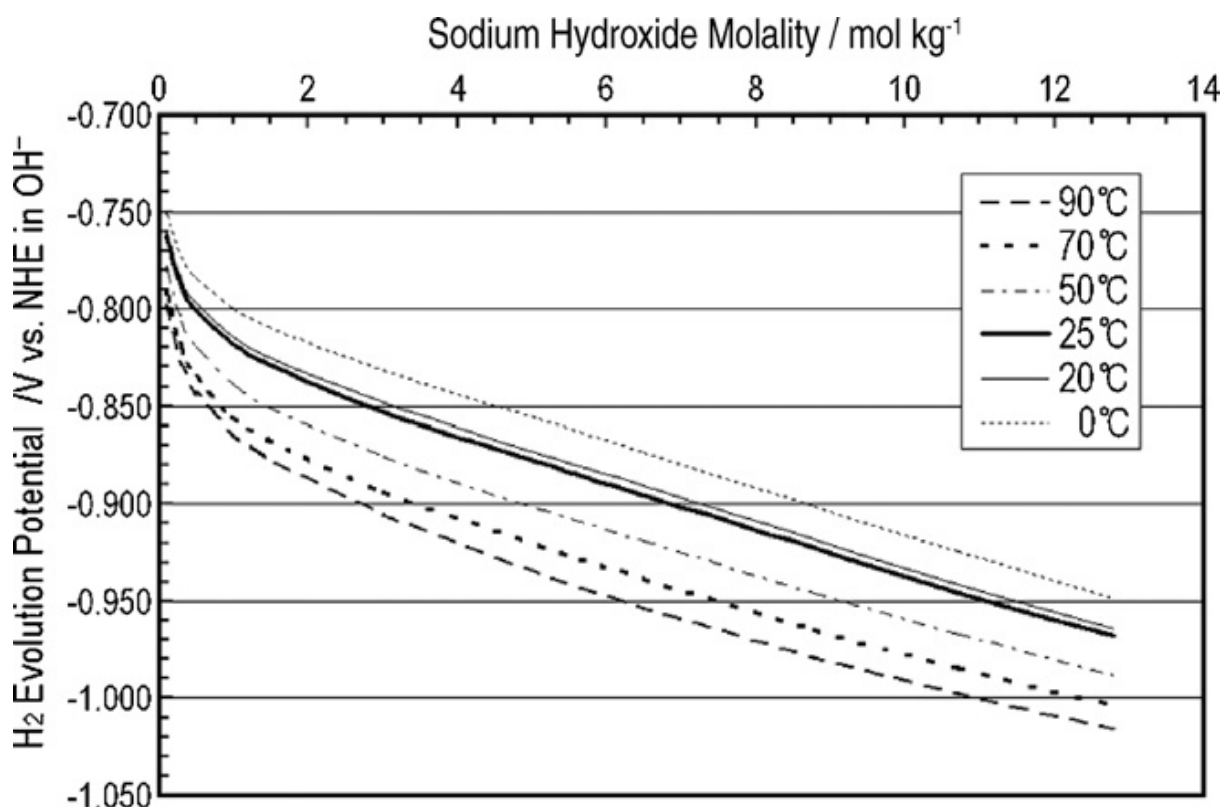


**Figure 9.** Calculations for half-cell potential of alkaline hydrogen evolution versus NHE based on an exact analysis of the relevant Nernst equation [31].

However, zinc deposition is only possible because of the hydrogen overpotential at the zinc electrode. The overvoltage is influenced by a number of factors. The exchange current density ( $i_0$ ) is surely the single most important variable that explains the large differences in the rate of hydrogen on metallic surfaces. Table 5 contains the approximate exchange current density for the reduction of hydrogen ions on a range of materials. Hydrogen evolution on platinum is thus ninety billion times easier than on zinc.

**Table 5.** Approximate exchange current density ( $i_0$ ) for the hydrogen oxidation reaction on different metals at 25°C (1M  $\text{H}_2\text{SO}_4$ )

Metal	$\text{Log}_{10} i_0 \text{ (A/cm}^2\text{)}$
Pb, Hg	-13
Zn	-11
Sn, Al, Be	-10
Ni, Ag, Cu, Cd	-7
Fe, Au, Mo	-6
W, Co, Ta	-5
Pd, Rh	-4
Pt	-2

Impurities, such as copper, antimony, arsenic, and antimony should be reduced to very low concentrations because they are more noble and lead to a reduction in the overpotential. The above mentioned metals can have a strongly detrimental effect on current yield due to formation of local elements on the cathode, leading to dissolution of the zinc. The maximum tolerable concentrations of these impurities are very low and require that the zinc electrolytes be rigorously purified.



Lead is also more noble than zinc (reactions 23 and 24), but has no detrimental effect due to higher overpotential for hydrogen evolution



Total reaction (reaction 20 + 23):



## 2.4 Operating conditions

The following operating conditions are deduced from a the literature review which will be used for the design of experiments in this study.

- *Pre- and post water washing step: [4, 5, 12]*

Two studies reported on water washing of EAFD. Xia and Pickles used the following conditions: 80 °C, liquid/solid ratio of 4, for 2h. Caravaca et al., used a two step process at 25 °C, liquid/solid ratio of 2, for 2h removing 90% and then 99% of total halides present.

- *First and secondary alkaline leaching step:[4, 5, 12, 18, 20, 21, 32, 33]*

Optimal conditions derived from the literature for temperature, concentration of NaOH, agitation speed, time: 90-95°C, 4-6 M NaOH,  $\geq 600$ rpm, >4h.

Removal of ZnO and PbO before roasting would increase recovery of the other impurities in the second alkaline leaching according to Zn > Pb > Al > Cr (III) > Cu.

An increase in recovery of zinc of 10% was achieved by washing the filter cake. This should be considered during experiment trials.

- *Roasting zinc ferrites: [5, 12, 22, 30, 34]*

By use of a pyrometallurgical step and addition of NaOH or Na<sub>2</sub>CO<sub>3</sub>, zinc ferrites are converted to zinc oxides. Optimal roasting conditions with NaOH are reported to be 350-400°C with stoichiometric additions between 3.6 and 7.4, for one hour. Optimal roasting conditions with Na<sub>2</sub>CO<sub>3</sub> are reported to be 850-950 °C, with stoichiometric additions between 2.9 and 4.5 for three to five hours.

- *Cementation to remove impurities:[18, 35, 36]*

Satisfactory results are achieved for cementation of impurities by use of zinc powder or Na<sub>2</sub>S. The optimal conditions to precipitate impurities using zinc powder for temperature, phase Zn/Pb ratio, agitation speed, and time are: 50°C, 1.2, 300 rpm, 3h.

- *Electrowinning in alkaline solution:[5, 37-42]*

Optimal conditions are largely dependent on required production capacity or energy consumption. Typical conditions are 65°C, 5-6M NaOH, 2.6 V, 1000 (Am<sup>-2</sup>) and total energy consumption of 2.5-2.7 kWh kg<sup>-1</sup> Zn.

### 3. Characterization of the raw materials

Characterization of zinc A and B is done by X-Ray Fluorescence (XRF), X-Ray Powder Diffraction (XRPD) and acidic digestion followed by ICP analyses. The equipment specifications are shortly described in Appendix II. From earlier chemical analysis of Zinc A and Zinc B, similar chemical and mineralogical compositions as EAFD became apparent [43].

#### 3.1 General characteristics for Zinc A and Zinc B

##### 3.1.1 Zinc A

Zinc A had high and variable moisture content according to 3 different measurements (Table 6). On appearance, Zinc A consisted of a heterogeneous coloration of “rusty” particles (Figure 10). Zinc A showed to possess magnetic properties (Figure 11). Zinc A was very coarse and hard, which was depicted by the angular shapes of the particles. From particle size distribution it became evident that a grinding step was necessary before any further processing could be done (Table 7). 62.65% of the particles were larger than 1 mm, implying that grinding was required in order to improve surface to volume ratios and hence reduce reaction time. A particle size distribution of <0.1mm was intended, similar to the particle size used for flotation in primary zinc processes [10].



Figure 10. Photo of as received Zinc A (09-09-2007).



Figure 11. Magnetic properties of Zinc A [2]

Table 6. Moisture content for 20kg as received Zinc A

Zinc A	Moisture %
Kemperman	22.3
Stewart [43]	21.12
Yang [2]	10.32

Table 7. Particle size distribution of zinc A [43]

Size range	Zinc A
0 – 1 mm	37.35
1 – 5 mm	33.41
5 – 10 mm	14.04
+10 mm	15.20

Table 8. Phases identified by XRPD analysis of Zinc A

XRPD	Identified Phases (in order of intensity)
Zinc A	ZnFe <sub>2</sub> O <sub>4</sub> , Iron oxides (FeO, Fe <sub>2</sub> O <sub>3</sub> , Fe <sub>3</sub> O <sub>4</sub> ), CaSO <sub>4</sub> *(H <sub>2</sub> O) <sub>0.67</sub> , SiO <sub>2</sub> , NaCl, Na <sub>2</sub> PbO <sub>3</sub> , NaFe <sub>3</sub> (SO <sub>4</sub> ) <sub>2</sub> (OH) <sub>6</sub> , Zn <sub>0.70</sub> Al <sub>0.30</sub> (OH) <sub>2</sub> (CO <sub>3</sub> ) <sub>0.15</sub> *xH <sub>2</sub> O

Table 9. XRPD analysis [43]

Compound	Zinc A (%)
ZnFe <sub>2</sub> O <sub>4</sub> (Franklinite)	30 ± 2
Zn <sub>5</sub> (OH) <sub>8</sub> Cl.nH <sub>2</sub> O (Simonkolleite)	10 ± 1
ZnO (zincite)	5 ± 0.5
SiO <sub>2</sub> (quartz)	5 ± 0.05
Amorphous	50 ± 2

Analyses showed significant presence of zinc ferrites, iron oxides and minor presence of quartz (Figure 12 and Figure 13). Zinc aluminumcarbonate hydroxide hydrate ( $\text{Zn}_{0.70}\text{Al}_{0.30}(\text{OH})_2(\text{CO}_3)_{0.15} \cdot x\text{H}_2\text{O}$ ), zinc hydroxyl chloride hydrate ( $\text{Zn}_5(\text{OH})_8\text{Cl}_2 \cdot x\text{H}_2\text{O}$ ) and zincite ( $\text{ZnO}$ ) were detected during two different XRD analyses in these materials [2, 43]. Calcium sulfates were present, though in numerous stoichiometric hydration forms. The most dominant Na-containing mineral, identified with XRPD, was  $\text{Na}_2\text{PbO}_3$ . In contrast to the finding of Yang (Figure 13), in which  $\text{NaCl}$  was detected. It was remarkable that no chloride salts were detected, although Cl contributed 12.64 wt% according to XRF analyses (Appendix IX). Probably chloride resides in the amorphous structures dominantly present in Zinc A. The background noise is (red line Figure 12) indicative for presense of amorphous structures. For most elements the chemical composition of Zinc A was in range with reported compositions of EAFD (Table 2).

From chemical and mineral characteristics, Zinc A shows many similarities with EAFD (Table 2 and Table 3). However, their morphology and particle size differ. The morphology of Zinc A shows more resemblance with solidified slag than with EAFD. This is possibly due to mineralogical alteration which occurred over at least 15 years of storage. The difference in moisture content can be caused by different sampling location and changes occurring over the years of storage. The differences detected in the mineralogical composition are most likely phases that are transformed into other minerals in the meanwhile or sample variance.

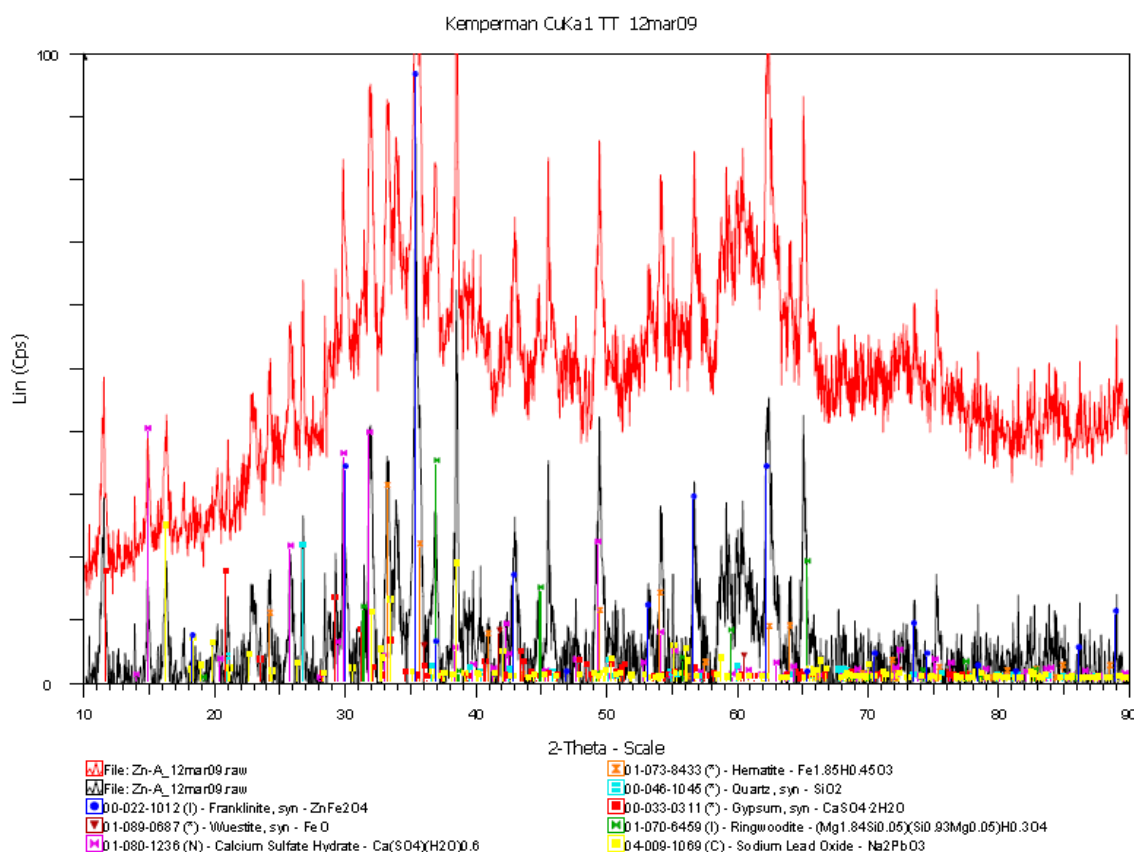
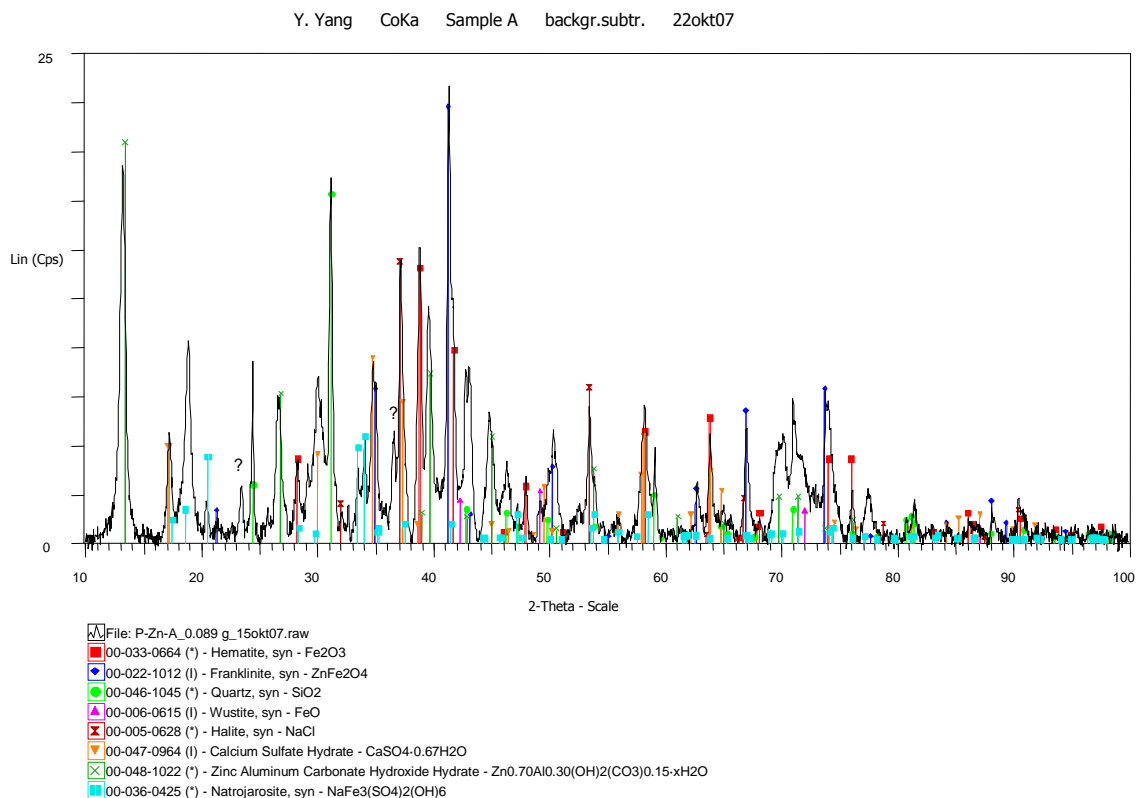


Figure 12. XRPD of Zinc A (Cu target)



**Figure 13. XRPD of Zinc A (Co target) [2]**

### 3.1.2 Zinc B

In contrast to Zinc A, Zinc B had very low moisture content, a homogenous coloration and upon applying some pressure larger particles easily disintegrated to fines (Table 10, Table 11 and Figure 14). Zinc B displayed stronger magnetic characteristics than zinc A (Figure 15). XRPD analysis confirmed these properties by showing strong presence of magnetite and zinc ferrite (Figure 16, Figure 17, Table 12). The phases of  $\text{NaCl}$ ,  $\text{KCl}$ ,  $\text{CaCO}_3$  and  $\text{SiO}_2$  were only detected when Co target was used. Both methods detected zinc oxides but differ in intensity of the signal. For most elements, the chemical composition of Zinc B was in range with reported compositions of EAFD (Appendix XI).



**Figure 14. As received Zinc B (EBS, 09-09-2007).**



**Figure 15. Magnetic properties of Zinc B [2]**

Table 10. Moisture content of as received Zinc B

Moisture	Zinc B %
Kemperman	3.46
Stewart [2]	5.12
Yang [43]	3.4

Table 11. Particle size distribution of Zinc B [43]

Size range	Concentrate B
0 – 1 mm	38.33
1 – 5 mm	29.06
5 – 10 mm	25.39
+10 mm	7.22

Table 12. Phases identified by XRPD analysis of Zinc B from figure 12 and 13

Sample	Identified Phases (in order of intensity)
Zinc B	Iron oxides (FeO, Fe <sub>2</sub> O <sub>3</sub> and Fe <sub>3</sub> O <sub>4</sub> ), ZnFe <sub>2</sub> O <sub>4</sub> , ZnO, SiO <sub>2</sub> , NaCl, CaCO <sub>3</sub> , KCl

Table 13. XRPD analysis of Zinc B [43]

Compound	Concentrate B (%)
ZnFe <sub>2</sub> O <sub>4</sub> (Franklinite)	60 ± 2
ZnO (zincite)	30 ± 2
CaCO <sub>3</sub> (lime stone)	5 ± 0.5
Rest (quartz, paragonite, MnSO <sub>4</sub> )	5 ± 0.5

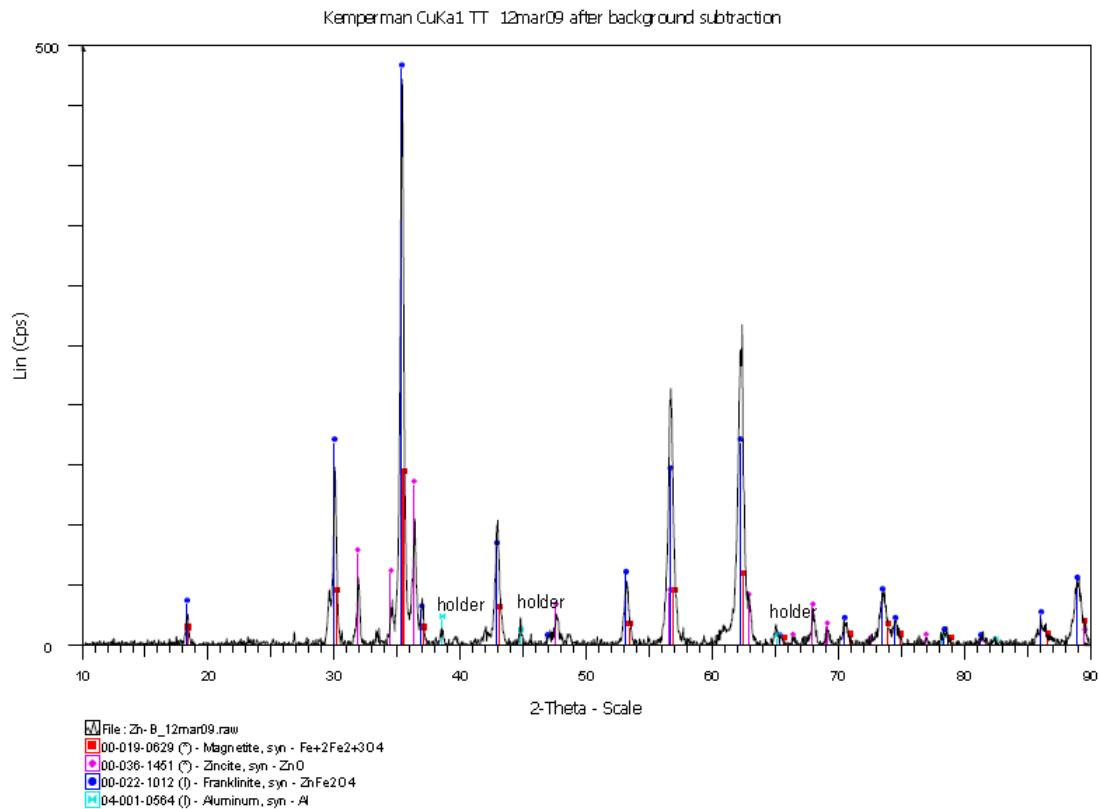
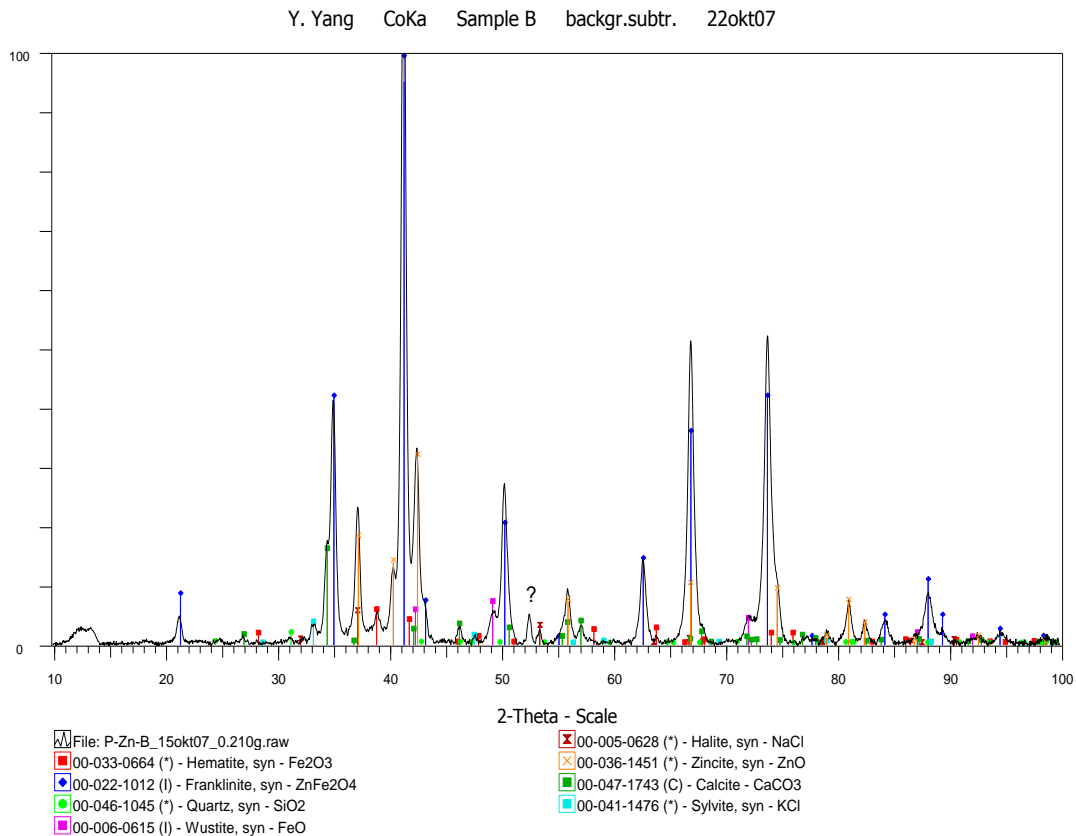


Figure 16. XRPD analysis of Zinc B (Cu target)



**Figure 17. XRPD analysis of Zinc B (Co target) [2]**

Overall, Zinc B shows more resemblance with EAFD than Zinc A. Not only chemical and mineralogical composition, but also its morphology shows many similarities. The long storage time probably increased the agglomeration of particles through surface alteration by weathering, hereby changing its chemical and physical characteristics.

It is very important to notice that, whenever zinc ferrites are detected by XRPD, magnetite can also be present due to exact overlapping patterns. Because of such overlapping, the presence of these phases cannot be unequivocally assured [17, 22].

## 4. Experimental

### 4.1 Raw Materials

Both Zinc A and Zinc B were dried to determine the moisture content and total weight of the dry solids. The material was then grinded in a jaw crusher followed by a Bond ball-mill, achieving sufficient material with a particle size less than 100 $\mu$ m. To insure that the material was below 100 $\mu$ m, sieving with an Allgaier and aperture of 90 $\mu$ m was used. After each process step the filter cake was dried and the moisture content determined. It was then ground for 30 seconds in a disk mill. After grinding the samples were sent for XRF, XRPD or after acid digestion for ICP analysis.

All chemicals used were of analytical grade. ZnO, NaOH, Na<sub>2</sub>CO<sub>3</sub>, Ca(OH)<sub>2</sub>, Mg(OH)<sub>2</sub> were from J.T. Baker and Fe<sub>2</sub>O<sub>3</sub> was obtained from Sigma-Aldrich. ZnO and Fe<sub>2</sub>O<sub>3</sub> were used for producing synthetic zinc ferrite. NaOH was used for roasting and leaching purposes. The use of Na<sub>2</sub>CO<sub>3</sub>, Ca(OH)<sub>2</sub>, Mg(OH)<sub>2</sub> was for roasting purposes.



## 4.2 Experiments

### 4.2.1 Roasting of synthetic zinc ferrites

The aim was to convert zinc ferrites into zinc oxides and to determine the most suitable reagent and final conversion of the zinc ferrites. Pure synthetic zinc ferrite was therefore used and prepared. After preparation it was roasted with suitable reagents according to thermodynamic calculations.

#### ***Zinc ferrite synthesis***

Equimolar amounts of zinc oxide and ferric oxide powders were mixed in an agate mortar and mechanically mixed by a turbula for a period of 30 minutes. The mixed powder was then compacted into briquettes at  $30 \text{ kg.cm}^{-2}$  and heated to  $1100^\circ\text{C}$  for 5 hours and cooled by air. The briquettes were then crushed into fine particles ( $<100\mu\text{m}$ ) by a disk mill in 30 seconds and analyzed by XRPD. Synthetic zinc ferrite was used to confirm the reaction kinetics for suitable reagents according to thermodynamic calculations.

#### ***Roasting of zinc ferrite***

The samples were then roasted using different stoichiometric additions of NaOH or  $\text{Na}_2\text{CO}_3$  ( $>100\mu\text{m}$ ) under different temperature conditions and time steps. After roasting, the samples were crushed into fine particles ( $<100\mu\text{m}$ ) by a disk mill in 30s. The batch samples were leached by 10M NaOH with a liquid/solid ratio of 5, at a constant temperature of  $90^\circ\text{C}$ , stirred by a mechanical device with 800 rpm over a period of 5h. After vacuum filtration, the filtrates were analyzed by AAS (PerkinElmer AA200) and residues by XRPD.

### 4.2.2 Water washing

Water washing experiments of Zinc A and B to remove halides by dissolution was done using different operating conditions (Table 14). The temperature remained constant by using a double walled glass beaker connected to a thermocouple with an accuracy of  $\pm 1^\circ\text{C}$ . Measurements of pH and conductivity were performed during the experiments. The samples were then filtrated. The filter cake was dried for 24h at  $105^\circ\text{C}$  and the moisture content was determined. It was then grinded by a disk mill for 30s and analyzed by XRF. Some of the filtrates were analyzed by ICP-OES.

**Table 14. Operating conditions used during first water washing step for Zinc A and preliminary test of Zinc B.**

Experiment	Temperature ( $^\circ\text{C}$ )	Liquid to solid Ratio (L/S)	Time (h)	Mechanical stirrer (RPM)
Zinc AWW <sup>2</sup>	25	5	1	800
Zinc A WW	50	5	1	800
Zinc A WW <sup>3</sup>	75	5	1	800
Zinc A WW <sup>4</sup>	50	10	1	800
Zinc B WW	50	5	1	1000

### 4.2.3 First NaOH leaching

Operating conditions used for leaching Zinc A and B are listed in Table 15.

Due to the high concentration of caustic soda instead of a glass beaker, a stainless steel beaker was used. The temperature was controlled as described in the water washing step. The evaporation was minimized by sealing the beakers air tight with a rubber lined lid. Samples of



15mL were taken at 5 and 60 minutes. After vacuum filtration, a batch sample was taken. The filtrate was analyzed by ICP-OES. The filter cake was dried for 24 hours at 105 °C, grinded by a disk mill for 30 seconds and analyzed by XRF or XRPD. Measurements of dry and wet weight of the filter cake and total volumetric measurements before and after leaching were performed for the mass balance.

**Table 15. Operating conditions used during first leaching step for Zinc A and Zinc B.**

Name	Lixiviant	Temperature	Time	L/S ratio	RPM
<b>Zinc A</b>	5 M NaOH	90	1h	5	1000
<b>Zinc B</b>	5 M NaOH	90	1h	5	1000

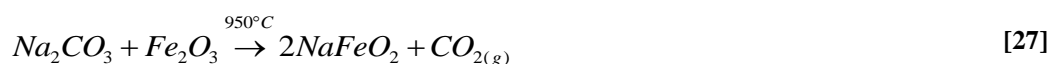
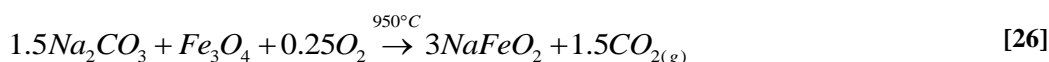
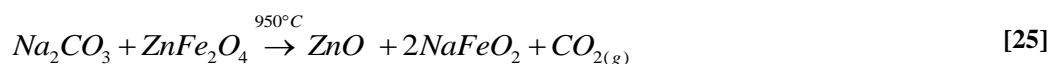
#### 4.2.4 Roasting of first leached filter cake

The additions of Na<sub>2</sub>CO<sub>3</sub> were determined by superimposing results obtained during the pre-feasibility study. The targeted stoichiometric addition was twice the Na<sub>2</sub>CO<sub>3</sub> requirement according to reaction 25-27. In Table 16 the theoretical stoichiometric additions and operating conditions are calculated from XRF analysis, assuming all zinc was present as ZnFe<sub>2</sub>O<sub>4</sub> after leaching, and remaining Fe was present as Fe<sub>2</sub>O<sub>3</sub> or Fe<sub>3</sub>O<sub>4</sub>.

After roasting the calcine was grinded by a disk mill for 30 seconds and analyzed by XRPD and XRF.

**Table 16. Operating conditions used for roasting of Zinc AL and Zinc BL.**

Experiment	Stoichiometric addition of Na <sub>2</sub> CO <sub>3</sub> relative to stoichiometry	Temperature (°C)	Time (h)
<b>Zinc AR</b>	2.6	950	2
<b>Zinc BR</b>	2.1	950	2



#### 4.2.5 Second NaOH leaching

In the second leaching step the same parameters apply as in the first leaching step. Some of the filter cakes were analyzed by XRF and XRPD and filtrates by ICP-OES.

#### 4.2.6 Post water washing

During roasting, formation of sodium iron oxides occurred. A useful residue can be obtained if the alkali metals are removed. Therefore, a final water washing step is used and of importance for the recovery of sodium hydroxides (reaction 28). Nearly similar operating conditions as for the water washing step are used (Table 17). The filter cake was analyzed by XRF and XRPD, the filtrate by ICP-OES.

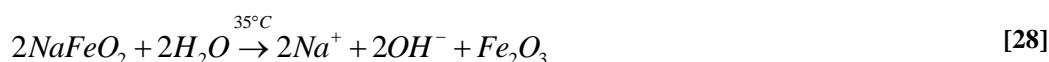


**Table 17. Operating conditions for post water washing of Zinc ARL and Zinc BRL.**

Sample	Temperature °C	Liquid to solid Ratio (L/S)	Time (h)	Mechanical stirrer (RPM)
Zinc ARLWW	50	5	1	800
Zinc BRLWW	50	5	1	800

#### 4.2.7 Cementation

Cementation was conducted on a mixture of filtrates. Equivalent amounts of volume of each filtrate were mixed and denoted as Zinc C. Zinc C was purified by adding zinc dust (Table 18). Lead and copper concentrations of Zinc C were calculated from previously obtained ICP analyses. Upon this estimate twice the stoichiometric addition of zinc dust was added, relative to cementation requirements of Pb and Cu. After measurement of Zinc C by ICP-OES only 1.43 times the stoichiometric dust addition appeared to be added. During cementation, the leachate was thoroughly mixed by an orbital mixer to maintain suspension. The leachate was filtered and used for electro-winning, the filtrate was analyzed by ICP-OES before and after cementation. Finally, the filter cake was analyzed by XRF.

**Table 18. Operating condition of zinc dust cementation of impurities from Zinc P**

Name	Temperature (°C)	Stoichiometric addition of Zn, relative to stoichiometric requirements for cementation of Pb and Cu	Time (h)
Zinc C	50	1.43	2.5

#### 4.2.8 Electrowinning

Direct electrowinning from solution, or after cementation process, was carried out in a 2.0 L volume Plexiglas cell where two anodes and a cathode were placed 20 mm apart (Figure 18). Anode and cathode materials were stainless steel 316L. Surface dimensions depended on the volume of the electrolyte used during experiments. Electrolyte circulation was determined to be sufficient by gas evolution and natural convection. Current was supplied by a DC (direct current) power supply (Delta Electronika), which could work either potential- or galvanostatical, at constant voltage or current respectively. During experimental work the power supply was used galvanostatically. The end solution was sent for ICP-OES analysis.

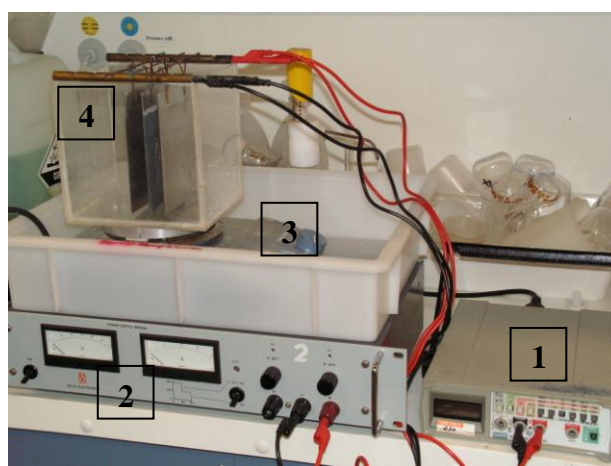


**Figure 18. Electrowinning set-up: 1) Multimeter Volt, 2) Delta Electronika 3) Heater, 4) Electrolytic cell containing one cathode and two anodes.**

## 5 Results and discussion

### 5.1 Zinc ferrite conversion

The conversion of zinc ferrite into zinc oxides is of major importance for the feasibility of the proposed flowsheet. Understanding of the basic chemical reactions involved during roasting is therefore of key importance.

The aim was to convert zinc ferrites into zinc oxides and to determine a suitable reagent and conversion ratio of the zinc ferrites. Pure synthetic zinc ferrite was therefore used and prepared. After preparation it was roasted with suitable reagents according to thermodynamic calculations. Four reagents were selected; NaOH, Na<sub>2</sub>CO<sub>3</sub>, Ca(OH)<sub>2</sub>, and Mg(OH)<sub>2</sub>. The calcined product was then leached in 10M NaOH to determine the final conversion rate.

#### 5.1.1 Zinc ferrite synthesis

Synthesis of zinc ferrite for this research is deduced from the following articles [30] [44] [45] (reaction 29).



A batch production of ~500g was made of the sample which showed complete conversion of ZnO and Fe<sub>2</sub>O<sub>3</sub> according to XRPD analysis (Figure 19 and Figure 20). The major phase was ZnFe<sub>2</sub>O<sub>4</sub>, and minor impurities consisted of ZnO and Fe<sub>2</sub>O<sub>3</sub>. After synthesis of the zinc ferrite pellets a decrease in volume and a small weight loss of ~ 0.5% was seen.

Presence of ZnO<sub>2</sub> in XRPD analysis is unlikely and is probably caused by overlapping of other phases present. The changes in volume and weight losses during roasting are consistent with research done by Rigden [46].

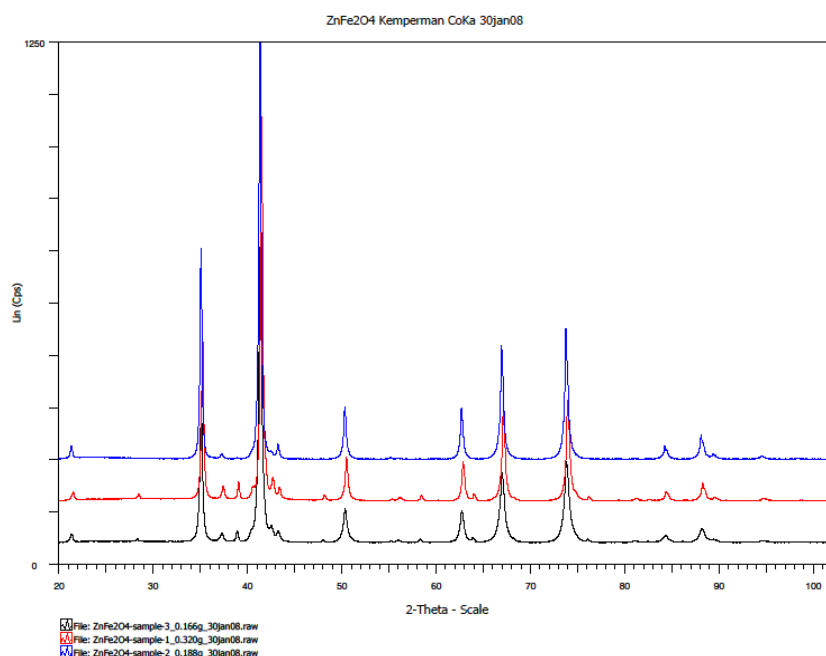


Figure 19. XRPD of zinc ferrite synthesis

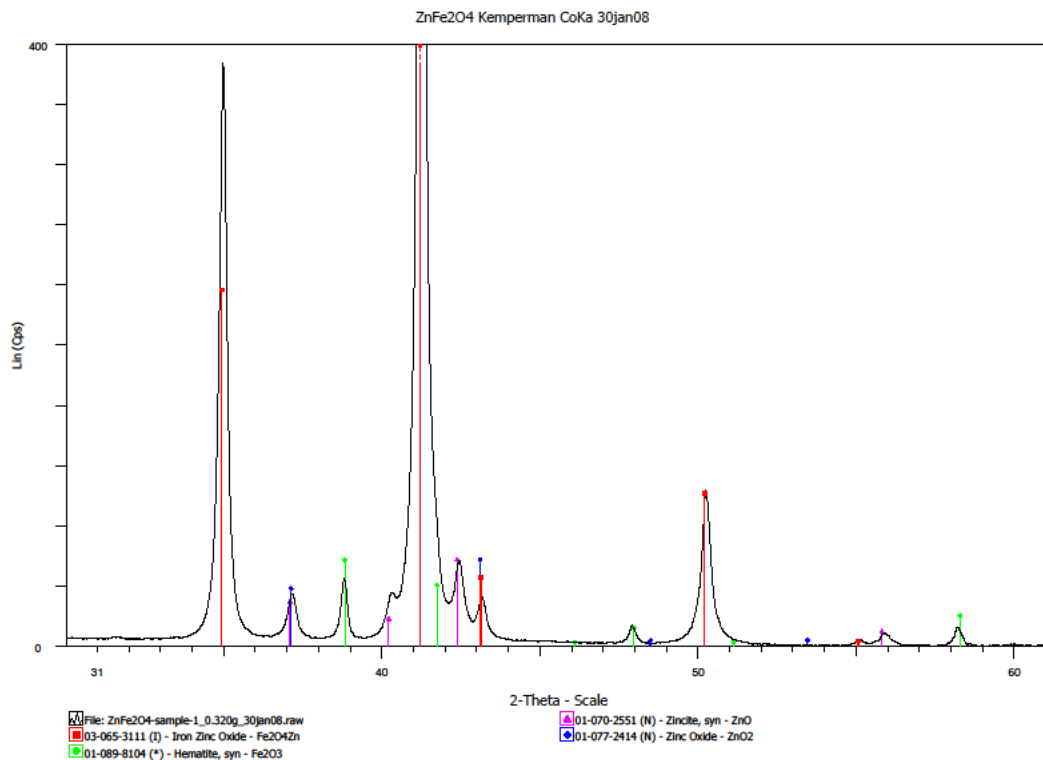


Figure 20. Blow-up of ZnFe<sub>2</sub>O<sub>4</sub>-1.

### 5.1.2 Roasting of synthetic zinc ferrite

#### Reagents

In search of suitable reagents for roasting zinc ferrites, hydroxide groups and other alkaline groups were investigated. This was done using HSC Chemistry [28], which is designed for various kinds of thermodynamic calculations of chemical reactions and equilibrium phases. Using HSC Chemistry 6.12 and review of the relevant literature the following additives were chosen: NaOH, Ca(OH)<sub>2</sub>, Mg(OH)<sub>2</sub> and Na<sub>2</sub>CO<sub>3</sub>.

The reactions and thermodynamic modeling of each reagent showed that soluble zinc oxides are formed when roasted at sufficiently high temperatures (reactions 30-33, Figure 21- Figure 24 and Table 19-Table 22).

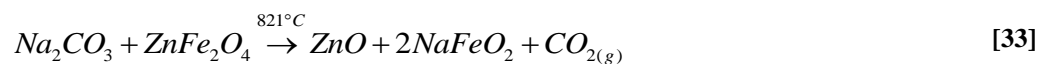
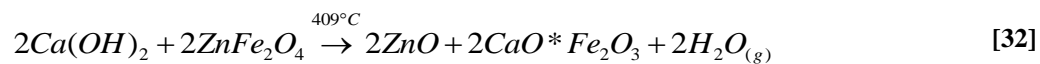
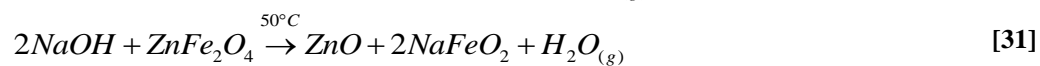
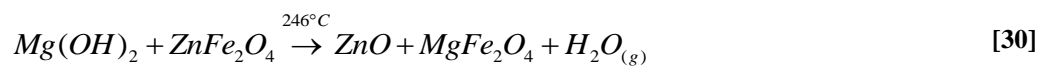


Figure 21 and Table 19 showed that  $\text{MgFe}_2\text{O}_4$ ,  $\text{ZnO}$  and  $\text{MgO}$  were the major products when roasting  $\text{ZnFe}_2\text{O}_4$  with  $\text{Mg}(\text{OH})_2$ . The conversion of zinc ferrite into zinc oxide was highest at  $300^\circ\text{C}$  and slowly decreased at higher temperatures. The conversion of zinc ferrite was not completed within the calculated temperature range, although twice the stoichiometric requirement of  $\text{Mg}(\text{OH})_2$  was added. At elevated temperatures  $\text{Mg}(\text{OH})_2$  dehydrates and was converted into  $\text{MgO}$ . At even higher temperature the equilibrium of preciously formed  $\text{MgFe}_2\text{O}_4$  and  $\text{ZnO}$  became lower as  $\text{MgO}$ ,  $\text{Fe}_2\text{O}_3$  and  $\text{ZnFe}_2\text{O}_3$  were formed.

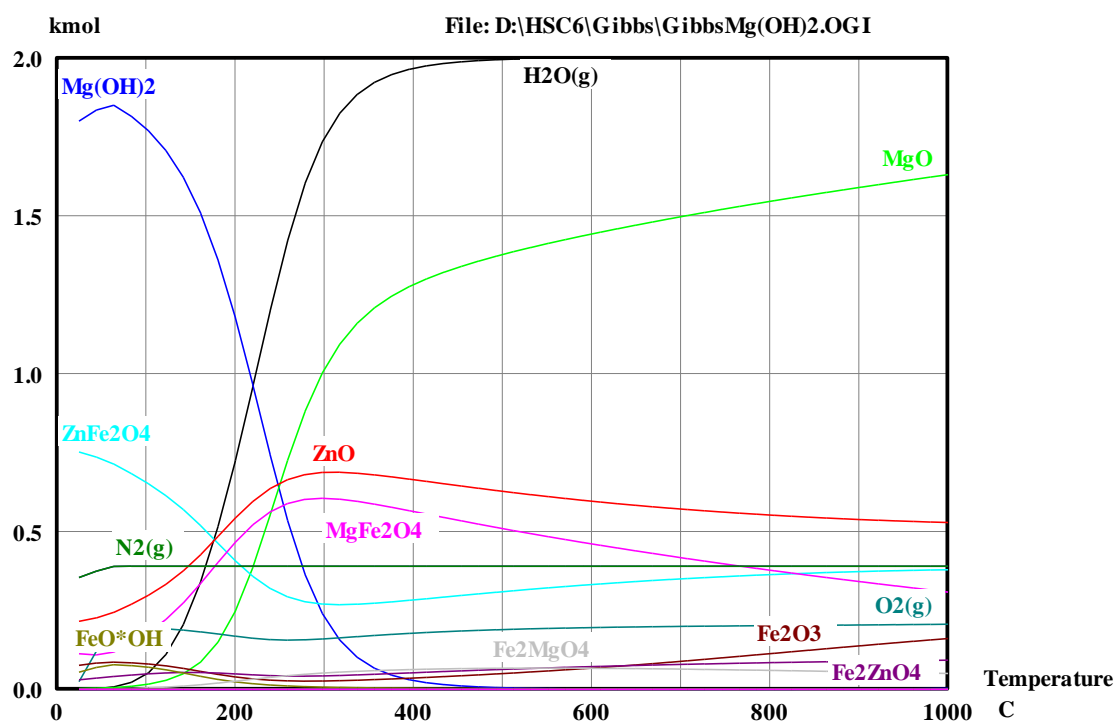


Figure 21. Calculated equilibrium compositions when roasting  $\text{ZnFe}_2\text{O}_4$  with  $\text{Mg}(\text{OH})_2$  in isobaric conditions over a temperature range of 25 to  $1000^\circ\text{C}$  [28]

Table 19. Reaction system  $\text{Na}_2\text{CO}_3$  in -and output at 25 -and  $1000^\circ\text{C}$  respectively (Kmol)

HSC 6.1	Input	Output
$\text{Mg}(\text{OH})_2$	2	-
$\text{ZnFe}_2\text{O}_4$	1	0.38
$\text{N}_2(\text{g})$	0.78	0.39
$\text{O}_2(\text{g})$	0.21	0.21
$\text{H}_2\text{O}(\text{g})$	0.01	2.00
$\text{ZnO}$	-	0.53
$\text{MgO}$	-	1.63
$\text{MgFe}_2\text{O}_4$	-	0.31
$\text{Fe}_2\text{ZnO}_4$	-	0.09
$\text{Fe}_2\text{O}_3$	-	0.16
$\text{Fe}_2\text{MgO}_4$	-	0.05

Figure 22 and Table 20 showed that ZnO,  $*2\text{CaO}*\text{Fe}_2\text{O}_3$ , and CaO were the major products when roasting  $\text{ZnFe}_2\text{O}_4$  with  $\text{Ca}(\text{OH})_2$ . The conversion of zinc ferrite reached completion at 600°. At 500°C 98% of the zinc ferrite was converted an one and a half times the stoichiometric requirement of  $\text{Ca}(\text{OH})_2$  was needed. At more elevated temperature dehydration of residual  $\text{Ca}(\text{OH})_2$  into CaO was completed.

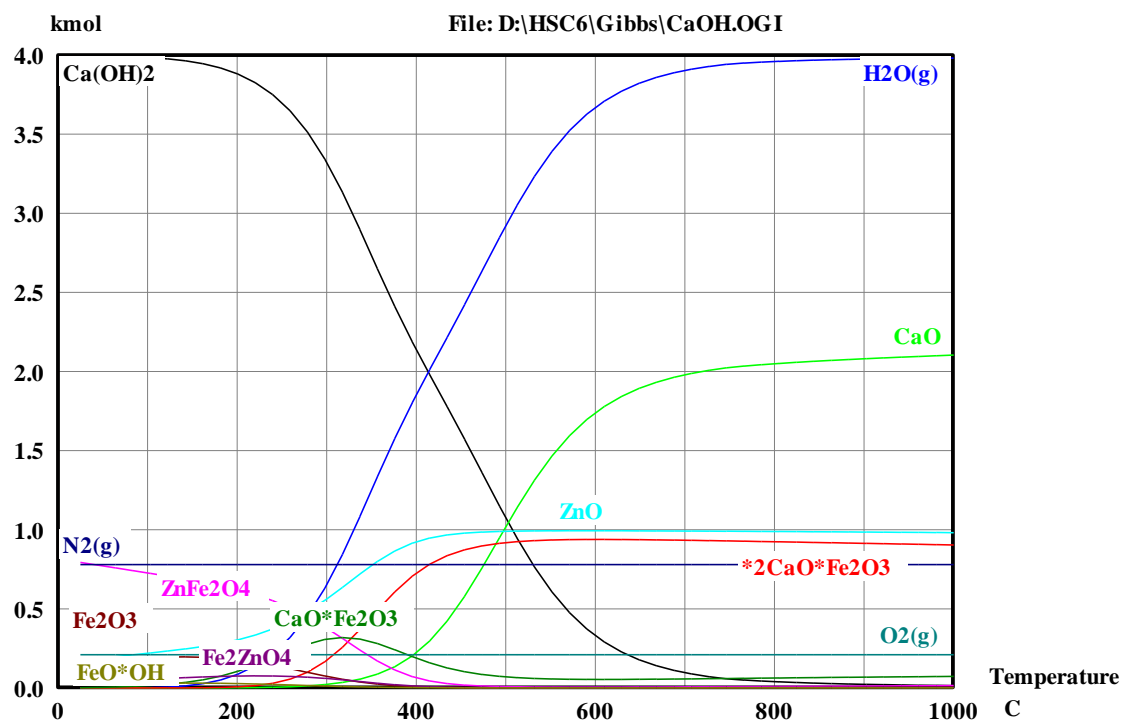


Figure 22. Calculated equilibrium compositions when roasting  $\text{ZnFe}_2\text{O}_4$  with  $\text{Ca}(\text{OH})_2$  in isobaric conditions over a temperature range of 25 to 1000°C [28]

Table 20. Reaction system  $\text{Ca}(\text{OH})_2$  in -and output at 25 -and 1000°C respectively (Kmol)

HSC 6.1	Input (Kmol)	Output (Kmol)
$\text{Ca}(\text{OH})_2$	4	0.02
$\text{ZnFe}_2\text{O}_4$	1	0.01
$\text{N}_2(\text{g})$	0.78	0.78
$\text{O}_2(\text{g})$	0.21	0.21
$\text{H}_2\text{O}(\text{g})$	0.01	3.98
ZnO	-	0.98
$*2\text{CaO}*\text{Fe}_2\text{O}_3$	-	0.90
CaO	-	2.10
$\text{CaO}*\text{Fe}_2\text{O}_3$	-	0.07

The major products when roasting  $\text{ZnFe}_2\text{O}_4$  with twice the stoichiometric addition of NaOH were ZnO, NaOH,  $\text{Na}_2\text{O} \cdot \text{Fe}_2\text{O}_3$  and  $\text{NaFeO}_2$  (Figure 23 and Table 21). The conversion was already completed and required the stoichiometric addition of 2M NaOH, therefore no zinc ferrite was found in the calculated temperature range. The absence of  $\text{ZnFe}_2\text{O}_4$  is probably due to the low reaction temperatures at which conversion of zinc ferrite into zinc oxide in excess presence of NaOH is thermodynamically favorable (reaction 31).

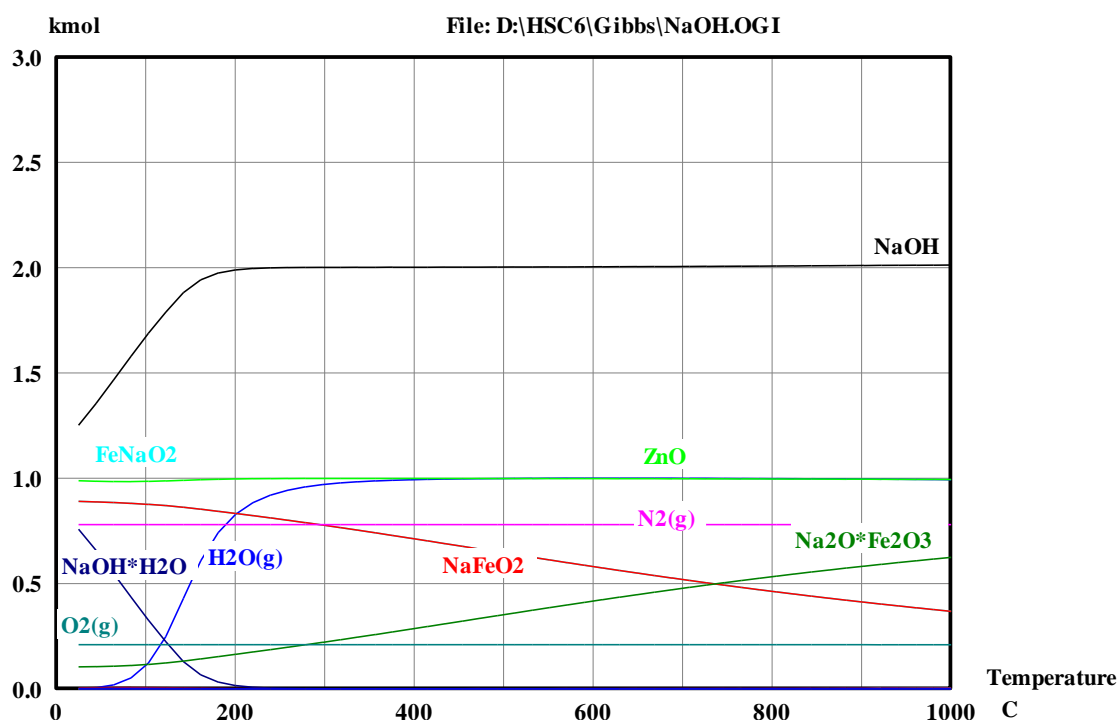


Figure 23. Calculated equilibrium compositions when roasting  $\text{ZnFe}_2\text{O}_4$  with NaOH in isobaric conditions over a temperature range of 25 to 1000°C [28]

Table 21. Reaction system NaOH in -and output at 25 -and 1000°C respectively (Kmol)

HSC 6.1	Input (Kmol)	Output (Kmol)
NaOH	4.00	2.01
$\text{ZnFe}_2\text{O}_4$	1.00	-
$\text{N}_2(\text{g})$	0.78	0.78
$\text{O}_2(\text{g})$	0.21	0.21
$\text{H}_2\text{O}(\text{g})$	0.01	0.99
ZnO	-	0.99
$\text{Na}_2\text{O} \cdot \text{Fe}_2\text{O}_3$	-	0.62
$\text{NaFeO}_2$	-	0.37



The major products when roasting  $\text{ZnFe}_2\text{O}_4$  with twice the stoichiometric addition of  $\text{Na}_2\text{CO}_3$  were  $\text{ZnO}$ ,  $\text{Na}_2\text{CO}_3$ ,  $\text{Na}_2\text{O} \cdot \text{Fe}_2\text{O}_3$  and  $\text{NaFeO}_2$  (Figure 24 and Table 22). The reaction started at  $350^\circ\text{C}$  and reached a maximal conversion of zinc ferrite into zinc oxide at  $1000^\circ\text{C}$  of 0.81 respectively. The onset of formation of  $\text{Na}_2\text{O} \cdot \text{Fe}_2\text{O}_3$  occurred at  $520^\circ\text{C}$ .

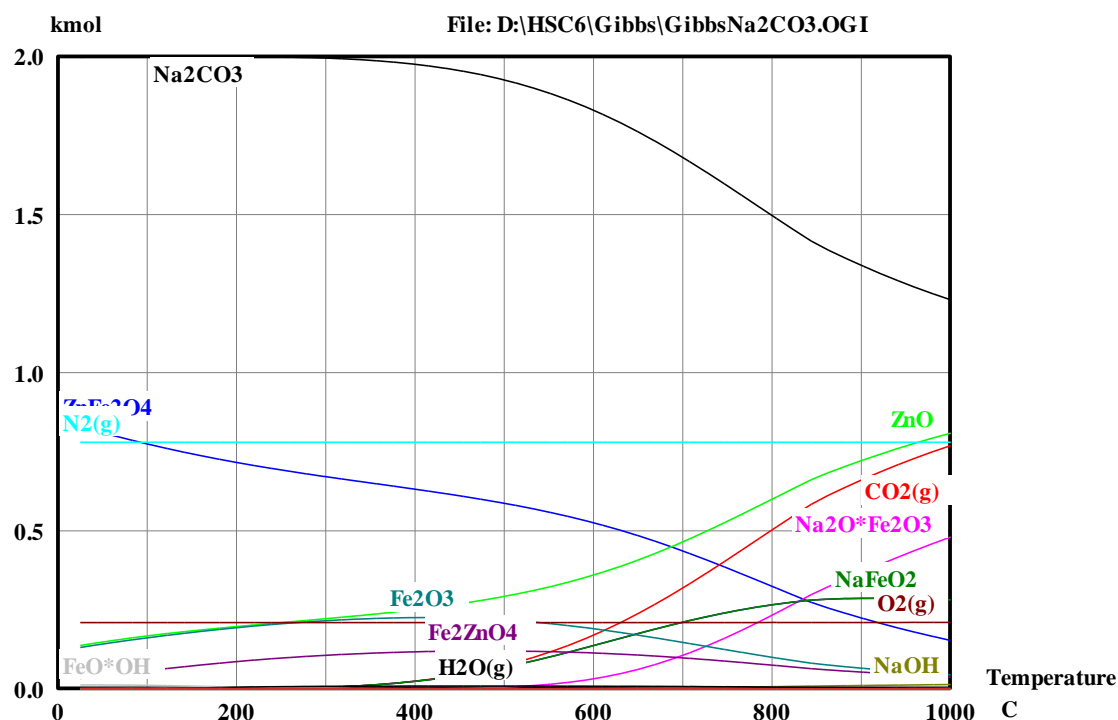


Figure 24. Calculated equilibrium compositions when roasting  $\text{ZnFe}_2\text{O}_4$  with  $\text{Na}_2\text{CO}_3$  in isobaric conditions over a temperature range of 25 to  $1000^\circ\text{C}$  [28]

Table 22. Reaction system  $\text{Na}_2\text{CO}_3$  in -and output at 25 -and  $1000^\circ\text{C}$  respectively (Kmol)

HSC 6.1	Input (Kmol)	Output (Kmol)
$\text{Na}_2\text{CO}_3$	2	1.23
$\text{ZnFe}_2\text{O}_4$	1	0.15
$\text{N}_2(\text{g})$	0.78	0.78
$\text{O}_2(\text{g})$	0.21	0.21
$\text{ZnO}$	-	0.81
$\text{CO}_2(\text{g})$	-	0.77
$\text{Na}_2\text{O} \cdot \text{Fe}_2\text{O}_3$	-	0.48
$\text{NaFeO}_2$	-	0.28
$\text{Fe}_2\text{O}_3$	-	0.04
$\text{Fe}_2\text{ZnO}_4$	-	0.04
$\text{NaOH}$	-	0.01

## Roasting

From preliminary roasting experiments it became apparent that both  $Mg(OH)_2$  and  $Ca(OH)_2$  showed very slow reaction kinetics. This was determined by no detectable changes in color and morphology after 24h of roasting. Holloway et al. found that upon addition of  $Mg(OH)_2$  and  $Ca(OH)_2$  to La Oroya zinc ferrite at  $900^\circ C$  and 5 hours retention conversion of zinc ferrite into zinc oxide remained low, ~30% respectively [34].

Dimensions of surface area, thickness of the layer and crucible shape influenced the reaction rate, change in coloration, and morphology of the calcined product. Therefore, after preliminary experiments, crucibles with similar dimensions were used.

To determine the optimal operating conditions for conversion of zinc ferrites with NaOH and  $Na_2CO_3$  the following variables were changed: Temperature, stoichiometric additions, and residence time (Table 23).

After roasting visual inspection of morphology (texture, structure, porosity, consistency), change of color, and weight loss determined which sample was sent for analysis. The samples sent for analyses were from test 4 (Table 23). After roasting with NaOH the reddish synthetic zinc ferrite changed into a product with a green surface with red interior and large “cavities” (Figure 25). Roasting with  $Na_2CO_3$  produced a brownish, porous, and sintered product (Figure 26). During sample preparations for XRPD analysis strong hygroscopic behavior of NaOH was detected. Phases identified from XRPD analysis showed that no residual NaOH or  $Na_2CO_3$  was present and that most zinc ferrite transformed into ZnO and  $NaFeO_2$  (Figure 28, Figure 28 and Table 24).

Weighing samples before and after roasting showed a significant weight loss. This was expected due to gas formation of  $H_2O$  and  $CO_2$  (reaction 31 and 33). For different stoichiometric additions of NaOH and  $Na_2CO_3$  the theoretical and experimental weight losses expected by gas formation showed large differences (Figure 29 and Figure 30).

$$W_{loss} = 100 * \left( \frac{H_2O}{((S * NaOH) + ZnFe_2O_4)} \right) \quad W_{loss} = 100 * \left( \frac{CO_2}{((S * Na_2CO_3) + ZnFe_2O_4)} \right) \quad [34]$$

Theoretical weightloss was calculated by assuming zinc ferrite stoichiometrically reacted, denoted as S, with soda ash or caustic soda (reaction 34). For  $Na_2CO_3$  a decreased weigh loss was seen from experimental results, whereas NaOH showed an opposing trend indicative for increased stoichiometric reactions.

Both NaOH and  $Na_2CO_3$  become liquid at the temperatures used during roasting. The high porosity present in both samples is probably caused by the gas formation during reaction. Changes in color are most likely caused by changes in mineralogy. Sintering of the calcine product with addition  $Na_2CO_3$  has great implications on the flowsheet development because an additional crushing step is then necessary. However, the hydrophobic behavior of NaOH and handling proves to be more difficult and would require specialized equipment and construction materials because of its corrosive behavior.

Remarkable is that no residual reagents are present, although twice the stoichiometric requirements were used. One explanation for the absence of reagents can be that both reactants solidified in an amorphous phase and were not detected during XRPD analysis. The hydrophobic behavior of NaOH can be an explanation for the presence of  $Na_2Zn(OH)_4$  by moisture from the air (reaction 35). Or additional reagent present reacts to form  $Na_2Zn(OH)_4$  and  $Na_2(Zn_2O_3)$ . This is in compliance with the excess weight loss measured when higher stoichiometric additions of NaOH are used.



**Table 23. Operating conditions for roasting of zinc ferrite for 2 hours. Stoichiometry additions are determined according to Eq. 5 and 6.**

Reagent	Parameters	Test 1	Test 2	Test 3	Test 4	Test 5
NaOH	Temperature	325 °C	425 °C	350 °C	350 °C	350 °C
	Stoichiometry	2	2	1	2	4
Na <sub>2</sub> CO <sub>3</sub>	Temperature	850 °C	950 °C	950 °C	950 °C	950 °C
	Stoichiometry	2	2	1	2	4



**Figure 25. Synthetic zinc ferrite roasted with NaOH (350°C, 2h, 2S)**



**Figure 26. Synthetic zinc ferrite roasted with Na<sub>2</sub>CO<sub>3</sub> (950°C, 2h, 2S)**

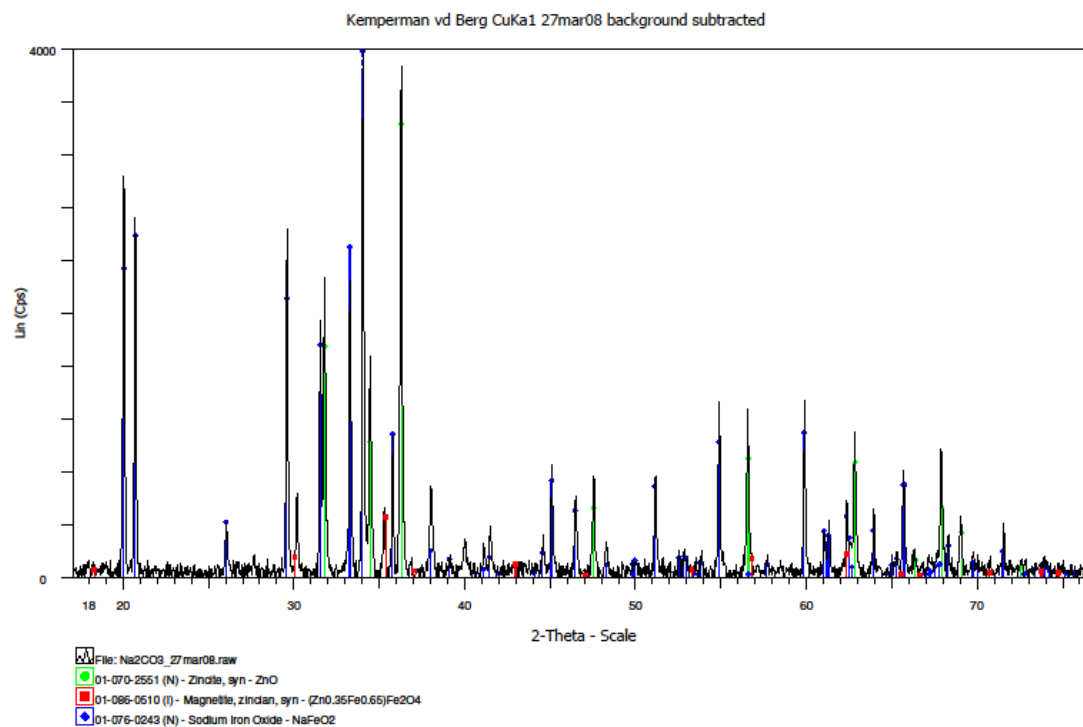


**Figure 27. XRPD analysis of synthetic zinc ferrite roasted with Na<sub>2</sub>CO<sub>3</sub>**

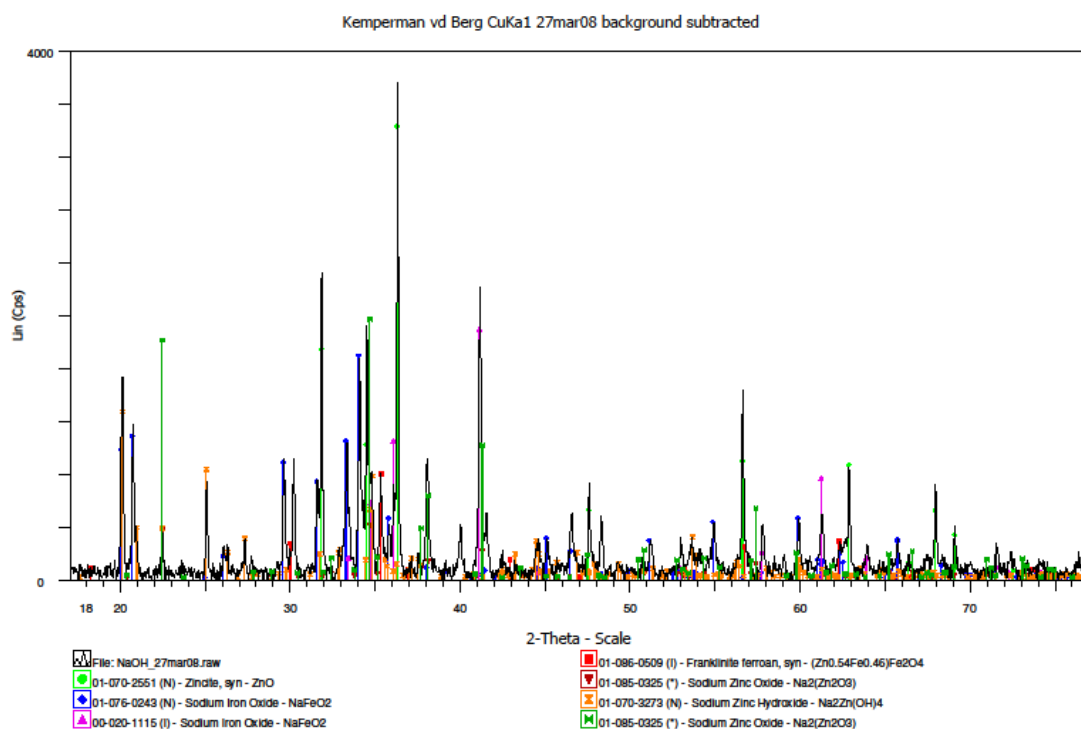


Figure 28. XRPD analysis of synthetic zinc ferrite roasted with NaOH

Table 24. Phases identified by XRPD analysis of synthetic zinc ferrite roasted with NaOH or Na<sub>2</sub>CO<sub>3</sub>

Sample	Identified Phases (in order of intensity)
NaOH: 350 °C, 2t, 2S	ZnO, NaFeO <sub>2</sub> , Na <sub>2</sub> Zn(OH) <sub>4</sub> , (Zn <sub>0.54</sub> Fe <sub>0.46</sub> )Fe <sub>2</sub> O <sub>4</sub> , Na <sub>2</sub> (Zn <sub>2</sub> O <sub>3</sub> )
Na <sub>2</sub> CO <sub>3</sub> : 950 °C, 2t, 2S	NaFeO <sub>2</sub> , ZnO, (Zn <sub>0.35</sub> Fe <sub>0.65</sub> )Fe <sub>2</sub> O <sub>4</sub>

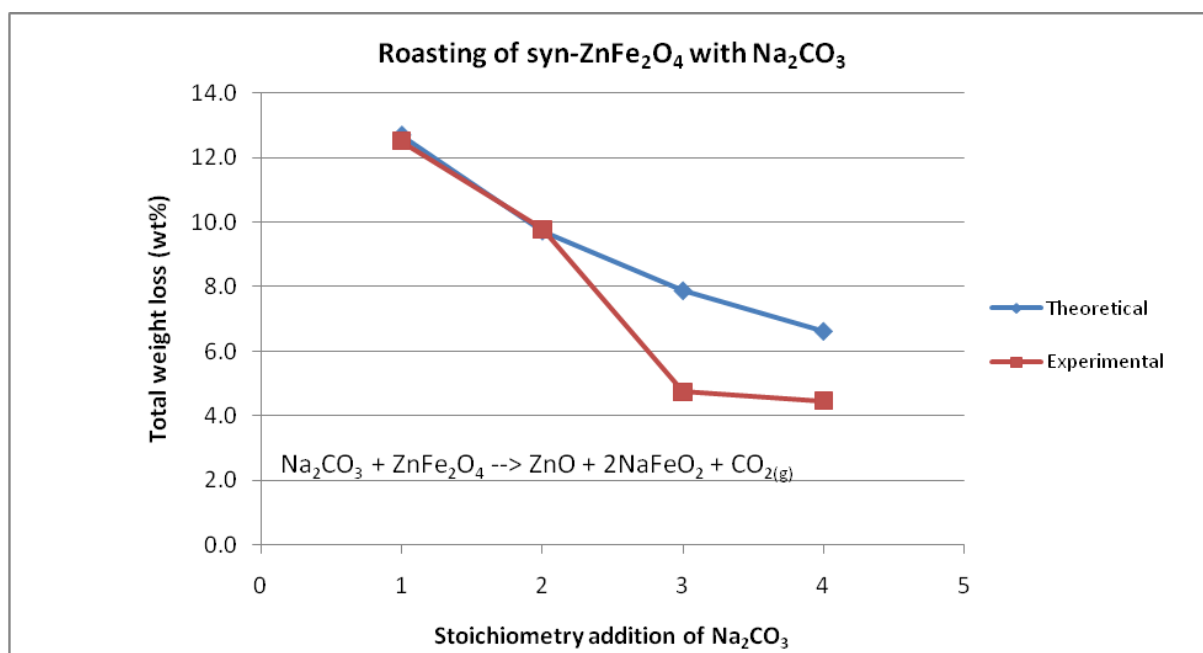


Figure 29. Roasting of syn-ZnFe<sub>2</sub>O<sub>4</sub> with Na<sub>2</sub>CO<sub>3</sub> for 2h at 950 °C; “Theoretical” stands for the theoretical weightloss of carbon dioxide when sample reacted according to stoichiometry

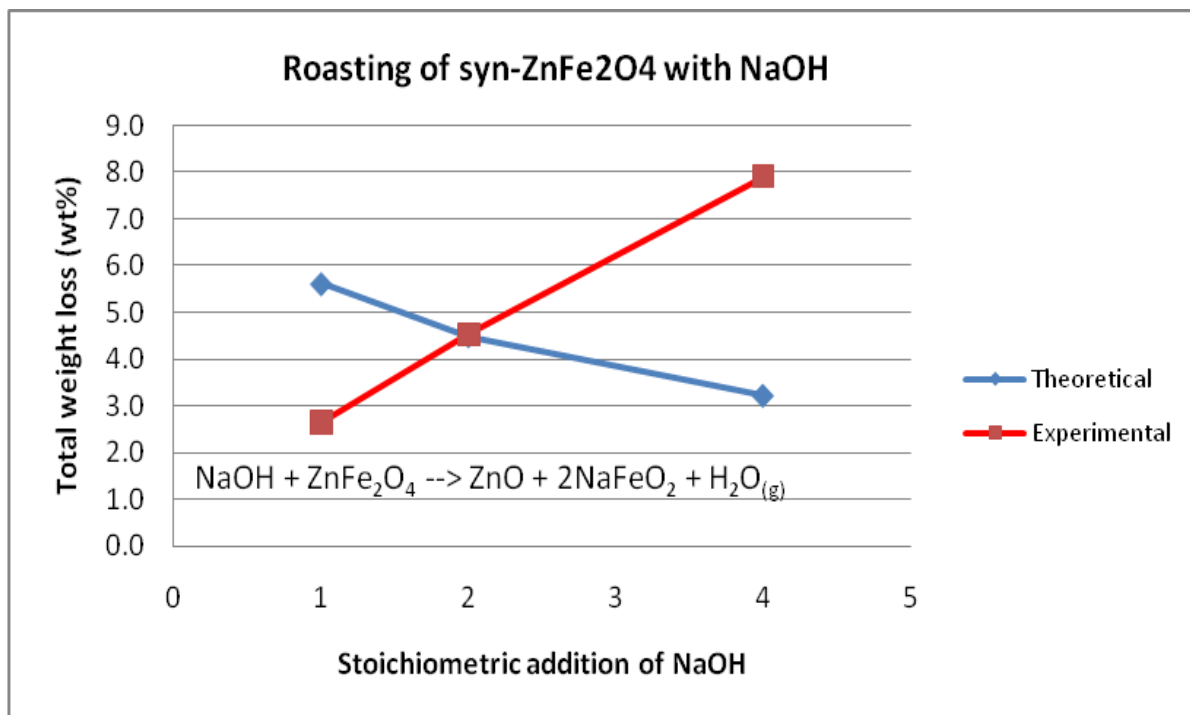


Figure 30. Roasting of syn-ZnFe<sub>2</sub>O<sub>4</sub> with NaOH for 2h at 350°C; “Theoretical” stands for the theoretical weightloss of water vapor when sample reacted according to stoichiometry

### 5.1.3 Leaching of roasted synthetic zinc ferrite

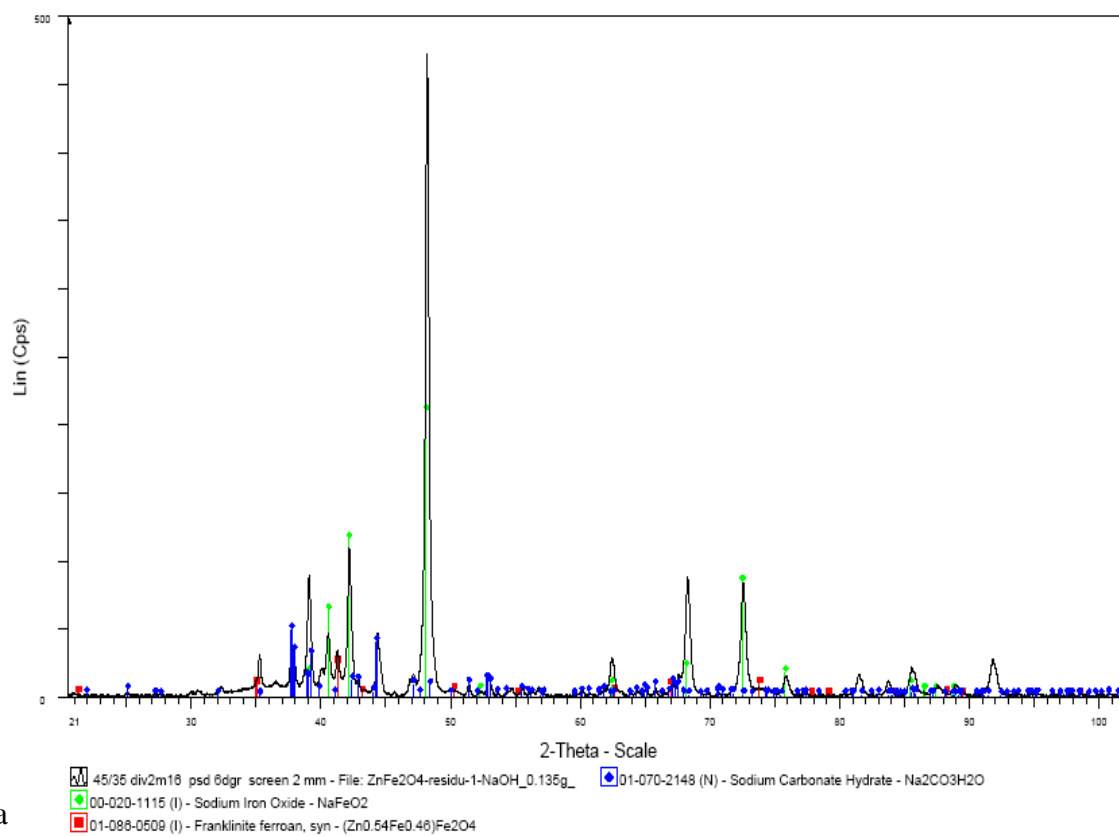
The total conversion of zinc ferrites into zinc oxides was determined by recovery of zinc through NaOH leaching. The recovery was calculated by multiplying the zinc concentration in solution with the total volume used during leaching and divided by total zinc present in the sample. Total dissolution of zinc oxides was ensured by using exceptionally high caustic soda solution of 10M NaOH.

The leachate was filtrated and analyzed by AAS for iron and zinc (Appendix III). The obtained leaching profiles showed that dissolution of zinc was very fast and almost completed within the first 10 minutes (Figure 32), except for sample Na<sub>2</sub>CO<sub>3</sub>-1. The dissolution profile of iron showed to decrease over time and was very low (Figure 33). Final recoveries for both zinc and iron showed that both roasting with NaOH and Na<sub>2</sub>CO<sub>3</sub> could almost completely converted zinc ferrites into soluble zinc compounds and that dissolution of iron was negligible (Table 25). XRPD analysis of the filter cake showed that NaFeO<sub>2</sub> was the dominant phase present followed by Na<sub>2</sub>CO<sub>3</sub>·H<sub>2</sub>O, with exception of sample Na<sub>2</sub>CO<sub>3</sub>-1 (Figure 31 and Table 24).

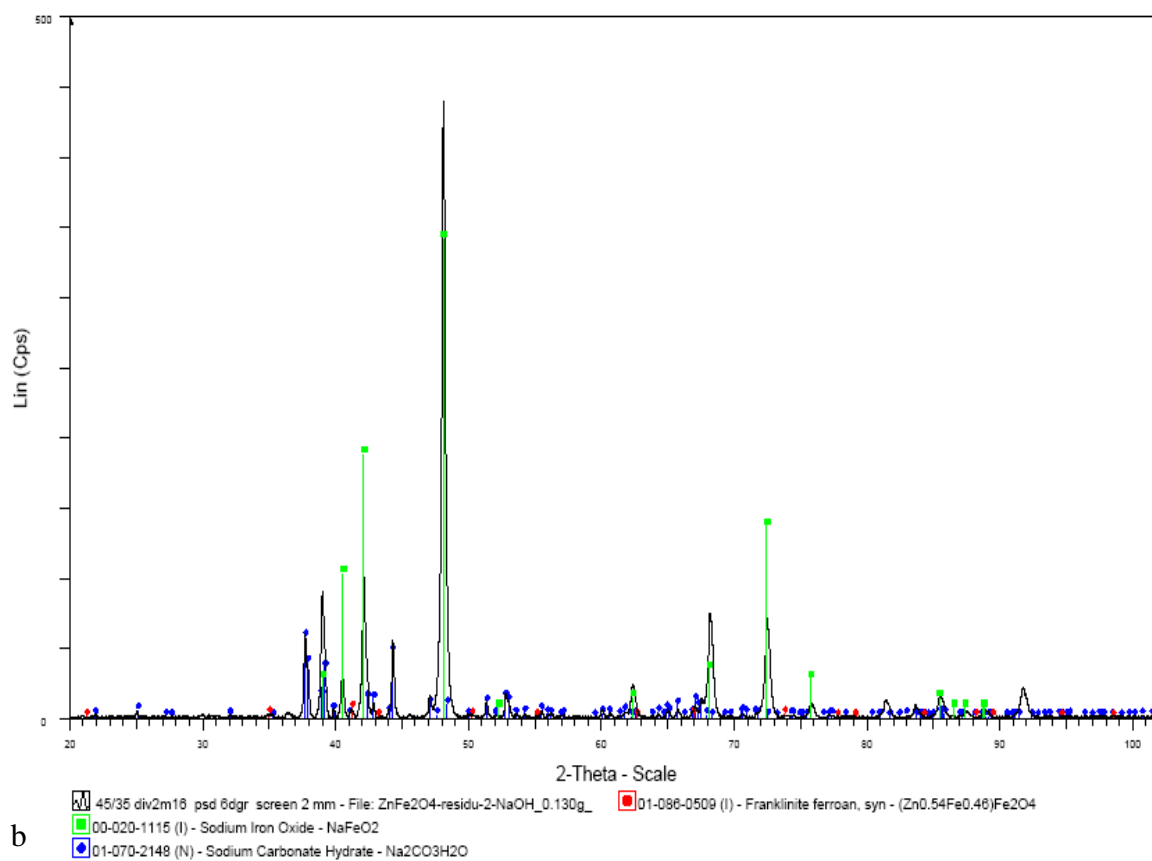
Table 25. Roasting conditions for NaOH and Na<sub>2</sub>CO<sub>3</sub> and final recoveries of zinc and iron after leaching

Tests	NaOH-1	NaOH-2	Na <sub>2</sub> CO <sub>3</sub> -1	Na <sub>2</sub> CO <sub>3</sub> -2
<b>Zinc Ferrite(g)</b>	24	24	24	24
<b>Reagent (g)</b>	16	16	21	21
<b>Temperature (°C)</b>	350	350	950	950
<b>Time (h)</b>	2	2	2	2
<b>Zinc recovery (%)</b>	96.8	88.9	44.7	87.1
<b>Iron dissolution (%)</b>	0.43	0.48	0.13	0.25

Kemperman CoKa 02jul08 background subtracted



a



b

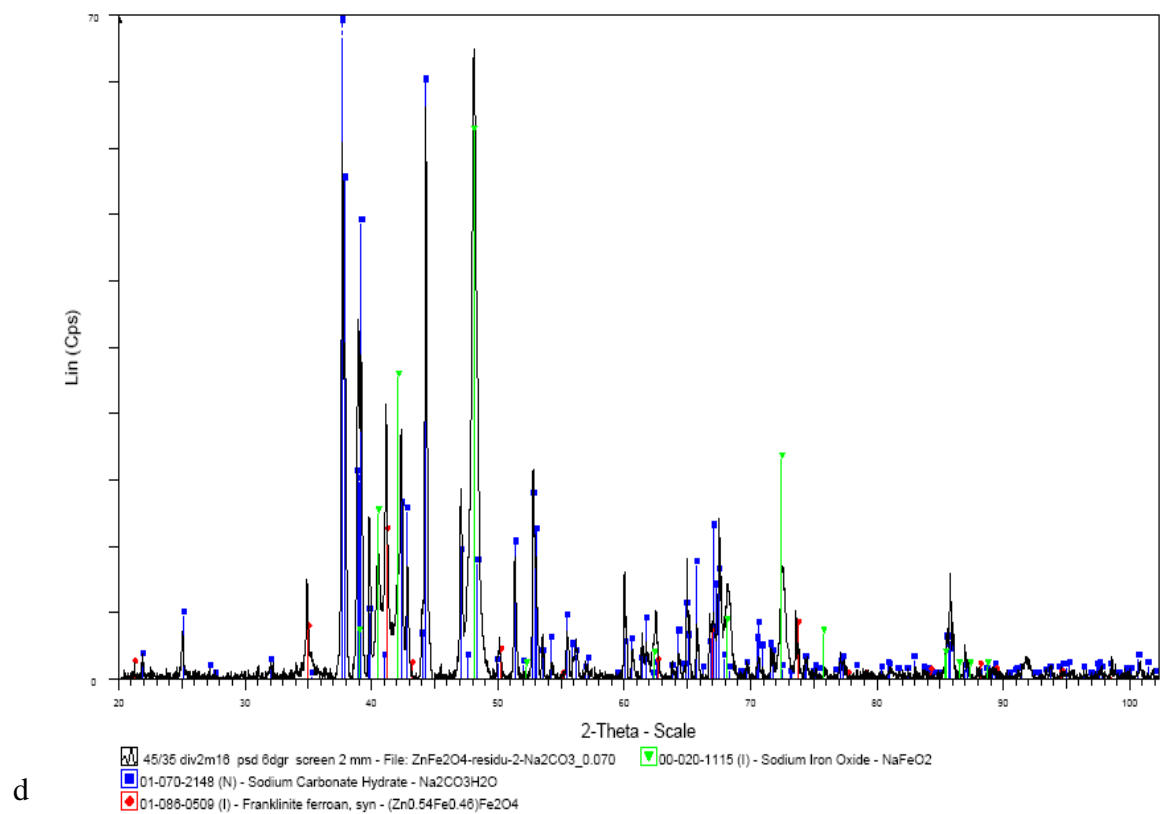
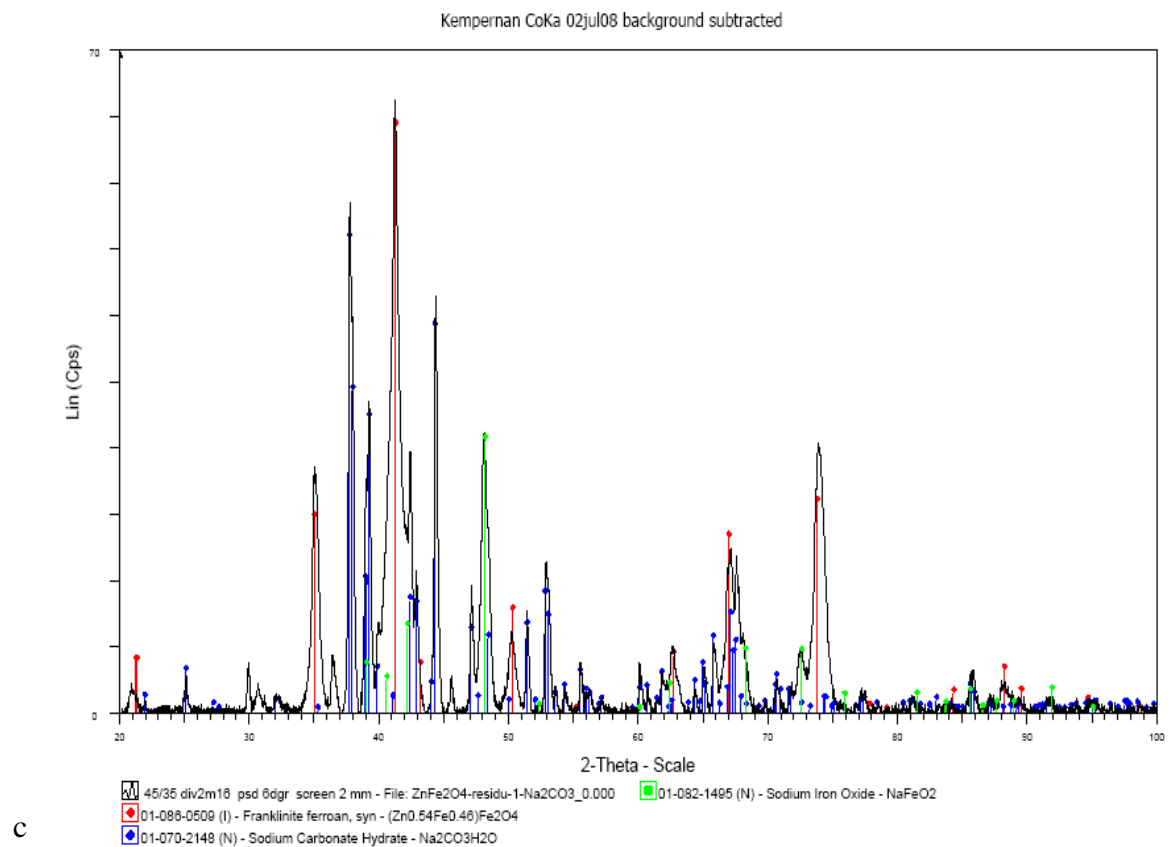


**Figure 31. XRPD analysis of leached calcine product (a) NaOH-1, (b) NaOH-2, (c) Na<sub>2</sub>CO<sub>3</sub>-1 and (d) Na<sub>2</sub>CO<sub>3</sub>-2**



**Table 26. Phases identified by XRPD analysis of synthetic zinc ferrite roasted with NaOH or Na<sub>2</sub>CO<sub>3</sub> after leaching for 1h with 10M NaOH at 90°C, L:S 10, 800 RPM.**

Sample*	Identified Phases (in order of intensity)
NaOH residue 1	NaFeO <sub>2</sub> , (Zn <sub>0.54</sub> Fe <sub>0.46</sub> )Fe <sub>2</sub> O <sub>4</sub> , Na <sub>2</sub> CO <sub>3</sub> H <sub>2</sub> O
NaOH residue 2	NaFeO <sub>2</sub> , (Zn <sub>0.54</sub> Fe <sub>0.46</sub> )Fe <sub>2</sub> O <sub>4</sub> , Na <sub>2</sub> CO <sub>3</sub> H <sub>2</sub> O
Na <sub>2</sub> CO <sub>3</sub> residue 1	(Zn <sub>0.54</sub> Fe <sub>0.46</sub> )Fe <sub>2</sub> O <sub>4</sub> , NaFeO <sub>2</sub> , Na <sub>2</sub> CO <sub>3</sub> H <sub>2</sub> O
Na <sub>2</sub> CO <sub>3</sub> residue 2	Na <sub>2</sub> CO <sub>3</sub> H <sub>2</sub> O, NaFeO <sub>2</sub> , (Zn <sub>0.54</sub> Fe <sub>0.46</sub> )Fe <sub>2</sub> O <sub>4</sub>

\*Roasting conditions (Table 23)

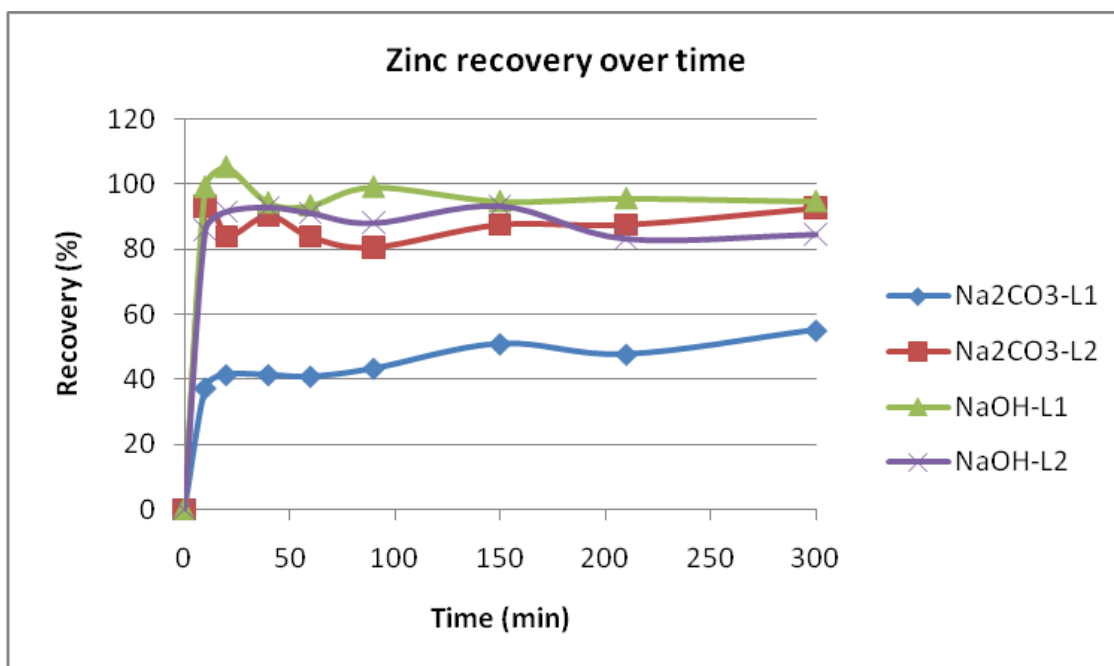


**Figure 32. Zn recovery over time. (90°C, 5h, 800 RPM, L:S 10, 10M NaOH)**

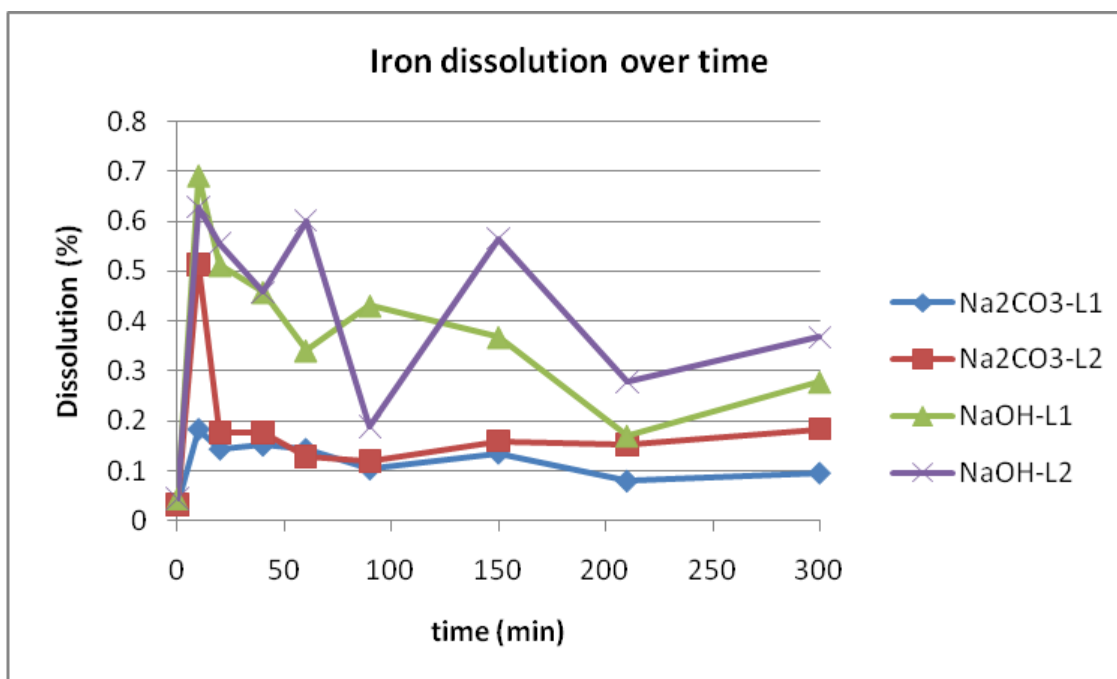


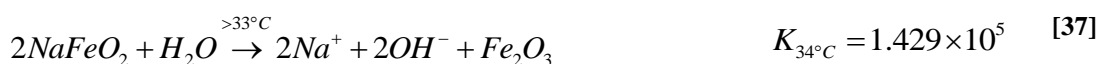
**Figure 33. Iron dissolution over time. (90°C, 5h, 800 RPM, L:S 10, 10M NaOH)**

The decreasing concentration of iron can be caused by slow equilibrium reactions. The large presence of  $\text{Na}_2\text{CO}_3 \cdot \text{H}_2\text{O}$  in XRPD analysis is an indication for excess  $\text{Na}_2\text{CO}_3$  used during roasting and that it is only partially dissolved in strong alkaline solutions. The low recovery of zinc from sample  $\text{Na}_2\text{CO}_3$ -1 can be attributed to poor suspension of the material during leaching. Fluctuations in the recovery might thus be caused by insufficient suspension and/or inadequate mixing preceding the roasting step. An adjustment of 800 to 1000 rpm for the mechanical stirrer for further experiments is used to decrease the chance of poor suspension.

### **Water washing of leach residue**

Water washing of the leach residues had the objective to obtain a clean by-product and simultaneously recover sodium hydroxide.

Sodium iron oxides formed an important byproduct after roasting. According to thermodynamic calculations  $\text{NaFeO}_2$  is highly soluble in water (reaction 36 and 37). However, the results cannot be unequivocally assured as residual caustic soda after filtration was present after filtration. Dissolution of 1,109g (~0.01M  $\text{NaFeO}_2$ ) of Zinc  $\text{Na}_2\text{CO}_3$ -L2 in 500 mL demi-water caused a change in pH of 5.58 to 11.96 within 10 min. According to the equilibrium constant this was expected.



Occurrence of this reaction will be of great importance for the recycling of NaOH and for producing a saleable product for the steel making industry. Furthermore, it closes the loop for the excessive amount of reagent needed to convert zinc ferrites and iron oxides. Closing of the reagent loop is of major importance for economic, environmental and industrial application.

## **5.1.4 Conclusions**

In conclusion, preparation of synthetic zinc ferrite was achieved with only minor impurities. Roasting with NaOH and  $\text{Na}_2\text{CO}_3$  converted the synthetic zinc ferrite into zinc oxides or other soluble zinc compounds. Finally, high recoveries of zinc was achieved while iron dissolution was negligible.

When choosing a suitable reagent the ease of operation and expenses should also be taken into account. NaOH is much more expensive with 546-907 \$/ton than  $\text{Na}_2\text{CO}_3$  with 165\$/ton (accessing data at [www.icis.com](http://www.icis.com)). Additionally, the hygroscopic behavior of NaOH and apparent higher stoichiometric requirements would greatly complex and increase the capital costs of the equipment and process. Therefore it was decided to continue processing Zinc A and B with  $\text{Na}_2\text{CO}_3$ . Disadvantages of using  $\text{Na}_2\text{CO}_3$  as reagent are operations at higher temperatures and higher  $\text{CO}_2$  emissions.

## **5.2 Water washing of Zinc A**

The aim for water washing of Zinc A (Zinc AWW) was removal of chlorides by dissolution. XRF analyses showed that Zinc A was very rich in chlorides with 9.07 wt% (Table 28). Because operating conditions from the literature were not conclusive, different operating conditions were applied (Table 27).

Removal efficiency calculated from XRF analysis showed that 62% of chlorides present in Zinc A was removed by dissolution (Table 28). Sodium, potassium and magnesium

were removed for 42% , 71%, and 19% respectively. Calcium and cadmium were removed to a certain extent and their presence in the leachate was confirmed by ICP analyses of the filtrate. Lead and zinc also dissolved to a certain extent according to ICP analysis, but showed a negative removal efficiency according to calculations based on XRF analyses.

ICP analyses of the filtrate from Zinc B showed that potassium was almost completely removed (Table 29). For more detailed information on dissolution, concentration and removal efficiency of other elements please be referred to Appendix IV and X.

Conductivity and pH measurements were continuously monitored and measurements were taken at t=0, 5 and 60 minutes. In most experiments no significant changes were seen after 5 minutes. Correct calibration of the conductivity apparatus conductivity was not achieved. Therefore conductivity measurements were only indicative. According to conductivity measurements in the first 5 minutes approximately 97% of the final ionic concentration was dissolved (Figure 34).

During water washing a thin grey film appeared on top of the filtrate (Figure 35). This occurrence was seen often, but formation and thickness of the film varied throughout experiments. It looked like zinc dust and reminds of froth flotation processes.

Based on XRF analyses all of the dissolved salts originated from chlorides. This was calculated using the ionic balance (equation 38).

$$\frac{M_{T,1} \times X - M_{T,2} \times X}{M_{W_x}} \times Z_x \quad [38]$$

Where  $M_{T,1}$  denotes total mass in grams before water washing,  $M_{T,2}$  total mass in grams after water washing.  $X$  is the weight percentage determined by XRF analyses of a specific element.  $Z_x$  is the ionic charge of element  $x$ ,  $M_{W_x}$  is molecular weight of element  $X$ .

Dissolution of zinc is caused by the low pH during water washing. According to Figure 6 zinc oxides are soluble at pH 6. Furthermore, loss of zinc can be increased by film formation because it displays adhesive behavior to the walls of equipment.

$\text{CaSO}_4$  formed a minor part of Zinc A (Figure 12 and Figure 13). ICP analyses of the leachate Zinc AWW showed that none of sulfate was dissolved during water washing. The solubility product of  $\text{CaSO}_4$  is low with  $K$  being  $2.2 \times 10^{-5}$  BINAS, or  $1.38 \times 10^{-5}$  [28]. The high recovery of Ca is therefore caused by presence of soluble complexes such as  $\text{CaCl}_2$ . Removal of chloride by water washing could also decrease the recovery of lead, causing decreased formation of soluble Pb-Cl complexes during leaching [33]. Presence of dissolved lead can therefore be explained by dissolution of  $\text{Na}_2\text{PbO}_3$  which was detected in XRPD analyses and presence of chloride ions to form soluble complexes.

Process water with Cd concentrations of 25mg/L imposes large environmental problems and health risks. According to European law the maximum concentration of cadmium in process water is 0.2 mg/L (<http://wetten.overheid.nl/>). This means that the waste water needs to be cleaned.

**Table 27. Water washing operating conditions for Zinc A and B.**

Sample	Temperature	L:S	pH	Residual fraction
Zinc A WW 25	25	5	6.17	0.82
Zinc AWW*	50	5	6.02	0.85
Zinc A WW L:S 10 50	50	10	5.26	0.82
Zinc A WW 75	75	5	5.2	0.81
Zinc B WW 50	50	5	8.88	0.96

\* Average of 6 batches

**Table 28. Analysis of the filtrate (ICP), filter cake (XRF) and calculated removal efficiency after water washing of Zinc A**

Element	Zinc AWW (g/L)	Zinc A (wt%)	Zinc AWW (wt%)	Removal efficiency (%)
<b>Ca</b>	4.72	3.76	2.10	52.54
<b>Cd</b>	0.025	0.03	0.02	19.25
<b>Cl</b>	-	9.07	4.03	62.24
<b>K</b>	1.32	0.67	0.23	71.33
<b>Mg</b>	0.158	0.12	0.11	18.62
<b>Na</b>	-	1.37	0.93	42.31
<b>Pb</b>	0.091	3.10	4.29	-17.60
<b>Sx</b>	-	2.47	3.24	-11.47
<b>Zn</b>	3.9	18.61	23.70	-8.23

**Table 29. Recovery of Zinc B-WW, based on ICP analysis**

Element	Zinc B (Wt%)	Zinc BWW (g/L)	Removal efficiency (%)
<b>Ca</b>	5.26	0.124	1.18
<b>K</b>	0.76	1.440	94.99
<b>Mg</b>	1.78	0.043	1.21
<b>Pb</b>	1.81	0.001	0.03
<b>Zn</b>	15.90	0.004	0.01

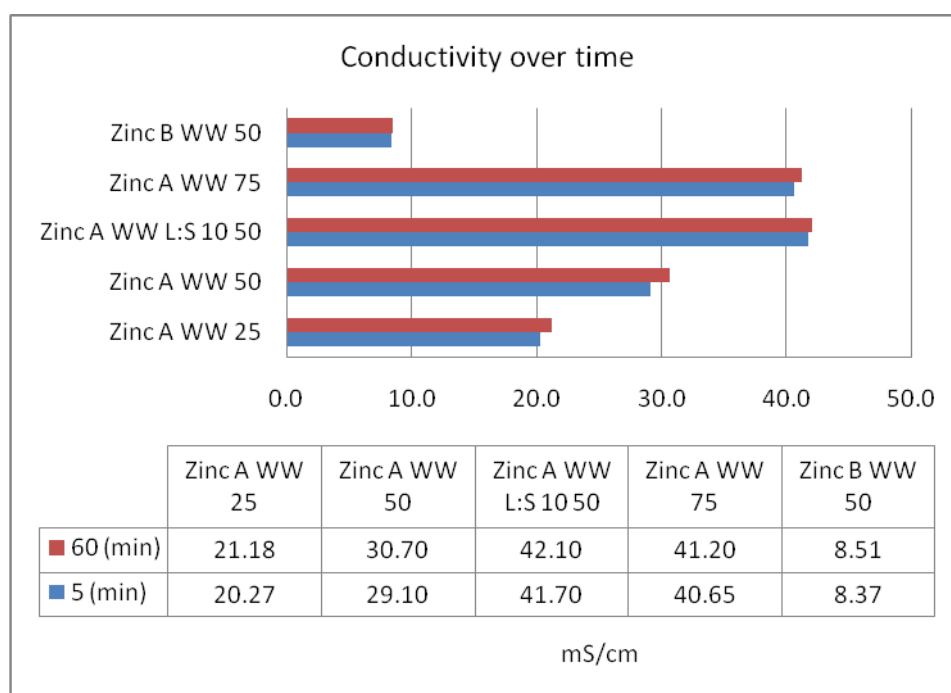


**Figure 34. Conductivity profile over time from water washing experiments, (normalized to 100g/L)**



**Figure 35. “Zinc” film formation during water washing.**

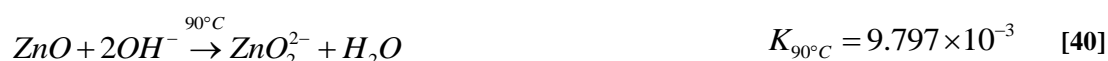
In conclusion, the removal efficiency of chloride from Zinc A was 62% when water washing the material at 50°C with liquid/solid ratio of 5 for 1 hour. This proves that most chlorides are readily soluble and can be removed by a simple water washing step. To further improve the removal efficiency, water washing should be done at higher temperatures using a higher L:S ratio. Furthermore, according to conductivity measurements the dissolution of salts was very fast. Therefore the retention time for washing could be decreased considerably.

To decrease losses of Zn, Pb, and Cd by dissolution, reducing agents should be added or pH of the washing water could be increased.

### 5.3 First leaching step

The aim was to selectively dissolve zinc and other heavy metals from water washed Zinc A (Zinc AL), and Zinc B (Zinc BL). The optimal operating conditions for alkaline leaching for EAFD were derived from the literature: 90-95°C, Liquid to solid ratio of 5-10, 4-6 M NaOH,  $\geq 600$ rpm,  $>4$ h [4, 5, 12, 18, 20, 21, 33].

ZnO was readily soluble in strong alkaline solutions (Figure 32, Reaction 39 and 40). Dutra and Antrekowitsch [21, 32] both concluded that ZnO dissolution is very fast in alkaline solution. Thereafter slow diffusion of zinc ferrites seemed to be the dominant reaction for dissolution of zinc. Because its two stage leaching processes a shorter leaching time was applied. It was therefore determined to operate at the following conditions: a solution of 5M NaOH at 90°C with a liquid/solid ratio of 5 being stirred at 1000 rounds per minute for 1 hour. Samples for ICP-OES analyses were taken at 5 and 60 minutes. Intermediate samples were not taken, because they were thought to contain little additional information.



### 5.3.1 First leaching step of water washed Zinc A

Recovery of zinc was calculated to be 66% and achieved a concentration of 25.6 g/L (Table 32). The recovery denoted the dissolved fraction of total zinc present in water washed Zinc A (Zinc AWW). Lead was recovered with 46% reaching concentrations of 2.83 g/L. Copper was recovered with 33% reaching concentrations of 0.279g/L.

Overall dissolution accounted for a total weight loss of 19.3wt%. Approximately 54% was attributed to dissolution of zinc; the other 46% was mostly represented by Cl, Sx, Fe, Pb, Cu, and Ca.

From XRPD analysis the predominant phases remained zinc ferrite/magnetite, hematite, followed by silica (Figure 36 and Figure 37, Table 30 and Table 31). Newly detected phases were; zinc aluminum oxide, sodium zinc silicate and sodium aluminum silicate. Both aluminum and silica dissolved in strong alkaline conditions and form complexes with sodium. In the pre-feasibility study of Yang [2] direct leaching without pre-washing step was conducted. Additional phases of calcium iron oxides, iron oxide and sodium chlorides were found.

**Table 30. Phases identified by XRPD analysis of water washed Zinc A (Zinc AL\*)**

Sample	Identified Phases (in order of intensity)
<b>Zinc AL*</b>	ZnFe <sub>2</sub> O <sub>4</sub> , SiO <sub>2</sub> , ZnAl <sub>2</sub> O <sub>4</sub> , Fe <sub>2</sub> O <sub>3</sub> , Na <sub>2</sub> ZnSiO <sub>4</sub> , Na <sub>1.54</sub> Al <sub>2</sub> SiO <sub>8.5</sub> O <sub>20.83</sub>

**Table 31. Phases identified by XRPD analysis of directly leached Zinc A (Zinc ALD) [2]**

Sample	Identified Phases (in order of intensity)
<b>Zinc ALD</b>	ZnFe <sub>2</sub> O <sub>4</sub> , Fe <sub>2</sub> O <sub>3</sub> , SiO <sub>2</sub> , ZnAl <sub>2</sub> O <sub>4</sub> , Ca <sub>3</sub> Fe <sub>15</sub> O <sub>25</sub> , NaCl, FeO, Al <sub>2</sub> O <sub>3</sub> , Zn <sub>6</sub> Al <sub>2</sub> O <sub>9</sub>

**Table 32. Analysis of the filtrate, filter cake and calculated recovery after leaching of water washed Zinc A (Zinc AL)**

Element	Zinc AL (g/L)	Zinc A-WW (wt%)	Zinc AL (wt%)	Recovery (%)
<b>Al</b>	1.65	1.05	0.98	28.93
<b>Ca</b>	0.02	2.10	2.11	23.57
<b>Cu</b>	0.28	1.59	1.40	33.02
<b>Fe</b>	0.01	20.76	22.18	18.73
<b>Si</b>	0.02	0.81	0.96	9.63
<b>Sx</b>	-	3.24	0.45	89.48
<b>Pb</b>	2.83	4.29	3.05	45.92
<b>Zn</b>	25.60	23.70	10.52	66.24

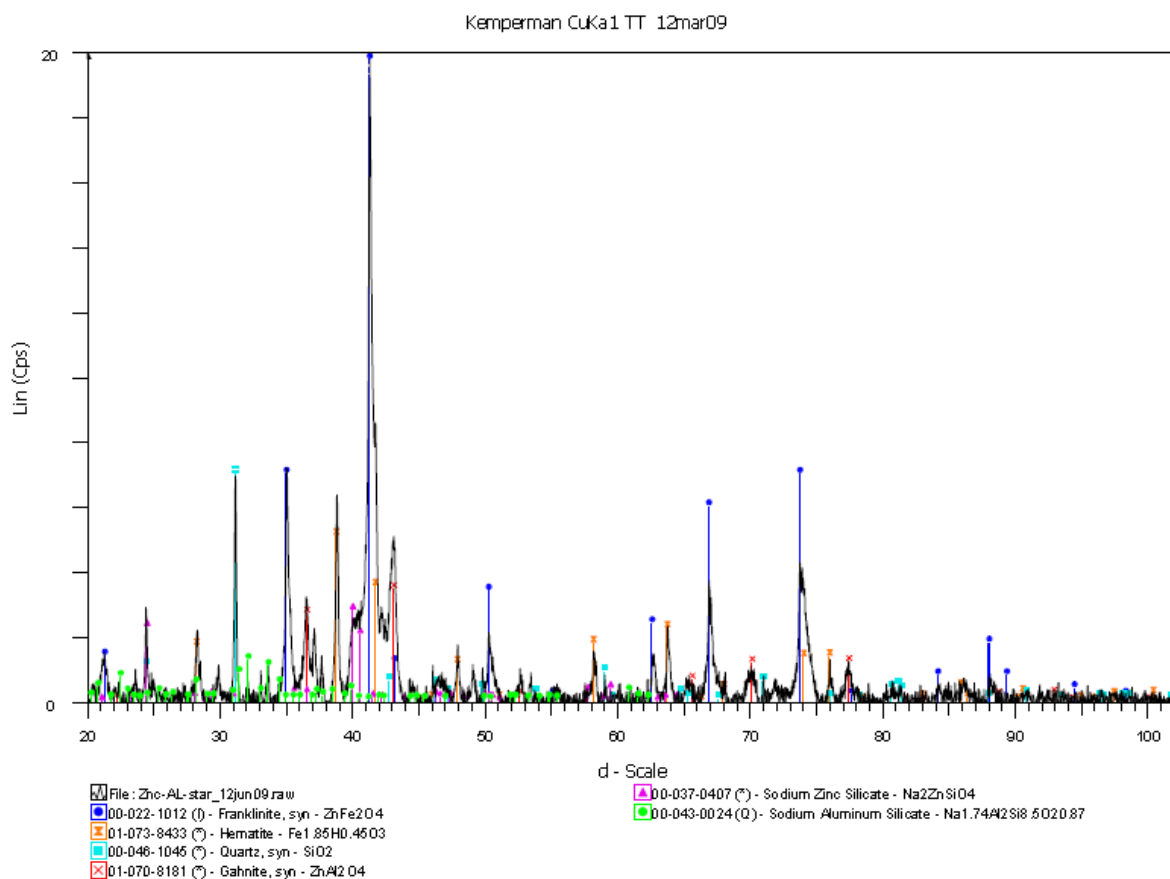


**Figure 36. XRPD analysis of residue of leached Zinc AL\* (5M NaOH, 50°C, 1h, L:S 5)**

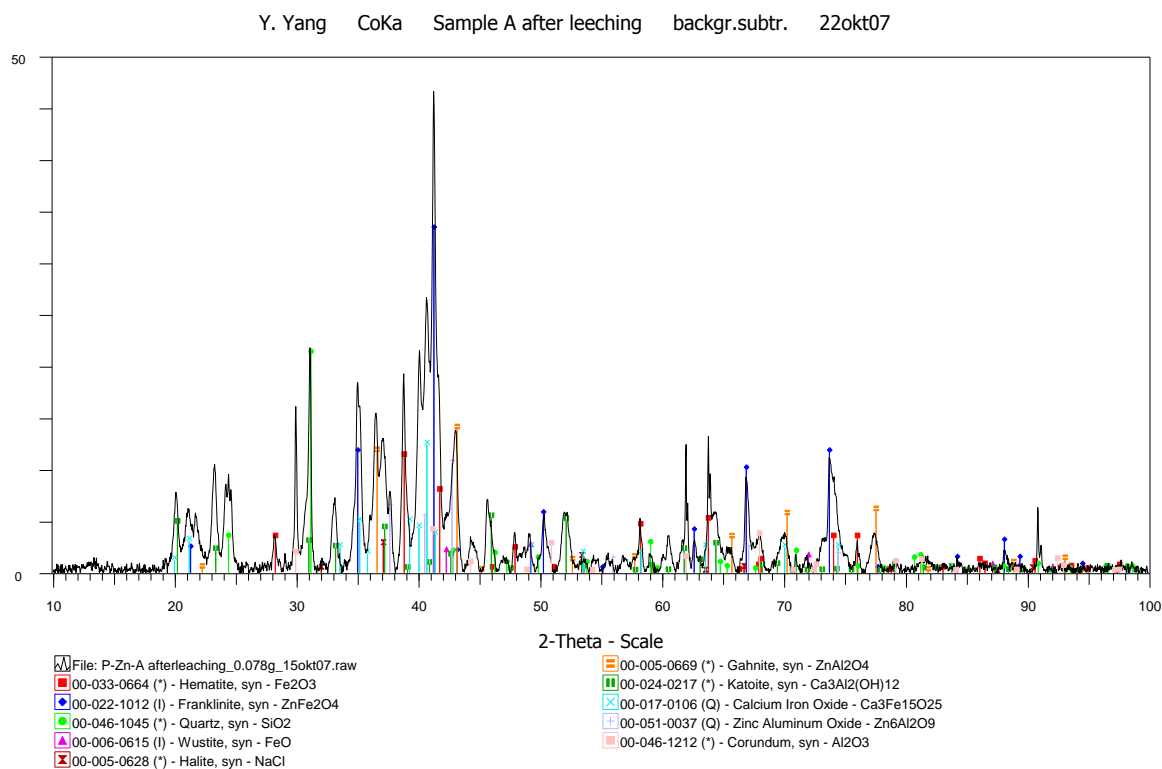


**Figure 37. XRPD analysis of residue of direct leached Zinc ALD (10M NaOH, ~55°C, 3h, L:S 10) [2]**

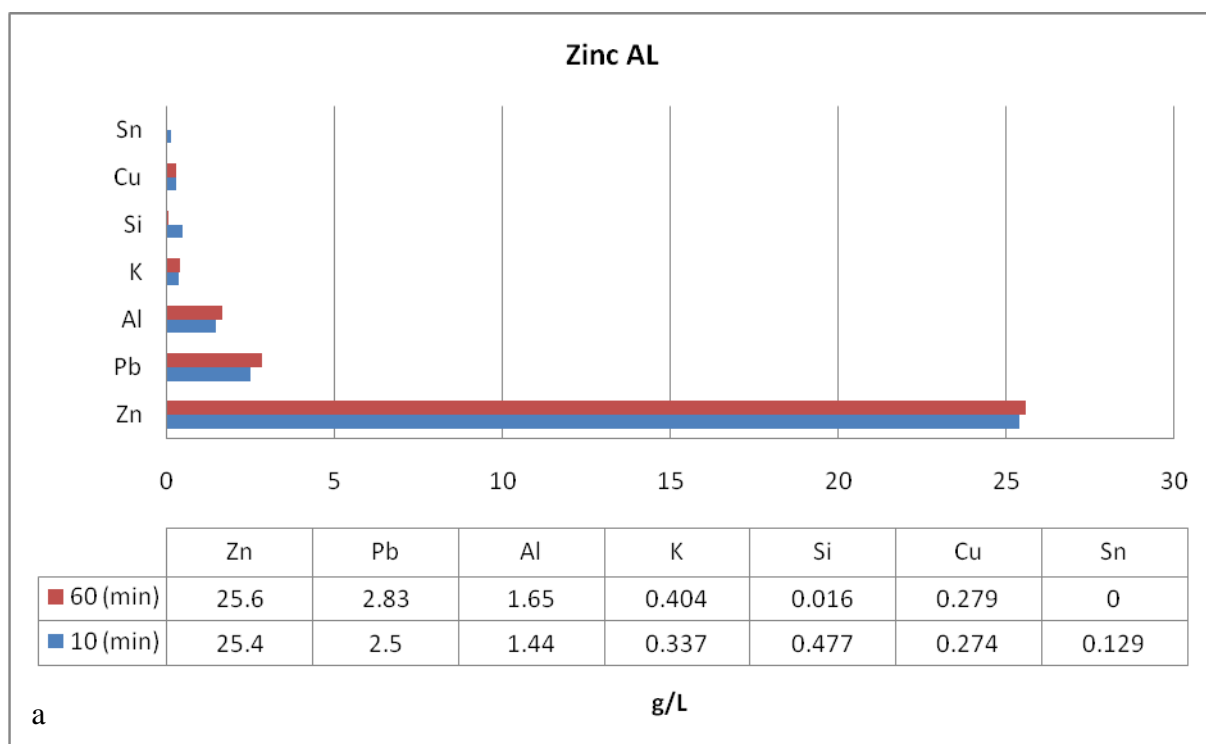
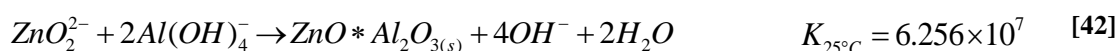


ICP analysis showed that most elements dissolved within the first 10 minutes (Figure 38<sub>a</sub> and Figure 38<sub>b</sub>). Zinc concentration slightly increased from 25.4 to 25.6g/L within the hour. As in earlier experiments zinc, presents as soluble zinc compounds, almost instantly dissolved.

Iron, chromium and cadmium had very low concentrations in the filtrate (Appendix IV). These metals showed reasonable dissolution yields in contrast to observed concentrations in the leachate (Appendix IX). Arsenic had concentrations as high as 52mg/L, and although boron could not be detected by XRF, it was present in small concentrations in the filtrate as  $B(OH)_4^-$ . The concentration of arsenic could pose environmental and health risks when accumulated by regeneration of lixiviate.

It was expected that aluminum and silica dissolved in strong alkaline conditions. Additionally, this phenomenon could have impeded zinc recovery by forming zinc aluminum or zinc silicate complexes, which were detected in XRPD analysis. The decrease of Si in solution over time is probably due to these complex formations and precipitation. The small increase of zinc in solution over time is probably caused by diffusion of zinc ferrites. Xia et al. [47] have found that at 353K ~2.5 % of synthetic zinc ferrite decomposes when leached for 3 hours in 5M NaOH.

The high recovery of sulfur compounds ( $S_x$ ) of 89% and low recovery of Ca of 24% is expected.  $CaSO_4$  probably dissolved in strong alkaline conditions according to reaction 41. The presence of  $ZnAl_2O_4$  can be explained thermodynamically; however formation is a function of concentration, temperature and pH (reaction 42).



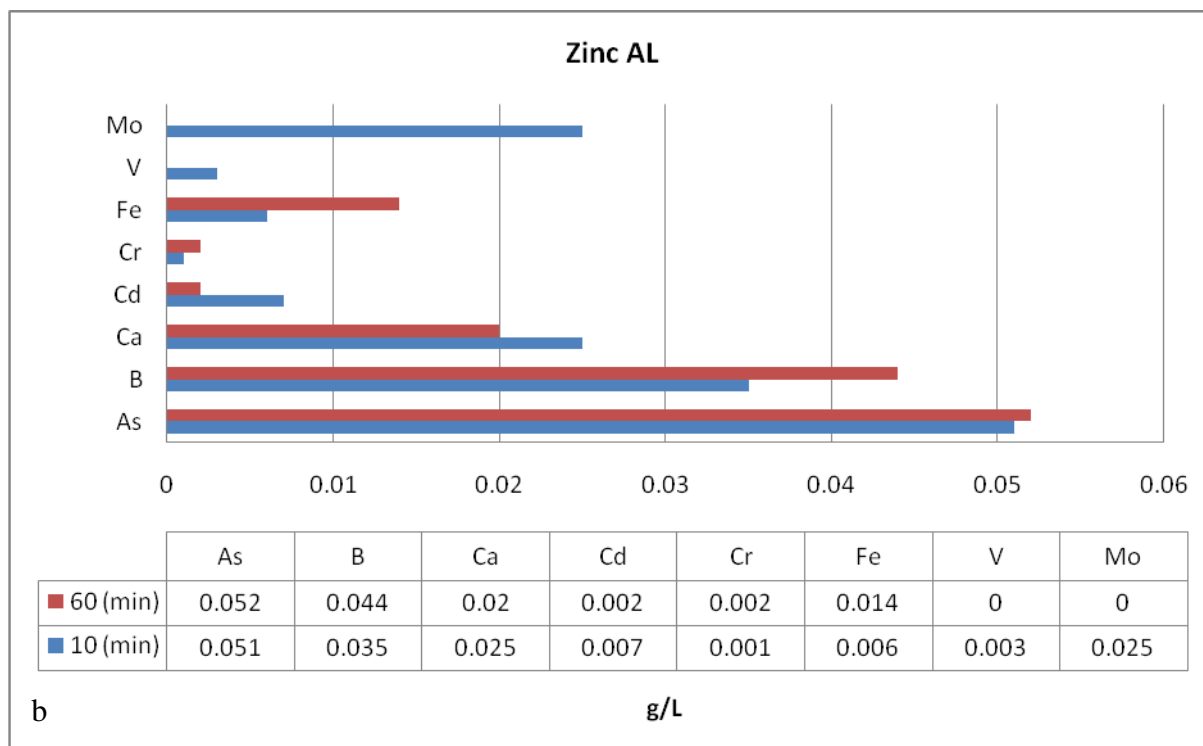


**Figure 38. Concentration of elements in filtrate Zinc AL after 10 and 60 minutes of leaching.**

### **Technical implication**

Filtration of the leachate was impeded by the increased viscosity of the liquid when cooling down from reaction temperature (Table 4). Additionally a white gelatinous precipitate formed after vacuum filtration. The cooling rate influenced the size and stability of the gelatinous particles. Nagib et al. [27] also mentioned a similar problem during filtration and observed  $Zn(OH)_2$  and  $3PbO \cdot H_2O$  as the predominant phases of the white precipitate.

Pourbaix diagram of zinc showed that zinc oxides need stronger alkaline conditions to be dissolved at low temperatures than at higher temperatures (Figure 39). Decreasing temperature of the filtrate would enhance formation of precipitates as hydroxides or zinc oxides, impeding the filtration process (reaction 43).



This also applies for aluminum and silica which were more likely to form complexes with zinc at lower temperatures, thereby impeding recovery of zinc.

Thermodynamic modeling and interpretation of pourbaix diagrams is therefore a very important tool to estimate the correct pH and temperature for optimal zinc recovery.

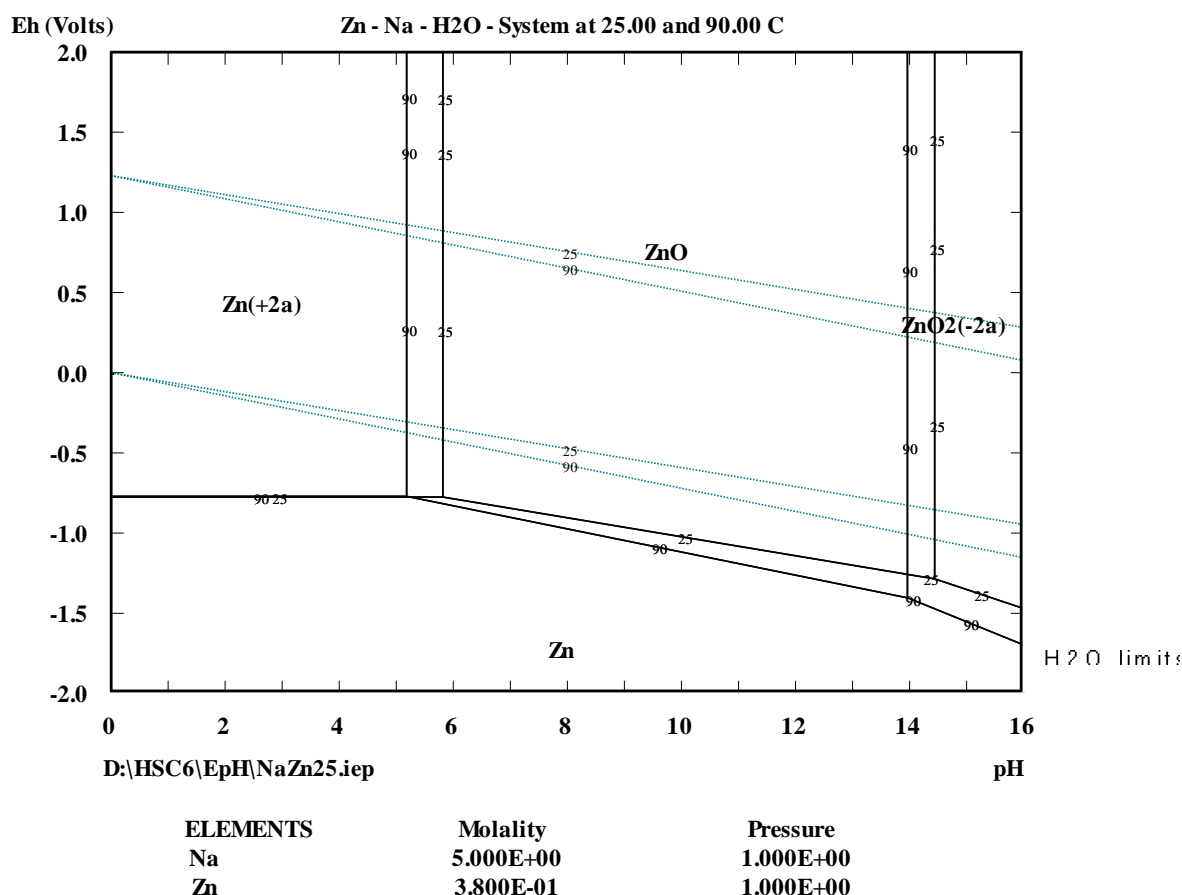


Figure 39. Stability diagram of Zn, 0.38M at 25 and 90°C in 5M NaOH solution [28].

### Mass balance implications

Large discrepancies between ICP and XRF analyses for leaching Zinc AWW were detected. According to XRF analyses about 175g of zinc should be recovered in 4.575 L of 5M NaOH, expected concentration in the filtrate would be ~38g/L Zn. However, only a concentration of 25.6 g/L of zinc was found. This leaves a total discrepancy of 59g zinc. Interpretation of XRF analyses for mass balance purposes and interpretation of the results should therefore be carefully considered.

Due to consequent use of XRF analysis relative differences and thus calculated recoveries are representative and could be used. Errors due to differences in samples, sample preparation, loss during experiments and analytical errors should be considered to have caused this discrepancy.

### 5.3.2 First leaching step of Zinc B

According to XRF analysis, the recovery of zinc from Zinc B was 57% and achieved a concentration of 20.2 g/L (Table 33). In contrast to recoveries found for water washed and leached Zinc A (Zinc AL), leached Zinc B (Zinc BL) showed high recovery for Pb with 70% and 2.54 g/L. The recovery of Cu was negligible and had a concentration of 0.014g/L. Overall dissolution accounts for a total weight loss of 9.4%. Approximately 54% was attributed to zinc dissolution with the remainder mostly comprised of Fe, Pb, K, Cl, Mn, Sx, Ca and Mo. ICP analysis showed a more significant increase of Zn, Pb, Cu and K over time than was seen for Zinc AL (Figure 42). Most other elements decreased over time.

When comparing XRPD Zinc B and Zinc BL\* a large difference in intensity of the phases was seen (Figure 16 and Figure 40, Table 34 and Table 35). After leaching less crystalline zinc ferrites were detected. ZnO were not detected and presumed to be totally dissolved. Calcium manganese hydroxide was the only other phase detected. Calcium formed (hydr)oxide complexes with aluminum and iron. As for directly leached Zinc B (Zinc BLD) iron oxides and zinc aluminum oxides were detected (Figure 41). Zinc B was not water washed, therefore halides K and Cl showed high recoveries of 89% and 91% respectively (Table 33). For detailed information please be referred to Appendix XI.

**Table 33. Analysis of the filtrate, filter cake and calculated recovery after leaching of Zinc BL**

Element	Zinc BL (g/L)	Zinc B (wt%)	Zinc BL (wt%)	Recovery (%)
Cl	-	0.80	0.08	91.01
K	3.86	0.89	0.11	89.04
Fe	<	34.97	33.89	12.17
Sx	-	0.55	0.07	88.52
Pb	2.54	1.98	0.65	70.25
Zn	20.2	18.14	8.66	56.73

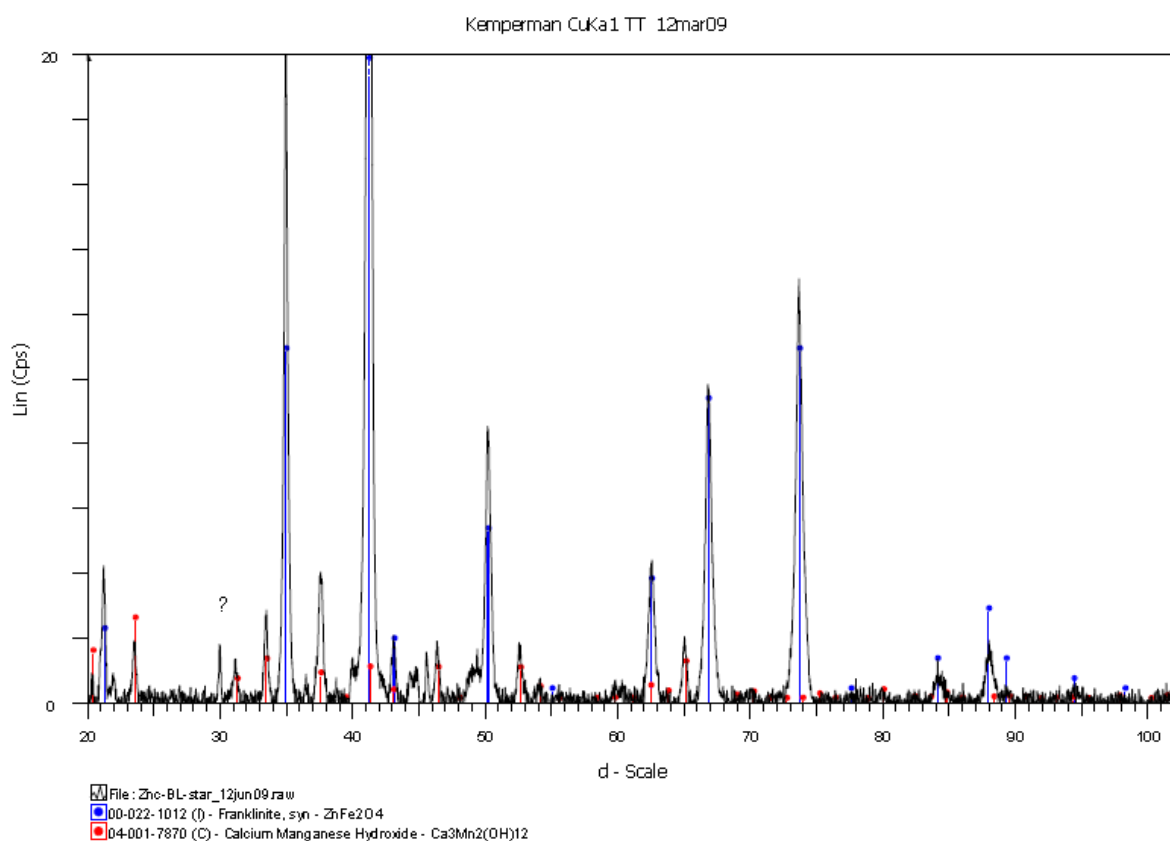


**Figure 40. XRPD analysis of residue of leached Zinc BL\* (5M NaOH, 50°C, 1h, L:S 5)**

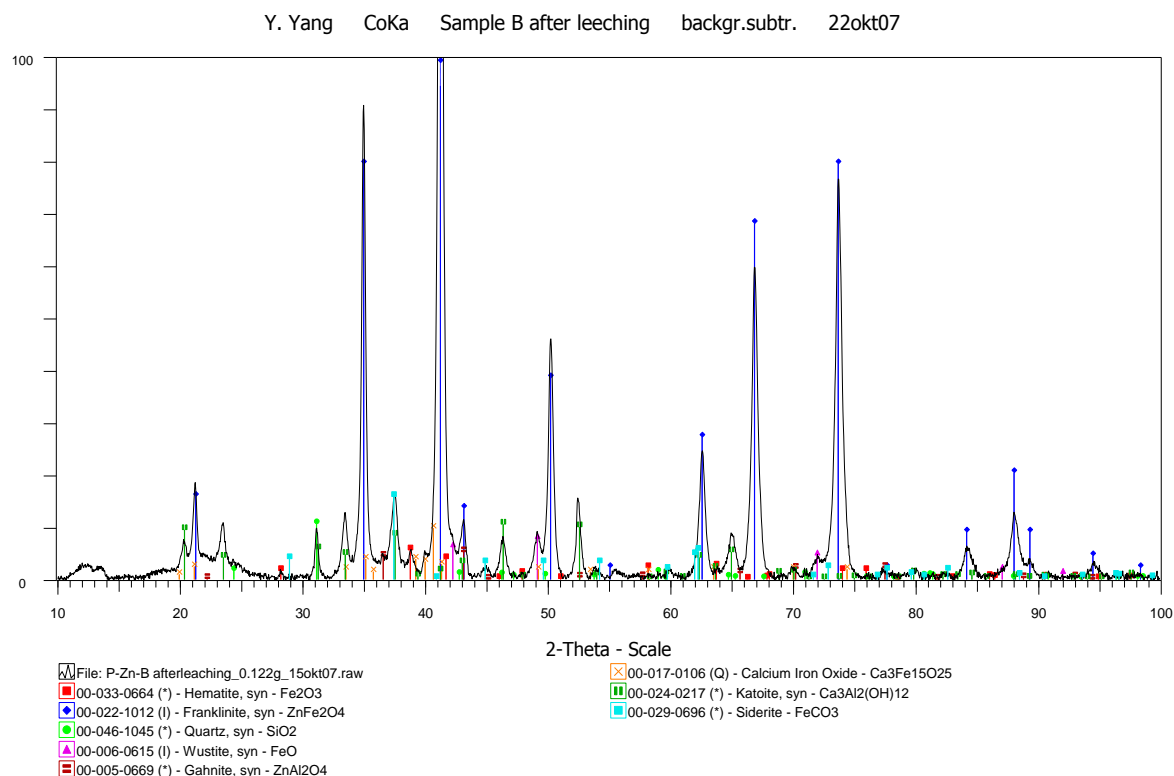


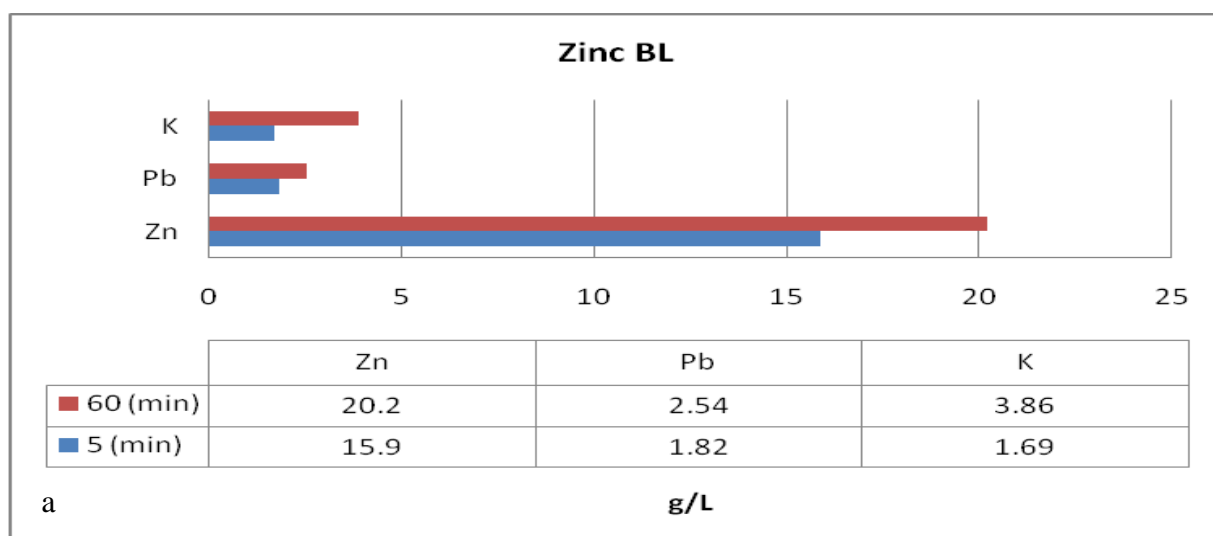
Figure 41. XRPD analysis of residue of leached Zinc BLD (10M NaOH, ~55°C, 3h, L:S 10) [2]

Table 34. Phases identified by XRPD analysis of Zinc BL\* filter cake

Sample	Identified Phases (in order of intensity)
Zinc BL*	ZnFe <sub>2</sub> O <sub>4</sub> , Ca <sub>3</sub> Mn <sub>2</sub> (OH) <sub>12</sub>

Table 35. Phases identified by XRPD analysis of Zinc BLD filter cake

Sample	Identified Phases (in order of intensity)
Zinc BLD	ZnFe <sub>2</sub> O <sub>4</sub> , Fe <sub>2</sub> O <sub>3</sub> , FeO, SiO <sub>2</sub> , FeCO <sub>3</sub> , ZnAl <sub>2</sub> O <sub>4</sub> , Ca <sub>3</sub> Fe <sub>15</sub> O <sub>25</sub> , Ca <sub>3</sub> Al <sub>2</sub> (OH) <sub>12</sub>



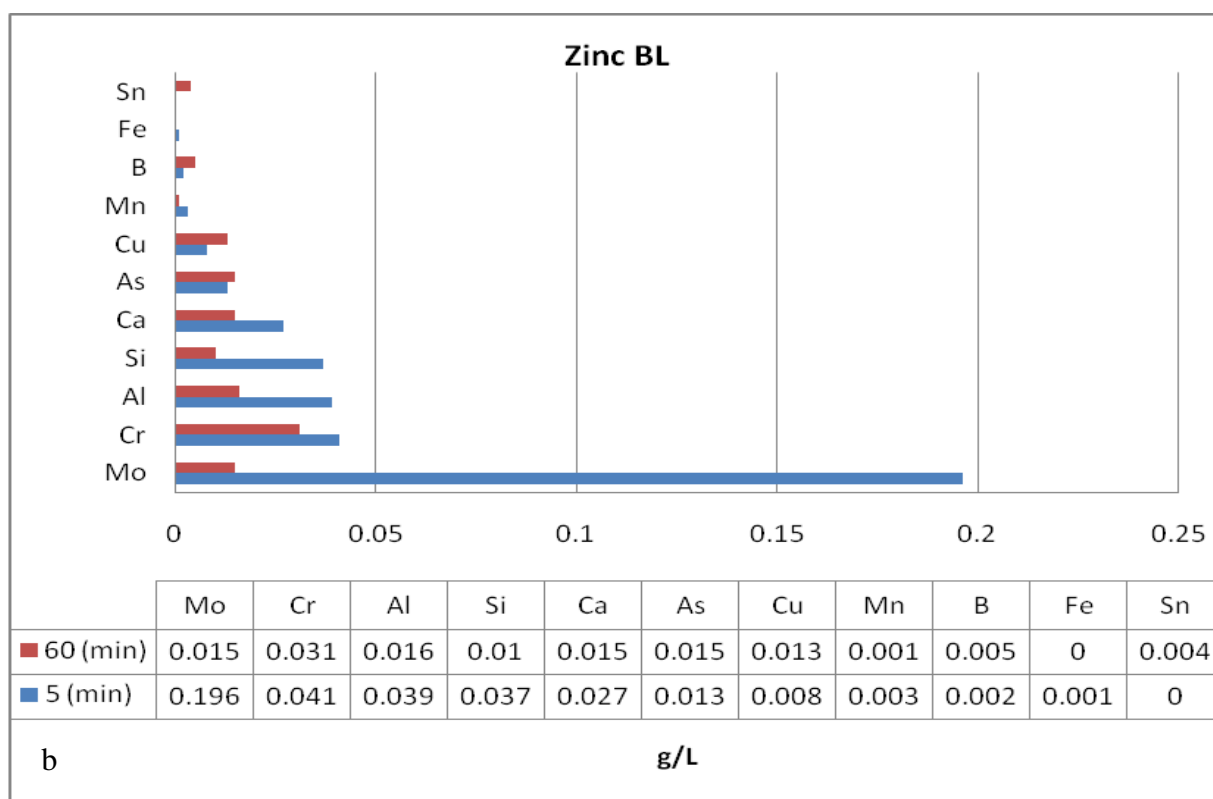


**Figure 42. Concentration of elements in Zinc BL filtrate after 5 and 60 minutes of leaching**

In conclusion, 66% of zinc from Zinc AWW and 57% of Zinc B was dissolved and recovered. Although no zinc oxide compounds were detected in XRPD analysis, zinc was probably present in soluble amorphous form ( Figure 12 and Figure 16). Recovery of lead was much higher for leached Zinc B (Zinc BL) with 70% than for Zinc AL with 46%. Cu recovery was low for Zinc AL and negligible for Zinc BL. Iron concentrations during both leaching experiments remained very low. These experiments prove that through a simple alkaline leaching step over 60% of the zinc can be recovered without considerable iron dissolution.

As seen in leaching experiments from synthetic zinc ferrite, dissolution of soluble zinc compounds was very fast. It is therefore recommended that the retention time can be reduced. Additionally, filtration at high temperatures will reduce the formation of precipitates and decrease the viscosity of the leachate, thereby enhancing overall filtration efficiency.

## 5.4 Roasting

The aim of roasting, was to convert zinc ferrites into zinc oxides. From roasting experiments on synthetic zinc ferrite  $\text{Na}_2\text{CO}_3$  was chosen as reagent. Roasting was done for 2 hours at  $950^\circ\text{C}$ .

### 5.4.1 Roasting of water washed and leached Zinc A

XRPD analyses of calcined product of water washed and leached Zinc A (Zinc AR) showed that not all zinc ferrites were converted (Figure 43 and Table 36). Magnetite was the dominant phase followed by zinc ferrite, however as mentioned before these minerals overlap. It was expected that  $\text{ZnO}$  and  $\text{NaFeO}_2$  were formed.

Reactions 25-27 showed that large quantities of  $\text{Na}_2\text{CO}_3$  were needed to convert not only zinc ferrite but also hematite and magnetite. Assuming that zinc was only present as zinc

ferrites and residual iron as magnetite or hematite, stoichiometric addition of  $\text{Na}_2\text{CO}_3$  was calculated from XRF analyses of Zinc AL (Appendix IX). A weight ratio of Zinc AL to  $\text{Na}_2\text{CO}_3$  of 1:0.54 resulted in a stoichiometric addition of 2.6.

After roasting, an average weight loss of 11.45% was detected. Assuming the weightloss was only caused by loss of  $\text{CO}_2$ , the stoichiometric requirement was 2.02.

Roasting of Zinc A with  $\text{Na}_2\text{CO}_3$  resulted in a sintered very porous product, adhered strongly to the crucible and was difficult to remove (Figure 44). Furthermore a fibrous mineral on the surface was formed, which changed color from yellow to white during cooling in air.

Formation or presence of FeO could indicates that a reducing environment was present during roasting due to formation of carbon dioxide. Formation of  $\text{Na}_2\text{Fe}(\text{SO}_4)_2$  probably arises from reaction with residual  $\text{S}_x$ , although most  $\text{S}_x$  was dissolved during the first leaching step. From roasting experiments on synthetic zinc ferrite it was expected that  $\text{NaFeO}_2$  should be the major phase present. Thus, presence of zinc ferrite and magnetite imply that insufficient  $\text{Na}_2\text{CO}_3$  was added.

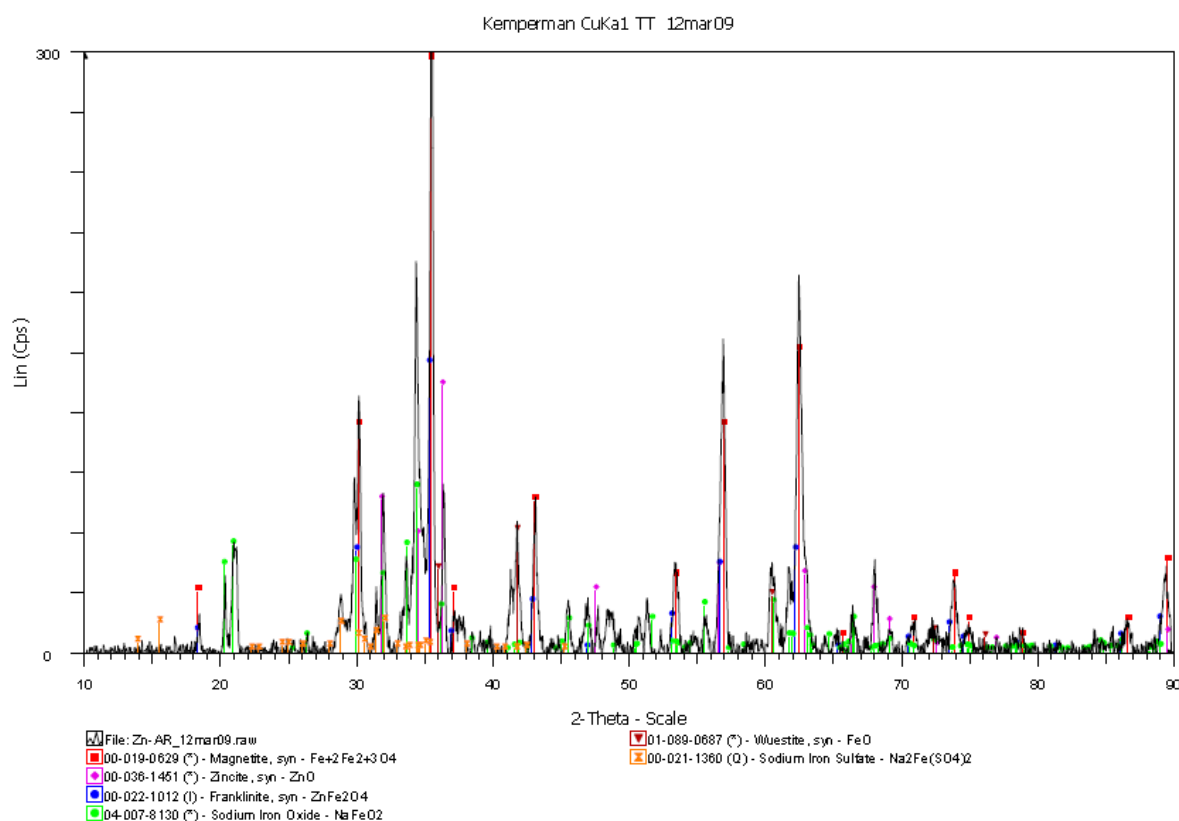


Figure 43. XRPD analysis of Zinc AR

Table 36. Phases identified by XRPD analysis of Zinc AR

Sample	Identified Phases (in order of intensity)
Zinc AR	$\text{Fe}_3\text{O}_4$ , $\text{ZnFe}_2\text{O}_4$ , $\text{ZnO}$ , $\text{NaFeO}_2$ , $\text{FeO}$ , $\text{Na}_2\text{Fe}(\text{SO}_4)_2$



**Figure 44. Roasting products of water washed and leached Zinc A (left; hot, right; cold)**

### **Mass balance implications**

Upon addition of  $\text{Na}_2\text{CO}_3$  it was expected that absolute weight of Na increased. Comparing the absolute weight before and after roasting resulted in a positive absolute weight difference (Table 37). The very large increase of Na measured by XRF cannot be explained. Calculation of total Na ( $\text{Na}_T$ ) after roasting should yield 22.7 wt%, taking into account residual Na concentration after leaching, and the addition of  $\text{Na}_2\text{CO}_3$ , and the weight loss during roasting. Compare this with 37.94 wt% from XRF analyses of Zinc ARL, a very large discrepancy becomes evident.

During roasting a large tray of stainless steel was used because large quantities needed to be processed. However, the mixture of Zinc AL and  $\text{Na}_2\text{CO}_3$  appeared to be highly corrosive (Figure 45). Stainless steel is made of Fe, Cr, and Ni. This explains the positive weight differences found for these elements (Table 37). Furthermore, corrosion of the crucible also reduces availability of  $\text{Na}_2\text{CO}_3$  for conversion of zinc ferrites. In future experiments it is recommended that a nickel tray (99%) must be used.

Mass balance calculations of the roasting step showed mostly negative and some positive differences in absolute weight, for more detailed information see Appendix XIV. Such inconsistencies show that large errors are involved when analyses only depend on one sample. Additionally, the matrix of the sample can also have a profound effect on analysis. When a powder is compressed the finer minerals concentrate at the surface and could cause overestimations of this mineral. Furthermore, line overlapping and overestimation of certain elements can occur e.g. between sodium  $\text{K}\alpha$  and zinc  $\text{L}\beta_2$  (L2-M4). Overestimation of zinc could have caused the missing zinc found during comparison of XRF and ICP analyses from leaching experiments (section 5.3.1, mass balance implication).

**Table 37. Analysis of filter cake Zinc AL, calcine product Zinc AR and absolute weight difference**

<b>Element</b>	<b>Zinc AL (wt%)</b>	<b>Zinc AR (wt%)</b>	<b>Absolute weight difference (g)</b>
<b>Cr</b>	0.30	0.60	5.35
<b>Fe</b>	22.18	20.80	63.99
<b>Na</b>	10.39	37.94	181.03
<b>Ni</b>	0.09	0.23	2.19





**Figure 45. Corrosion effect of tray after roasting Zinc A with  $\text{Na}_2\text{CO}_3$ .**

#### **5.4.2 Roasting of leached Zinc B**

XRPD analyses showed that  $\text{NaFeO}_2$  was the dominant phase present. Similar to Zinc AR, zinc ferrite and magnetite were still present in leached and roasted Zinc B (Zinc BR). In contrast to Zinc AL, Zinc BL had higher iron and lower zinc content. A higher weight ratio addition of Zinc BL and  $\text{Na}_2\text{CO}_3$  of 1:0.69 finally resulted in a stoichiometric addition of 2.1. After roasting the average weight loss was 10.27%, Assuming the weightloss was only caused by loss of  $\text{CO}_2$ , the stoichiometric requirement was 1.3.

Zinc BR showed similar properties as synthetic zinc ferrite. It became sintered, very porous and darker of color (Figure 47). It was easily removed and did not adhere to the crucible.

Similar results were seen for Zinc BR regarding absolute weight increase for Na, Ni, Fe and Cr (Table 39). Mg, Sn, and Al also increased, whereas for the rest a negative absolute weight difference was calculated. For more detailed information see Appendix XIV.

The incomplete conversion of zinc ferrites could be an indication for insufficient addition of  $\text{Na}_2\text{CO}_3$ .

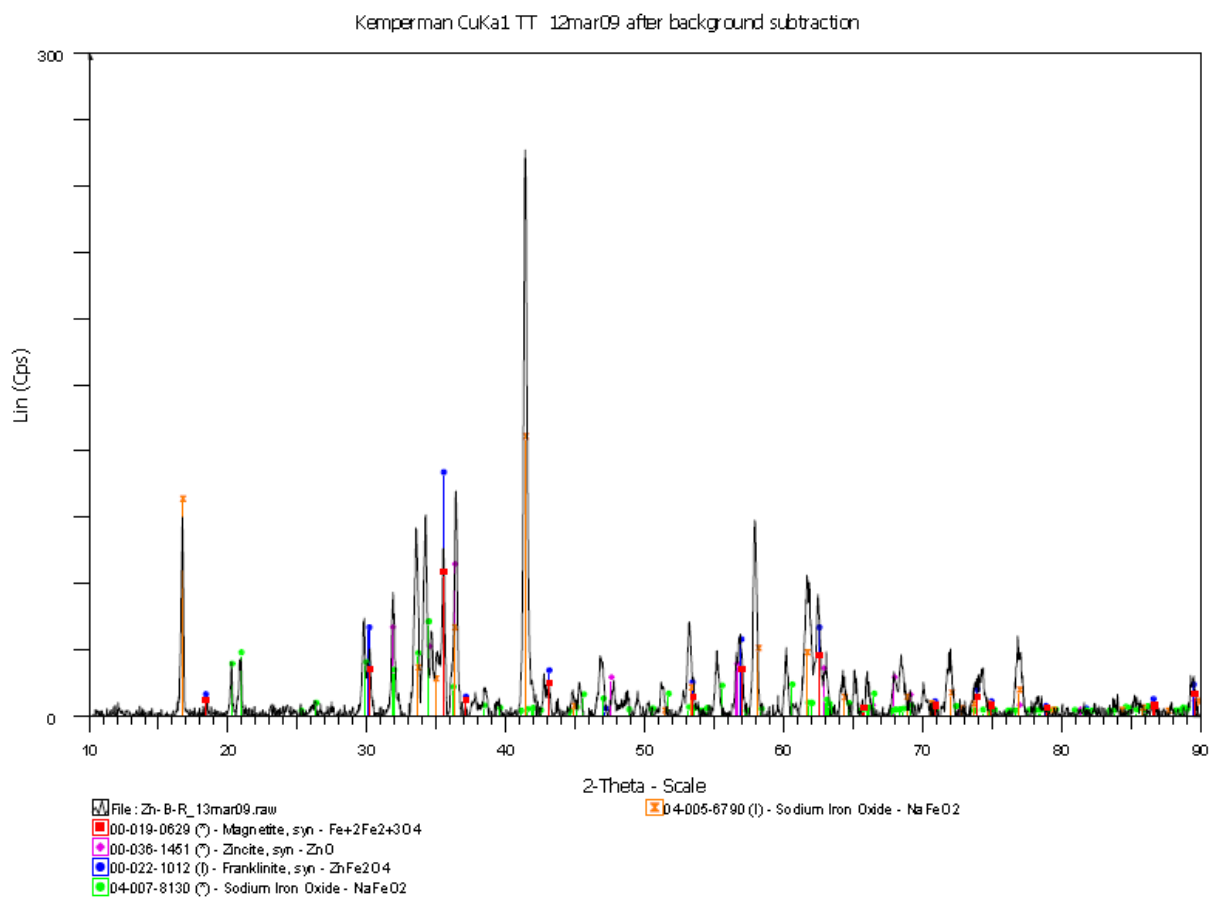


Figure 46. XRPD analysis of Zinc BR

Table 38. Phases identified by XRPD analysis of Zinc BR

Sample	Identified Phases (in order of intensity)
Zinc BR	$\text{NaFeO}_2$ , $\text{ZnFe}_2\text{O}_4$ , $\text{ZnO}$ , $\text{Fe}_3\text{O}_4$



Figure 47. Roasting products of Zinc BR

**Table 39. Analysis of filter cake Zinc BL, calcine product Zinc BR and absolute weight difference**

<b>Element</b>	<b>Zinc BL (wt%)</b>	<b>Zinc BR (wt%)</b>	<b>Absolute weight difference (g)</b>
<b>Cr</b>	0.33	0.52	5.80
<b>Fe</b>	33.89	25.75	64.91
<b>Na</b>	5.67	30.52	135.24
<b>Ni</b>	0.02	0.05	0.62

### 5.4.3 Additional roasting experiments

Because XRPD analysis of Zinc AR and Zinc BR implied that the conversion of zinc ferrites was incomplete and contamination of Ni and Cr was seen, another experiment was set up. By increasing the stoichiometric additions of  $\text{Na}_2\text{CO}_3$  in the roasting test, complete conversion of zinc ferrite was intended. The samples obtained from these experiments were denoted with the star (\*) symbol.

To increase the conversion of zinc ferrites into zinc oxides the stoichiometric  $\text{Na}_2\text{CO}_3$  addition for zinc AL\* and Zinc BL\* was increased to 3.6 and 3.1 respectively. Preceding process steps used the same operating conditions as before to isolate the effect of additional reagent addition.

#### **Water washing of Zinc A\* (Zinc AWW\*)**

Zinc A\* comes from the same sampling poule and therefore XRF results from Zinc A and obtained during water washing of Zinc A are superimposed. For the water washing step a weight loss of 19.2% was found.

#### **Leaching of Zinc AWW\* and Zinc B\* (Zinc AL\* and Zinc BL\*)**

Dissolution during leaching of Zinc AWW\* was accountable for a total weight loss of 19.8% with zinc as major contributor. The chemical composition of water washed and leached Zinc A (Zinc AL\*) was higher in Fe, Zn, Pb and Si and lower in Al and probably caused due to reduced presence of oxides in the sample (Table 40).

Using Zinc A\* and superimposing water washing results as a reference seems therefore incorrect for mass balance calculation, although the sample originates from the same sampling pool. These differences in chemical compositions show that, even within the same sampling pool, large chemical variations exist or large analytical faults can be made.

**Table 40. Recovery of water washed and leached Zinc A\* using XRF analysis of Zinc AWW and filter cake Zinc AL\***

<b>Element</b>	<b>Zinc AWW (wt%)</b>	<b>Zinc AL* (wt%)</b>	<b>Recovery (%)</b>
<b>Al</b>	1.05	0.55	57.99
<b>Mg</b>	0.11	0.88	-523.22
<b>Pb</b>	4.29	3.75	29.89
<b>Si</b>	0.81	3.40	-237.52
<b>Zn</b>	23.70	13.10	55.66

Overall dissolution of Zinc B during leaching accounted for a total weight loss of 8.01%, with zinc and lead as major contributors. Zinc BL\* showed a large increase in presence of Fe, Zn, Si, Mg, Ca, Mn, and Al and caused by reduced presence of oxides in the sample. No

significant decrease was detected (Table 41, Appendix XII and XIII). Recoveries obtained by XRF analyses for the first leaching step for both zinc AL\* and BL\* showed similar trends as observed for Zinc AL, BL with exception for the elements mentioned above.

**Table 41. Recovery of water washed and leached Zinc B\* using XRF analysis of Zinc B and filter cake Zinc BL\***

Element	Zinc B (wt%)	Zinc BL* (wt%)	Recovery (%)
<b>Al</b>	0.13	0.62	-357.24
<b>Mg</b>	0.53	2.21	-286.81
<b>Pb</b>	1.98	0.82	61.90
<b>Si</b>	0.51	1.90	-239.67
<b>Zn</b>	18.14	10.47	46.96

#### ***Roasting of Zinc AL\* and Zinc BL\* (Zinc AR\* and Zinc BR\*)***

Water washed and leached Zinc A (Zinc AR\*) was roasted in alumina trays and leached Zinc B (Zinc BR\*) in alumina crucibles. As in earlier experiments Zinc AR\* showed adhesive characteristics to the crucibles and was difficult to remove. Zinc BR\* was easily removed due to shrinkage of the sample and no adhesive characteristics.

The increased concentrations of Al and Si were reflected in XRPD analysis. This was shown by inclusions of these metals in  $\text{NaFeO}_2$  and presence of other phases such as,  $\text{Al}_3\text{Fe}_5\text{O}_{12}$  and  $\text{Ca}_{2.93}\text{Al}_{1.97}\text{Si}_{0.64}\text{O}_{2.56}(\text{OH})_{9.44}$  (Figure 48 and Figure 49). Zinc ferrite remained the dominant phase in both samples and implied incomplete conversion. Zinc oxide was not detected in Zinc AR\* or showed poor intensities in Zinc BR\*. This indicates that increasing the stoichiometric addition of  $\text{Na}_2\text{CO}_3$  does not necessarily increase the conversion of zinc ferrite.

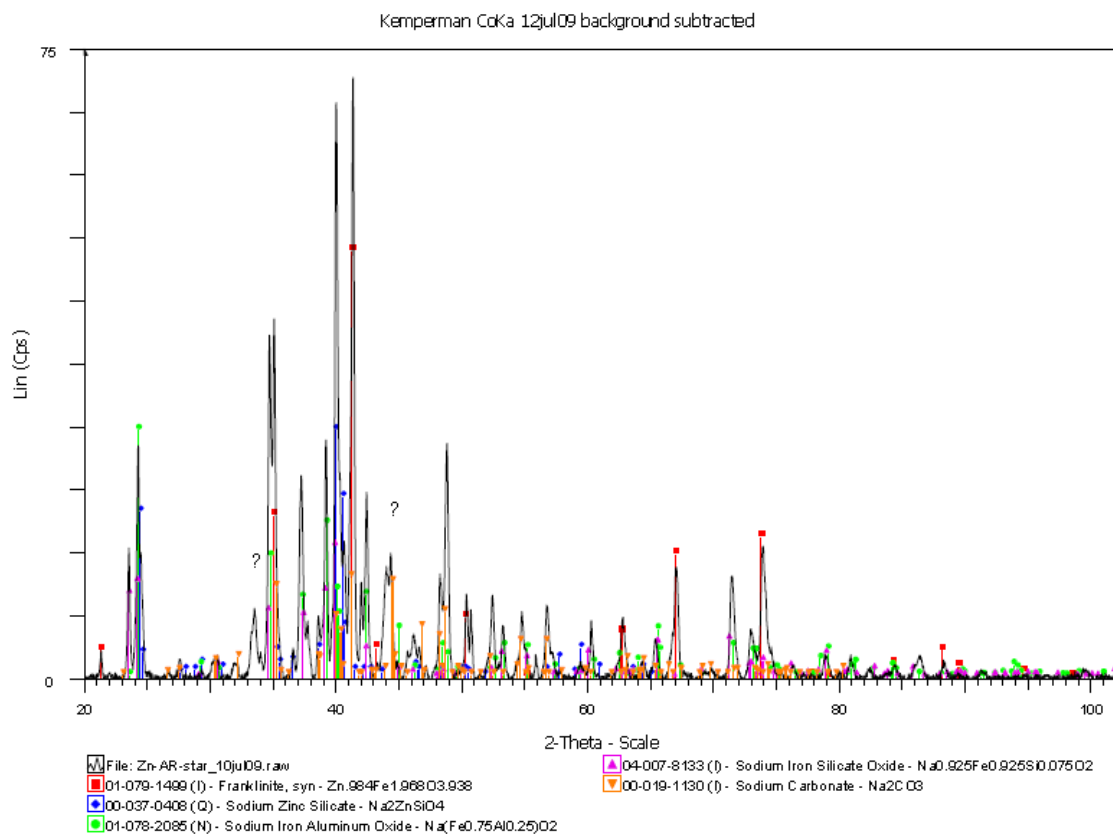


Figure 48. XRPD analyses of Zinc AR\*

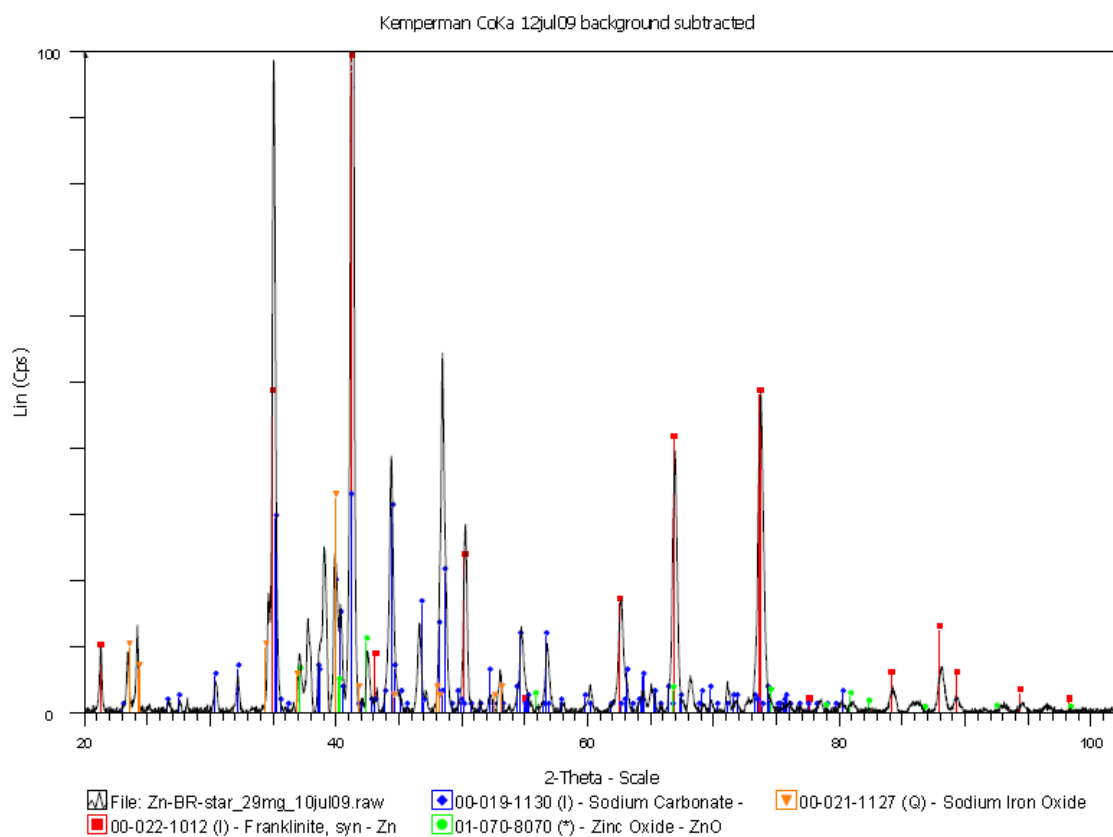


Figure 49. XRPD analyses of Zinc BR\*



**Table 42. Phases identified by XRPD analysis of Zinc AR\***

Sample	Identified Phases (in order of intensity)
Zinc AR*	$\text{ZnFe}_2\text{O}_4$ , $\text{Na}_2\text{ZnSiO}_4$ , $\text{Na}(\text{Fe}_{0.75}\text{Al}_{0.25})\text{O}_2$ , $\text{Na}_{0.925}\text{Fe}_{0.925}\text{Si}_{0.075}\text{O}_2$ , $\text{Na}_2\text{CO}_3$

**Table 43. Phases identified by XRPD analysis of Zinc AR\***

Sample	Identified Phases (in order of intensity)
Zinc BR*	$(\text{Fe}_{0.4}\text{Zn}_{0.6})(\text{Fe}_{1.6}\text{Ni}_{0.2}\text{Mg}_{0.2})\text{O}_4$ , $\text{FeO}$ , $\text{Al}_3\text{Fe}_5\text{O}_{12}$ , $\text{Ca}_{2.93}\text{Al}_{1.97}\text{Si}_{0.64}\text{O}_{2.56}(\text{OH})_{9.44}$ , $\text{Na}_2\text{CO}_3$

### **Technical and mass balance implications**

In earlier experiments the use of a stainless steel crucible resulted in contaminations of Cr, Ni, and Fe. Therefore in these experiments alumina crucibles were used. The excessive additions of  $\text{Na}_2\text{CO}_3$  resulted in violent reactions and for most experiments in loss of material due to spillages (Figure 50). Unknown was what caused the green color seen on the surface of the crucibles and spillages. The weightloss is thus not representative for stoichiometric requirements. In addition to above mentioned losses, repetitive use of crucibles caused cracking and resulted in additional loss of material due to oozing through the cracks.



**Figure 50. Roasting samples of Zinc AR\* and Zinc BR\***

In conclusion, roasting of Zinc AL and Zinc BL showed that zinc ferrites were partially converted into zinc oxides and sodium iron oxides, thereby proving the technical feasibility. Overestimation of Zn and Na in XRF samples could be caused by overlapping signals. In additional roasting experiments with increased stoichiometric addition of  $\text{Na}_2\text{CO}_3$  the conversion reaction became more violent and did not necessarily increase the conversion of zinc ferrite. The inconsistency of the results show that more research is necessary. Therefore, it is recommended that a more thorough investigation on optimal roasting conditions for Zinc AL and Zinc BL should be conducted.

## **5.5 Secondary leaching step**

The aim of the secondary leaching step was to selectively dissolve zinc and other heavy metals from Zinc AR and Zinc BR.

The operating conditions were similar to the once used in the first leaching step. In the roasting step zinc ferrites were partially converted to zinc oxides and sodium iron oxides. According to leaching experiments on synthetic zinc ferrite, zinc oxides were readily dissolved when leached in 10M NaOH. The dissolution of zinc, and thus the recovery, was therefore a measurement for the conversion ratio of zinc ferrites.

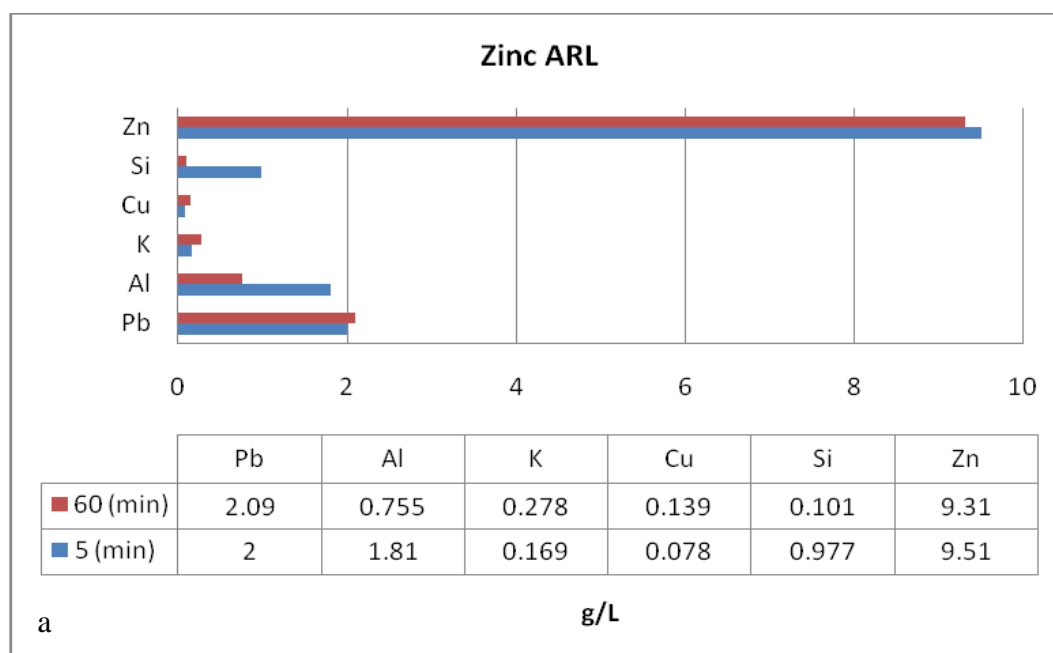
### 5.5.1 Leaching of water washed, leached and roasted Zinc A

The recovery of water washed, leached and roasted Zinc A (Zinc ARL) was 48% and reached a concentration 9.31 g/L in the filtrate (Table 44). Recoveries of Na and Pb were 67% and 34% respectively. Dissolution during the leaching test was accountable for a total weight loss of 38.37%. Approximately 81% of this loss was subscribed to dissolution of Na from NaFeO<sub>2</sub>, remainder was mostly attributed by dissolution of Zn, Pb, and Cl. However, Zinc ARL still had high concentrations of Zn, Pb and Na. Roasting of Zinc AL changed insoluble P<sub>x</sub> compounds into soluble compounds. High recoveries were seen for Cl, K and especially P<sub>x</sub> with 89%, 91% and 89% respectively. For more detailed information on other elements please be referred to Appendix X.

The zinc oxides formed after roasting dissolved within the first 5 minutes (Figure 51a). The high residual zinc concentration in Zinc ARL confirmed that not all zinc was leached or otherwise converted into soluble zinc oxides. Other elements showed the same trend as observed during leaching experiments, which were decreasing concentrations over time (Figure 47b).

**Table 44. Analysis of the filtrate, filter cake and recovery of Zinc ARL**

Element	Zinc ARL (g/L)	Zinc AR (wt%)	Zinc ARL (wt%)	Recovery (%)
Al	-	0.59	1.56	-62.67
Cl	-	0.51	0.09	89.28
Na	-	37.94	20.03	67.46
K	0.278	0.12	0.02	90.89
Pb	2.09	2.25	2.42	33.72
Px	-	0.18	0.03	88.98
Zn	9.31	8.54	7.23	47.83



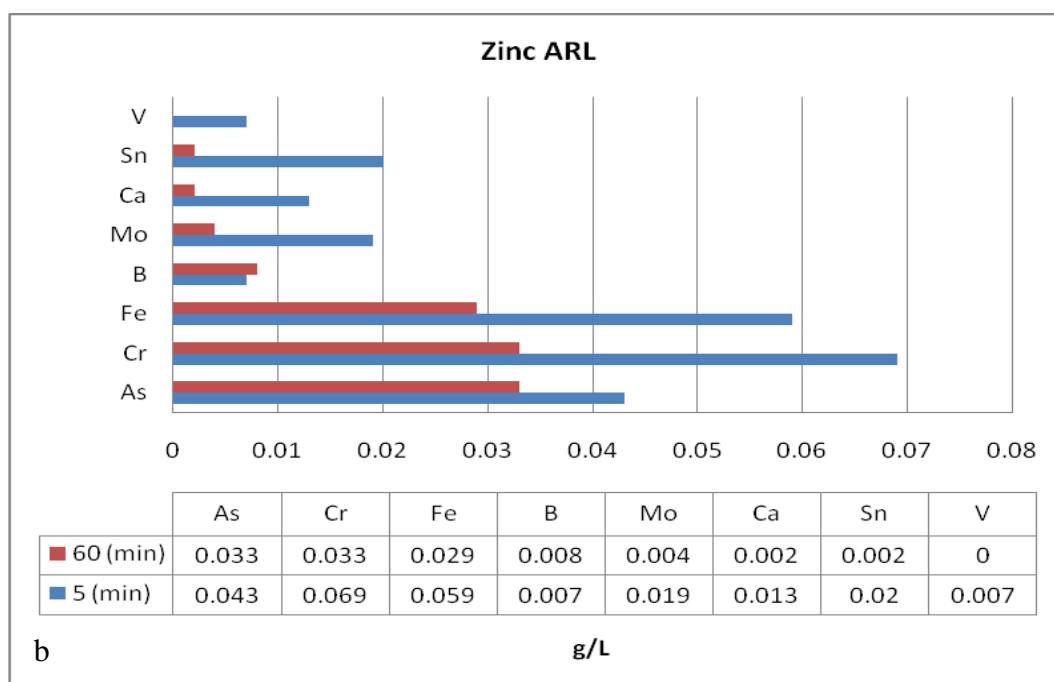


**Figure 51. Concentration of elements in Zinc ARL filtrate after 5 and 60 minutes of leaching**

### 5.5.2 Leaching of leached and roasted Zinc B

Leaching of leached and roasted Zinc B (Zinc BRL) showed many similarities with Zinc ARL regarding recoveries of Zn, K, and Cl (Table 45). The recoveries of Na and Pb were 60% and 25% respectively. In contrast to Zinc ARL, dissolution of Zinc BR was only accountable for a total weight loss of 27.03%. Dissolution of Na was the major cause, followed by Zn and Cr. Striking was the high recovery of Cr and concentration, with 87% and 0.996 g/L. The presence of soluble Cr compounds was due to contaminations of the crucible. ICP analyses of Zinc BRL showed that most elements remained steady during leaching. (Figure 52a and b).

**Table 45. Analysis of the filtrate, filter cake and recovery of Zinc BRL**

Element	Zinc BRL (g/L)	Zinc BR (wt%)	Zinc BRL (wt%)	Recovery (%)
Cl	-	0.06	0.01	88.79
Cr	0.996	0.52	0.09	87.02
K	-	0.08	0.01	87.02
Na	-	30.52	16.67	60.14
Pb	0.149	0.49	0.50	25.25
Px	-	0.07	0.03	68.12
Zn	6.62	6.51	4.10	54.04



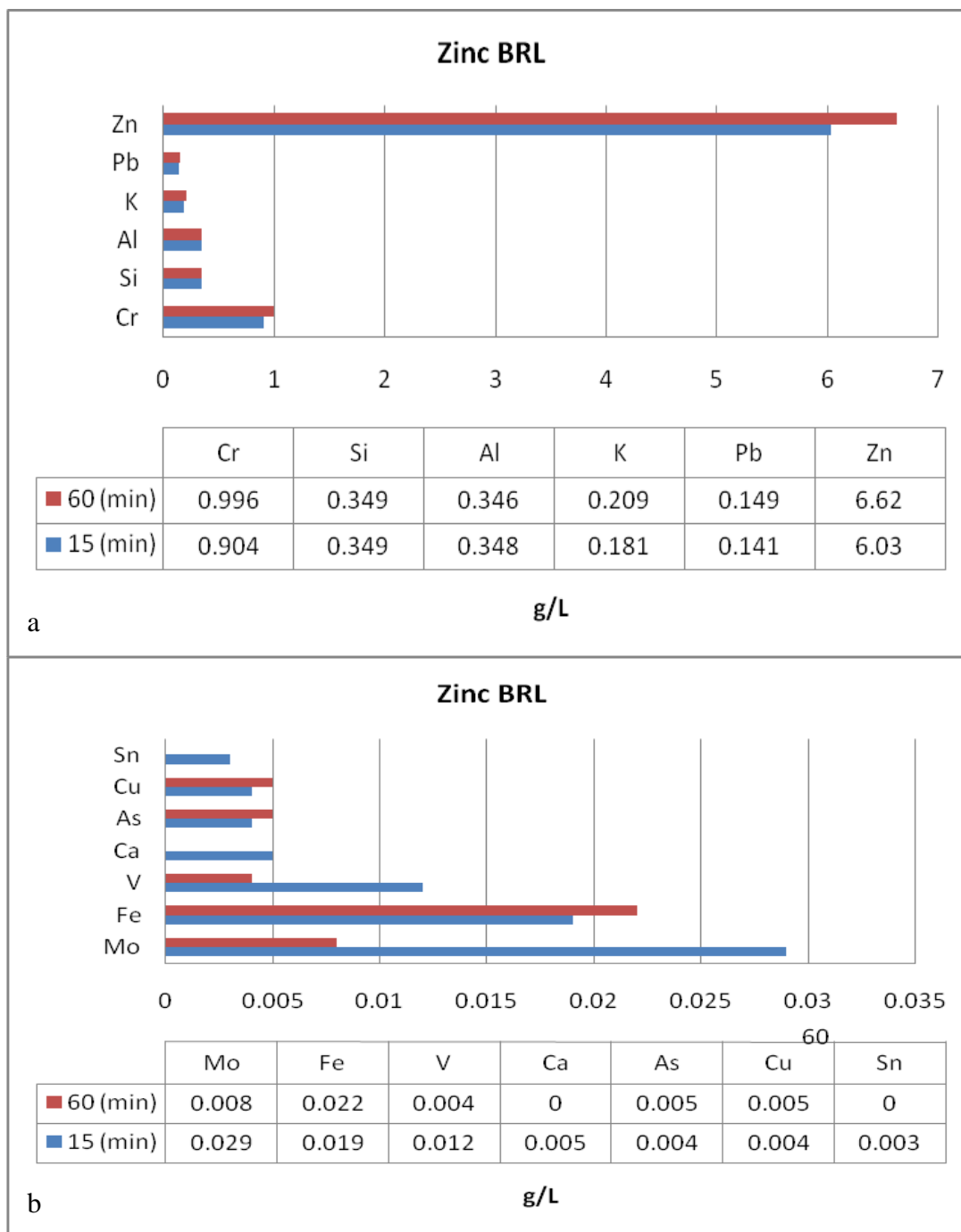


**Figure 52. Concentration of elements in Zinc BRL filtrate after 15 and 60 minutes of leaching.**

### 5.5.3 Leaching of water washed, leached and roasted Zinc A\* and Zinc B\*

To both Zinc AR\* and Zinc BR\* higher additions of  $\text{Na}_2\text{CO}_3$  during roasting resulted in higher weight losses during leaching, 50.09% and 46.59% respectively.

Although not detected by XRPD, soluble zinc oxides probably in amorphous form were present in both Zinc AR\* and Zinc BR\*. The recovery of Zn from Zinc AR\* compared to Zinc AR increased from 48% to 53%, and decreased for lead from 34% to 17% (Table 44 and Table 46). Zinc BR\* showed a large decrease in recovery for zinc from 54% to 4%, and for lead a large increase of 25% to 41% (Table 45 and Table 47). The large decrease in zinc recovery was unexpected. A higher conversion of zinc ferrite to zinc oxides was expected,

hence a higher recovery. Zinc ferrite remained present as dominant phase in both Zinc ARL\* and Zinc BRL\*(Figure 53 and Figure 54, Table 48 and Table 49). Furthermore, residual fractions of excess  $\text{Na}_2\text{CO}_3$  were detected. Apparently  $\text{Na}_2\text{CO}_3$  did not dissolve completely in strong alkaline solutions.

**Table 46. Analysis of filtrate, filter cake and recovery of Zinc ARL\***

Element	Zinc AR* (wt%)	Zinc ARL* (wt%)	Recovery (%)
Al	0.78	2.05	-30.67
Cl	0.17	0.05	86.47
Fe	9.65	22.20	-14.81
Na	17.90	12.08	66.32
Pb	1.07	1.79	16.51
Si	0.91	2.53	-38.76
Zn	4.38	4.13	52.94

**Table 47. Analysis of filtrate, filter cake and recovery of Zinc BRL\***

Element	Zinc BR* (wt%)	Zinc BRL* (wt%)	Recovery (%)
Al	0.15	0.25	7.18
Cl	0.09	0.00	100.00
Fe	13.96	27.28	-4.37
Na	19.50	8.26	77.34
Pb	0.25	0.28	40.56
Si	0.45	0.78	7.57
Zn	3.29	5.93	3.74

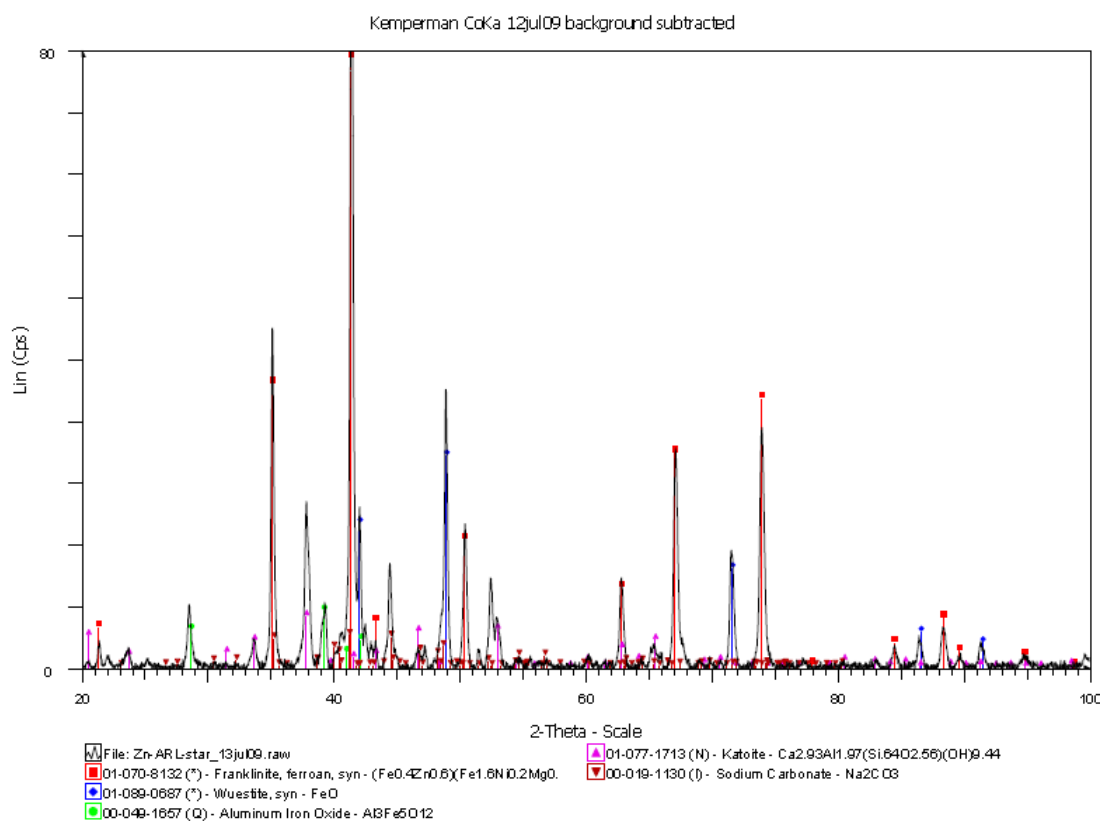


**Figure 53. XRPD analyses of Zinc ARL\***

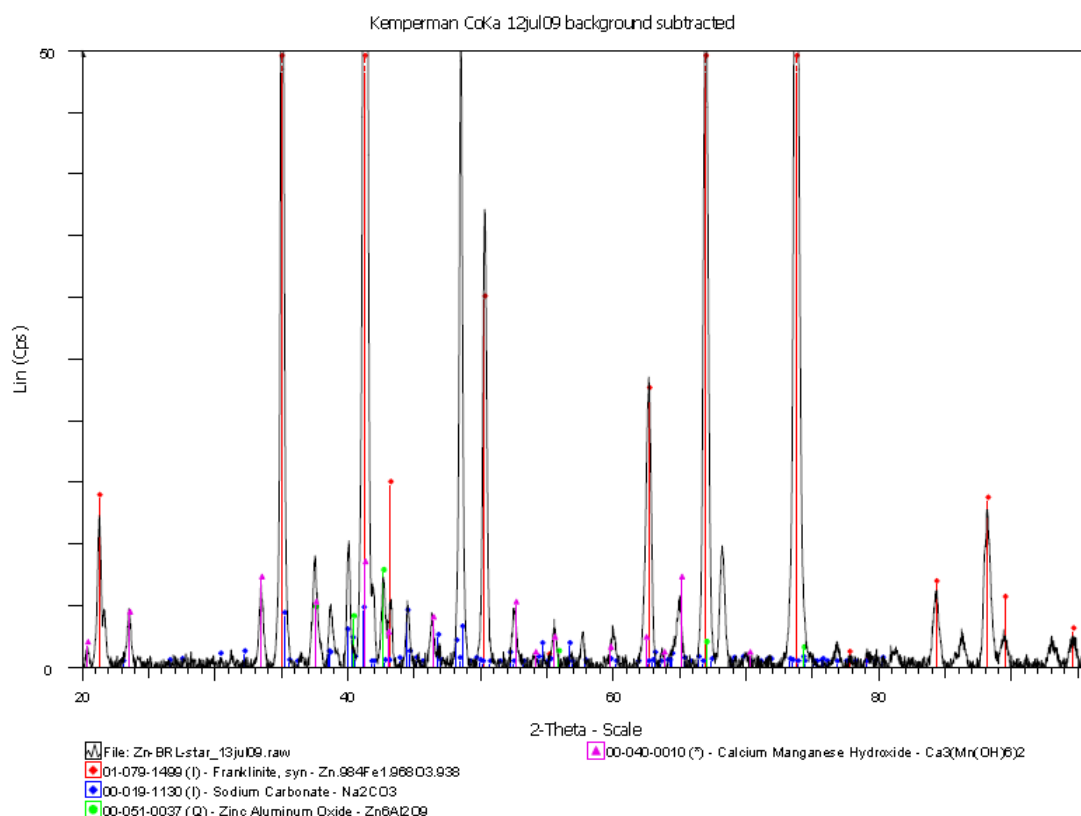


**Figure 54. XRPD analyses of Zinc BRL\***

**Table 48. Phases identified by XRPD analysis of Zinc ARL\***

Sample	Identified Phases (in order of intensity)
Zinc ARL*	(Fe <sub>0.4</sub> Zn <sub>0.6</sub> )(Fe <sub>1.6</sub> Ni <sub>0.2</sub> Mg <sub>0.2</sub> )O <sub>4</sub> , FeO, Al <sub>3</sub> Fe <sub>5</sub> O <sub>12</sub> , Ca <sub>2.93</sub> Al <sub>1.97</sub> (Si <sub>1.64</sub> O <sub>2.56</sub> )(OH) <sub>9.44</sub> , Na <sub>2</sub> CO <sub>3</sub>

**Table 49. Phases identified by XRPD analysis of Zinc BRL\***

Sample	Identified Phases (in order of intensity)
Zinc BRL*	ZnFe <sub>2</sub> O <sub>4</sub> , Na <sub>2</sub> CO <sub>3</sub> , Zn <sub>6</sub> Al <sub>2</sub> O <sub>9</sub> , Ca <sub>3</sub> (Mn(OH) <sub>6</sub> ) <sub>2</sub>

For both Zinc A\* and Zinc B\* batches residual contents of Mg and Si were much higher than in earlier experiments. Zinc recovery can be impeded by complex formation with Si and Al. The increase of these elements could have been one of the causes why the recovery was unexpectedly low. Detection of Zn<sub>6</sub>Al<sub>2</sub>O<sub>9</sub> confirms that presence of aluminum impede zinc dissolution and thus recovery. For more detailed information on dissolution and recovery see Appendix XII and XIII.

In conclusion, during roasting approximately 50% of the zinc ferrites are converted into soluble zinc compounds. This implies that without optimization of individual processing steps this innovative flowsheet is feasible to recover 81% of total zinc. Inconsistent results were obtained during additional roasting experiments, therefore more research is necessary to increase the conversion and to understand the underlying effects.

After roasting of synthetic zinc ferrite additional experiments showed that NaFeO<sub>2</sub> is very soluble. Dissolving NaFeO<sub>2</sub> in an additional water washing step would simultaneously

recover and remove residual Na as NaOH from the residue. So, in addition to the process steps from proposed flowsheet, another water washing step would be useful to remove and recover NaOH and obtain a useful residue for steelmaking industries.

## 5.6 Post water washing

The aim of post water washing was to recover Na as NaOH from Zinc ARL and Zinc BRL. This was achieved by using the same operating conditions which were applied during the first water washing step.

Sodium accounted over 8-20% of the total weight of the filter cake, after second leaching experiments (Table 44 - Table 47). Modeling of 1kmol dissolution of NaFeO<sub>2</sub> using Gibbs solver from HSC 6.1[28] showed that NaFeO<sub>2</sub> readily dissolved in water (Figure 55). Formation of goethite and hematite were favored according to thermodynamics. The Pourbaix diagram showed that favorable formation of goethite and hematite changed between 32 and 33 °C (Figure 56 a, b). From preliminary experiments it was shown that NaFeO<sub>2</sub> readily dissolved in water and that at 50°C hematite was the dominant precipitate formed (reaction 44).

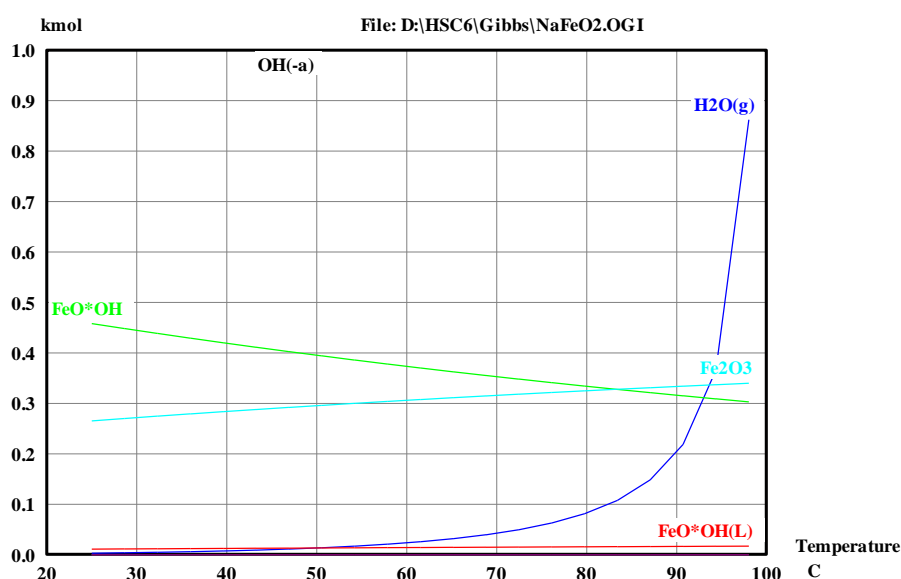


Figure 55. Equilibrium amount of products (1M NaFeO<sub>2</sub>/L) 25-100°C.

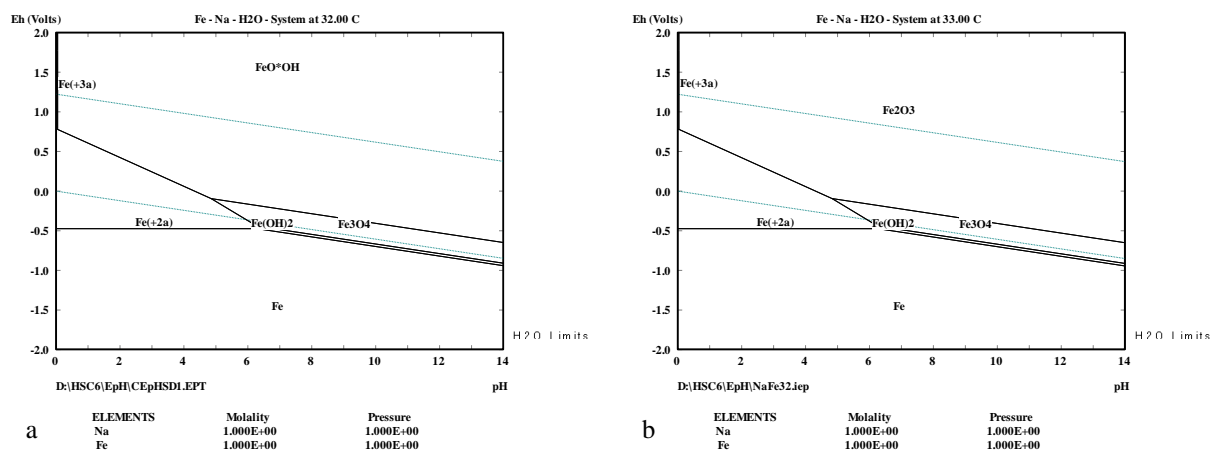


Figure 56. Eh pH diagram of Na-Fe-O-H at a) 32°C b) 33°C

### 5.6.1 Water washing of water washed, leached, roasted and leached Zinc A

The recoveries of Na, K and Cl were 62%, 100% and 36% respectively (Table 50). Dissolution was accountable for a total weight loss of 16.51%. Within 5 minutes the pH increased to 11.89 and the conductivity to 120mS/Cm. Both did not change over the remaining time. Dissolution of Na was almost solely responsible for the entire weight loss measured. However, ICP analyses showed that Zn, Pb, Al, and Cr dissolved to some extent (Table 50). Even at these low alkaline concentrations silica dissolved and achieved a concentration of 0.668 g/L (Table 50). For more detailed information on other elements see Appendix IX.

**The residue of water washing of water washed, leached, roasted and leached Zinc A (Zinc ARLWW) displayed strong intensities of zinc ferrites and FeO (Figure 57 and**

**Table 51).**

This presence confirmed the incomplete conversion of zinc ferrites and removal of residual  $\text{Na}_2\text{CO}_3$ .

Table 50. Analysis of filtrate, filter cake and recovery of Zinc ARLWW

Element	Zinc ARLWW (g/L)	Zinc ARL (wt%)	Zinc ARLWW (wt%)	Recovery (%)
Al	0.164	1.56	1.93	-3.29
Cl	-	0.09	0.07	35.68
Cr	0.153	1.02	1.09	10.78
Na	-	20.03	9.01	62.44
K	0.016	0.02	0.00	100.00
Si	0.668	1.80	2.26	-4.83
Pb	0.167	2.42	2.67	7.88
Zn	0.214	7.23	8.27	4.50

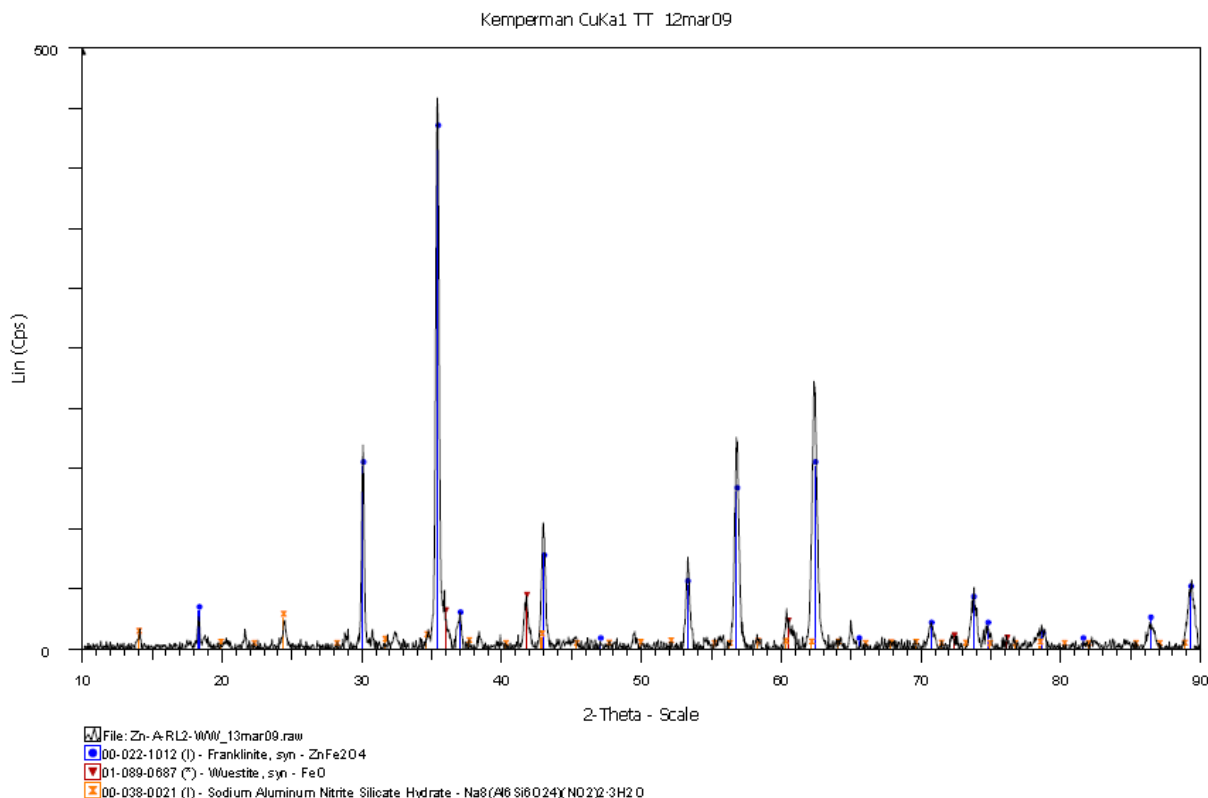


**Figure 57. XRPD analysis of Zinc ARLWW**

**Table 51 Phases identified by XRPD analysis of Zinc ARLWW**

Sample	Identified Phases (in order of intensity)
Zinc ARLWW	ZnFe <sub>2</sub> O <sub>4</sub> , FeO, Na <sub>8</sub> (Al <sub>6</sub> Si <sub>6</sub> O <sub>24</sub> )(NO <sub>2</sub> ) <sub>2</sub> ·3H <sub>2</sub> O

### 5.6.2 Water washing of leached, roasted and leached Zinc B

The recoveries of Na and Cl were 61% and 100 % respectively. In contrast to the conductivity of Zinc ARLWW, Zinc BRLWW increased from 101 mS/cm to 145 mS/cm over time. Zinc BRLWW had similar pH displayed strong intensities for zinc ferrites, magnetite and calcium manganese hydroxides (Figure 58 and Table 53). The metals Zn, Si, Cr and Al dissolved to some extent (Table 52). Worth mentioning was that Cr showed a recovery of 41%. This was quite high in comparison with zinc ARL-WW of which only 11% was dissolved. For more detailed information see Appendix XI.

**Table 52. Analysis of filtrate, filter cake and recovery of Zinc BRLWW**

Element	Zinc ARLWW (g/L)	Zinc ARL (wt%)	Zinc ARLWW (wt%)	Recovery (%)
Al	0.057	0.09	0.11	-9.59
Cl	-	0.01	0.00	100.00
Cr	0.077	0.09	0.06	41.35
Na	-	16.67	7.61	60.91
K	0.011	0.01	0.01	38.57
Pb	0.015	0.50	0.60	-1.47
Si	0.157	0.43	0.62	-24.25
Zn	0.205	4.10	4.46	6.85

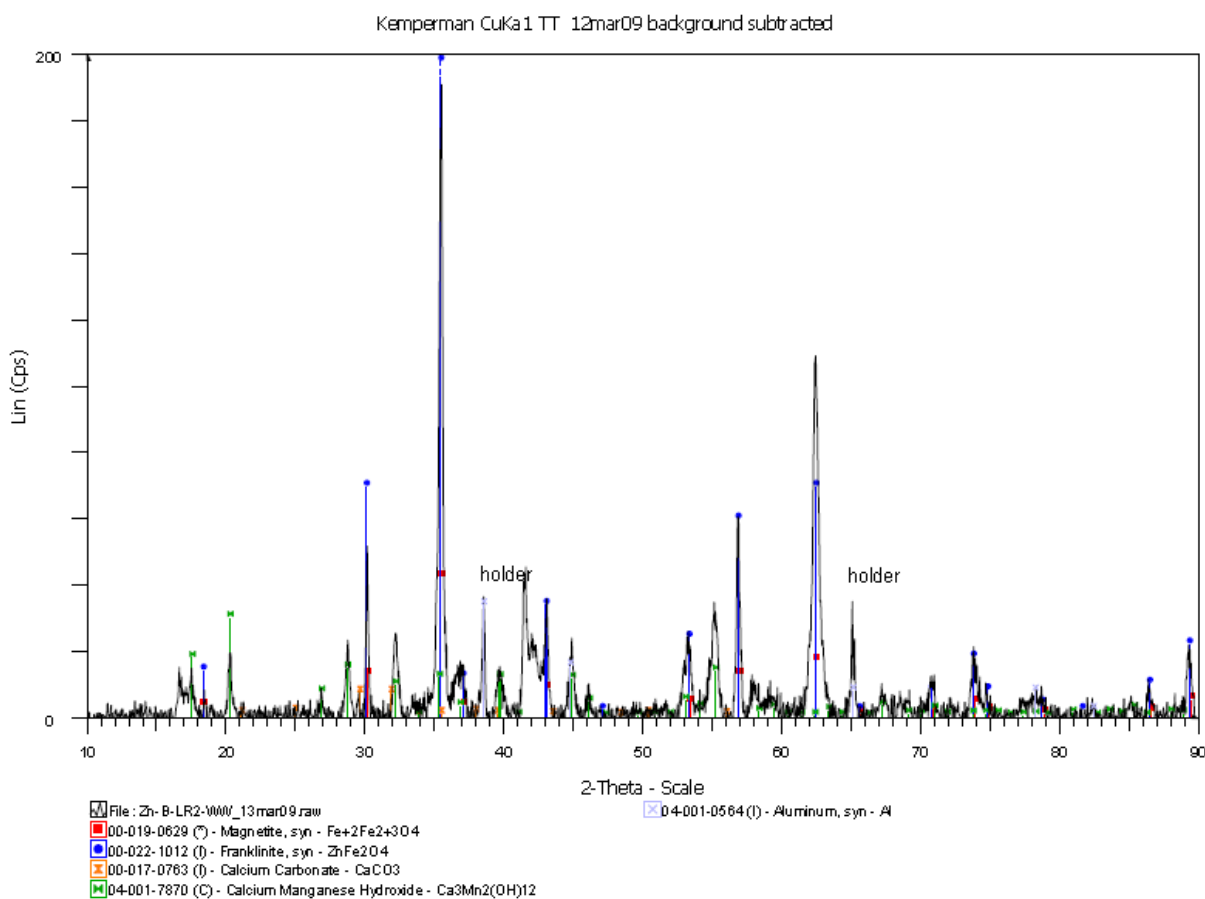


**Figure 58. XRPD analysis of Zinc BRLWW**

**Table 53. Phases identified by XRPD analysis of Zinc BRLWW**

Sample	Identified Phases (in order of intensity)
Zinc BRL-WW	ZnFe <sub>2</sub> O <sub>4</sub> , Fe <sub>+2</sub> Fe <sub>2+3</sub> O <sub>4</sub> , Ca <sub>3</sub> Mn <sub>2</sub> (OH) <sub>12</sub> , CaCO <sub>3</sub>

In conclusion, the recovery of sodium(hydroxide) was approximately 61%. According to XRF analyses the residues consisted of 8 to 9 wt% Na. Optimization of the post waterwashing test

is very important for closing the sodium(hydroxide) loop. To achieve a higher recovery similar recommendations apply which were mentioned for the first water washing step.

## **5.7 Residue**

The aim was to obtain a residue which could be used as aggregate in construction materials, serve as feeding stock for steel industries or be suitable for disposal. The final chemical composition of the residue was therefore of major importance. In Appendix XXV the intervention values are denoted and used for comparing the quality of the final residues.

### **5.7.1 Final residue of Zinc A**

The final residue of Zinc A remained high in zinc, lead, sodium and copper (Table 54 and Table 55). It was calculated that iron (hydr)oxides makes up 38 wt% of the final residue. Although most of the zinc, lead, sodium and copper was recovered the final residue of Zinc A had to high concentration of these elements to be used as an aggregate, feedstock or landfilled without additional treatment.

Assuming all zinc was present as zinc ferrite, and remaining iron as iron oxides. Iron ores used for the blast furnace usually range in the 60+% Fe, furthermore high concentrations of Na and K will cause problems during processing in blast furnaces, such as scaffolding. Furthermore processing residues with high concentrations of Zn and Pb, which end up in the off gasses and need scrubbing, cost additional energy. Therefore the residue was unsuitable as a feeding stock for steel industry.

Unfortunately it was not suitable as a building aggregate because it was too low in Ca, Al and Si which together must comprise more than 10 wt% of the total mass. For landfilling Zinc ARL-WW contains too high concentrations of Ba, Cr, Cu, Ni, Pb and Zn.

### **5.7.2 Final residue of Zinc B**

For Zinc BRLWW it was important to reduce the high Na concentration. The final residue of zinc B remained high in Na and high in Zn, Mn, Pb and Ca (Table 54 and Table 55). Iron (hydr)oxides make up 43 wt% of the final residue. Unfortunately it was not suitable as a building aggregate because of too low concentrations of Ca, Al and Si. Also landfilling of Zinc BRL-WW is not possible due to high concentrations of Cu, Pb and Zn.



**Table 54. XRF analysis of filter cake of Zinc ARLWW and Zinc BRLWW (wt%)**

<b>Element</b>	<b>Zinc ARL-WW</b>	<b>Zinc BRL-WW</b>
<b>Ag</b>	0.01	-
<b>Al</b>	1.93	0.11
<b>As</b>	-	-
<b>Ba</b>	0.74	0.06
<b>Bi</b>	0.02	-
<b>Br</b>	-	-
<b>Ca</b>	3.38	5.98
<b>Cd</b>	0.03	0.02
<b>Cl</b>	0.07	-
<b>Cr</b>	1.09	0.06
<b>Cs</b>	-	-
<b>Cu</b>	1.99	0.13
<b>Fe</b>	40.37	37.82
<b>Ga</b>	0.01	-
<b>Ge</b>	0.01	-
<b>In</b>	0.03	-
<b>K</b>	-	0.01
<b>La</b>	0.01	-
<b>Mg</b>	0.28	0.65
<b>Mn</b>	0.74	5.22
<b>Mo</b>	-	0.01
<b>Na</b>	9.01	7.61
<b>Ni</b>	0.49	0.07
<b>Pb</b>	2.67	0.60
<b>Px</b>	0.03	0.04
<b>Sb</b>	0.04	-
<b>Si</b>	2.26	0.62
<b>Sn</b>	0.32	0.02
<b>Sr</b>	0.04	-
<b>Sx</b>	0.24	-
<b>Ti</b>	0.32	0.04
<b>V</b>	-	-
<b>Zn</b>	8.27	4.46
<b>Zr</b>	0.02	0.06

**Table 55. Acid digestion ICP analysis of filter cake Zinc ARLWW and Zinc BRLWW (wt%)**

<b>Sample</b>	<b>Zinc ARLWW</b>	<b>Zinc B RLWW</b>
<b>Al</b>	2.660	0.262
<b>As</b>	<0.001	<0.001
<b>Ba</b>	0.672	0.029
<b>Ca</b>	3.080	5.800
<b>Cd</b>	0.003	<0.001
<b>Cr</b>	0.517	0.036
<b>Cu</b>	1.610	0.143
<b>Fe</b>	35.300	35.600
<b>K</b>	0.160	0.158
<b>Mg</b>	0.856	1.970
<b>Mn</b>	0.636	4.560
<b>Mo</b>	<0.001	<0.001
<b>Na</b>	2.970	4.720
<b>Ni</b>	0.376	<0.001
<b>Pb</b>	2.340	0.565
<b>Si</b>	2.770	1.130
<b>Sn</b>	0.284	<0.001
<b>Zn</b>	7.240	3.980

In conclusion, optimization of the operating conditions of individual processing steps should notably improve the quality of the residue and increase recovery zinc, lead, copper sodium and other heavy metals.

## 5.8 Cementation

The aim of cementation was to recover heavy metals in solution by precipitation by adding zinc powder dust.

Cementation was conducted following experimental set up and results obtained by Orhan, [18] (Table 18). Zinc dust addition of 1.8020 gr. resulted in a 1.4 Zn/Pb+Cu ratio and stoichiometric addition of 1.13 for all impurities (Cr, Cd, Fe). Calculation of the stoichiometric addition was done using reaction 45.



ICP analysis showed that copper was completely recovered and lead for 61% (Table 56). From metallurgical principles, Pb and Cu showed the highest reaction potential and were expected to be reduced and precipitated first (reaction 11 and 12). Most of the zinc dust was consumed by these two metals.

The heavy metal residue was rich in Pb, Na, Cu, Zn, and Cr (Table 57). Still 2% residual zinc remained in the residue, indicating that 96% of the added zinc dust was used for precipitation of heavy metals.

**Table 56. Recovery by cementation using zinc dust/Pb ratio of 1.7 (50°C, 2.5h)**

Element	Zinc C g/L	Zinc P g/L	Recovery %
<b>Al</b>	0.836	0.816	2.39
<b>B</b>	0.019	0.018	5.26
<b>Ca</b>	0.009	0.007	22.22
<b>Fe</b>	0.018	0.017	5.56
<b>Cu</b>	0.128	<	100.00
<b>Cr</b>	0.281	0.255	9.25
<b>K</b>	0.927	0.965	-4.10
<b>Pb</b>	2.25	0.88	60.89
<b>Zn</b>	18.3	20.4	-11.48

**Below detection limit of 0.001 g/l: Ag, Ba, Bi, Cd, Co, Ga, In, Li, Mg, Mn, Ni, Sr, Tl**

Probably coating of zinc dust occurs by precipitated impurities, impeding dissolution, precipitation of heavy metals, and thus recoveries. The high concentration of Na present in the Zinc CR could be removed by water washing. The cementation product will then approach the following theoretical chemical composition (Table 58). The cementation product could then be sold to a lead smelter which processes the material in a reverberatory furnace for lead recovery and removal of impurities such as oxides and copper.

**Table 57. XRF analyses of cementation residue using zinc dust addition of 1.7 Zn/Pb ratio (50°C, 2.5h)**

Zinc CR	wt%	wt%	wt%
<b>Al</b>	0.06	<b>Fe</b> 0.22	<b>Pb</b> 70.60
<b>Ba</b>	0.04	<b>I</b> 0.01	<b>Px</b> 0.01
<b>Ca</b>	0.23	<b>K</b> 0.08	<b>Sx</b> 0.14
<b>Cd</b>	0.02	<b>La</b> 0.02	<b>Ti</b> 0.01
<b>Cl</b>	0.23	<b>Mg</b> 0.16	<b>U</b> 0.05
<b>Cr</b>	1.26	<b>Mn</b> 0.02	<b>Zn</b> 2.08
<b>Cu</b>	8.40	<b>Na</b> 16.38	

**Table 58. Theoretical chemical composition of cementation product after removal of Na using water washing.**

Zinc CR(WW)	wt%	wt%	wt%
<b>Al</b>	0.08	<b>Fe</b> 0.27	<b>Pb</b> 84.43
<b>Ba</b>	0.04	<b>I</b> 0.01	<b>Px</b> 0.02
<b>Ca</b>	0.27	<b>K</b> 0.09	<b>Sx</b> 0.16
<b>Cd</b>	0.02	<b>La</b> 0.02	<b>Ti</b> 0.01
<b>Cl</b>	0.27	<b>Mg</b> 0.19	<b>U</b> 0.06
<b>Cr</b>	1.51	<b>Mn</b> 0.02	<b>Zn</b> 2.49
<b>Cu</b>	10.05	<b>Na</b> 0.00	

In conclusion, a saleable lead cake can be recovered suitable as feedstock for lead blast furnaces. Thereby proving that cementation of heavy metals can be achieved by addition of zinc dust. Although the recovery of Pb and Cr were too low, it is believed that a higher addition of zinc dust should be eligible to further reduce their concentrations, achieving an electrolyte that is suitable for zinc electrowinning.

## 5.9 Electrowinning

The aim of electrowinning was to recover zinc from a strong alkaline solution.

The decomposition voltage for purified electrolyte (E.P. at 40°C) and electrolyte used for direct electrowinning (D.E. at 20°C) was determined by stepwise increase of the voltage by 0.2V and measuring the mA (Figure 59). The average value was 1.67V which was close to the theoretical value of 1.6V (reaction 21), and in agreement with pourbaix diagrams for zinc concentrations of 0.25M/l zinc at 40°C [28].

With increasing potential a higher current was seen for the purified electrolyte. This was caused by the increased temperature which lowers the viscosity and thus cell resistance (Appendix XVI).

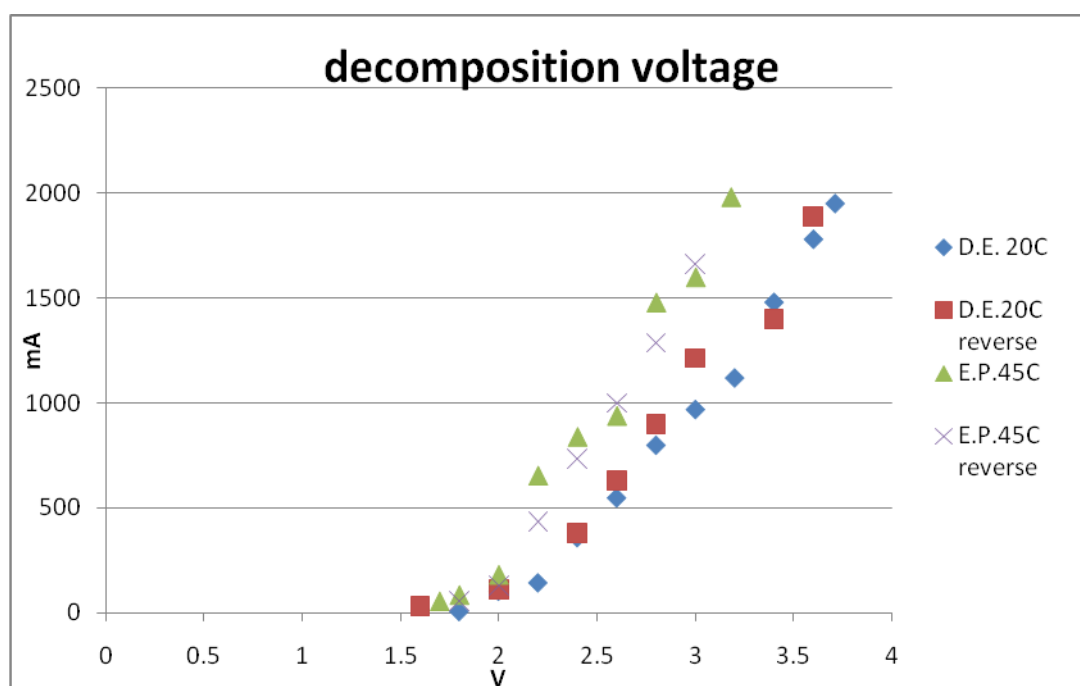


**Figure 59. Decomposition voltage for  $\text{Zn}(\text{OH})_4^{2-}|\text{Zn}$ . D.E.= direct electrolyte at 20°C, E.P = Electrolyte purified at 45°C.**

From the weight of the cathodic deposit  $W$ , current efficiency was calculated.

$$CE = \frac{W_z F}{ItM} \times 100\% \quad [46]$$

Where  $CE$  denotes the current efficiency,  $z$  is the charge of ion,  $F$  is the faradays constant and  $M$  is the molecular weight of specific element,  $I$  is the total cell current in amperes, and  $t$  is the time of deposition in seconds. Current efficiency and specific energy consumption were calculated with respect to Zn.

### 5.9.1 Direct electrowinning

Direct electrowinning was applied to determine the product quality, current efficiency and specific energy consumption (Table 59). XRF analyses showed that direct electrowinning produced a product of very low quality with 77% zinc, 21% Pb and 1% Cu at current efficiency of 83%. During electrowinning hydrogen evolution was considerable at the beginning, but decreased after zinc covered the cathode. Microphotographs showed that a granular, cauliflower and poorly dendritic deposit was formed (Figure 60). The deposit was dark grey to metallic silver. The dark grey coloration of the granules was predominantly on the outer surface; the matrix was comprised of metallic deposits with silver luster. After removal of this poorly defined layer, a thin compact layer on the electrode was found. This compact layer was relatively hard to remove.

**Table 59. Typical direct electrowinning conditions for zinc**

Current density $\text{A m}^{-2}$	Zn g/L	NaOH M	Electrode	Average Voltage V	Specific energy consumption	Current efficiency	Zn wt%	Pb wt%	Cu wt%	°C	Time
81	15.43	~4-5	SS 316-L	-	-	93.7	-	-	-	20	30 min
200	15.43	~4-5	SS 316-L	2.7	1.73 $\text{kWh kg}^{-1}$	127.53*	-	-	-	40	20 min
750	15.43	~4-5	SS 316-L	3.0	1.91 $\text{kWh kg}^{-1}$	83.06	77.21	20.91	1.21	40	1h

\* CE calculation was very high and caused by oxidation of the deposit.

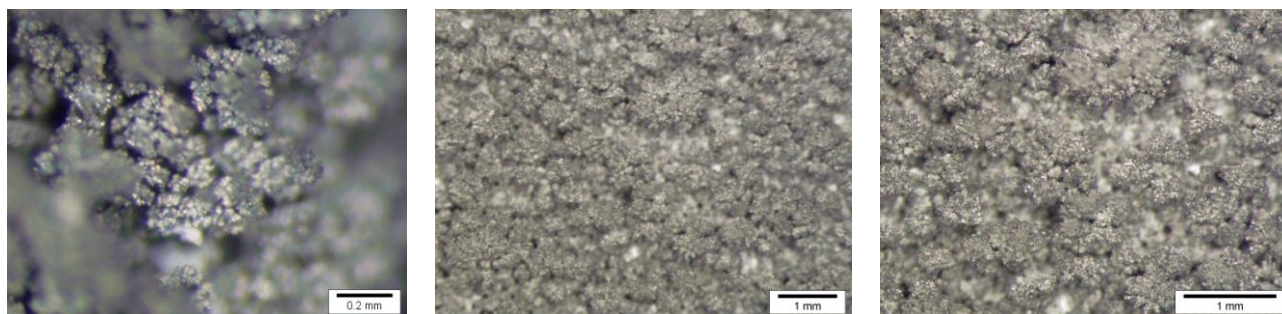


**Figure 60. Microphotographs of zinc deposit after direct electrowinning. (750  $\text{A m}^{-2}$ , 1h, 40°C)**

## 5.9.2 Electrowinning after cementation

In contrast to direct electrowinning experiments, only little hydrogen evolved during these experiments. However, by depletion of zinc during it showed to increase significantly. This became evident during depletion electrowinning experiments; Nr1, Nr 2, and Nr 3 (Table 60). XRF analyses showed that zinc purity was still too low, with 94% instead of the aimed 99.95%. A current efficiency of 89% was achieved. ICP analyses of the purified electrolyte showed that lead had a concentration of 0.88g/L. Therefore lead contamination was considerable. This confirmed that the purification step insufficiently removed heavy metals from solutions. XRPD analyses showed that the sample existed purely from elemental zinc and lead and were hardly oxidized (Figure 61). From microphotographs of the deposit, large fernlike, dendritic deposits were visible (Figure 62 Nr.1 and Table 61). The dendritic “branches” usually end in nodules, which were predominantly grey bluish of color. The “trunk” of the fern and finer matrix usually had a silver metallic color. The dark bluish color was probably indicative for Pb and the silver metallic color for zinc. Microphotographs of trail Nr. 2 showed cauliflower deposits with similar characteristics. Nr. 3 displayed a sparsely covered electrode with tiny cauliflowers deposits of different colors. Removals of the powdery deposits were very easy and Nr. 1 deposit could even be brushed off. For every trial a thin compact layer of zinc was found on the surface of the cathode which was difficult to remove.

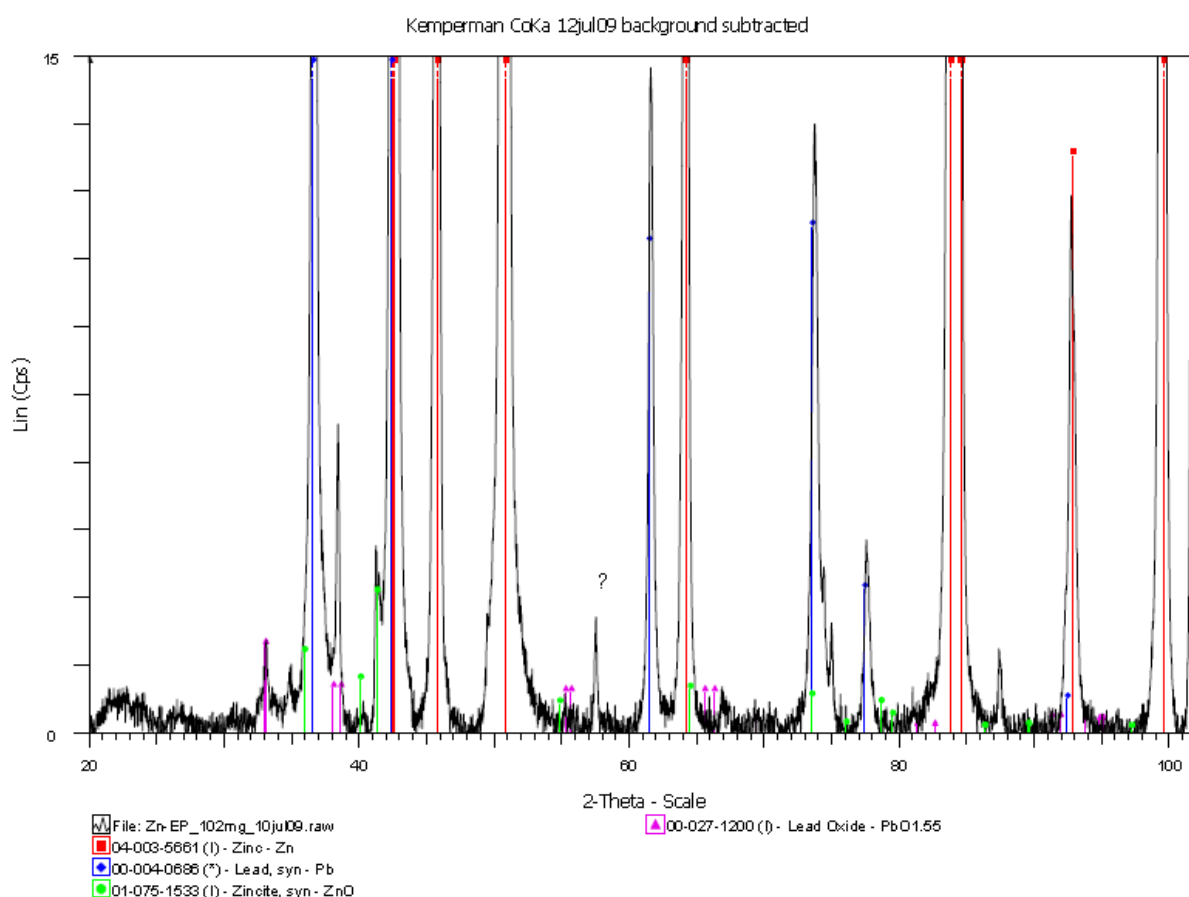


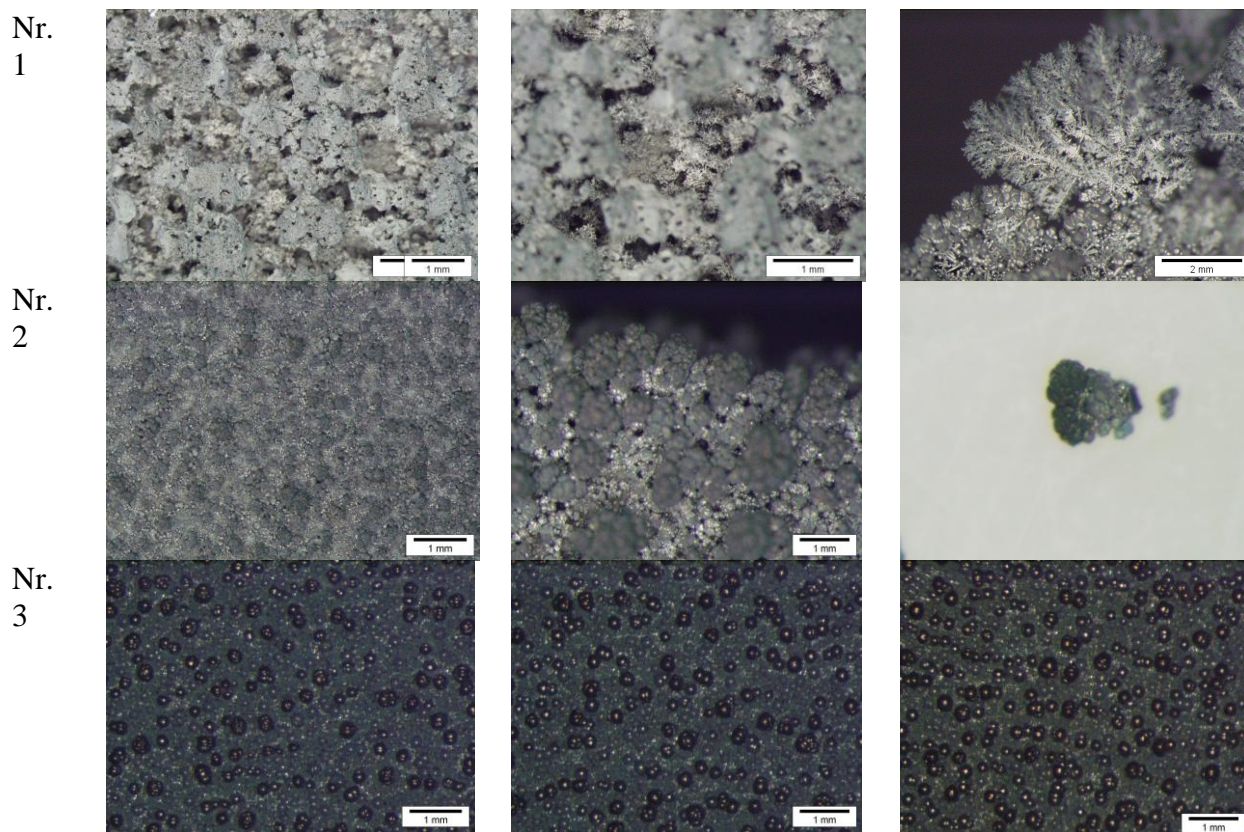
Figure 61. XRPD analyses of Nr.1 zinc product from electrowinning

Table 60. Typical electrowinning conditions of 1.5L purified electrolyte for zinc.

Current	Zn, Pb	NaOH	Electrode	Average	Specific	Current	Zn	Pb	Cr	°C	Time
---------	--------	------	-----------	---------	----------	---------	----	----	----	----	------



density (A m-2)	(g/L)	(M)		Voltage (V)	energy consumption	efficiency	wt%	wt%	wt%		
673 Nr.1	20.4	~4-5	SS 316-L	2.55	2.33 kWh kg <sup>-1</sup>	89.4	94.04	5.26	0.12	20	1h
673 Nr.2	13.22 Est.	~4-5	SS 316-L	2.7	5.21 kWh kg <sup>-1</sup>	42.24	-	-	-	40	1h
673 Nr.3	-	~4-5	SS 316-L	3.13	7.80 kWh kg <sup>-1</sup>	32.87	-	-	-	40	1h



**Figure 62. Microphotographs of zinc deposit of depletion electrowinning from purified electrolyte nr1, nr2 and nr3. (673 Am-2, 1h, 40°C)**

Changes in voltage measured for Nr. 2 and 750 Am-2 D.E. were remarkable (Figure 63). It shows that during electrowinning the dominant reaction changed, or is indicative for increased overvoltages due to smooth surfaces of the electrodes. When a decrease in V is measured, according to ohms law the resistance decreases when the current is kept constant. A decrease in resistivity, thus an increase in conductivity could have been caused by change in mineral growth. Type of mineral growth is depends on current density (Table 61). When 3D growth is preferred it could close the distance between the cathode and anodes, hence reduce the cell resistivity and lower the potential.

In the beginning of these experiments hydrogen evolution was significant but decreased during the experiment after the cathode was coated with Zn due to overpotential of hydrogen evolution on Zn. The smooth surface, clean stainless steel cathode followed by deposition and coating of Zn by dendritic growth probably caused the decreasing voltage observed.

**Table 61. Description of zinc deposits obtained in unstirred alkaline solutions [41].**

Name	Description	Macroscopic	Range of current density (A m <sup>-2</sup> )
Lamellar	Microscopic Composed of ridges and layers with well-defined crystal faces	Compact, sheet-like and very thin (<0.1 mm)	200-358
Spongy	Also referred to as mossy; dull, light to dark grey, composed of very fine grains without well defined faces	Powdery with very loose grains and crystals	40-250
Granular	Also referred to as bouldery or nodular; brilliant with well defined faces	Powdery with very loose grains and crystals	200-448
Dendritic	Fern-like and brilliant with well defined faces	Powdery with very loose grains and crystals	500-1000

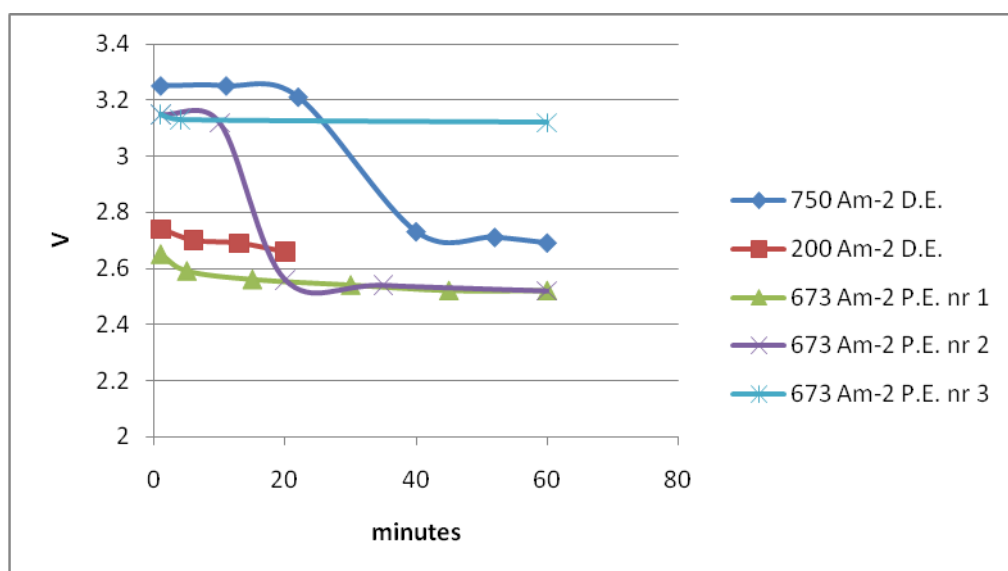


**Figure 63. Voltage change during electrolyse.**

In conclusion, electrowinning of zinc from purified solution produced a product of 94% zinc with a current efficiency of 89%, thereby proving the feasibility of this entire flowsheet. At the beginning of electrolysis hydrogen evolution was evident and decreased when a compact layer of zinc coated the cathode. Electrowinning of solutions with low zinc or high concentrations of heavy metals was accompanied by significant hydrogen evolution and lower current efficiencies.

To decrease the specific energy consumption of this process, it is recommended to increase the temperature. This lowers the viscosity of solution (Table 4), reduces the cell resistivity and therefore decreases the specific energy consumption (Appendix XVI). However, the hydrogen overvoltage decreases with increasing temperature and balance between these two parameters must be found.

Research on suitable anode and cathode materials, such as magnesium, should be conducted. Use of a magnesium cathode could potentially further reduce the hydrogen evolution and make automated recovery of zinc possible.

## 6 Mass balance

### 6.1 Mass flow in the conceptual flowsheet

The aim was to obtain a mass balance from measurements during processing of Zinc A and Zinc B. The mass flows of process water, chemicals and elements were calculated for processing the zinc bearing residues from the Rotterdam harbor, Zinc A and B comprised of 3000 and 1700 tons respectively using Appendix IX as baseline. By extrapolating XRF results, the mass flows were calculated using the recoveries found in the laboratory experiments. The results were summarized in Table 62 - Table 65.

#### **Considerations**

As mentioned before mass balance calculations were deduced from XRF analysis with rest % measured as oxygen. Only calculations of positive recoveries are reported. For cementation and electrowinning mass balance calculation results from filtrates, analyzed by ICP-OES, were extrapolated.

#### 6.1.1 Water washing

Due to the chemical composition water washing of Zinc A was necessary. The moisture content of Zinc A and B was determined to be 22.32% and 3.46% (Table 6 and 8). The residual moisture was included with the total processing water to obtain a liquid solid ratio of 5.

Thus, Zinc A contained 669.6 tons of moisture and 2330.4 tons of dry solids (Appendix XVII). For processing 2330.4 tons of Zinc A, 11652 tons of total processing water was necessary. Reducing the moisture already present, the pre-water washing step needed an addition of 10982.4 tons of processing water. After processing the slurry was filtered. The cake moisture content using industrial processes would have been approximately 25wt% [48], however using laboratory equipment an average moisture content of 45% was determined (Table 65).

Extrapolating XRF analyses K, Na, Ca and Cl dissolve and amount to 11, 14, 46, and 132 tons respectively (Appendix XVIII). In addition to XRF analysis, ICP analysis showed that considerable amounts of zinc dissolved during water washing and amount to a loss of 45 tons.

Remaining moisture after water washing could have lead to high Cl concentration in Zinc AWW. A cake washing step could then be used, however a repulping and an additional filtration step is than necessary. When operating at a wash ratio of 1.5 to 2 approximately 6 to 4% of the solute will remain present. Use of such a wash ratio of 1.5 to 2 means an additional 745 and 990 tons of processing water[48].

To recover the dissolved salts, the bleed stream should first be purified to obtain brine existing solely of Ca, Cl, K, and Na. One of the possibilities is using  $\text{NaHCO}_3$  to precipitate impurities as carbonate compounds. This is more effective at high pH and effluent of water washing of  $\text{NaFeO}_2$  could be used for this purpose. However, one should take into account the tentative dissolution of  $\text{CaCl}_2$  which will precipitate at high pH as  $\text{Ca(OH)}_2$  consuming hydroxides. Furthermore, formed  $\text{Ca(OH)}_2$  will probably end up in the final residue as calcium iron oxide. Additional benefit is that it could substitute part of the soda ash necessary during roasting because it will also convert zinc ferrites, although its reaction rate is much slower.



More investigation for selective purification should be conducted as the proposed implications of higher Ca in the residue and use of effluent of washing of  $\text{NaFeO}_2$ . After purification the evaporate product can then be sold as feed stock for chemical companies.

### 6.1.2 First leaching

According to water washing experiments 15.02% of Zinc A total dry solids dissolved. Adding Zinc A (1980 tons) and Zinc B (1641) total dry solids amount to 3972 tons which needed to be leached. Water in situ was 1679 tons which meant an additional 13411 tons of process water and 3018 tons of NaOH was necessary to obtain the experimental 5:1 L:S (w:w) ratio.

The theoretical requirement to dissolve 1 ton of Zn as  $\text{ZnO}$  is 1.22 ton NaOH (reaction 1). Zinc oxide dissolution for Zinc AWW and B amounted to 585 tons of NaOH consumption. An approximation of additional consumption by other minerals amounted to 39 % for Zinc A and 41% for Zinc B, resulting in a total consumption by mineral dissolution of 966 tons NaOH. Dissolution of Zinc AWW and BWW amounted to 19.28 and 9.37 wt% respectively. The residual moisture content for zinc A and B was 35 and 25 wt% respectively. Residual moisture amounted in an additional loss of process water and NaOH, 932 and 186 tons respectively. Residual NaOH contributed in the roasting step (reaction 6).

The four main constituents of the filtrate were Zn, Fe, Cl,  $\text{S}_x$ , and Pb with 311, 77, 71, 57, and 39 tons respectively. For more detailed information see Appendix XIX.

During leaching experiments the loss of water due to evaporation was kept to a minimum. However, significant losses were detected after and during filtration. For Zinc A and Zinc B the ratios of evaporation and loss during drying are 53% and 61% to 47% and 39% respectively.

The end temperature of solution upon mixing additional process water with caustic soda is calculated and a temperature of  $84.4^\circ\text{C}$  can be achieved. This arises from the exothermic reaction upon dissolution of NaOH. Due to the very corrosive behavior of high caustic soda solution external heating is advisable and a lot of thought should go to materials of construction. Additional heating to operate at  $90^\circ\text{C}$  could be provided by a jacketed vessel, which has high wall thicknesses and is often used for vessels which need frequent cleaning[48]. In these vessels only a very short retention time is needed because  $\text{ZnO}$  readily dissolves. Complete suspension and agitation is therefore of great importance for the recovery of zinc from the zinc oxides. This can be provided by batch stirred tanks.

### 6.1.3 Roasting

According to first leaching experiments 19.3% of Zinc A and 9.4% of Zinc B dissolved. The total dry solids of zinc AL, BL were 1596 and 1487 tons. According to reactions 25-27 roasting 1 ton of Zn in the form of  $\text{ZnFe}_2\text{O}_4$  required at least 1.62 tons of  $\text{Na}_2\text{CO}_3$ . The total consumption of  $\text{Na}_2\text{CO}_3$  for roasting Zinc AL and Zinc BL amounted to 873 and 1024 tons respectively. Loss of ignition for zinc AL and BL were 11.46 and 10.27wt%. After roasting the total dry solids for zinc AR, BR comprised 2186 and 2253 tons respectively.

### 6.1.4 Secondary leaching

During roasting the material became sintered and totaled at 4440 tons, 2186 tons of Zinc AR and 2253 tons of Zinc BR. The operating conditions were similar as for the first leaching step, utilizing 18498 tons of process water and 3700 tons NaOH. Substantial dissolution of  $\text{NaFeO}_2$

had taken place. This accounted for approximately 973 tons (73-81 wt%) of the total dissolved solids for Zinc ARL and BRL with 169 ton Zn (13-14 wt%) and the remainder being Pb, Fe, Cl, Cr, and Ca. The total dissolved solids were 1260 tons (Appendix XXI). For Zinc ARL and Zinc BRL the ratios of evaporation and loss during drying are 67% and 61% to 33% and 39% respectively. Dissolution of Zinc AR and BR amounted to 38.4 and 27.0 wt% respectively. The residual moisture content for Zinc ARL and BRL was 21.9 and 19.3 wt% respectively.

Because sintering occurred during roasting experiments, a grinding step is necessary. For achieving a narrow particle size a rod mill is more suitable than a ball mill. In principle the secondary leaching step would not consume NaOH if appropriate pH, temperature and L:S ratio conditions are maintained. Upon mixing the fresh lixiviant a temperature of 76.6°C can be reached.

### **6.1.5 Post water washing**

The post water washing was conducted to recover residual soluble constituents (Appendix XXII). Similar operating conditions as for the water washing step were used. Zinc ARL and Zinc BRL, 1347 and 1645 tons respectively needed 11694 tons of additional process water because 771 tons residual moisture was present. Dissolution of Zinc ARL and BRL were 16.5 and 14.4 wt% with residual moisture content of 23.5 and 23.3 wt%.

### **6.1.6 Residue**

The final residue consisted of 2533 tons; 1125 tons of Zinc ARLWW and 1408 tons of Zinc BRLWW. The main constituents were Fe, Zn, Na, Ca and Mn (Appendix XXIII).

### **6.1.7 Cementation**

The filtrates from the two leaching steps were 33588 tons. Regarding losses of evaporation and drying of the filter cakes, the final filtrates calculated for Zinc AL, Zinc BL, Zinc ARL and Zinc BRL were 6463, 7568, 5496, and 8051 tons respectively adding up to 27578 tons. These filtrates, Zinc C, were purified and if similar results were achieved as in the cementation experiment, a sponge comprised of Pb, Cu and Zn and 30, 3 and 1 tons was produced respectively (Appendix I).

After filtration this product could be sent to a lead smelter and the remaining filtrate would be used for electrowinning purposes.

### **6.1.8 Electrowinning**

Assuming that 80% of total zinc was recovered through the electrowinning route and extrapolating the results from electrowinning experiments, it was expected that 357 tons of zinc with a purity of 94% could be produced. The remaining 6% were 20 tons of Pb and 0.45 tons of Cr and other metals (Appendix XXV). With a current efficiency of 90% the total electrowinning step would consume 832 MWh. The regenerated solution would attain 9.8kM OH<sup>-</sup> and could be reused for leaching purposes.

Finally a more detailed flowsheet with additional water washing step and other recommended processes was constructed (Figure 64).

**Table 62. Estimated input of materials for processing Zinc A and Zinc B according to experimental results**

Input	Tons	Description
Zinc A	3000	Zinc A – 22.32wt% H <sub>2</sub> O; dry solids 19% Zn (434tons)
Zinc B	1700	Zinc B – 3.46wt% H <sub>2</sub> O; dry solids 18% Zn (298 tons)
NaOH	3018	First and second leaching step
Na <sub>2</sub> CO <sub>3</sub>	1897	Roasting
Water	37891	Water washing, leaching and 5% loss
Zinc dust	26	purification
Total	5895	Dry solids (Zinc A + Zinc B + Zn dust + Na <sub>2</sub> CO <sub>3</sub> )

**Table 63. Estimated output of materials after processing Zinc A and Zinc B according to experimental results**

Output	Tons	Description
Residues	2533	leach residue (38-40% Fe-bearing)
Salt	203	CaCl <sub>2</sub> , NaCl, KCl
Heavy metal cake	34	metal cake from purification stage (Pb, Cu)
Zinc	474	metallic zinc (assuming recovery of 81% and 80% during electrowinning)
NaOH	522	NaOH regenerated during electrowinning of zinc (with a CE of 90%)
CO <sub>2</sub>	541	CO <sub>2</sub> loss during roasting reaction
NaOH	1229	$\left( \begin{array}{l} Na_2CO_3 + Fe_2O_3 \xrightarrow{950^\circ C} 2NaFeO_2 + CO_{2(g)} \\ 2NaFeO_2 + H_2O \rightarrow 2NaOH + Fe_2O_3 \end{array} \right)$
Total	5536	Dry solids (residue + gas and NaOH generation)

**Table 64. Total possible recovery of Zinc A and Zinc B**

XRF	Total recovery Zinc A %	Total recovery Zinc B %
Cl	62	-
Cu	33	28
K	71	-
Pb	64	78
Zn	82	80

Table 65. Mass balance of conceptual flowsheet

Process step	Sample	Total weight (tons)	Process water in tons (needed)	NaOH (tons)	Na <sub>2</sub> CO <sub>3</sub> (tons)	L.O.I. (%)	Dissolved (%)	Total dry solids (tons)	Moisture (wt%)
<b>Zinc bearing residues</b>	Zinc A	3000	-	-	-	-	-	2330	22.32
	Zinc B	1700	-	-	-	-	-	1641	3.46
<b>Water washing</b>	Zinc A	3000	11652 (10982)	-	-	-	15.02	1980	45.00
	Zinc B	1700	-	-	-	-	-	1641	3.46
<b>First leaching</b>	Zinc AWW	3601	8252 (6631)	1650	-	-	19.40	1596	35
	Zinc B	1700	6838 (6779)	1368	-	-	9.40	1487	25
<b>Roasting</b>	Zinc AL	1596)	-	-	873	11.46		2186	0
	Zinc BL	1487	-	-	1024	10.27		2253	0
<b>Secondary leaching</b>	Zinc AR	2186	(9109)	1822	-	-	38.40	1347	22
	Zinc BR	2253	(9389)	1878	-	-	27.00	1645	19
<b>Post water washing</b>	Zinc ARL	1724	5611 (5234)	-	-	-	16.50	1124	23
	Zinc BRL	2038	6854 (6461)	-	-	-	14.40	1408	23
<b>Residue</b>	Zinc ARLWW	1469	-	-	-	-	-	1125	-
	Zinc BRLWW	1836	-	-	-	-	-	1408	-



## 7 Conclusions and recommendations

The aim of this study was to establish the feasibility and efficiency of processes from the proposed flowsheet [2]. Zinc A and B showed many similarities with electric arc furnace dust. From the literature review, appropriate leaching and roasting agents were selected and optimal operating conditions for water washing, leaching, cementation and electrowinning were determined.

Finally, through conducting many experiments it can be concluded that the feasibility of the entire flowsheet has been proven.

### *Zinc ferrite synthesis*

- Synthetic zinc ferrite can be converted into zinc oxide by roasting with NaOH or  $\text{Na}_2\text{CO}_3$
- Zinc can be selectively recovered by dissolving the calcine product in strong basic solutions
- Minor dissolution of iron in strong alkaline solutions

Synthesis zinc ferrite can be achieved by mixing  $\text{ZnO}$  and  $\text{Fe}_2\text{O}_3$  and roasting for 5h at  $1100^\circ\text{C}$ . By use of HSC 6.1 and the literature review, appropriate roasting agents were tested. Optimal roasting conditions were determined by an orthogonal study of roasting synthetic zinc ferrite with NaOH and  $\text{Na}_2\text{CO}_3$  using different retention times, temperatures, and stoichiometric additions. Due to hygroscopic characteristics of the NaOH calcine product, corrosive behavior and cost of reagent, finally  $\text{Na}_2\text{CO}_3$  was chosen as roasting reagent. Leaching experiments using L:S of 10,  $90^\circ\text{C}$ , 800 rpm and 10M NaOH showed high recovery of zinc (90%) and very low recovery of iron (0.2%) can be achieved. The dissolution of  $\text{ZnO}$  was very fast.

### *Water washing*

- Dissolution and removal of halides from Zinc A through water washing is feasible
- Dissolution of heavy metals necessitate additional treatment of the filtrate

Water washing of Zinc A was conducted using the following operating conditions: Liquid/solid ratio of 5 at  $50^\circ\text{C}$  for 1 hour. The objective of water washing was to dissolve and remove halides from Zinc A.

The dissolution of halogens and (earth)alkali elements was very fast, chloride, potassium, sodium, and magnesium showed recoveries of 62%, 71%, 42%, and 19% respectively. Furthermore, dissolution of Zn, Pb, and especially Cd necessitates additional treatment of solution.

To further increase the recovery of halides and remove the heavy metals from solution it is suggested that the washing water should an increased pH of approximately 12. Addition of  $\text{NaHCO}_3$  can be used for precipitation of the heavy metals in carbonate form, if not already precipitated as their hydroxide form caused by the increased pH. The washing water from the final residue can be used for this purpose and closes the loop. According to XRF results there is an excess of  $\text{Cl}^-$  ions, and to achieve a clean salt product it is necessary to have stoichiometric availability of  $\text{Na}^+$  ions. Furthermore the increase of temperature and L:S in additional experiments showed an increase in conductivity. Therefore water washing at a higher temperature of  $80^\circ\text{C}$  and higher L:S ratio 7 with a shorter retention time is also recommended. Later recommendations also apply for the post water washing step.

### *First leaching step*

- Zinc is selectively recovered by dissolution in strong alkaline solution with minor dissolution of iron
- Dissolution of Al and Si impede filtration and zinc recovery
- Filtration of the filtrate becomes problematic upon cooling, due to precipitation of zinc, lead, and aluminum (hydr)oxides and increased viscosity of leachate at lower temperatures

Leaching of water washed Zinc A and Zinc B was conducted using the following operating conditions: L:S of 5, at 90°C, 1000 rpm and 5M NaOH solution for 1 hour. The objective of leaching with strong alkaline solutions was to selectively dissolve zinc and other heavy metals, leaving iron oxides in the solution.

Of water washed Zinc A 19.3wt% of the filtercake dissolved, of which 54% was attributed to dissolution of zinc, the other 46% was mainly dissolution of Cl, Sx, Fe, Pb, Cu and Ca. The recovery of zinc and lead was 66% and 46% respectively. Of Zinc B 9.4wt% of the solid dissolved, of which 54% was attributed to zinc dissolution. The remainder was mainly Fe, Pb, K, Cl, Mn, Sx, Ca and Mo. The recovery of zinc and lead was 57% and 70% respectively.

Dissolution of Al and Si impeded the recovery of Zn by forming complexes and consuming additional NaOH. Upon cooling of the filtrates during filtration the viscosity increased and caused filtration problems. Additionally, filtration problems occurred due to formation of a white gelatinous phase, which probably consisted of zinc hydroxides and lead oxides. Zinc AL\* and Zinc BL\* showed comparable characteristics.

### *Roasting*

- Zinc ferrite in the residue of water washed and leached Zinc A and Zinc B are partially converted by roasting with  $\text{Na}_2\text{CO}_3$
- During roasting  $\text{ZnO}$  and  $\text{NaFeO}_2$  are formed
- More research is necessary

Roasting of first leaching filtercakes, Zinc AL and Zinc BL, was conducted using the following operating conditions: Stoichiometric additions of 2.6 and 2.1  $\text{Na}_2\text{CO}_3$ , a retention time of 2h at 950°C. The objective was to convert zinc ferrite into soluble zinc oxides. As expected formation of  $\text{ZnO}$  and  $\text{NaFeO}_2$  were detected. However, presence of  $\text{ZnFe}_2\text{O}_4$  in XRPD analysis were detected and implied that conversion of zinc ferrite was incomplete. Albeit, over 50% of the zinc ferrite was converted. Additional experiments to increase the conversion by adding additional reagent showed inconsistent results. Therefore, a more thorough investigation on roasting parameters must be considered.

### *Secondary leaching step*

- Similar conclusions apply as for the first leaching step
- Conversion of zinc ferrite into zinc oxide was determined to be ~50%
- Considerable dissolution of  $\text{NaFeO}_2$  in strong alkaline solutions

Similar operating conditions and objectives as in the first leaching step were intended. Of Zinc ALR 38 wt% was dissolved, approximately 81% can be attributed to dissolution of Na. The recoveries of Na, Zn, Pb were respectively 67%, 48% and 34%. Of zinc BRL 27 wt% was dissolved, the major constituent was Na. The recoveries of Na, Zn, Pb were respectively 60%, 54% and 25%. The overall zinc recover, without optimization, is approximately 81%.



Soluble zinc compounds were almost completely dissolved within 10 minutes. The retention time for leaching processes can therefore be reduced. During filtration the filtrate cooled down and became more viscous. At the same time formation of precipitates upon cooling impeded the rate of filtration. It is therefore recommended that hot filtration takes place, reducing the change of precipitate formation and decrease the viscosity of the filtrate.

#### *Post water washing*

- Considerable amounts of sodium(hydroxide) can be recovered during the post water washing step
- Operating conditions need to be optimized

The same operating condition and objectives as in water washing of Zinc A were intended. Of Zinc ARL and Zinc BRL 16.51% and 14.37 wt% dissolved respectively. The losses were almost entirely by dissolution of Na(hydroxide). Minor elements that dissolved were Si, Zn, Al and Cr. For both solutions the pH increased immediately to 12, partially due to residual presence of NaOH from secondary leaching step. The recovery of Na was insufficient and the residual concentration would still cause problems for utilization of the residue as an aggregate, feedstock or for landfilling purposes.

The post water washing step deserves more investigation. For industrial and economic feasibility of the developed flowsheet it is highly important to have an accurate sodium (hydroxide) mass balance. Whether sodium hydroxide or sodium carbonate is the suitable reagent for roasting largely depends to which extent the sodium hydroxide loop can be closed. Intuitively, higher capital expenditures are necessary to use sodium hydroxide as reagent, whereas operating with sodium carbonate will result in higher operating expenditures.

#### *Residue*

- Most of the heavy metals from Zinc A and Zinc B are removed and recovered

The additional objective was to obtain a residue which could be used as a feed stock for steel making industry, serve as an aggregate or be disposed of in a landfill without further specialized treatment. Optimization of each individual process step could potentially produce a residual product useful as feedstock for bricks, pigments or suitable for landfilling.

#### *Cementation*

- Cementation of heavy metals by addition of zinc dust is feasible
- A saleable lead cake is obtained
- Stoichiometric addition of zinc dust was insufficient to precipitate all impurities

Cementation was conducted using the following operation conditions: Zinc dust addition of 1.4 Zn/Pb+Cu ratio for 2.5 hours at 50°C. The objective was to obtain a purified leachate suitable for electrowinning purposes by cementation of heavy metals using zinc dust addition. Lead recovery was 61% and a product consisting of 71% Pb, 15 % Na and 8% Cu was obtained. After electrowinning experiments it was determined that the cementation process was unsatisfactory, with lead being the main impurity in the zinc deposit.

Especially the lead removal during cementation process was insufficient and higher zinc dust addition is recommended to increase the efficiency.



### *Electrowinning*

- Electrowinning of Zn in strong alkaline solutions is feasible and less energy intensive in comparison with conventional acidic solutions
- Considerable hydrogen evolution can occur at high current densities and low zinc concentrations

Electrowinning of Zn in alkaline conditions was less energy intensive than in acidic conditions, 2.33 and 3.3 kWh kg<sup>-1</sup> respectively. From the purified solution a product of 94 wt% Zn and 5 wt% Pb was produced. The product had a specific energy consumption of 2.33 kWh kg<sup>-1</sup> with a current efficiency of ~90% deposit when 653 A m<sup>-2</sup> was applied resulting in potential of 2.57V. Hydrogen evolution was substantial at the start of the experiments until a zinc layer was deposited on the stainless steel cathode. The deposits were dendritic at high concentrations and became granular or formed boulderlike cauliflower deposits at lower concentrations.

Use of higher temperature can reduce the specific energy consumption bearing in mind the decreasing hydrogen overpotential. Other materials for anodes and cathodes should be researched for automation of the process.

### *Mass Balance*

The major in-, and outputs were determined by calculating a mass balance from measurements taken during experiments.

## 8 Acknowledgements

Yongxiang Yang:	For his supervision and many pleasant discussions over these last years
Thilo Behrends:	For giving me this opportunity
Yanping Xiao:	For her assistance and discussions in the lab
Harald Oosterhof:	For trying to make sense of it all
Hans de Ruiter:	For his financial, logistical, and moral support
Ron Penners:	For his assistance and everlasting enthusiasm over a cup of coffee
John van den Berg:	For his support in and around the laboratories
Ruud Hendrikx:	For analyzing the XRPD and XRF samples
Joop Padmos:	For analyzing the filtrate samples with ICP-OES
My family:	For keeping supportive and believing in me
My friends:	For laughing through the years of study
My girlfriend:	For all the fun delays and help

## 9 References

1. Tolcin, A.C., *Minerals yearbook: Zinc*, U.S.G. Survey, Editor. 2007.
2. Yang, Y., *Metallurgical processing of zinc bearing residues at Rotterdam Harbour*. 2007, Metals production, Refining and Recycling; Department of Materials science and Engineering; Delft University of Technology: Delft. p. 1-45.
3. Eacott, J.G., *Techno-economic feasibility of zinc and lead recovery from electric arc furnace baghouse dust*. CIM BULLETIN, 1984. **77**(869): p. 75-81.
4. Caravaca, C., A. Cobo, and F.J. Alguacil, *Considerations about the recycling of EAF flue dusts as source for the recovery of valuable metals by hydrometallurgical processes*. Resources, Conservation and Recycling, 1994. **10**(1-2): p. 35-41.
5. Youcai, Z. and R. Stanforth, *Integrated hydrometallurgical process for production of zinc from electric arc furnace dust in alkaline medium*. Journal of Hazardous Materials, 2000. **80**(1-3): p. 223-240.
6. Dreisinger, D.B., E. Peters, and G. Morgan, *The hydrometallurgical treatment of carbon steel electric arc furnace dusts by the UBC-Chaparral process*. Hydrometallurgy, 1990. **25**(2): p. 137-152.
7. Nyirenda, R.L., *The processing of steelmaking flue-dust: A review*. Minerals Engineering, 1991. **4**(7-11): p. 1003-1025.
8. Consultancy, W., *Terugwinning van zink bij de recycling van verzinkt staal(schroot)*. 2008, WBM Consultancy. p. 33.
9. Honingh, S., G. van Weert, and W.A. Reuter. *Turning blast furnace dust into a source of zinc and lead units: A progress report on testwork at Corus IJmuiden*. in *Recycling of metals and engineered materials*. 2000. Pittsburg, Pennsylvania: TMS.
10. Reuter, M.A., J.E. Dutrizac, and S.C. Lans, eds. *Zinc College*. 2nd ed. Zinc College. 2002, TU Delft.
11. Van Herck, P. and C. Vandecasteele, *Zinc and Lead Removal from Blast Furnace Sludge with a Hydrometallurgical Process*. Environmental Science & Technology, 2000. **34**(17): p. 3802.
12. Xia, D.K. and C.A. Pickles, *Caustic roasting and leaching of electric arc furnace dust*. Canadian Metallurgical Quarterly, 1999. **38**(3): p. 175-186.
13. Das, B., et al., *An overview of utilization of slag and sludge from steel industries*. Resources, Conservation and Recycling, 2007. **50**(1): p. 40-57.
14. Kelebek, S., S. Yörük, and B. Davis, *Characterization of basic oxygen furnace dust and zinc removal by acid leaching*. Minerals Engineering, 2004. **17**(2): p. 285-291.
15. Mikhail, S.A. and A.-M. Turcotte, *Thermal reduction of steel-making secondary materials I. Basic-oxygen-furnace dust*. Thermochemica Acta, 1998. **311**(1-2): p. 113-119.
16. Guezennec, A.-G., et al., *Dust formation in Electric Arc Furnace: Birth of the particles*. Powder Technology, 2005. **157**(1-3): p. 2-11.
17. Machado, J.G.M.S., et al., *Chemical, physical, structural and morphological characterization of the electric arc furnace dust*. Journal of Hazardous Materials, 2006. **136**(3): p. 953-960.
18. Orhan, G., *Leaching and cementation of heavy metals from electric arc furnace dust in alkaline medium*. Hydrometallurgy, 2005. **78**(3-4): p. 236-245.
19. Ruiz, O., et al., *Recycling of an electric arc furnace flue dust to obtain high grade ZnO*. Journal of Hazardous Materials, 2007. **141**(1): p. 33-36.

20. Jarupisitthorn, C., T. Pimtong, and G. Lothongkum, *Investigation of kinetics of zinc leaching from electric arc furnace dust by sodium hydroxide*. Materials Chemistry and Physics, 2003. **77**(2): p. 531-535.
21. Dutra, A.J.B., P.R.P. Paiva, and L.M. Tavares, *Alkaline leaching of zinc from electric arc furnace steel dust*. Minerals Engineering, 2006. **19**(5): p. 478-485.
22. Holloway, P.C., T.H. Etsell, and A.L. Murland, *Roasting of La Oroya Zinc Ferrite with Na<sub>2</sub>CO<sub>3</sub>*. Metallurgical and Materials Transactions B, 2007. **38**(5): p. 781-791.
23. Ye, G., et al. *Elimination of zinc ferrite for hydrometallurgical recovery of zinc from EAF dust*. in *Advanced processing of metals and materials*. 2006: TMS.
24. Jha, M.K., V. Kumar, and R.J. Singh, *Review of hydrometallurgical recovery of zinc from industrial wastes*. Resources, Conservation and Recycling, 2001. **33**(1): p. 1-22.
25. Rao, S.R., *Recourse recovery and recycling from metallurgical wastes*. Waste management. 2006: Elsevier. 557.
26. Sahu, K.K., A. Agrawal, and B.D. Pandey, *Recent trend and current practices for secondary processing of zinc and lead. Part II: zinc recovery from secondary sources*. Sage Journals: Waste Manage Research, 2004. **22**: p. 248-254.
27. Nagib, S. and K. Inoue, *Recovery of lead and zinc from fly ash generated from municipal incineration plants by means of acid and/or alkaline leaching*. Hydrometallurgy, 2000. **56**(3): p. 269-292.
28. Roine, A., *HSC Chemistry 6.0*. 2006, Outotec.
29. Drever, J.I., *The geochemistry of natural waters: surface and groundwater environments*. Third edition ed. 1997: Prentice Hall.
30. Youcai, Z. and R. Stanforth, *Extraction of zinc from zinc ferrites by fusion with caustic soda*. Minerals Engineering, 2000. **13**(13): p. 1417-1421.
31. Nickell, R.A., et al., *Hg/HgO electrode and hydrogen evolution potentials in aqueous sodium hydroxide*. Journal of Power Sources, 2006. **161**(2): p. 1217-1224.
32. Antrekowitsch, J., Antrekowitsch, H., *Hydrometallurgically recovering zinc from electric arc furnace dusts*. JOM, 2001. **53**(12): p. 26-28.
33. Zhao, Y. and R. Stanforth, *Production of Zn powder by alkaline treatment of smithsonite Zn-Pb ores*. Hydrometallurgy, 2000. **56**(2): p. 237-249.
34. Holloway, P.C., T.H. Etsell, and A.L. Murland, *Use of Secondary Additives to Control the Dissolution of Iron during Na<sub>2</sub>CO<sub>3</sub> Roasting of La Oroya Zinc Ferrite*. Metallurgical and Materials Transactions B, 2007. **38**(5): p. 793-808.
35. Lenz, D.M., Martins, F.B., *Lead and zinc selective precipitation from leach electric arc furnace dust solutions*. Revista Materia, 2007. **12**(3): p. 503-509.
36. Youcai, Z., Stanforth, R., *Selective separation of lead from alkaline zinc solution by sulfide precipitation*. Separation science and technology, 2001. **36**(11): p. 2561-2570.
37. Afifi, S., et al., *On the electrowinning of zinc from alkaline zincate solutions*. Journal of electrochemical society, 1991. **139**(7): p. 1929-1933.
38. Brown, A.P., Meisenhelder, J.H., Yao, N.P., *The alkaline electrolytic process for zinc production: a critical evaluation*. Ind. Eng. Chem. Prod. Res. Dev., 1983. **22**(2): p. 263-272.
39. Gurmen, S. and M. Emre, *A laboratory-scale investigation of alkaline zinc electrowinning*. Minerals Engineering, 2003. **16**(6): p. 559-562.
40. Saleh, M.M., et al., *Electrowinning of non-noble metals with simultaneous hydrogen evolution at flow-through porous electrodes .3. Time effects*. Journal of the Electrochemical society, 1997. **144**(3): p. 922-927.
41. St-Pierre, J. and D.L. Piron, *Electrowinning of zinc from alkaline solutions*. Journal of Applied Electrochemistry, 1986. **16**(3): p. 447-456.

42. St-Pierre, J. and D.L. Piron, *Electrowinning of zinc from alkaline solutions at high current densities*. Journal of Applied Electrochemistry, 1990. **20**(1): p. 163-165.
43. Stewart, A. 2005, Alex Stewart International Corporation B.V.
44. Konvička, T., P. Mošner, and Z. Šolc, *Investigation of the Non-isothermal Kinetics of the Formation of ZnFe<sub>2</sub>O<sub>4</sub> and ZnCr<sub>2</sub>O<sub>4</sub>*. Journal of Thermal Analysis and Calorimetry, 2000. **60**(2): p. 629-640.
45. Kolta, G.A., et al., *Kinetics and mechanism of zinc ferrite formation*. Thermochemica Acta, 1980. **36**(3): p. 359-366.
46. Rigden, C.J., *Weight losses from zinc ferrite and nickel ferrite during sintering*. Journal of Materials Science, 1969. **4**(12): p. 1084-1087.
47. Xia, D.K. and C.A. Pickles, *Kinetics of zinc ferrite leaching in caustic media in the deceleratory period*. Minerals Engineering, 1999. **12**(6): p. 693-700.
48. Perry, R.H., Green, D.W., *Perry's Chemical Engineers' Handbook*. 8th ed. 2007: McGraw-Hill.

## 10 Appendices

### I. Treatment technologies of iron-making dusts

Table 66. Criteria and sub-criteria to treat iron-making dusts via hydrometallurgical processes [9]

<b>A. Type of raw material the process is developed for: EAF dust, BOF dust, BF dust, others;</b>
<b>B. Stage of commercialisation:</b>
<ul style="list-style-type: none"> <li>• (o) once tested in laboratory</li> <li>• (oo) intensively tested in laboratory</li> <li>• (ooo) tested on pilot scale</li> <li>• (oooo) in use on technical scale</li> </ul>
<b>C. Zinc/lead product:</b>
<ul style="list-style-type: none"> <li>• (h) refined metal</li> <li>• (l) low grade metal</li> <li>• (d) mixed Zn/Pb oxides dust or zinc compounds</li> </ul>
<b>D. Metallic or oxide iron product</b>
<b>E. Zinc yield</b>
<b>F. Pre-treatment part of the proposed processing:</b>
<ul style="list-style-type: none"> <li>• (a) agglomerating</li> <li>• (dry) drying</li> <li>• (no) no pre-treatment necessary</li> <li>• (roast) roasting</li> <li>• (calc) calcination</li> </ul>
<b>G. Evaluation of environmental effect:</b>
<ul style="list-style-type: none"> <li>• (tw) possible problematic toxic waste generated</li> <li>• (a) possible problematic air pollution</li> <li>• (wp) possible problematic water pollution</li> <li>• (s) soil pollution can be expected.</li> </ul>

Table 67. Comparing hydrometallurgical technologies to treat iron-making dusts [9]

	Raw material	Status	Zn product	Fe product	Zn yield	Pre-treatment environ.	Effect on
Pressurised leaching	BFD	ooo	1	o	>95	no	
Chlorine leaching	BF/BOFD	ooo	1	o	90	no	
NH <sub>4</sub> Cl-leaching	BF/BOFD	o	1	o	90	no	wp
NaOH-leaching	BF/BOFD	oooo	1	o	85	no	
NH <sub>4</sub> Cl-Ezinex	EAFD	oooo	1	o		no	wp
Zincex	Pyrite	oooo	1	o	96	no	wp
UBC	EAFD	ooo	h	o	60	no	wp
Unimetal	EAFD	ooo	h	o	75	no	wp

**Table 68. Criteria and sub-criteria to treat iron-making dusts via pyrometallurgical processes [9]**

<b>A. Type of raw material the process is developed to treat: EAF dust, BOF dust, BF dust, others;</b>
<b>B. Stage of commercialisation:</b>
<ul style="list-style-type: none"> <li>• (o) once tested in laboratory</li> <li>• (oo) intensively tested in laboratory</li> <li>• (ooo) tested on pilot scale</li> <li>• (oooo) in use on technical scale</li> </ul>
<b>C. Zinc/lead product:</b>
<ul style="list-style-type: none"> <li>• (h) refined metal</li> <li>• (l) low grade metal</li> <li>• (d) mixed Zn/Pb oxides dust or zinc compounds</li> </ul>
<b>D. Metallic or oxide iron product</b>
<b>E. Zinc yield</b>
<b>F. Pre-treatment part of the proposed processing:</b>
<ul style="list-style-type: none"> <li>• (a) agglomerating</li> <li>• (dry) drying</li> <li>• (no) no pre-treatment necessary</li> <li>• (roast) roasting</li> <li>• (calc) calcination</li> </ul>
<b>G. Evaluation of environmental effect:</b>
<ul style="list-style-type: none"> <li>• (tw) possible problematic toxic waste generated</li> <li>• (a) possible problematic air pollution</li> <li>• (wp) possible problematic water pollution</li> <li>• (s) soil pollution can be expected.</li> </ul>

**Table 69. Comparing pyrometallurgical technologies to treat iron-making dusts [9]**

	Raw material	Status	Zn product	Fe product	Zn yield	Pre-treatment	Effect on environ.
<b>a) IMMOBILISATION:</b>							
To non toxic waste		o			100	no	Tw
In concrete products					100	no	
In clinker production					100	no	tw
Melting and pouring to blocks					100	dry	a, tw
In BF slag sand		oo			100	calc	a, s
<b>b) ELECTRIC FURNACES</b>							
Tetronics	EAFD	oooo	d	m		dry	a, wp
ZIP	EAFD		h	m		a	a
HI PLAS	EAFD		h	m			a
Scan Dust	EAFD	oooo	h	m		dry	a
Outokumpu	EAFD		d	m			a, wp
Enviroplas (Mintek)	EAFD	ooo	d	m		dry	a
Elkem	Alloy	oooo	l	m		dry	a, wp
<b>c) SHAFT FURNACES</b>							
PTC	BF/BOFD	o	d	m		a	a
Cupola	BFD	oooo	d	m		a	a
Kawasaki	EAFD		d	m		dry	a
DK Recycling	BFD	oooo	d	m		a	a
<b>d) FLAME FURNACES</b>							
IRRS	EAFD	oo	h	o		a	a
Waelz	Zn waste	oooo	d	o		no	a
Inmetco	EAF	oooo	d	m	>90	a	a
Circulating fluidised bed	BF/BOFD	ooo	d	o	80	dry	a
<b>e) FLASH REACTORS</b>							
Contop converter	Pb wastes	oooo	d	o		dry	a
Oxysmelt	Jarosite		d	o		dry	a
Flame/St Joe	EAFD	ooo	d	o	92	dry	a
<b>f) PYROHYDROMETALLURGY</b>							
Pyrohydrolysis-HCl	BF/BOFD	o	d	o	>95	no	a
Pyrohydrolysis-CaCl <sub>2</sub>	EAF/BOF	oo	d	o	40	no	a
Kowa-Seiko	Pyrite	oooo	d	o	97	roast, a	a



## II. Analytical techniques

X-ray powder diffraction (XRPD) patterns were recorded in a Bragg-Brentano geometry in a Bruker D8 Advance diffractometer equipped with a Vantec position sensitive detector. Data collection was carried out at room temperature using monochromatic Co K $\alpha$  radiation ( $\lambda = 0.179026$  nm) in the  $2\theta$  region between  $20^\circ$  and  $100^\circ$ , step size  $0.026$  degrees  $2\theta$ . Step time  $1$  s. The sample was placed on a Si substrate and rotated during measurement. Data evaluation was done with the Bruker program EVA.

X-ray fluorescence (XRF) analyses were done using the Spectrometer configuration Philips PW2400 Rh 60kV + Uniquant 5.16 + SuperQ 3.0G (wavelength dispersive).

Atomic absorption spectrometer (AAS) analyses were conducted using a PerkinElmer AA200 spectrometer.

Inductively coupled plasma optical emission spectrometer (ICP-OES) analyses were conducted using a PerkinElmer Optima 5300dv spectrometer.

### III. AAS analyses of synthetic zinc ferrite leachates

Monster	time	mg Zn/ml	mg Fe/ml	Monster	time	mg Zn/ml	mg Fe/ml
Na <sub>2</sub> CO <sub>3</sub> -L1	0	0.001	0.004	NaOH-L1	0	0.003	0.005
	10	8.05	0.023		5	21.7	0.066
	20	8.94	0.018		10	22.5	0.077
	40	8.94	0.019		20	23.9	0.057
	60	8.83	0.018		40	21.4	0.051
	90	9.36	0.013		60	21.2	0.038
	150	11	0.017		90	22.5	0.048
	210	10.3	0.01		150	21.5	0.041
	300	11.9	0.012		210	21.7	0.019
Na <sub>2</sub> CO <sub>3</sub> -L2	0	0.003	0.004	NaOH-L2	300	21.5	0.031
	1	18.4	0.08		0	0.004	0.005
	10	20.1	0.064		5	20.3	0.075
	20	18.1	0.022		10	19.5	0.07
	40	19.5	0.022		20	20.8	0.062
	60	18.1	0.016		40	21.1	0.051
	90	17.4	0.015		60	20.7	0.067
	150	18.9	0.02		90	20	0.021
	210	18.9	0.019		150	21.2	0.063
	300	20	0.023		210	18.9	0.031
					300	19.2	0.041

The samples taken from the leaching of synthetic zinc ferrite after roasting with NaOH or Na<sub>2</sub>CO<sub>3</sub> were diluted 1:10 and immediately acidified by HNO<sub>3</sub> (1ml concentrated HNO<sub>3</sub> per 10 ml end volume).

The samples were diluted 1000 to 2000x in 0,5 M HNO<sub>3</sub> for determination of zinc concentration. Due to the fact that salt concentrations were extremely high determination of the iron concentration samples dilution couldn't be more than 1:10. Therefore only semi-quantitatively results were obtained due to the high salt levels.

#### IV. ICP-OES analyses

Sample	Lab.Id.	Al	As	B	Ca	Cd	Cr	Cu	Fe	K
Zinc AWW	09/04/015	<	<	0.028	4.72	0.025	<	<	<	1.32
Zinc AL	09/04/016	1.65	0.052	0.044	0.02	0.002	0.002	0.279	0.014	0.404
Zinc AL t10	09/04/017	1.44	0.051	0.035	0.025	0.007	0.001	0.274	0.006	0.337
Zinc ARWW	09/04/018	0.018	0.002	<	0.005	<	0.014	<	<	0.009
Zinc ARL	09/04/019	0.755	0.033	0.008	0.002	<	0.033	0.139	0.029	0.278
Zinc ARL t5	09/04/020	1.81	0.043	0.007	0.013	<	0.069	0.078	0.059	0.169
Zinc ARLWW	09/04/021	0.164	0.005	<	0.002	<	0.153	0.003	0.002	0.016
D Elec	09/04/022	0.699	0.03	0.012	0.005	<	0.259	0.07	0.011	0.83
Zinc BWW	09/04/023	<	<	<	0.124	<	0.006	<	0.005	1.44
Zinc BL	09/04/024	0.016	0.015	0.005	0.015	<	0.031	0.013	<	3.86
Zinc BL t5	09/04/025	0.039	0.013	0.002	0.027	<	0.041	0.008	0.001	1.69
Zinc BRWW	09/04/026	0.003	<	<	0.01	<	0.09	<	<	0.007
Zinc BRL	09/04/027	0.346	0.005	<	<	<	0.996	0.005	0.022	0.209
Zinc BRL t15	09/04/028	0.348	0.004	<	0.005	<	0.904	0.004	0.019	0.181
Zinc BRLWW	09/04/029	0.057	<	<	0.003	<	0.077	<	0.002	0.011

Sample	Lab.Id.	Mg	Mn	Mo	Pb	Si	Sn	Sr	Tl	V	Zn
Zinc AWW	09/04/015	0.158	0.032	<	0.091	<	<	0.027	0.006	<	3.9
Zinc AL	09/04/016	<	<	<	2.83	0.016	<	<	<	<	25.6
Zinc AL t10	09/04/017	<	<	0.025	2.5	0.477	0.129	<	<	0.003	25.4
Zinc ARWW	09/04/018	<	<	0.008	0.003	0.143	0.051	<	<	<	<
Zinc ARL	09/04/019	<	<	0.004	2.09	0.101	0.002	<	<	<	9.31
Zinc ARL t5	09/04/020	<	<	0.019	2	0.977	0.02	<	<	0.007	9.51
Zinc ARLWW	09/04/021	<	<	0.007	0.167	0.668	0.007	<	<	0.003	0.214
D Elec	09/04/022	<	<	0.007	1.13	0.576	0.025	<	<	0.001	14.1
Zinc BWW	09/04/023	0.043	<	0.023	0.001	0.174	0.019	<	<	0.002	0.004
Zinc BL	09/04/024	<	0.001	0.015	2.54	0.01	0.004	<	<	<	20.2
Zinc BL t5	09/04/025	<	0.003	0.196	1.82	0.037	<	<	<	<	15.9
Zinc BRWW	09/04/026	<	0.002	0.048	0.001	0.048	<	<	<	<	0.001
Zinc BRL	09/04/027	<	<	0.008	0.149	0.349	<	<	<	0.004	6.62
Zinc BRL t15	09/04/028	<	<	0.029	0.141	0.349	0.003	<	<	0.012	6.03
Zinc BRLWW	09/04/029	<	<	0.01	0.015	0.157	<	<	<	0.004	0.205

Lab.Id. Sample	09/04/030 Zinc A	09/04/031 Zinc ARLWW	09/04/032 Zinc B	09/04/033 Zinc BRLWW
Al	1.130	2.660	0.295	0.262
As	0.039	<0.001	0.003	<0.001
Ba	0.323	0.672	0.014	0.029
Ca	3.730	3.080	5.260	5.800
Cd	0.013	0.003	<0.001	<0.001
Cr	0.054	0.517	0.295	0.036
Cu	1.040	1.610	0.128	0.143
Fe	17.000	35.300	32.600	35.600
K	0.644	0.160	0.758	0.158
Mg	0.446	0.856	1.780	1.970
Mn	0.292	0.636	4.320	4.560
Mo	0.011	<0.001	0.081	<0.001
Na	0.574	2.970	0.391	4.720
Ni	<0.001	0.376	<0.001	<0.001
Pb	3.250	2.340	1.810	0.565
Si	0.580	2.770	0.861	1.130
Sn	0.158	0.284	0.018	<0.001
Zn	19.200	7.240	15.900	3.980

Lab. Id Sample	09/04/019 Zinc C	09/04/020 Zinc P	09/04/021 Zinc P*
Ag	<	<	<
Al	0.836	0.816	0.931
B	0.019	0.018	0.018
Ba	<	<	<
Bi	<	<	<
Ca	0.009	0.007	0.005
Cd	<	<	<
Co	<	<	<
Cr	0.281	0.255	0.228
Cu	0.128	<	<
Fe	0.018	0.017	0.009
Ga	<	<	<
In	<	<	<
K	0.927	0.965	1.16
Li	<	<	<
Mg	<	<	<
Mn	<	<	<
Ni	<	<	<
Pb	2.25	0.88	0.112
Sr	<	<	<
Tl	<	<	<
Zn	18.3	20.4	4.8

## V. XRF analyses – Zinc A

```
*****
* TU-Delft*Faculty 3mE * Section Structure & Change * R.W.A. Hendrikx *
* Mekelweg 2 * Tel. 015-2782255 * *
* 2628 CD Delft * Fax 015-2786730 * *
*****Semi-Quantitative XRF analysis*****
C:\UQ5\USER\TUD_TA\Jobs\JOB.126 2009-03-12
ZnA Kemperman (Zinc A)
```

Spectrometer's configuration: PW2400 Rh 60kV Measure Prog. : UniQuant

C:\UQ5\USER\TUD\_TA\Appl\AnySample.kap 2009-09-18

Calculated as : Elements Matrix (Shape & ImpFc) : 1|Teflon

X-ray path = Vacuum Film type = No supporting film

Case number = 2 %Rest unknown

Eff.Diam. = 23.0 mm Eff.Area = 415.3 mm2

KnownConc = 0 %

Rest = ? % Oxygen Viewed Mass = 2000.000 mg

Dil/Sample = 0.184 Licowax C Sample Height = 1.00 mm

< means that the concentration is < 50 mg/kg  
<2e means wt% < 2 StdErr. A + or & means: Part of 100% sum

Z	wt%	StdErr	Z	wt%	StdErr	Z	wt%	StdErr
SumBe..F	0	0.052	29+Cu	1.14	0.12	52 Te	<	
11+Na	1.37	0.16	30+Zn	18.61	0.24	53+I	<	
12+Mg	0.118	0.013	31+Ga	0.0088	0.0020	55 Cs	<	
13+Al	0.860	0.056	32+Ge	<		56+Ba	0.342	0.018
14+Si	0.672	0.075	33+As	0.0233	0.0057	SumLa..Lu	0.02	0.12
15+Px	0.162	0.002	34 Se	<		72 Hf	<	
15 P			35+Br	<		73 Ta	<	
16+Sx	2.47	0.18	37 Rb	<		74 W	<2e	0.0081
16 S			38+Sr	0.0290	0.0032	75 Re	<	
17+Cl	9.07	0.34	39+Y	<		76+Os	<	
18 Ar	<		40+Zr	0.0059	0.0020	77 Ir	<2e	0.016
19+K	0.670	0.074	41 Nb	<		78+Pt	<	
20+Ca	3.76	0.22	42+Mo	0.0223	0.0029	79+Au	<	
21 Sc	<		44+Ru	<		80 Hg	<	
22+Ti	0.119	0.013	45 Rh	<		81+Tl	<	
23+V	<		46 Pd	<		82+Pb	3.10	0.04
24+Cr	0.204	0.023	47 Ag	<		83 Bi	<	
25+Mn	0.294	0.015	48+Cd	0.0261	0.0022	90 Th	<	
26+Fe	15.11	0.50	49+In	0.0085	0.0018	92 U	<	
27+Co	<		50+Sn	0.215	0.011	94 Pu		
28+Ni	0.0628	0.0070	51+Sb	0.0131	0.0019	95 Am		

==== Light Elements =====			==== Noble Elements =====			===== Lanthanides =====		
SumBe..F	0	0.052	44+Ru	<		57+La	0.0062	0.0016
4 Be			45 Rh	<		58 Ce	<	
5 B			46 Pd	<		59 Pr	<2e	0.0067
6 C			47 Ag	<		60 Nd	<	
7 N			75 Re	<		62+Sm	<	
8 O			76+Os	<		63 Eu	<	
9 F	<		77 Ir	<2e	0.016	64 Gd	<	
			78+Pt	<		65+Tb	<	
			79+Au	<		66 Dy	<	
						67 Ho	<	
						68+Er	<	
						69 Tm	<	
						70 Yb	<	
						71 Lu	<	

KnownConc= 0

REST=41.50 Oxygen

D/S= 0.184Licowax C

\*\*\*\*\*  
 \* TU-Delft\*Faculty 3mE \* Section Structure & Change \* R.W.A. Hendrikx \*  
 \* Mekelweg 2 \* Tel. 015-2782255 \*  
 \* 2628 CD Delft \* Fax 015-2786730 \*  
 \*\*\*\*\*Semi-Quantitative XRF analysis \*\*\*\*\*  
 C:\UQ5\USER\TUD\_TA\Jobs\JOB.132 2009-03-12  
 batch Kemperman (Zinc AWW)

Spectrometer's configuration: PW2400 Rh 60kV Measure Prog. : UniQuant  
 C:\UQ5\USER\TUD\_TA\Appl\AnySample.kap 2009-09-18  
 Calculated as : Elements Matrix (Shape & ImpFc) : 1|Teflon  
 X-ray path = Vacuum Film type = No supporting film  
 Case number = 2 %Rest unknown  
 Eff.Diam. = 23.0 mm Eff.Area = 415.3 mm2  
 KnownConc = 0 %  
 Rest = ? % Oxygen Viewed Mass = 2000.000 mg  
 Dil/Sample = 0.184 Licowax C Sample Height = 1.00 mm

< means that the concentration is < 50 mg/kg  
 <2e means wt% < 2 StdErr. A + or & means: Part of 100% sum

Z	wt%	StdErr	Z	wt%	StdErr	Z	wt%	StdErr
SumBe..F	0	0.052	29+Cu	1.59	0.14	52 Te	<	
11+Na	0.93	0.20	30+Zn	23.70	0.26	53+I	<	
12+Mg	0.113	0.012	31+Ga	0.0067	0.0028	55 Cs	<	
13+Al	1.05	0.07	32 Ge	<		56+Ba	0.484	0.026
14+Si	0.808	0.090	33+As	0.0378	0.0071	SumLa..Lu	0.02	0.15
15+Px	0.206	0.002	34 Se	<		72 Hf	<	
15 P			35 Br	<		73 Ta	<	
16+Sx	3.24	0.20	37 Rb	<		74+W	<	
16 S			38+Sr	0.0257	0.0029	75 Re	<	
17+Cl	4.03	0.22	39+Y	<		76+Os	<	
18 Ar	<		40+Zr	0.0088	0.0025	77+Ir	<	
19+K	0.226	0.025	41 Nb	<		78+Pt	<	
20+Ca	2.10	0.16	42+Mo	0.0251	0.0035	79+Au	<	
21 Sc	<		44 Ru	<		80 Hg	<	
22+Ti	0.165	0.018	45 Rh	<		81+Tl	<	
23+V	0.0087	0.0010	46 Pd	<		82+Pb	4.29	0.05
24+Cr	0.285	0.032	47 Ag	<		83+Bi	0.0095	0.0035
25+Mn	0.374	0.019	48+Cd	0.0248	0.0025	90 Th	<	
26+Fe	20.76	0.61	49+In	0.0143	0.0022	92 U	<	
27+Co	<		50+Sn	0.308	0.015	94 Pu		
28+Ni	0.0859	0.0095	51+Sb	0.0246	0.0023	95 Am		

==== Light Elements =====			==== Noble Elements =====			===== Lanthanides =====		
SumBe..F	0	0.052	44 Ru	<		57+La	0.0066	0.0016
4 Be			45 Rh	<		58 Ce	<	
5 B			46 Pd	<		59 Pr	<	
6 C			47 Ag	<		60+Nd	0.0088	0.0036
7 N			75 Re	<		62+Sm	<	
8 O			76+Os	<		63 Eu	<	
9 F	<		77+Ir	<		64 Gd	<	
			78+Pt	<		65+Tb	<	
			79+Au	<		66 Dy	<	
						67 Ho	<	
						68+Er	<	
						69 Tm	<	
						70 Yb	<	
						71 Lu	<	

KnownConc= 0

REST=35.06 Oxygen

D/S= 0.184Licowax C

\*\*\*\*\*  
 \* TU-Delft\*Faculty 3mE \* Section Structure & Change \* R.W.A. Hendrikx \*  
 \* Mekelweg 2 \* Tel. 015-2782255 \*  
 \* 2628 CD Delft \* Fax 015-2786730 \*  
 \*\*\*\*\*Semi-Quantitative XRF analysis \*\*\*\*\*  
 C:\UQ5\USER\TUD\_TA\Jobs\JOB.127 2009-03-12  
 Zn A mix 11st Kemperman (Zinc AL)

Spectrometer's configuration: PW2400 Rh 60kV Measure Prog. : UniQuant  
 C:\UQ5\USER\TUD\_TA\Appl\AnySample.kap 2009-09-18  
 Calculated as : Elements Matrix (Shape & ImpFc) : 1|Teflon  
 X-ray path = Vacuum Film type = No supporting film  
 Case number = 2 %Rest unknown  
 Eff.Diam. = 23.0 mm Eff.Area = 415.3 mm2  
 KnownConc = 0 %  
 Rest = ? % Oxygen Viewed Mass = 2000.000 mg  
 Dil/Sample = 0.184 Licowax C Sample Height = 1.00 mm

< means that the concentration is < 50 mg/kg  
 <2e means wt% < 2 StdErr. A + or & means: Part of 100% sum

Z	wt%	StdErr	Z	wt%	StdErr	Z	wt%	StdErr
SumBe..F	0	0.049	29+Cu	1.40	0.13	52 Te	<	
11+Na	10.39	0.33	30+Zn	10.52	0.17	53+I	<	
12+Mg	0.189	0.021	31+Ga	0.0069	0.0016	55 Cs	<	
13+Al	0.981	0.064	32+Ge	<		56+Ba	0.483	0.026
14+Si	0.96	0.11	33+As	0.0243	0.0048	SumLa..Lu	0.01	0.15
15+Px	0.160	0.002	34 Se	<		72 Hf	<	
15 P			35 Br	<		73 Ta	<	
16+Sx	0.448	0.050	37+Rb	<		74+W	<	
16 S			38+Sr	0.0268	0.0030	75 Re	<	
17+Cl	0.536	0.059	39+Y	<		76+Os	<	
18 Ar	<		40+Zr	0.0091	0.0018	77 Ir	<2e	0.015
19+K	0.131	0.015	41 Nb	<		78+Pt	<	
20+Ca	2.11	0.16	42+Mo	0.0081	0.0023	79+Au	<	
21 Sc	<		44 Ru	<		80 Hg	<	
22+Ti	0.182	0.020	45 Rh	<		81+Tl	<	
23+V	0.0066	0.0008	46+Pd	<		82+Pb	3.05	0.04
24+Cr	0.300	0.033	47+Ag	0.0073	0.0018	83+Bi	0.0100	0.0023
25+Mn	0.415	0.021	48+Cd	0.0255	0.0019	90 Th	<	
26+Fe	22.18	0.71	49+In	0.0141	0.0017	92 U	<	
27+Co	<		50+Sn	0.203	0.010	94 Pu		
28+Ni	0.094	0.010	51+Sb	0.0277	0.0019	95 Am		

==== Light Elements =====			==== Noble Elements =====			===== Lanthanides =====		
SumBe..F	0	0.049	44 Ru	<		57+La	0.0054	0.0013
4 Be			45 Rh	<		58 Ce	<	
5 B			46+Pd	<		59 Pr	<	
6 C			47+Ag	0.0073	0.0018	60 Nd	<	
7 N			75 Re	<		62+Sm	<	
8 O			76+Os	<		63 Eu	<	
9 F	<		77 Ir	<2e	0.015	64 Gd	<	
			78+Pt	<		65+Tb	<	
			79+Au	<		66 Dy	<	
						67 Ho	<	
						68+Er	<	
						69 Tm	<	
						70 Yb	<	
						71 Lu	<	

KnownConc= 0

REST=45.08 Oxygen

D/S= 0.184Licowax C



\*\*\*\*\*  
 \* TU-Delft\*Faculty 3mE \* Section Structure & Change \* R.W.A. Hendrikx \*  
 \* Mekelweg 2 \* Tel. 015-2782255 \*  
 \* 2628 CD Delft \* Fax 015-2786730 \*  
 \*\*\*\*\*Semi-Quantitative XRF analysis \*\*\*\*\*  
 C:\UQ5\USER\TUD\_TA\Jobs\JOB.128 2009-03-12  
 Zn A R Kemperman (Zinc AR)

Spectrometer's configuration: PW2400 Rh 60kV Measure Prog. : UniQuant  
 C:\UQ5\USER\TUD\_TA\Appl\AnySample.kap 2009-09-18  
 Calculated as : Elements Matrix (Shape & ImpFc) : 1|Teflon  
 X-ray path = Vacuum Film type = No supporting film  
 Case number = 2 %Rest unknown  
 Eff.Diam. = 23.0 mm Eff.Area = 415.3 mm2  
 KnownConc = 0 %  
 Rest = ? % Oxygen Viewed Mass = 2000.000 mg  
 Dil/Sample = 0.184 Licowax C Sample Height = 1.00 mm

< means that the concentration is < 50 mg/kg  
 <2e means wt% < 2 StdErr. A + or & means: Part of 100% sum

Z	wt%	StdErr	Z	wt%	StdErr	Z	wt%	StdErr
SumBe..F	0	0.038	29+Cu	1.00	0.11	52 Te	<	
11+Na	37.94	0.51	30+Zn	8.54	0.15	53+I	<	
12+Mg	0.0481	0.0053	31+Ga	<		55 Cs	<	
13+Al	0.591	0.038	32+Ge	<		56+Ba	0.360	0.019
14+Si	0.852	0.095	33+As	0.0152	0.0042	SumLa..Lu	0.01	0.14
15+Px	0.180	0.002	34 Se	<		72 Hf	<	
15 P			35 Br	<		73 Ta	<	
16+Sx	0.632	0.070	37+Rb	<		74+W	<	
16 S			38+Sr	0.0218	0.0024	75 Re	<	
17+Cl	0.508	0.056	39+Y	<		76 Os	<	
18 Ar	<		40+Zr	0.0085	0.0015	77 Ir	<2e	0.011
19+K	0.115	0.013	41 Nb	<		78+Pt	<	
20+Ca	1.83	0.15	42+Mo	0.0215	0.0025	79+Au	<	
21 Sc	<		44 Ru	<		80 Hg	<	
22+Ti	0.158	0.018	45 Rh	<		81+Tl	<	
23+V	0.0054	0.0008	46 Pd	<		82+Pb	2.25	0.04
24+Cr	0.604	0.067	47 Ag	<		83+Bi	0.0084	0.0020
25+Mn	0.370	0.019	48+Cd	0.0080	0.0016	90 Th	<	
26+Fe	20.80	0.66	49+In	0.0107	0.0016	92 U	<	
27 Co	<		50+Sn	0.161	0.008	94 Pu		
28+Ni	0.226	0.025	51+Sb	0.0208	0.0018	95 Am		

==== Light Elements =====			==== Noble Elements =====			===== Lanthanides =====		
SumBe..F	0	0.038	44 Ru	<		57+La	0.0055	0.0013
4 Be			45 Rh	<		58 Ce	<	
5 B			46 Pd	<		59 Pr	<	
6 C			47 Ag	<		60 Nd	<	
7 N			75 Re	<		62+Sm	<	
8 O			76 Os	<		63 Eu	<	
9 F	<		77 Ir	<2e	0.011	64 Gd	<	
			78+Pt	<		65+Tb	<	
			79+Au	<		66 Dy	<	
						67 Ho	<	
						68+Er	<	
						69 Tm	<	
						70 Yb	<	
						71 Lu	<	

KnownConc= 0

REST=22.71 Oxygen

D/S= 0.184Licowax C

\*\*\*\*\*  
 \* TU-Delft\*Faculty 3mE \* Section Structure & Change \* R.W.A. Hendrikx \*  
 \* Mekelweg 2 \* Tel. 015-2782255 \*  
 \* 2628 CD Delft \* Fax 015-2786730 \*  
 \*\*\*\*\*Semi-Quantitative XRF analysis \*\*\*\*\*  
 C:\UQ5\USER\TUD\_TA\Jobs\JOB.129 2009-03-12  
 Zn A R L2 Kemperman (Zinc ARL)

Spectrometer's configuration: PW2400 Rh 60kV Measure Prog. : UniQuant  
 C:\UQ5\USER\TUD\_TA\Appl\AnySample.kap 2009-09-18  
 Calculated as : Elements Matrix (Shape & ImpFc) : 1|Teflon  
 X-ray path = Vacuum Film type = No supporting film  
 Case number = 2 %Rest unknown  
 Eff.Diam. = 23.0 mm Eff.Area = 415.3 mm2  
 KnownConc = 0 %  
 Rest = ? % Oxygen Viewed Mass = 2000.000 mg  
 Dil/Sample = 0.184 Licowax C Sample Height = 1.00 mm

< means that the concentration is < 50 mg/kg  
 <2e means wt% < 2 StdErr. A + or & means: Part of 100% sum

Z	wt%	StdErr	Z	wt%	StdErr	Z	wt%	StdErr
SumBe..F	0	0.034	29+Cu	1.70	0.14	52 Te	<	
11+Na	20.03	0.43	30+Zn	7.23	0.14	53+I	<	
12+Mg	0.239	0.027	31+Ga	0.0058	0.0016	55 Cs	<	
13+Al	1.56	0.08	32+Ge	<		56+Ba	0.653	0.035
14+Si	1.80	0.15	33 As	<2e	0.0045	SumLa..Lu	0.01	0.22
15+Px	0.0322	0.0010	34 Se	<		72 Hf	<	
15 P			35 Br	<		73 Ta	<	
16+Sx	0.358	0.040	37+Rb	<		74 W	<	
16 S			38+Sr	0.0372	0.0041	75 Re	<2e	0.0041
17+Cl	0.0884	0.0098	39+Y	<		76+Os	<	
18 Ar	<		40+Zr	0.0133	0.0018	77 Ir	<2e	0.012
19+K	0.0170	0.0019	41 Nb	<		78+Pt	<	
20+Ca	2.91	0.19	42+Mo	0.0073	0.0027	79+Au	<	
21 Sc	<		44 Ru	<		80 Hg	<	
22+Ti	0.278	0.031	45 Rh	<		81+Tl	<	
23 V	<		46 Pd	<		82+Pb	2.42	0.04
24+Cr	1.02	0.11	47+Ag	0.0059	0.0021	83+Bi	0.0156	0.0023
25+Mn	0.634	0.032	48+Cd	0.0169	0.0021	90 Th	<	
26+Fe	35.00	0.89	49+In	0.0229	0.0021	92 U	<	
27+Co	<		50+Sn	0.272	0.014	94 Pu		
28+Ni	0.422	0.047	51+Sb	0.0363	0.0022	95 Am		

==== Light Elements =====			==== Noble Elements =====			===== Lanthanides =====		
SumBe..F	0	0.034	44 Ru	<		57+La	0.0086	0.0014
4 Be			45 Rh	<		58+Ce	<	
5 B			46 Pd	<		59 Pr	<	
6 C			47+Ag	0.0059	0.0021	60 Nd	<	
7 N			75 Re	<2e	0.0041	62+Sm	<	
8 O			76+Os	<		63 Eu	<	
9 F	<		77 Ir	<2e	0.012	64 Gd	<	
			78+Pt	<		65+Tb	<	
			79+Au	<		66 Dy	<	
						67 Ho	<	
						68+Er	<	
						69 Tm	<	
						70+Yb	<	
						71 Lu	<	

KnownConc= 0

REST=23.15 Oxygen

D/S= 0.184Licowax C

\*\*\*\*\*  
 \* TU-Delft\*Faculty 3mE \* Section Structure & Change \* R.W.A. Hendrikx \*  
 \* Mekelweg 2 \* Tel. 015-2782255 \*  
 \* 2628 CD Delft \* Fax 015-2786730 \*  
 \*\*\*\*\*Semi-Quantitative XRF analysis \*\*\*\*\*  
 C:\UQ5\USER\TUD\_TA\Jobs\JOB.130 2009-03-12  
 Zn A R L2 WW Kemperman (Zinc ARL-WW)

Spectrometer's configuration: PW2400 Rh 60kV Measure Prog. : UniQuant  
 C:\UQ5\USER\TUD\_TA\Appl\AnySample.kap 2009-09-18  
 Calculated as : Elements Matrix (Shape & ImpFc) : 1|Teflon  
 X-ray path = Vacuum Film type = No supporting film  
 Case number = 2 %Rest unknown  
 Eff.Diam. = 23.0 mm Eff.Area = 415.3 mm2  
 KnownConc = 0 %  
 Rest = ? % Oxygen Viewed Mass = 2000.000 mg  
 Dil/Sample = 0.184 Licowax C Sample Height = 1.00 mm

< means that the concentration is < 50 mg/kg  
 <2e means wt% < 2 StdErr. A + or & means: Part of 100% sum

Z	wt%	StdErr	Z	wt%	StdErr	Z	wt%	StdErr
SumBe..F	0	0.036	29+Cu	1.99	0.15	52 Te	<	
11+Na	9.01	0.31	30+Zn	8.27	0.14	53+I	<	
12+Mg	0.277	0.031	31+Ga	0.0078	0.0017	55 Cs	<	
13+Al	1.93	0.09	32+Ge	0.0055	0.0014	56+Ba	0.740	0.039
14+Si	2.26	0.17	33 As	<		SumLa..Lu	0.01	0.25
15+Px	0.0312	0.0009	34 Se	<		72+Hf	<	
15 P			35 Br	<		73 Ta	<	
16+Sx	0.243	0.027	37+Rb	<		74+W	<	
16 S			38+Sr	0.0440	0.0049	75 Re	<	
17+Cl	0.0681	0.0076	39+Y	<		76+Os	<	
18 Ar	<		40+Zr	0.0165	0.0020	77 Ir	<2e	0.013
19+K	<		41 Nb	<		78+Pt	<	
20+Ca	3.38	0.21	42 Mo	<2e	0.0027	79+Au	<	
21 Sc	<		44 Ru	<		80 Hg	<	
22+Ti	0.318	0.035	45 Rh	<		81+Tl	<	
23 V	<		46+Pd	<		82+Pb	2.67	0.04
24+Cr	1.09	0.12	47+Ag	0.0145	0.0023	83+Bi	0.0185	0.0025
25+Mn	0.738	0.037	48+Cd	0.0258	0.0023	90 Th	<	
26+Fe	40.37	0.95	49+In	0.0259	0.0022	92 U	<	
27+Co	<		50+Sn	0.320	0.016	94 Pu		
28+Ni	0.490	0.054	51+Sb	0.0432	0.0024	95 Am		

==== Light Elements =====			==== Noble Elements =====			===== Lanthanides =====		
SumBe..F	0	0.036	44 Ru	<		57+La	0.0075	0.0015
4 Be			45 Rh	<		58 Ce	<	
5 B			46+Pd	<		59+Pr	<	
6 C			47+Ag	0.0145	0.0023	60 Nd	<	
7 N			75 Re	<		62+Sm	<	
8 O			76+Os	<		63 Eu	<	
9 F	<		77 Ir	<2e	0.013	64 Gd	<	
			78+Pt	<		65+Tb	<	
			79+Au	<		66 Dy	<	
						67 Ho	<	
						68+Er	<	
						69 Tm	<	
						70+Yb	<	
						71 Lu	<	

KnownConc= 0

REST=25.58 Oxygen

D/S= 0.184Licowax C

## VI. XRF analyses – Zinc B

```
*****
* TU-Delft*Faculty 3mE * Section Structure & Change * R.W.A. Hendrikx *
* Mekelweg 2 * Tel. 015-2782255 *
* 2628 CD Delft * Fax 015-2786730 *
*****Semi-Quantitative XRF analysis*****
C:\UQ5\USER\TUD_TA\Jobs\JOB.133 2009-03-12
Zn B Kemperman (Zinc B)
```

Spectrometer's configuration: PW2400 Rh 60kV Measure Prog. : UniQuant

C:\UQ5\USER\TUD\_TA\Appl\AnySample.kap 2009-09-18

Calculated as : Elements Matrix (Shape & ImpFc) : 1|Teflon

X-ray path = Vacuum Film type = No supporting film

Case number = 2 %Rest unknown

Eff.Diam. = 23.0 mm Eff.Area = 415.3 mm2

KnownConc = 0 %

Rest = ? % Oxygen Viewed Mass = 2000.000 mg

Dil/Sample = 0.184 Licowax C Sample Height = 1.00 mm

< means that the concentration is < 50 mg/kg

<2e means wt% < 2 StdErr. A + or & means: Part of 100% sum

Z	wt%	StdErr	Z	wt%	StdErr	Z	wt%	StdErr
SumBe..F	0	0.058	29+Cu	0.139	0.015	52 Te	<	
11+Na	1.41	0.16	30+Zn	18.14	0.21	53 I	<	
12+Mg	0.525	0.058	31+Ga	0.0128	0.0018	55 Cs	<	
13+Al	0.125	0.008	32 Ge	<		56+Ba	0.0433	0.0048
14+Si	0.514	0.057	33 As	<		SumLa..Lu	0.02	0.23
15+Px	0.0827	0.0015	34 Se	<		72 Hf	<2e	0.0060
15 P			35+Br	0.0163	0.0013	73 Ta	<	
16+Sx	0.548	0.061	37+Rb	0.0074	0.0014	74 W	<2e	0.0091
16 S			38+Sr	0.0051	0.0011	75 Re	<	
17+Cl	0.801	0.089	39+Y	<		76 Os	<	
18 Ar	<		40 Zr	<		77 Ir	<2e	0.011
19+K	0.885	0.098	41 Nb	<		78+Pt	<	
20+Ca	5.14	0.26	42+Mo	0.122	0.014	79+Au	<	
21 Sc	<		44 Ru	<		80 Hg	<	
22+Ti	0.0256	0.0028	45 Rh	<		81+Tl	<	
23+V	0.0111	0.0010	46 Pd	<		82+Pb	1.98	0.03
24+Cr	0.379	0.042	47 Ag	<		83 Bi	<	
25+Mn	5.03	0.12	48+Cd	0.0184	0.0021	90 Th	<	
26+Fe	34.97	0.87	49 In	<		92 U	<	
27+Co	<		50+Sn	0.0177	0.0020	94 Pu		
28+Ni	0.0246	0.0027	51 Sb	<		95 Am		

==== Light Elements =====

SumBe..F	0	0.058
4 Be		
5 B		
6 C		
7 N		
8 O		
9 F	<	

==== Noble Elements =====

44 Ru	<	
45 Rh	<	
46 Pd	<	
47 Ag	<	
75 Re	<	
76 Os	<	
77 Ir	<2e	0.011
78+Pt	<	
79+Au	<	

===== Lanthanides =====

57+La	0.0071	0.0015
58 Ce	<	
59 Pr	<	
60 Nd	<	
62+Sm	<	
63+Eu	<	
64 Gd	<	
65+Tb	<	
66 Dy	<	
67 Ho	<2e	0.014
68+Er	<	
69 Tm	<	
70 Yb	<	
71 Lu	<	

KnownConc= 0

REST=29.02 Oxygen

D/S= 0.184Licowax C

\*\*\*\*\*  
 \* TU-Delft\*Faculty 3mE \* Section Structure & Change \* R.W.A. Hendrikx \*  
 \* Mekelweg 2 \* Tel. 015-2782255 \*  
 \* 2628 CD Delft \* Fax 015-2786730 \*  
 \*\*\*\*\*Semi-Quantitative XRF analysis \*\*\*\*\*  
 C:\UQ5\USER\TUD\_TA\Jobs\JOB.134 2009-03-12  
 Zn B L1st Kemperman (Zinc BL)

Spectrometer's configuration: PW2400 Rh 60kV Measure Prog. : UniQuant  
 C:\UQ5\USER\TUD\_TA\Appl\AnySample.kap 2009-09-18  
 Calculated as : Elements Matrix (Shape & ImpFc) : 11|Sc Ti V  
 X-ray path = Vacuum Film type = No supporting film  
 Case number = 2 %Rest unknown  
 Eff.Diam. = 23.0 mm Eff.Area = 415.3 mm2  
 KnownConc = 0 %  
 Rest = ? % Oxygen Viewed Mass = 2000.000 mg  
 Dil/Sample = 0 Sample Height = 1.00 mm

< means that the concentration is < 50 mg/kg  
 <2e means wt% < 2 StdErr. A + or & means: Part of 100% sum

Z	wt%	StdErr	Z	wt%	StdErr	Z	wt%	StdErr
SumBe..F	0	0.049	29+Cu	0.109	0.012	52 Te	<	
11+Na	5.67	0.25	30+Zn	8.66	0.15	53 I	<	
12+Mg	0.597	0.066	31+Ga	0.0074	0.0013	55 Cs	<	
13+Al	0.174	0.011	32+Ge	<		56+Ba	0.0442	0.0046
14+Si	0.563	0.063	33 As	<		SumLa..Lu	0.04	0.21
15+Px	0.0631	0.0012	34 Se	<		72 Hf	<	
15 P			35 Br	<		73 Ta	<	
16 Sx			37 Rb	<		74 W	<	
16+S	0.0694	0.0035	38 Sr	<		75 Re	<	
17+Cl	0.0795	0.0088	39 Y	<		76 Os	<	
18 Ar	<		40+Zr	0.0058	0.0008	77+Ir	0.0103	0.0050
19+K	0.107	0.012	41+Nb	<		78+Pt	<	
20+Ca	5.41	0.27	42+Mo	0.0256	0.0028	79+Au	<	
21+Sc	<		44 Ru	<		80 Hg	<	
22+Ti	0.0271	0.0030	45 Rh	<		81 Tl	<	
23+V	0.0089	0.0009	46 Pd	<		82+Pb	0.650	0.015
24+Cr	0.334	0.037	47 Ag	<		83+Bi	<	
25+Mn	5.00	0.12	48+Cd	0.0188	0.0017	90 Th	<	
26+Fe	33.89	0.89	49 In	<		92 U	<	
27+Co	<		50+Sn	0.0170	0.0016	94 Pu		
28+Ni	0.0214	0.0024	51 Sb	<		95 Am		

==== Light Elements =====			==== Noble Elements =====			===== Lanthanides =====		
SumBe..F	0	0.049	44 Ru	<		57 La	<	
4 Be			45 Rh	<		58 Ce	<	
5 B			46 Pd	<		59 Pr	<	
6 C			47 Ag	<		60 Nd	<	
7 N			75 Re	<		62+Sm	<	
8 O			76 Os	<		63+Eu	<	
9 F	<		77+Ir	0.0103	0.0050	64 Gd	<	
			78+Pt	<		65+Tb	<	
			79+Au	<		66+Dy	<	
						67+Ho	0.035	0.011
						68+Er	<	
						69+Tm	<	
						70+Yb	<	
						71 Lu	<	

KnownConc= 0 REST=38.38 Oxygen D/S= 0

\*\*\*\*\*  
 \* TU-Delft\*Faculty 3mE \* Section Structure & Change \* R.W.A. Hendrikx \*  
 \* Mekelweg 2 \* Tel. 015-2782255 \*  
 \* 2628 CD Delft \* Fax 015-2786730 \*  
 \*\*\*\*\*Semi-Quantitative XRF analysis \*\*\*\*\*  
 C:\UQ5\USER\TUD\_TA\Jobs\JOB.135 2009-03-12  
 Zn B R Kemperman (Zinc BR)

Spectrometer's configuration: PW2400 Rh 60kV Measure Prog. : UniQuant  
 C:\UQ5\USER\TUD\_TA\Appl\AnySample.kap 2009-09-18  
 Calculated as : Elements Matrix (Shape & ImpFc) : 11|Sc Ti V  
 X-ray path = Vacuum Film type = No supporting film  
 Case number = 2 %Rest unknown  
 Eff.Diam. = 23.0 mm Eff.Area = 415.3 mm2  
 KnownConc = 0 %  
 Rest = ? % Oxygen Viewed Mass = 2000.000 mg  
 Dil/Sample = 0.184 Licowax C Sample Height = 1.00 mm

< means that the concentration is < 50 mg/kg  
 <2e means wt% < 2 StdErr. A + or & means: Part of 100% sum

Z	wt%	StdErr	Z	wt%	StdErr	Z	wt%	StdErr
SumBe..F	0	0.034	29+Cu	0.0862	0.0093	52 Te	<	
11+Na	30.52	0.48	30+Zn	6.51	0.13	53 I	<	
12+Mg	0.307	0.034	31+Ga	0.0079	0.0011	55 Cs	<	
13+Al	0.0847	0.0055	32+Ge	<		56+Ba	0.0409	0.0051
14+Si	0.448	0.050	33 As	<		SumLa..Lu	0.03	0.17
15+Px	0.0682	0.0013	34 Se	<		72 Hf	<2e	0.0036
15 P			35 Br	<		73 Ta	<	
16+Sx	0.0703	0.0078	37 Rb	<		74 W	<	
16 S			38 Sr	<		75 Re	<	
17+Cl	0.0560	0.0062	39 Y	<		76 Os	<	
18 Ar	<		40+Zr	<		77 Ir	<	
19+K	0.0776	0.0086	41+Nb	<		78 Pt	<	
20+Ca	4.44	0.24	42+Mo	0.0219	0.0024	79+Au	<	
21+Sc	<		44 Ru	<		80 Hg	<	
22+Ti	0.0233	0.0026	45 Rh	<		81 Tl	<	
23+V	0.0075	0.0008	46 Pd	<		82+Pb	0.491	0.011
24+Cr	0.523	0.058	47 Ag	<		83 Bi	<	
25+Mn	3.38	0.10	48+Cd	0.0126	0.0015	90 Th	<	
26+Fe	25.75	0.78	49 In	<		92 U	<	
27+Co	<		50+Sn	0.0089	0.0014	94 Pu		
28+Ni	0.0467	0.0052	51 Sb	<		95 Am		

==== Light Elements =====			==== Noble Elements =====			===== Lanthanides =====		
SumBe..F	0	0.034	44 Ru	<		57 La	<	
4 Be			45 Rh	<		58 Ce	<	
5 B			46 Pd	<		59 Pr	<	
6 C			47 Ag	<		60 Nd	<	
7 N			75 Re	<		62+Sm	<	
8 O			76 Os	<		63+Eu	<	
9 F	<		77 Ir	<		64 Gd	<	
			78 Pt	<		65+Tb	<	
			79+Au	<		66 Dy	<	
						67+Ho	0.0286	0.0094
						68+Er	<	
						69+Tm	<	
						70 Yb	<	
						71 Lu	<	

KnownConc= 0

REST=26.97 Oxygen

D/S= 0.184Licowax C

\*\*\*\*\*  
 \* TU-Delft\*Faculty 3mE \* Section Structure & Change \* R.W.A. Hendrikx \*  
 \* Mekelweg 2 \* Tel. 015-2782255 \*  
 \* 2628 CD Delft \* Fax 015-2786730 \*  
 \*\*\*\*\*Semi-Quantitative XRF analysis \*\*\*\*\*  
 C:\UQ5\USER\TUD\_TA\Jobs\JOB.136 2009-03-12  
 Zn B RL2 Kemperman (Zinc BRL)

Spectrometer's configuration: PW2400 Rh 60kV Measure Prog. : UniQuant  
 C:\UQ5\USER\TUD\_TA\Appl\AnySample.kap 2009-09-18  
 Calculated as : Elements Matrix (Shape & ImpFc) : 11|Sc Ti V  
 X-ray path = Vacuum Film type = No supporting film  
 Case number = 2 %Rest unknown  
 Eff.Diam. = 23.0 mm Eff.Area = 415.3 mm2  
 KnownConc = 0 %  
 Rest = ? % Oxygen Viewed Mass = 2000.000 mg  
 Dil/Sample = 0.184 Licowax C Sample Height = 1.00 mm

< means that the concentration is < 50 mg/kg  
 <2e means wt% < 2 StdErr. A + or & means: Part of 100% sum

Z	wt%	StdErr	Z	wt%	StdErr	Z	wt%	StdErr
SumBe..F	0	0.042	29+Cu	0.118	0.013	52 Te	<	
11+Na	16.67	0.40	30+Zn	4.10	0.10	53 I	<	
12+Mg	0.561	0.062	31+Ga	0.0055	0.0012	55 Cs	<	
13+Al	0.0883	0.0057	32 Ge	<		56+Ba	0.0521	0.0051
14+Si	0.428	0.048	33 As	<		SumLa..Lu	0.02	0.21
15+Px	0.0298	0.0009	34 Se	<		72 Hf	<2e	0.0040
15 P			35 Br	<		73 Ta	<	
16+Sx	0.0085	0.0009	37 Rb	<		74 W	<	
16 S			38 Sr	<		75 Re	<	
17+Cl	0.0086	0.0010	39 Y	<		76 Os	<	
18 Ar	<		40+Zr	0.0056	0.0007	77 Ir	<2e	0.0041
19+K	0.0138	0.0015	41+Nb	<		78 Pt	<	
20+Ca	5.08	0.26	42+Mo	0.0060	0.0020	79+Au	<	
21+Sc	<		44 Ru	<		80 Hg	<	
22+Ti	0.0308	0.0034	45 Rh	<		81 Tl	<	
23+V	<		46 Pd	<		82+Pb	0.503	0.012
24+Cr	0.093	0.010	47 Ag	<		83+Bi	<	
25+Mn	4.59	0.11	48+Cd	0.0168	0.0016	90 Th	<	
26+Fe	33.11	0.97	49 In	<		92 U	<	
27+Co	<		50+Sn	0.0127	0.0015	94 Pu		
28+Ni	0.0641	0.0071	51 Sb	<		95 Am		

==== Light Elements =====			==== Noble Elements =====			===== Lanthanides =====		
SumBe..F	0	0.042	44 Ru	<		57 La	<	
4 Be			45 Rh	<		58 Ce	<	
5 B			46 Pd	<		59 Pr	<	
6 C			47 Ag	<		60 Nd	<	
7 N			75 Re	<		62+Sm	<	
8 O			76 Os	<		63+Eu	<	
9 F	<		77 Ir	<2e	0.0041	64 Gd	<	
			78 Pt	<		65+Tb	<	
			79+Au	<		66+Dy	<	
						67 Ho	<2e	0.011
						68+Er	<	
						69+Tm	<	
						70+Yb	<	
						71 Lu	<	

KnownConc= 0

REST=34.41 Oxygen

D/S= 0.184Licowax C



\*\*\*\*\*  
 \* TU-Delft\*Faculty 3mE \* Section Structure & Change \* R.W.A. Hendrikx \*  
 \* Mekelweg 2 \* Tel. 015-2782255 \*  
 \* 2628 CD Delft \* Fax 015-2786730 \*  
 \*\*\*\*\*Semi-Quantitative XRF analysis \*\*\*\*\*  
 C:\UQ5\USER\TUD\_TA\Jobs\JOB.137 2009-03-12  
 Zn B RL2 WW Kemperman (Zinc BRLWW)

Spectrometer's configuration: PW2400 Rh 60kV Measure Prog. : UniQuant  
 C:\UQ5\USER\TUD\_TA\Appl\AnySample.kap 2009-09-18  
 Calculated as : Elements Matrix (Shape & ImpFc) : 11|Sc Ti V  
 X-ray path = Vacuum Film type = No supporting film  
 Case number = 2 %Rest unknown  
 Eff.Diam. = 23.0 mm Eff.Area = 415.3 mm2  
 KnownConc = 0 %  
 Rest = ? % Oxygen Viewed Mass = 2000.000 mg  
 Dil/Sample = 0.184 Licowax C Sample Height = 1.00 mm

< means that the concentration is < 50 mg/kg  
 <2e means wt% < 2 StdErr. A + or & means: Part of 100% sum

Z	wt%	StdErr	Z	wt%	StdErr	Z	wt%	StdErr
SumBe..F	0	0.048	29+Cu	0.128	0.014	52 Te	<	
11+Na	7.61	0.29	30+Zn	4.46	0.11	53 I	<	
12+Mg	0.649	0.072	31 Ga	<		55 Cs	<	
13+Al	0.113	0.007	32 Ge	<		56+Ba	0.0631	0.0045
14+Si	0.621	0.069	33 As	<		SumLa..Lu	0.02	0.23
15+Px	0.0353	0.0009	34 Se	<		72 Hf	<	
15 P			35 Br	<		73 Ta	<	
16 Sx	<		37 Rb	<		74 W	<	
16 S			38 Sr	<		75 Re	<	
17 Cl	<		39 Y	<		76 Os	<	
18 Ar	<		40+Zr	0.0055	0.0008	77+Ir	<	
19+K	0.0099	0.0011	41+Nb	<		78+Pt	<	
20+Ca	5.98	0.29	42+Mo	0.0072	0.0021	79 Au	<	
21+Sc	<		44 Ru	<		80 Hg	<	
22+Ti	0.0351	0.0039	45 Rh	<		81 Tl	<	
23 V	<		46 Pd	<		82+Pb	0.596	0.014
24+Cr	0.0637	0.0071	47+Ag	<		83+Bi	<	
25+Mn	5.22	0.12	48+Cd	0.0202	0.0017	90 Th	<	
26+Fe	37.82	1.04	49 In	<		92 U	<	
27+Co	<		50+Sn	0.0191	0.0016	94 Pu		
28+Ni	0.0717	0.0080	51+Sb	<		95 Am		

==== Light Elements =====			==== Noble Elements =====			===== Lanthanides =====		
SumBe..F	0	0.048	44 Ru	<		57 La	<	
4 Be			45 Rh	<		58 Ce	<	
5 B			46 Pd	<		59 Pr	<	
6 C			47+Ag	<		60 Nd	<	
7 N			75 Re	<		62+Sm	<	
8 O			76 Os	<		63+Eu	<	
9 F	<		77+Ir	<		64 Gd	<	
			78+Pt	<		65+Tb	<	
			79 Au	<		66+Dy	<	
						67 Ho	<2e	0.012
						68+Er	<	
						69+Tm	<	
						70 Yb	<	
						71 Lu	<	

KnownConc= 0

REST=36.46 Oxygen

D/S= 0.184Licowax C

## VII. XRF analyses – Zinc A\*

```
*****
* TU-Delft*Faculty 3mE * Section Structure & Change * R.W.A. Hendrikx *
* Mekelweg 2 * Tel. 015-2782255 * *
* 2628 CD Delft * Fax 015-2786730 * *
*****Semi-Quantitative XRF analysis*****
C:\UQ5\USER\TUD_TA\Jobs\JOB.312 2009-06-19
Zn AL Kemperman18jun09 (Zinc AL*)
```

Spectrometer's configuration: PW2400 Rh 60kV Measure Prog. : UniQuant

C:\UQ5\USER\TUD\_TA\Appl\AnySample.kap 2009-09-18

Calculated as : Elements Matrix (Shape & ImpFc) : 1|Teflon

X-ray path = Vacuum Film type = No supporting film

Case number = 2 %Rest unknown

Eff.Diam. = 23.0 mm Eff.Area = 415.3 mm2

KnownConc = 0 %

Rest = ? % Oxygen Viewed Mass = 18000.00 mg

Dil/Sample = 0 Sample Height = 5.00 mm

< means that the concentration is < 50 mg/kg

<2e means wt% < 2 StdErr. A + or & means: Part of 100% sum

Z	wt%	StdErr	Z	wt%	StdErr	Z	wt%	StdErr
SumBe..F	0	0.038	29+Cu	1.57	0.14	52 Te	<	
11+Na	11.05	0.33	30+Zn	13.10	0.18	53+I	<	
12+Mg	0.878	0.097	31+Ga	0.0070	0.0021	55 Cs	<	
13+Al	3.55	0.12	32+Ge	<		56+Ba	0.607	0.032
14+Si	3.40	0.20	33+As	0.0326	0.0056	SumLa..Lu	0.02	0.18
15+Px	0.185	0.002	34 Se	<		72 Hf	<	
15 P			35 Br	<		73 Ta	<	
16+Sx	0.572	0.063	37 Rb	<		74+W	<	
16 S			38+Sr	0.0281	0.0031	75 Re	<	
17+Cl	0.672	0.075	39+Y	<		76+Os	<	
18 Ar	<		40+Zr	0.0115	0.0022	77 Ir	<2e	0.018
19+K	0.152	0.017	41 Nb	<		78+Pt	<	
20+Ca	2.53	0.18	42+Mo	0.0131	0.0030	79+Au	<	
21 Sc	<		44 Ru	<		80 Hg	<	
22+Ti	0.216	0.024	45 Rh	<		81+Tl	<	
23+V	0.0058	0.0010	46 Pd	<		82+Pb	3.75	0.05
24+Cr	0.386	0.043	47+Ag	0.0079	0.0022	83+Bi	0.0154	0.0028
25+Mn	0.516	0.026	48+Cd	0.0315	0.0024	90 Th	<	
26+Fe	27.39	0.71	49+In	0.0216	0.0021	92 U	<	
27 Co	<		50+Sn	0.263	0.013	94 Pu		
28+Ni	0.114	0.013	51+Sb	0.0313	0.0023	95 Am		

==== Light Elements =====

SumBe..F	0	0.038
4 Be		
5 B		
6 C		
7 N		
8 O		
9 F	<	

==== Noble Elements =====

44 Ru	<	
45 Rh	<	
46 Pd	<	
47+Ag	0.0079	0.0022
75 Re	<	
76+Os	<	
77 Ir	<2e	0.018
78+Pt	<	
79+Au	<	

===== Lanthanides =====

57+La	0.0099	0.0016
58 Ce	<	
59 Pr	<2e	0.0079
60 Nd	<	
62+Sm	<	
63+Eu	<	
64 Gd	<	
65+Tb	<	
66 Dy	<	
67 Ho	<	
68+Er	<	
69+Tm	<	
70 Yb	<	
71 Lu	<	

KnownConc= 0

REST=28.88 Oxygen

D/S= 0

\*\*\*\*\*  
 \* TU-Delft\*Faculty 3mE \* Section Structure & Change \* R.W.A. Hendrikx \*  
 \* Mekelweg 2 \* Tel. 015-2782255 \* \*  
 \* 2628 CD Delft \* Fax 015-2786730 \* \*  
 \*\*\*\*\*Semi-Quantitative XRF analysis \*\*\*\*\*  
 C:\UQ5\USER\TUD\_TA\Jobs\JOB.362 2009-07-17  
 Zn AR Kemperrman 17jul09 (Zinc AR\*)

Spectrometer's configuration: PW2400 Rh 60kV Measure Prog. : UniQuant  
 C:\UQ5\USER\TUD\_TA\Appl\AnySample.kap 2009-09-18

Calculated as : Elements Matrix (Shape & ImpFc) : 1|Teflon

X-ray path = Vacuum Film type = No supporting film

Case number = 2 %Rest unknown

Eff.Diam. = 23.0 mm Eff.Area = 415.3 mm2

KnownConc = 0 %

Rest = ? % Oxygen

Viewed Mass = 18000.00 mg

Dil/Sample = 0 Sample Height = 5.00 mm

< means that the concentration is < 50 mg/kg

<2e means wt% < 2 StdErr. A + or & means: Part of 100% sum

Z	wt%	StdErr	Z	wt%	StdErr	Z	wt%	StdErr
SumBe..F	0	0.036	29+Cu	0.421	0.045	52 Te	<	
11+Na	17.90	0.40	30+Zn	4.38	0.11	53+I	<	
12+Mg	0.139	0.015	31+Ga	<		55 Cs	<	
13+Al	0.783	0.051	32+Ge	<		56+Ba	0.147	0.008
14+Si	0.91	0.10	33+As	0.0112	0.0025	SumLa..Lu	0.011	0.069
15+Px	0.0681	0.0011	34 Se	<		72 Hf	<	
15 P			35 Br	<		73 Ta	<	
16+Sx	0.275	0.031	37 Rb	<		74 W	<	
16 S			38+Sr	0.0098	0.0011	75 Re	<	
17+Cl	0.169	0.019	39+Y	<		76+Os	<	
18 Ar	<		40+Zr	<		77 Ir	<	
19+K	0.0601	0.0067	41 Nb	<		78 Pt	<	
20+Ca	0.856	0.095	42+Mo	<		79+Au	<	
21 Sc	<		44 Ru	<		80 Hg	<	
22+Ti	0.0778	0.0086	45 Rh	<		81+Tl	<	
23+V	<		46 Pd	<		82+Pb	1.07	0.03
24+Cr	0.131	0.015	47 Ag	<		83+Bi	<	
25+Mn	0.173	0.009	48+Cd	<		90 Th	<	
26+Fe	9.65	0.45	49+In	<		92 U	<	
27 Co	<		50+Sn	0.0802	0.0040	94 Pu		
28+Ni	0.0403	0.0045	51+Sb	0.0068	0.0013	95 Am		

==== Light Elements =====

SumBe..F	0	0.036
4 Be		
5 B		
6 C		
7 N		
8 O		
9 F	<	

==== Noble Elements =====

44 Ru	<
45 Rh	<
46 Pd	<
47 Ag	<
75 Re	<
76+Os	<
77 Ir	<
78 Pt	<
79+Au	<

===== Lanthanides =====

57+La	<	
58 Ce	<	
59 Pr	<	
60 Nd	<	
62+Sm	<	
63 Eu	<	
64 Gd	<	
65+Tb	<	
66 Dy	<	
67 Ho	<2e	0.0046
68+Er	<	
69+Tm	<	
70+Yb	<	
71 Lu	<	

KnownConc= 0

REST=62.62 Oxygen

D/S= 0

\*\*\*\*\*  
 \* TU-Delft\*Faculty 3mE \* Section Structure & Change \* R.W.A. Hendrikx \*  
 \* Mekelweg 2 \* Tel. 015-2782255 \*  
 \* 2628 CD Delft \* Fax 015-2786730 \*  
 \*\*\*\*\*Semi-Quantitative XRF analysis \*\*\*\*\*  
 C:\UQ5\USER\TUD\_TA\Jobs\JOB.363 2009-07-17  
 Zn ARL Kemperrman 17jul09 (Zinc ARL\*)

Spectrometer's configuration: PW2400 Rh 60kV Measure Prog. : UniQuant  
 C:\UQ5\USER\TUD\_TA\Appl\AnySample.kap 2009-09-18  
 Calculated as : Elements Matrix (Shape & ImpFc) : 1|Teflon  
 X-ray path = Vacuum Film type = No supporting film  
 Case number = 2 %Rest unknown  
 Eff.Diam. = 23.0 mm Eff.Area = 415.3 mm2  
 KnownConc = 0 %  
 Rest = ? % Oxygen Viewed Mass = 18000.00 mg  
 Dil/Sample = 0 Sample Height = 5.00 mm

< means that the concentration is < 50 mg/kg  
 <2e means wt% < 2 StdErr. A + or & means: Part of 100% sum

Z	wt%	StdErr	Z	wt%	StdErr	Z	wt%	StdErr
SumBe..F	0	0.030	29+Cu	0.877	0.095	52 Te	<	
11+Na	12.08	0.35	30+Zn	4.13	0.10	53+I	<	
12+Mg	0.379	0.042	31 Ga	<		55 Cs	<	
13+Al	2.05	0.09	32+Ge	<		56+Ba	0.405	0.021
14+Si	2.53	0.17	33 As	<		SumLa..Lu	0.01	0.14
15+Px	0.0131	0.0006	34 Se	<		72 Hf	<	
15 P			35 Br	<		73 Ta	<	
16+Sx	0.158	0.018	37 Rb	<		74 W	<	
16 S			38+Sr	0.0216	0.0024	75 Re	<	
17+Cl	0.0458	0.0051	39+Y	<		76+Os	<	
18 Ar	<		40+Zr	0.0098	0.0013	77 Ir	<2e	0.0089
19+K	0.0066	0.0011	41 Nb	<		78 Pt	<	
20+Ca	1.93	0.16	42 Mo	<		79+Au	<	
21 Sc	<		44 Ru	<		80 Hg	<	
22+Ti	0.186	0.021	45 Rh	<		81 Tl	<	
23 V	<		46 Pd	<		82+Pb	1.79	0.03
24+Cr	0.293	0.033	47 Ag	<		83+Bi	0.0094	0.0016
25+Mn	0.419	0.021	48+Cd	0.0154	0.0016	90 Th	<	
26+Fe	22.20	0.73	49+In	0.0132	0.0015	92 U	<	
27+Co	<		50+Sn	0.169	0.008	94 Pu		
28+Ni	0.092	0.010	51+Sb	0.0205	0.0018	95 Am		

==== Light Elements =====			==== Noble Elements =====			===== Lanthanides =====		
SumBe..F	0	0.030	44 Ru	<		57+La	0.0060	0.0011
4 Be			45 Rh	<		58 Ce	<	
5 B			46 Pd	<		59 Pr	<	
6 C			47 Ag	<		60 Nd	<	
7 N			75 Re	<		62+Sm	<	
8 O			76+Os	<		63 Eu	<	
9 F	<		77 Ir	<2e	0.0089	64 Gd	<	
			78 Pt	<		65+Tb	<	
			79+Au	<		66 Dy	<	
						67 Ho	<	
						68+Er	<	
						69 Tm	<	
						70 Yb	<	
						71 Lu	<	

KnownConc= 0

REST=50.15 Oxygen

D/S= 0

# VIII. XRF analyses – Zinc B\*

```
*****
* TU-Delft*Faculty 3mE * Section Structure & Change * R.W.A. Hendrikx *
* Mekelweg 2 * Tel. 015-2782255 * *
* 2628 CD Delft * Fax 015-2786730 * *
*****Semi-Quantitative XRF analysis*****
C:\UQ5\USER\TUD_TA\Jobs\JOB.313 2009-06-19
Zn BL Kemperman18jun09 (Zinc BL*)
```

Spectrometer's configuration: PW2400 Rh 60kV Measure Prog. : UniQuant

C:\UQ5\USER\TUD\_TA\Appl\AnySample.kap 2009-09-18

Calculated as : Elements Matrix (Shape & ImpFc) : 12|Cr-Fe-Ni

X-ray path = Vacuum Film type = No supporting film

Case number = 2 %Rest unknown

Eff.Diam. = 23.0 mm Eff.Area = 415.3 mm2

KnownConc = 0 %

Rest = ? % Oxygen Viewed Mass = 18000.00 mg

Dil/Sample = 0 Sample Height = 5.00 mm

< means that the concentration is < 50 mg/kg

<2e means wt% < 2 StdErr. A + or & means: Part of 100% sum

Z	wt%	StdErr	Z	wt%	StdErr	Z	wt%	StdErr
SumBe..F	0	0.036	29+Cu	0.129	0.014	52 Te	<	
11+Na	11.80	0.34	30+Zn	10.47	0.16	53 I	<	
12+Mg	2.21	0.16	31 Ga	<		55+Cs	0.0077	0.0033
13+Al	0.622	0.040	32 Ge	<		56+Ba	0.0687	0.0043
14+Si	1.90	0.15	33 As	<		SumLa..Lu	0	0.26
15+Px	0.0621	0.0013	34 Se	<		72 Hf	<	
15 P			35 Br	<		73 Ta	<	
16 Sx			37 Rb	<		74 W	<	
16+S	0.0570	0.0029	38 Sr	<		75 Re	<	
17+Cl	0.094	0.010	39 Y	<		76 Os	<	
18+Ar	0.0086	0.0016	40+Zr	<		77+Ir	<	
19+K	0.222	0.025	41+Nb	<		78+Pt	<	
20+Ca	6.16	0.28	42+Mo	0.0351	0.0039	79 Au	<	
21 Sc	<		44 Ru	<		80 Hg	<	
22+Ti	0.0308	0.0034	45 Rh	<		81 Tl	<	
23+V	0.0128	0.0011	46 Pd	<		82+Pb	0.821	0.019
24+Cr	0.403	0.045	47 Ag	<		83+Bi	0.0068	0.0023
25+Mn	5.77	0.12	48+Cd	0.0220	0.0020	90 Th	<	
26+Fe	40.16	0.88	49 In	<		92 U	<	
27+Co	<		50+Sn	0.0188	0.0019	94 Pu	<	
28+Ni	0.0109	0.0032	51+Sb	<		95 Am	<	

==== Light Elements ===== Noble Elements ===== Lanthanides =====

SumBe..F	0	0.036	44 Ru	<	57 La	<
4 Be			45 Rh	<	58 Ce	<
5 B			46 Pd	<	59 Pr	<
6 C			47 Ag	<	60 Nd	<
7 N			75 Re	<	62+Sm	<
8 O			76 Os	<	63+Eu	<
9 F	<		77+Ir	<	64 Gd	<
			78+Pt	<	65+Tb	<
			79 Au	<	66 Dy	<
					67 Ho	<
					68+Er	<
					69 Tm	<
					70 Yb	<
					71 Lu	<

KnownConc= 0

REST=18.88 Oxygen

D/S= 0

\*\*\*\*\*  
 \* TU-Delft\*Faculty 3mE \* Section Structure & Change \* R.W.A. Hendrikx \*  
 \* Mekelweg 2 \* Tel. 015-2782255 \*  
 \* 2628 CD Delft \* Fax 015-2786730 \*  
 \*\*\*\*\*Semi-Quantitative XRF analysis \*\*\*\*\*  
 C:\UQ5\USER\TUD\_TA\Jobs\JOB.364 2009-07-17  
 Zn BR Kemperrman 17jul09 (Zinc BR\*)

Spectrometer's configuration: PW2400 Rh 60kV Measure Prog. : UniQuant  
 C:\UQ5\USER\TUD\_TA\Appl\AnySample.kap 2009-09-18  
 Calculated as : Elements Matrix (Shape & ImpFc) : 1|Teflon  
 X-ray path = Vacuum Film type = No supporting film  
 Case number = 2 %Rest unknown  
 Eff.Diam. = 23.0 mm Eff.Area = 415.3 mm2  
 KnownConc = 0 %  
 Rest = ? % Oxygen Viewed Mass = 18000.00 mg  
 Dil/Sample = 0 Sample Height = 5.00 mm

< means that the concentration is < 50 mg/kg  
 <2e means wt% < 2 StdErr. A + or & means: Part of 100% sum

Z	wt%	StdErr	Z	wt%	StdErr	Z	wt%	StdErr
SumBe..F	0	0.030	29+Cu	0.0497	0.0054	52 Te	<	
11+Na	19.50	0.41	30+Zn	3.29	0.09	53 I	<	
12+Mg	0.353	0.039	31+Ga	<		55 Cs	<	
13+Al	0.145	0.009	32 Ge	<		56+Ba	0.0105	0.0039
14+Si	0.453	0.050	33 As	<		SumLa..Lu	0.013	0.093
15+Px	0.0297	0.0008	34 Se	<		72 Hf	<	
15 P			35 Br	<		73 Ta	<	
16+Sx	0.0283	0.0031	37 Rb	<		74 W	<	
16 S			38+Sr	<		75 Re	<	
17+Cl	0.0294	0.0033	39 Y	<		76 Os	<	
18 Ar	<		40 Zr	<		77 Ir	<	
19+K	0.0443	0.0049	41 Nb	<		78 Pt	<	
20+Ca	2.03	0.16	42+Mo	0.0089	0.0013	79+Au	<	
21 Sc	<		44+Ru	<		80 Hg	<	
22+Ti	0.0103	0.0011	45 Rh	<		81 Tl	<	
23+V	<		46 Pd	<		82+Pb	0.248	0.006
24+Cr	0.141	0.016	47 Ag	<		83+Bi	<	
25+Mn	1.91	0.07	48+Cd	0.0066	0.0009	90 Th	<	
26+Fe	13.96	0.58	49 In	<		92 U	<	
27+Co	<		50+Sn	0.0056	0.0009	94 Pu		
28+Ni	0.0139	0.0015	51 Sb	<		95 Am		

==== Light Elements =====			==== Noble Elements =====			===== Lanthanides =====		
SumBe..F	0	0.030	44+Ru	<		57+La	<	
4 Be			45 Rh	<		58 Ce	<	
5 B			46 Pd	<		59 Pr	<	
6 C			47 Ag	<		60 Nd	<	
7 N			75 Re	<		62+Sm	<	
8 O			76 Os	<		63+Eu	<	
9 F	<		77 Ir	<		64+Gd	<	
			78 Pt	<		65+Tb	<	
			79+Au	<		66 Dy	<	
						67 Ho	<2e	0.0055
						68+Er	<	
						69+Tm	<	
						70 Yb	<	
						71 Lu	<	

KnownConc= 0 REST=57.72 Oxygen D/S= 0

\*\*\*\*\*  
 \* TU-Delft\*Faculty 3mE \* Section Structure & Change \* R.W.A. Hendrikx \*  
 \* Mekelweg 2 \* Tel. 015-2782255 \*  
 \* 2628 CD Delft \* Fax 015-2786730 \*  
 \*\*\*\*\*Semi-Quantitative XRF analysis \*\*\*\*\*  
 C:\UQ5\USER\TUD\_TA\Jobs\JOB.365 2009-07-17  
 Zn BRL Kemperrman 17jul09 (Zinc BRL\*)

Spectrometer's configuration: PW2400 Rh 60kV Measure Prog. : UniQuant  
 C:\UQ5\USER\TUD\_TA\Appl\AnySample.kap 2009-09-18  
 Calculated as : Elements Matrix (Shape & ImpFc) : 12|Cr-Fe-Ni  
 X-ray path = Vacuum Film type = No supporting film  
 Case number = 2 %Rest unknown  
 Eff.Diam. = 23.0 mm Eff.Area = 415.3 mm2  
 KnownConc = 0 %  
 Rest = ? % Oxygen Viewed Mass = 18000.00 mg  
 Dil/Sample = 0 Sample Height = 5.00 mm

< means that the concentration is < 50 mg/kg  
 <2e means wt% < 2 StdErr. A + or & means: Part of 100% sum

Z	wt%	StdErr	Z	wt%	StdErr	Z	wt%	StdErr
SumBe..F	0	0.039	29+Cu	0.0747	0.0081	52 Te	<	
11+Na	8.26	0.30	30+Zn	5.93	0.12	53 I	<	
12+Mg	0.852	0.095	31+Ga	<		55+Cs	0.0131	0.0029
13+Al	0.252	0.016	32 Ge	<		56+Ba	0.0473	0.0038
14+Si	0.784	0.087	33 As	<		SumLa..Lu	0	0.17
15+Px	0.0126	0.0006	34 Se	<		72 Hf	<	
15 P			35 Br	<		73 Ta	<	
16 Sx	<		37 Rb	<		74 W	<	
16 S			38 Sr	<		75 Re	<	
17+Cl	<		39 Y	<		76 Os	<	
18 Ar	<		40+Zr	<		77+Ir	<	
19 K	<		41+Nb	<		78+Pt	<	
20+Ca	4.01	0.23	42+Mo	0.0111	0.0019	79+Au	<	
21+Sc	<		44 Ru	<		80 Hg	<	
22+Ti	0.0227	0.0025	45 Rh	<		81 Tl	<	
23+V	<		46 Pd	<		82+Pb	0.276	0.006
24+Cr	0.150	0.017	47 Ag	<		83+Bi	<	
25+Mn	3.80	0.10	48+Cd	0.0153	0.0015	90 Th	<	
26+Fe	27.28	0.86	49 In	<		92 U	<	
27+Co	<		50+Sn	0.0118	0.0014	94 Pu		
28+Ni	0.0134	0.0021	51+Sb	<		95 Am		

==== Light Elements =====			==== Noble Elements =====			===== Lanthanides =====		
SumBe..F	0	0.039	44 Ru	<		57 La	<	
4 Be			45 Rh	<		58 Ce	<	
5 B			46 Pd	<		59 Pr	<	
6 C			47 Ag	<		60 Nd	<	
7 N			75 Re	<		62+Sm	<	
8 O			76 Os	<		63+Eu	<	
9 F	<		77+Ir	<		64+Gd	<	
			78+Pt	<		65+Tb	<	
			79+Au	<		66 Dy	<	
						67 Ho	<	
						68+Er	<	
						69 Tm	<	
						70 Yb	<	
						71 Lu	<	

KnownConc= 0 REST=48.16 Oxygen D/S= 0

## IX. Weight of samples before and after experiments

**Table 70. Weights of samples at start and end of their corresponding experiment**

<b>Experiments</b>	<b>Start (g)</b>	<b>End (g)</b>
<b>Zinc A</b>		
Water washing of Zinc A	1685	1432
Leaching of water washed Zinc A	1401.9	1066.4
Roasting of water washed and leached Zinc A	1014.27 (554.72)	1389.2
Leaching of roasted Zinc A	1344.7	828.69
Water washing of leached and roasted Zinc A	300	250.47
<b>Zinc B</b>		
Leaching of water washed Zinc B	1503.5	1362.6
Roasting of water washed and leached Zinc B	1263.82 (870.62)	1915.4
Leaching of roasted Zinc B	1787.2	1304.1
Water washing of leached and roasted Zinc B	300	256.9
<b>Zinc A*</b>		
Water washing of Zinc A*	200	161.8
Leaching of water washed Zinc A*	161.8	130
Roasting of water washed and leached Zinc A*	45.169 (41.665)	75.578
Leaching of roasted Zinc A*	103.31	51.56
<b>Zinc B*</b>		
Leaching of water washed Zinc B*	200	184
Roasting of water washed and leached Zinc B*	56.50192 (65.818)	111.23
Leaching of roasted Zinc B*	95	50.74



## X. Overview Zinc A

XRF analysis of Zinc A products from processing steps (wt%, rest % oxygen);

Abbreviations: Zinc A as received raw material; Zinc A-WW Filter cake after first water washing step; Zinc AL, Filter cake after first leaching step; Zinc AR, calcine product; Zinc ARL, Filter cake of secondary leaching step; Zinc ARL-WW, Filter cake after secondary water washing step.

Element	Zinc A	Zinc AWW	Zinc AL	Zinc AR	Zinc ARL	Zinc ARLWW
Ag	-	-	0.01	-	0.01	0.01
Al	0.86	1.05	0.98	0.59	1.56	1.93
As	0.02	0.04	0.02	0.02	-	-
Ba	0.34	0.48	0.48	0.36	0.65	0.74
Bi	-	0.01	0.01	0.01	0.02	0.02
Br	-	-	-	-	-	-
Ca	3.76	2.10	2.11	1.83	2.91	3.38
Cd	0.03	0.02	0.03	0.01	0.02	0.03
Cl	9.07	4.03	0.54	0.51	0.09	0.07
Cr	0.20	0.29	0.30	0.60	1.02	1.09
Cs	-	-	-	-	-	0.00
Cu	1.14	1.59	1.40	1.00	1.70	1.99
Fe	15.11	20.76	22.18	20.80	35.00	40.37
Ga	0.01	0.01	0.01	-	0.01	0.01
Ge	-	-	-	-	-	0.01
In	0.01	0.01	0.01	0.01	0.02	0.03
K	0.67	0.23	0.13	0.12	0.02	-
La	0.01	0.01	0.01	0.01	0.01	0.01
Mg	0.12	0.11	0.19	0.05	0.24	0.28
Mn	0.29	0.37	0.42	0.37	0.63	0.74
Mo	0.02	0.03	0.01	0.02	0.01	-
Na	1.37	0.93	10.39	37.94	20.03	9.01
Nd	-	0.01	-	-	-	-
Ni	0.06	0.09	0.09	0.23	0.42	0.49
Pb	3.10	4.29	3.05	2.25	2.42	2.67
Px	0.16	0.21	0.16	0.18	0.03	0.03
Rb	-	-	-	-	-	-
Ru	-	-	-	-	-	-
Sb	0.01	0.02	0.03	0.02	0.04	0.04
Si	0.67	0.81	0.96	0.85	1.80	2.26
Sn	0.22	0.31	0.20	0.16	0.27	0.32
Sr	0.03	0.03	0.03	0.02	0.04	0.04
Sx	2.47	3.24	0.45	0.63	0.36	0.24
Ti	0.12	0.17	0.18	0.16	0.28	0.32
V	-	0.01	0.01	0.01	-	-
Zn	18.61	23.70	10.52	8.54	7.23	8.27
Zr	0.01	0.09	0.01	0.01	0.01	0.02

**Recovery of elements per processing step of Zinc A (%); X denotes newly detected elements**

<b>Element</b>	<b>Water washing 1</b>	<b>Leaching 1</b>	<b>Leaching 2</b>	<b>Water washing 2</b>
<b>Ag</b>	-	X	X	-105.19
<b>Al</b>	-3.76	28.93	-62.67	-3.29
<b>As</b>	-37.87	51.10	100.00	-
<b>Ba</b>	-20.27	24.09	-11.78	5.39
<b>Bi</b>	X	19.93	-14.45	0.99
<b>Br</b>	-	-	-	-
<b>Ca</b>	52.54	23.57	2.00	3.02
<b>Cd</b>	19.25	21.79	-30.19	-27.46
<b>Cl</b>	62.24	89.88	89.28	35.68
<b>Cr</b>	-18.73	19.93	-4.07	10.78
<b>Cs</b>	-	-	-	-
<b>Cu</b>	-18.53	33.02	-4.77	2.27
<b>Fe</b>	-16.76	18.73	-3.70	3.70
<b>Ga</b>	35.30	21.66	X	-12.28
<b>Ge</b>	-	-	-	X
<b>In</b>	-42.97	25.00	-31.89	5.57
<b>K</b>	71.33	55.91	90.89	100.00
<b>La</b>	9.54	37.76	3.64	27.19
<b>Mg</b>	18.62	-27.22	-206.21	3.23
<b>Mn</b>	-8.11	15.60	-5.60	2.81
<b>Mo</b>	4.35	75.45	79.08	100.00
<b>Na</b>	42.31	-749.80	67.46	62.44
<b>Nd</b>	X	100.00	-	-
<b>Ni</b>	-16.24	16.76	-15.07	3.06
<b>Pb</b>	-17.60	45.92	33.72	7.88
<b>Px</b>	-8.06	40.92	88.98	19.10
<b>Rb</b>	-	-	-	-
<b>Ru</b>	-	-	-	-
<b>Sb</b>	-59.58	14.35	-7.55	0.64
<b>Si</b>	-2.18	9.63	-30.20	-4.83
<b>Sn</b>	-21.74	49.87	-4.11	1.78
<b>Sr</b>	24.69	20.68	-5.16	1.25
<b>Sx</b>	-11.47	89.48	65.09	43.33
<b>Ti</b>	-17.83	16.10	-8.43	4.50
<b>V</b>	X	42.30	100.00	-
<b>Zn</b>	-8.23	66.24	47.83	4.50
<b>Zr</b>	-1167.53	92.13	3.57	-3.58

ICP-OES analysis of Zinc A products from processing steps;

Abbreviations: Zinc AWW, sample of lixiviant of water washing batch 3; Zinc AL, lixiviant after first leaching step; Zinc ALB3-10; lixiviant of first leaching step at 10 minutes; Zinc AR-WW, lixiviant of water washing calcine product; Zinc ARL, lixiviant of secondary leaching step; Zinc ARL lixiviant of secondary leaching step; Zinc ARB5-5, lixiviant of secondary leaching step at 5 minutes of batch 5; Zinc ARL-WW, lixiviant of secondary water washing step.

g/L	ZincAWW	ZincAL <sup>#</sup>	ZincALB3-10	ZincAR-WW	ZincARL <sup>#</sup>	ZincARB5-5	ZincARL-WW
Al	<	1.65	1.44	0.018	0.755	1.81	0.164
As	<	0.052	0.051	0.002	0.033	0.043	0.005
B	0.028	0.044	0.035	<	0.008	0.007	<
Ca	4.72	0.02	0.025	0.005	0.002	0.013	0.002
Cd	0.025	0.002	0.007	<	<	<	<
Cr	<	0.002	0.001	0.014	0.033	0.069	0.153
Cu	<	0.279	0.274	<	0.139	0.078	0.003
Fe	<	0.014	0.006	<	0.029	0.059	0.002
K	1.32	0.404	0.337	0.009	0.278	0.169	0.016
Mg	0.158	<	<	<	<	<	<
Mn	0.032	<	<	<	<	<	<
Mo	<	<	0.025	0.008	0.004	0.019	0.007
Pb	0.091	2.83	2.5	0.003	2.09	2	0.167
Si	<	0.016	0.477	0.143	0.101	0.977	0.668
Sn	<	<	0.129	0.051	0.002	0.02	0.007
Sr	0.027	<	<	<	<	<	<
Tl	0.006	<	<	<	<	<	<
V	<	<	0.003	<	<	0.007	0.003
Zn	3.9	25.6	25.4	<	9.31	9.51	0.214

# Lixiviant derived from 6 batches

ICP-OES analysis of acidic digestion using aqua regia of Zinc A and filter cake Zinc ARL-WW.

wt%	ZincA	ZincARL-WW
Al	1.130	2.660
As	0.039	<0.001
Ba	0.323	0.672
Ca	3.730	3.080
Cd	0.013	0.003
Cr	0.054	0.517
Cu	1.040	1.610
Fe	17.000	35.300
K	0.644	0.160
Mg	0.446	0.856
Mn	0.292	0.636
Mo	0.011	<0.001
Na	0.574	2.970
Ni	<0.001	0.376
Pb	3.250	2.340
Si	0.580	2.770
Sn	0.158	0.284
Zn	19.200	7.240
total	48.484	61.474

## XI. Overview Zinc B

XRF analysis of Zinc B products from processing steps (wt%, rest % oxygen); Zinc B as received raw material; Zinc BL, filter cake after first leaching step; Zinc BR, calcine product; Zinc BRL, filter cake of secondary leaching step; Zinc BRL-WW, filter cake after first water washing step.

Element	Zinc B	Zinc BL	Zinc BR	Zinc BRL	Zinc BRL-WW
Al	0.13	0.17	0.08	0.09	0.11
As	-	-	-	-	-
Ba	0.04	0.04	0.04	0.05	0.06
Bi	-	-	-	-	-
Br	0.02	-	-	-	-
Ca	5.14	5.41	4.44	5.08	5.98
Cd	0.02	0.02	0.01	0.02	0.02
Cl	0.80	0.08	0.06	0.01	-
Cr	0.38	0.33	0.52	0.09	0.06
Cs	-	-	-	-	-
Cu	0.14	0.11	0.09	0.12	0.13
Fe	34.97	33.89	25.75	33.11	37.82
Ga	0.01	0.01	0.01	0.01	-
Ge	-	-	-	-	-
In	-	-	-	-	-
K	0.89	0.11	0.08	0.01	0.01
La	0.01	-	-	-	-
Mg	0.53	0.60	0.31	0.56	0.65
Mn	5.03	5.00	3.38	4.59	5.22
Mo	0.12	0.03	0.02	0.01	0.01
Na	1.41	5.67	30.52	16.67	7.61
Nd	-	-	-	-	-
Ni	0.02	0.02	0.05	0.06	0.07
Pb	1.98	0.65	0.49	0.50	0.60
Px	0.08	0.06	0.07	0.03	0.04
Rb	0.01	-	-	-	-
Ru	-	-	-	-	-
Sb	-	-	-	-	-
Si	0.51	0.56	0.45	0.43	0.62
Sn	0.02	0.02	0.01	0.01	0.02
Sr	0.01	-	-	-	-
Sx	0.55	0.07	0.07	0.01	-
Ti	0.03	0.03	0.02	0.03	0.04
V	0.01	0.01	0.01	-	-
Zn	18.14	8.66	6.51	4.10	4.46
Zr	-	0.01	-	0.01	0.06

Recovery of elements per processing step of Zinc B (%); X denotes newly detected elements.

Element	Leaching 1	Leaching 2	Water washing
Al	-26.15	23.93	-9.59
As	-	-	-
Ba	7.49	7.05	-3.71
Bi	-	-	-
Br	100.00	-	-
Ca	4.61	16.51	-0.81
Cd	7.40	2.71	-2.96
Cl	91.01	88.79	100.00
Cr	20.13	87.02	41.35
Cs	-	-	-
Cu	28.93	0.11	7.11
Fe	12.17	6.17	2.18
Ga	47.61	49.20	100.00
Ge	-	-	-
In	-	-	-
K	89.04	87.02	38.57
La	100.00	-	-
Mg	-3.06	-33.34	0.93
Mn	9.91	0.91	2.61
Mo	80.98	80.01	-2.76
Na	-264.44	60.14	60.91
Nd	-	-	-
Ni	21.16	-0.16	4.21
Pb	70.25	25.25	-1.47
Px	30.85	68.12	-1.44
Rb	100.00	-	-
Ru	-	-	-
Sb	-	-	-
Si	0.73	30.29	-24.25
Sn	12.96	-4.13	-28.79
Sr	100.00	-	-
Sx	88.52	91.18	100.00
Ti	4.06	3.54	2.41
V	27.33	100.00	-
Zn	56.73	54.04	6.85
Zr	-	-	-741.05

**ICP-OES analysis of Zinc B products from processing steps;**

**Abbreviations:** Zinc B-WW, sample of lixiviant of water washing; Zinc BL, lixiviant after first leaching step; Zinc BLB3-5; lixiviant of first leaching step at 5 minutes; Zinc BR-WW, lixiviant of water washing calcine product; Zinc BRL, lixiviant of secondary leaching step; Zinc BRL filtrate of secondary leaching step; Zinc BRL2-15, lixiviant of secondary leaching step at 15 minutes of batch 2; Zinc BRL-WW, lixiviant of secondary water washing step.

g/L	ZincB-WW	ZincBL <sup>#</sup>	ZincBLB3-5	ZincBR-WW	ZincBRL <sup>#</sup>	ZincBRL2-15	ZincBRL-WW
Al	<	0.016	0.039	0.003	0.346	0.348	0.057
As	<	0.015	0.013	<	0.005	0.004	<
B	<	0.005	0.002	<	<	<	<
Ca	0.124	0.015	0.027	0.01	<	0.005	0.003
Cd	<	<	<	<	<	<	<
Cr	0.006	0.031	0.041	0.09	0.996	0.904	0.077
Cu	<	0.013	0.008	<	0.005	0.004	<
Fe	0.005	<	0.001	<	0.022	0.019	0.002
K	1.44	3.86	1.69	0.007	0.209	0.181	0.011
Mg	0.043	<	<	<	<	<	<
Mn	<	0.001	0.003	0.002	<	<	<
Mo	0.023	0.015	0.196	0.048	0.008	0.029	0.01
Pb	0.001	2.54	1.82	0.001	0.149	0.141	0.015
Si	0.174	0.01	0.037	0.048	0.349	0.349	0.157
Sn	0.019	0.004	<	<	<	0.003	<
Sr	<	<	<	<	<	<	<
Tl	<	<	<	<	<	<	<
V	0.002	<	<	<	0.004	0.012	0.004
Zn	0.004	20.2	15.9	0.001	6.62	6.03	0.205

<sup>#</sup> Lixiviant derived from 6 batches

**ICP-OES analysis of acidic digestion using aqua regia of Zinc B and filter cake ZincBRL-WW.**

wt%	ZincB	ZincBRL-WW
Al	0.295	0.262
As	0.003	<0.001
Ba	0.014	0.029
Ca	5.260	5.800
Cd	<0.001	<0.001
Cr	0.295	0.036
Cu	0.128	0.143
Fe	32.600	35.600
K	0.758	0.158
Mg	1.780	1.970
Mn	4.320	4.560
Mo	0.081	<0.001
Na	0.391	4.720
Ni	<0.001	<0.001
Pb	1.810	0.565
Si	0.861	1.130
Sn	0.018	<0.001
Zn	15.900	3.980
total	64.514	58.953

## XII. Overview Zinc AL\*

XRF analysis of Zinc A \* products from processing steps (without normalisation to 100%); Zinc A as received raw material; Zinc AL\*, filter cake after first leaching step; Zinc AR\*, calcine product; Zinc ARL\*, filter cake of secondary leaching step.

Element	Zinc A	Zinc A-WW	Zinc AL*	Zinc AR*	Zinc ARL*
Ag	-	-	0.01	-	-
Al	0.86	1.05	0.55	0.78	2.05
As	0.02	0.04	0.03	0.01	-
Ba	0.34	0.48	0.61	0.15	0.41
Bi	-	0.01	0.02	-	0.01
Br	-	-	-	-	-
Ca	3.76	2.10	2.53	0.86	1.93
Cd	0.03	0.02	0.03	-	0.02
Cl	9.07	4.03	0.67	0.17	0.05
Cr	0.20	0.29	0.39	0.13	0.29
Cs	-	-	-	-	-
Cu	1.14	1.59	1.57	0.42	0.88
Fe	15.11	20.76	27.14	9.65	22.20
Ga	0.01	0.01	0.01	-	-
Ge	-	-	-	-	-
In	0.01	0.01	0.02	-	0.01
K	0.67	0.23	0.15	0.60	0.01
La	0.01	0.01	0.01	-	-
Mg	0.12	0.11	0.88	0.14	0.38
Mn	0.29	0.37	0.52	0.17	0.42
Mo	0.02	0.03	0.01	-	-
Na	1.37	0.93	11.05	17.90	12.08
Nd	-	0.01	-	-	-
Ni	0.06	0.09	0.11	0.04	0.09
Pb	3.10	4.29	3.75	1.07	1.79
Px	0.16	0.21	0.19	0.07	0.01
Rb	-	-	-	-	-
Ru	-	-	-	-	-
Sb	0.01	0.02	0.03	0.01	0.02
Si	0.67	0.81	3.40	0.91	2.53
Sn	0.22	0.31	0.26	0.08	0.17
Sr	0.03	0.03	0.01	0.01	0.02
Sx	2.47	3.24	0.57	0.28	0.16
Ti	0.12	0.17	0.22	0.08	0.19
V	-	0.01	0.01	-	-
Zn	18.61	23.70	13.10	4.38	4.13
Zr	0.01	0.09	0.01	-	0.01

**Recovery of elements per processing step of Zinc A\***  
(%); X denotes newly detected elements.

<b>Element</b>	<b>waterwashing</b>	<b>Leaching 1</b>	<b>Leaching 2</b>
<b>Ag</b>	-	X	-
<b>Al</b>	1.23	57.99	-30.67
<b>As</b>	-31.25	X	X
<b>Ba</b>	-14.49	-0.59	-37.50
<b>Bi</b>	-	-30.02	X
<b>Br</b>	-	-	-
<b>Ca</b>	54.82	3.37	-12.53
<b>Cd</b>	23.13	-1.88	X
<b>Cl</b>	64.05	86.63	86.47
<b>Cr</b>	-13.02	-8.63	-11.63
<b>Cs</b>	-	-	-
<b>Cu</b>	-12.83	20.80	-3.97
<b>Fe</b>	-11.15	-4.86	-14.81
<b>Ga</b>	38.41	16.20	-
<b>Ge</b>	-	-	-
<b>In</b>	-36.10	-21.16	X
<b>K</b>	72.71	46.05	99.45
<b>La</b>	13.88	-20.31	-
<b>Mg</b>	22.53	-523.22	-36.08
<b>Mn</b>	-2.91	-10.66	-20.88
<b>Mo</b>	8.94	58.14	100.00
<b>Na</b>	45.08	X	66.32
<b>Nd</b>	X	100.00	-
<b>Ni</b>	-10.66	-6.45	-13.93
<b>Pb</b>	-11.96	29.89	16.51
<b>Px</b>	-2.87	27.97	90.40
<b>Rb</b>	-	-	-
<b>Ru</b>	-	-	-
<b>Sb</b>	-51.92	-2.06	-50.46
<b>Si</b>	2.73	-237.52	-38.76
<b>Sn</b>	-15.89	31.51	-5.17
<b>Sr</b>	28.31	64.11	-10.00
<b>Sx</b>	-6.12	85.84	71.33
<b>Ti</b>	-12.17	-5.00	-19.32
<b>V</b>	X	46.53	-
<b>Zn</b>	-3.03	55.66	52.94
<b>Zr</b>	-1106.64	89.52	X



### XIII. Overview Zinc BL\*

XRF analysis of Zinc B \*products from processing steps (without normalization to 100%); Zinc B as received raw material; Zinc BL\*, filter cake after first leaching step; Zinc BR\*, calcine product; Zinc BRL\*, filter cake of secondary leaching step.

Wt%	Zinc B	Zinc BL*	Zinc BR*	Zinc BRL*
<b>Al</b>	0.13	0.62	0.15	0.25
<b>As</b>	-	-	-	-
<b>Ba</b>	0.04	0.07	0.01	0.05
<b>Bi</b>	-	0.01	-	-
<b>Br</b>	0.02	-	-	-
<b>Ca</b>	5.14	6.16	2.03	4.01
<b>Cd</b>	0.02	0.02	0.01	0.02
<b>Cl</b>	0.80	0.09	0.09	-
<b>Cr</b>	0.38	0.40	0.14	0.15
<b>Cs</b>	-	-	-	0.01
<b>Cu</b>	0.14	0.13	0.05	0.07
<b>Fe</b>	34.97	40.16	13.96	27.28
<b>Ga</b>	0.01	-	-	-
<b>Ge</b>	-	-	-	-
<b>In</b>	-	-	-	-
<b>K</b>	0.89	0.22	0.04	-
<b>La</b>	0.01	-	-	-
<b>Mg</b>	0.53	2.21	0.35	0.85
<b>Mn</b>	5.03	5.77	1.91	3.80
<b>Mo</b>	0.12	0.04	0.01	0.01
<b>Na</b>	1.41	11.80	19.50	8.26
<b>Nd</b>	-	-	-	-
<b>Ni</b>	0.02	0.01	0.01	0.01
<b>Pb</b>	1.98	0.82	0.25	0.28
<b>Px</b>	0.08	0.06	0.03	0.01
<b>Rb</b>	0.01	-	-	-
<b>Ru</b>	-	-	-	-
<b>Sb</b>	-	-	-	-
<b>Si</b>	0.51	1.90	0.45	0.78
<b>Sn</b>	0.02	0.02	0.01	0.01
<b>Sr</b>	0.01	-	-	-
<b>Sx</b>	0.55	0.06	0.03	-
<b>Ti</b>	0.03	0.03	0.01	0.02
<b>V</b>	0.01	0.01	-	-
<b>Zn</b>	18.14	10.47	3.29	5.93
<b>Zr</b>	-	-	-	-

Recovery of elements per processing step of Zinc B\* (%); X denotes newly detected elements.

Element	Leaching 1	Leaching 2
Al	-357.24	7.18
As	-	-
Ba	-45.79	-140.59
Bi	X	-
Br	100.00	-
Ca	-10.12	-5.50
Cd	-9.87	-23.81
Cl	89.22	100.00
Cr	2.29	43.18
Cs	X	X
Cu	14.72	19.73
Fe	-5.53	-4.37
Ga	100.00	-
Ge	-	-
In	-	-
K	76.95	100.00
La	100.00	-
Mg	-286.81	-28.90
Mn	-5.41	-6.26
Mo	73.56	33.39
Na	-669.00	77.38
Nd	-	-
Ni	59.28	48.51
Pb	61.90	40.56
Px	31.00	77.34
Rb	100.00	-
Ru	-	-
Sb	-	-
Si	-239.67	7.57
Sn	6.55	-12.54
Sr	100.00	-
Sx	90.44	100.00
Ti	-10.55	-17.70
V	-5.96	-
Zn	46.96	3.74
Zr	-	-

#### XIV. Overview absolute weight differences after roasting experiments

**Table 71. Absolute weight differences in gram after roasting**

<b>Element</b>	<b>Zinc AR</b>	<b>Zinc BR</b>
<b>Ag</b>	-0.07	-
<b>Al</b>	-1.74	-0.58
<b>As</b>	-0.04	-
<b>Ba</b>	0.10	0.22
<b>Bi</b>	0.02	-
<b>Br</b>	-	-
<b>Ca</b>	4.02	16.67
<b>Cd</b>	-0.15	0.00
<b>Cl</b>	1.62	0.07
<b>Cr</b>	5.35	5.80
<b>Cs</b>	-	-
<b>Cu</b>	-0.31	0.27
<b>Fe</b>	63.99	64.91
<b>Ga</b>	-0.07	0.06
<b>Ge</b>	-	-
<b>In</b>	0.01	-
<b>K</b>	0.27	0.13
<b>La</b>	0.02	-
<b>Mg</b>	-1.25	-1.66
<b>Mn</b>	0.93	1.55
<b>Mo</b>	0.22	0.10
<b>Na</b>	181.03	135.24
<b>Nd</b>	-	-
<b>Ni</b>	2.19	0.62
<b>Pb</b>	0.32	1.19
<b>Px</b>	0.88	0.51
<b>Rb</b>	-	-
<b>Ru</b>	-	-
<b>Sb</b>	0.01	-
<b>Si</b>	2.10	1.47
<b>Sn</b>	0.18	-0.04
<b>Sr</b>	0.03	-
<b>Sx</b>	4.24	0.47
<b>Ti</b>	0.35	0.10
<b>V</b>	0.01	0.03
<b>Zn</b>	11.94	15.25
<b>Zr</b>	0.03	-0.07

It is expected that no weightloss occurs during the roasting experiments. According to this assumption the absolute weight difference for elements should be 0.00. A positive value denotes that during the roasting experiment respective element increased, whereas a negative value denotes a decrease in weight compared to initial input (Zinc AL or Zinc BL)

## XV. Cementation and electrowinning

ICP-OES analysis of a mix with equivalent volume parts of lixiviants ZincAL, Zinc ARL, Zinc BL and Zinc BRL, respectively Z P start, Z P end; lixiviants before and after cementation step. Z P depleted; lixiviant after 3 trials of zinc electrolyzes.

g/l	Z P start	Z P end	Z P depleted
<b>Ag</b>	<	<	<
<b>Al</b>	0.836	0.816	0.931
<b>B</b>	0.019	0.018	0.018
<b>Ba</b>	<	<	<
<b>Bi</b>	<	<	<
<b>Ca</b>	0.009	0.007	0.005
<b>Cd</b>	<	<	<
<b>Co</b>	<	<	<
<b>Cr</b>	0.281	0.255	0.228
<b>Cu</b>	0.128	<	<
<b>Fe</b>	0.018	0.017	0.009
<b>Ga</b>	<	<	<
<b>In</b>	<	<	<
<b>K</b>	0.927	0.965	1.16
<b>Li</b>	<	<	<
<b>Mg</b>	<	<	<
<b>Mn</b>	<	<	<
<b>Ni</b>	<	<	<
<b>Pb</b>	2.25	0.88	0.112
<b>Sr</b>	<	<	<
<b>Tl</b>	<	<	<
<b>Zn</b>	18.3	20.4	4.8

## XVI. Electrowinning

$$V_{cell} = V_0 + V_{iR} + \eta_a + \eta_c \quad [47]$$

The total cell voltage can be subdivided according to equation 39.

Where  $V_0$  is the decomposition voltage,  $\eta_a$  and  $\eta_c$  the anodic and cathodic overpotentials, and  $V_{iR}$  is the ohmic electrolyte iR drop (equation 40).

$$V_{iR} = Il / k \quad [48]$$

Where  $I$  is the current density,  $l$  the electrode separation and  $k$  the conductivity.

To understand the differences in conductivity one must look into transport of ions. Transport of ions induced by application of a potential field are accelerated according to equations 41-43.

$$F_1 = z \cdot e \cdot F = m \cdot a \quad [49]$$

Where  $F$  denotes the force applied by an electric potential  $V$  on an ion with valence  $z$  and total charge  $z \cdot e$ . This ion with charge  $z \cdot e$  and mass  $m$ , is according to the law of Newton accelerated,  $a$ . Because an ion with radius  $r$  in a medium with viscosity  $\eta$  moves with velocity  $v$  a frictional force against the movement direction is exerted. For this frictional force the law of Stokes applies.

$$F_2 = 6 \cdot \pi \cdot \eta \cdot r \cdot v \quad [50]$$

Because after a short time  $F_1$  is  $F_2$ .

$$v = \frac{z \cdot e \cdot F}{6 \cdot \pi \cdot \eta \cdot r} \quad [51]$$

So, ions with similar charge and larger radius will move slower than ions with a small radius. By applying a higher current density the force becomes larger, hence the increase in conductivity. By increasing the temperature, the viscosity of the solution decreases. A decrease in viscosity directly decreases the frictional force, hence reducing the specific energy consumption.

# **XVII. Mass balance - Zinc A and B**

Appendix XVII-XXV are for mass balancing calculations when processing 4700 ton zinc bearing residues, superimposing results obtained and described in Appendix IX

<b>Zinc A (Rest % Oxygen)</b>			<b>Zinc B (Rest % oxygen)</b>		
<b>Element (XRF)</b>	<b>Zinc A (wt%)</b>	<b>Zinc A (tons)</b>	<b>Element (XRF)</b>	<b>Zinc B (wt%)</b>	<b>Zinc B (tons)</b>
Ag	-	-	Al	0.13	2.05
Al	0.86	20.04	As	-	-
As	0.02	0.54	Ba	0.04	0.71
Ba	0.34	7.97	Bi	-	-
Bi	-	-	Br	0.02	0.27
Br	-	-	Ca	5.14	84.36
Ca	3.76	87.62	Cd	0.02	0.30
Cd	0.03	0.61	Cl	0.80	13.15
Cl	9.07	211.37	Cr	0.38	6.22
Cr	0.20	4.75	Cs	-	-
Cs	-	-	Cu	0.14	2.28
Cu	1.14	26.57	Fe	34.97	573.92
Fe	15.11	352.12	Ga	0.01	0.21
Ga	0.01	0.21	Hf	-	-
Ge	-	-	I	-	-
In	0.01	0.20	K	0.89	14.52
K	0.67	15.61	La	0.01	-
La	0.01	0.14	Mg	0.53	8.62
Mg	0.12	2.75	Mn	5.03	82.55
Mn	0.29	6.85	Mo	0.12	2.00
Mo	0.02	0.52	Na	1.41	23.14
Na	1.37	31.93	Nb	-	-
Nd	-	-	Ni	0.02	0.40
Ni	0.06	1.46	Pb	1.98	32.50
Pb	3.10	72.24	Px	0.08	1.36
Px	0.16	3.78	Rb	0.01	0.12
Rb	-	-	S	-	-
Ru	-	-	Sb	-	-
Sb	0.01	0.31	Si	0.51	8.44
Si	0.67	15.66	Sn	0.02	0.29
Sn	0.22	5.01	Sr	0.01	-
Sr	0.03	0.68	Sx	0.55	8.99
Sx	2.47	57.56	Ti	0.03	0.42
Ti	0.12	2.77	V	0.01	0.18
V	-	-	Zn	18.14	297.71
Zn	18.61	433.69	Zr	-	-
Zr	0.01	0.14			
<b>Total</b>	<b>58.49</b>	<b>1363.10</b>	<b>Total</b>	<b>70.98</b>	<b>1164.71</b>



Zinc A chemical composition			Zinc B composition		
Element (ICP)	ZincA (wt%)	Zinc A (tons)	Element (ICP)	Zinc B (wt%)	Zinc B (tons)
Al	1.13	26.33	Al	0.30	4.84
As	0.04	0.91	As	0.00	0.05
Ba	0.32	7.53	Ba	0.01	0.23
Ca	3.73	86.92	Ca	5.26	86.33
Cd	0.01	0.30	Cd	<0.001	-
Cr	0.05	1.26	Cr	0.30	4.84
Cu	1.04	24.24	Cu	0.13	2.10
Fe	17.00	396.17	Fe	32.60	535.02
K	0.64	15.01	K	0.76	12.44
Mg	0.45	10.39	Mg	1.78	29.21
Mn	0.29	6.80	Mn	4.32	70.90
Mo	0.01	0.26	Mo	0.08	1.33
Na	0.57	13.38	Na	0.39	6.42
Ni	<0.001	-	Ni	<0.001	-
Pb	3.25	75.74	Pb	1.81	29.71
Si	0.58	13.52	Si	0.86	14.13
Sn	0.16	3.68	Sn	0.02	0.30
Zn	19.20	447.44	Zn	15.90	260.95



### XVIII. Mass balance - Water washing step

Water washing product of Zinc A (rest % oxygen)					Water washing product of Zinc A extrapolated		
XRF	Zinc A (wt%)	Zinc A (tons)	Water washing (%)	Lixiviant-1A (tons)	ICP	Zn A WW batch 3 (g/L)	Lixiviant-Zinc AWW (tons)
<b>Ca</b>	3.76	87.62	52.54	46.03	<b>B</b>	0.028	0.326
<b>Cd</b>	0.03	0.61	19.25	0.12	<b>Ca</b>	4.720	54.997
<b>Cl</b>	9.07	211.37	62.24	131.56	<b>Cd</b>	0.025	0.291
<b>Ga</b>	0.01	0.21	35.30	0.07	<b>K</b>	1.320	15.381
<b>K</b>	0.67	15.61	71.33	11.14	<b>Mg</b>	0.158	1.841
<b>La</b>	0.01	0.14	9.54	0.01	<b>Mn</b>	0.032	0.373
<b>Mg</b>	0.12	2.75	18.62	0.51	<b>Pb</b>	0.091	1.060
<b>Mo</b>	0.02	0.52	4.35	0.02	<b>Zn</b>	3.900	45.443
<b>Na</b>	1.37	31.93	42.31	13.51			
<b>Sr</b>	0.03	0.68	24.69	0.17			

XIX. Mass balance - First leaching step

Leaching product Zinc AL, extrapolated from XRF (rest % oxygen)					Leaching product Zinc BL, extrapolated from XRF (rest % oxygen)				
XRF	Zinc A- WW (wt%)	Zinc A- WW (tons)	Recovery (%)	Lixiviant- AL	XRF	Zinc B (wt%)	Zinc B (tons)	Recovery (%)	Lixiviant- BL
Al	1.05	20.79	28.93	6.02	Ba	0.04	0.71	7.49	0.05
As	0.04	0.75	51.10	0.38	Br	0.02	0.27	100.00	0.27
Ba	0.48	9.59	24.09	2.31	Ca	5.14	84.36	4.61	3.89
Bi	0.01	0.19	19.93	0.04	Cd	0.02	0.30	7.40	0.02
Ca	2.10	41.59	23.57	9.80	Cl	0.80	13.15	91.01	11.96
Cd	0.02	0.49	21.79	0.11	Cr	0.38	6.22	20.13	1.25
Cl	4.03	79.81	89.88	71.73	Cu	0.14	2.28	28.93	0.66
Cr	0.29	5.64	19.93	1.12	Fe	34.97	573.92	12.17	69.85
Cu	1.59	31.49	33.02	10.40	Ga	0.01	0.21	47.61	0.10
Fe	20.76	411.13	18.73	77.01	K	0.89	14.52	89.04	12.93
Ga	0.01	0.13	21.66	0.03	La	0.01	0.12	100.00	0.12
In	0.01	0.28	25.00	0.07	Mn	5.03	82.55	9.91	8.18
K	0.23	4.48	55.91	2.50	Mo	0.12	2.00	80.98	1.62
La	0.01	0.13	37.76	0.05	Ni	0.02	0.40	21.16	0.09
Mn	0.37	7.41	15.60	1.16	Pb	1.98	32.50	70.25	22.83
Mo	0.03	0.50	75.45	0.38	Px	0.08	1.36	30.85	0.42
Nd	0.01	0.17	100.00	0.17	Rb	0.01	0.12	100.00	0.12
Ni	0.09	1.70	16.76	0.29	Si	0.51	8.44	0.73	0.06
Pb	4.29	84.96	45.92	39.01	Sn	0.02	0.29	12.96	0.04
Px	0.21	4.08	40.92	1.67	Sr	0.01	0.08	100.00	0.08
Sb	0.02	0.49	14.35	0.07	Sx	0.55	8.99	88.52	7.96
Si	0.81	16.00	9.63	1.54	Ti	0.03	0.42	4.06	0.02
Sn	0.31	6.10	49.87	3.04	V	0.01	0.18	27.33	0.05
Sr	0.03	0.51	20.68	0.11	Zn	18.14	297.71	56.73	168.90
Sx	3.24	64.16	89.48	57.42					
Ti	0.17	3.27	16.10	0.53					
V	0.01	0.17	42.30	0.07					
Zn	23.70	469.35	66.24	310.88					
Zr	0.09	1.74	92.13	1.61					

Lixiviant Zinc AL and extrapolated recovery (ICP)						Lixiviant Zinc BL and extrapolated recovery (ICP)					
ICP	Zinc A-WW (wt%)	Zinc A-WW (tons)	Lixiviant Zinc AL (g/L)	Recovery (%)	Lixiviant Zinc AL (Tons)	ICP	Zinc B (wt%)	Zinc A-WW (tons)	Lixiviant Zinc BL (g/L)	Recovery (%)	Lixiviant Zinc BL (Tons)
<b>Al</b>	1.05	20.79	1.65	62.41	12.98	<b>Al</b>	0.13	2.05	0.016	4.29	0.09
<b>As</b>	0.04	0.75	0.052	54.64	0.41	<b>Ca</b>	5.14	84.36	0.015	0.10	0.08
<b>Ca</b>	2.10	41.59	0.02	0.38	0.16	<b>Cr</b>	0.38	6.22	0.031	2.74	0.17
<b>Cd</b>	0.02	0.49	0.002	3.20	0.02	<b>Cu</b>	0.14	2.28	0.013	3.13	0.07
<b>Cr</b>	0.29	5.64	0.002	0.28	0.02	<b>K</b>	0.89	14.52	3.86	146.06	21.21
<b>Cu</b>	1.59	31.49	0.279	6.97	2.19	<b>Mn</b>	5.03	82.55	0.001	0.01	0.01
<b>Fe</b>	20.76	411.13	0.014	0.03	0.11	<b>Mo</b>	0.12	2.00	0.015	4.12	0.08
<b>K</b>	0.23	4.48	0.404	71.00	3.18	<b>Pb</b>	1.98	32.50	2.54	42.96	13.96
<b>Pb</b>	4.29	84.96	2.83	26.20	22.26	<b>Si</b>	0.51	8.44	0.01	0.65	0.05
<b>Si</b>	0.81	16.00	0.016	0.79	0.13	<b>Sn</b>	0.02	0.29	0.004	7.57	0.02
<b>Zn</b>	23.70	469.35	25.6	42.90	201.36	<b>Zn</b>	18.14	297.71	20.2	37.29	111.02

## XX. Mass balance - Roasting step

### Roasting product Zinc AR XRF (rest % oxygen)

XRF	Zinc AL (wt%)	Zinc AL (tons)	Zinc AR (wt%)	Zinc AR (tons)	Loss or gain (tons)
Ag	0.01	0.12	0.00	0.00	-0.12
Al	0.98	15.66	0.59	12.92	-2.74
As	0.02	0.39	0.02	0.33	-0.06
Ba	0.48	7.71	0.36	7.87	0.16
Bi	0.01	0.16	0.01	0.18	0.02
Br	-	-	-	-	-
Ca	2.11	33.68	1.83	40.01	6.33
Cd	0.03	0.41	0.01	0.17	-0.23
Cl	0.54	8.56	0.51	11.11	2.55
Cr	0.30	4.79	0.60	13.20	8.42
Cs	-	-	-	-	-
Cu	1.40	22.35	1.00	21.86	-0.48
Fe	22.18	354.03	20.80	454.73	100.69
Ga	0.01	0.11	0.00	0.00	-0.11
Ge	-	-	-	-	-
In	0.01	0.23	0.01	0.23	0.01
K	0.13	2.09	0.12	2.51	0.42
La	0.01	0.09	0.01	0.12	0.03
Mg	0.19	3.02	0.05	1.05	-1.97
Mn	0.42	6.62	0.37	8.09	1.46
Mo	0.01	0.13	0.02	0.47	0.34
Na	10.39	165.84	37.94	829.44	663.60
Nd	-	-	-	-	-
Ni	0.09	1.50	0.23	4.94	3.44
Pb	3.05	48.68	2.25	49.19	0.51
Px	0.16	2.55	0.18	3.94	1.38
Rb	-	-	-	-	-
Ru	-	-	-	-	-
Sb	0.03	0.44	0.02	0.45	0.01
Si	0.96	15.32	0.85	18.63	3.30
Sn	0.20	3.24	0.16	3.52	0.28
Sr	0.03	0.43	0.02	0.48	0.05
Sx	0.45	7.15	0.63	13.82	6.67
Ti	0.18	2.91	0.16	3.45	0.55
V	0.01	0.11	0.01	0.12	0.01
Zn	10.52	167.92	8.54	186.70	18.78
Zr	0.01	0.15	0.01	0.19	0.04

**Roasting product Zinc BR XRF (Rest % oxygen)**

<b>XRF</b>	<b>Zinc BL (wt%)</b>	<b>Zinc BL (tons)</b>	<b>Zinc BR (wt%)</b>	<b>Zinc BR (tons)</b>	<b>Loss or gain (tons)</b>
<b>Al</b>	0.17	2.59	0.08	1.91	-0.68
<b>As</b>	-	-	-	-	-
<b>Ba</b>	0.04	0.66	0.04	0.92	0.26
<b>Bi</b>	-	-	-	-	-
<b>Br</b>	-	-	-	-	-
<b>Ca</b>	5.41	80.44	4.44	100.05	19.61
<b>Cd</b>	0.02	0.28	0.01	0.28	0.00
<b>Cl</b>	0.08	1.18	0.06	1.26	0.08
<b>Cr</b>	0.33	4.97	0.52	11.79	6.82
<b>Cs</b>	-	-	-	-	-
<b>Cu</b>	0.11	1.62	0.09	1.94	0.32
<b>Fe</b>	33.89	503.91	25.75	580.26	76.34
<b>Ga</b>	0.01	0.11	0.01	0.18	0.07
<b>Hf</b>	-	-	-	-	-
<b>I</b>	-	-	-	-	-
<b>K</b>	0.11	1.59	0.08	1.75	0.16
<b>La</b>	-	-	-	-	-
<b>Mg</b>	0.60	8.88	0.31	6.92	-1.96
<b>Mn</b>	5.00	74.35	3.38	76.17	1.82
<b>Mo</b>	0.03	0.38	0.02	0.49	0.11
<b>Na</b>	5.67	84.31	30.52	687.74	603.44
<b>Nb</b>	-	-	-	-	-
<b>Ni</b>	0.02	0.32	0.05	1.05	0.73
<b>Pb</b>	0.65	9.66	0.49	11.06	1.40
<b>Px</b>	0.06	0.94	0.07	1.54	0.60
<b>Rb</b>	-	-	-	-	-
<b>S</b>	-	-	-	-	-
<b>Sb</b>	-	-	-	-	-
<b>Si</b>	0.56	8.37	0.45	10.10	1.72
<b>Sn</b>	0.02	0.25	0.01	0.20	-0.05
<b>Sr</b>	-	-	-	-	-
<b>Sx</b>	0.07	1.03	0.07	1.58	0.55
<b>Ti</b>	0.03	0.40	0.02	0.53	0.12
<b>V</b>	0.01	0.13	0.01	0.17	0.04
<b>Zn</b>	8.66	128.77	6.51	146.70	17.93
<b>Zr</b>	0.01	0.09	0.00	0.00	-0.09

XXI. Mass balance - Secondary leaching step

Leaching product Zinc ARL, extrapolated from XRF (rest % oxygen)					Leaching product of Zinc BRL, extrapolated from XRF (rest % oxygen)				
XRF	Zinc AR (wt%)	Zinc AR (tons)	Recovery (%)	Lixiviant Zinc ARL (tons)	XRF	Zinc BR (wt%)	Zinc BR (tons)	Recovery (%)	Lixiviant Zinc BRL (tons)
As	0.02	0.33	100.00	0.33	Al	0.08	1.91	23.93	0.46
Ca	1.83	40.01	2.00	0.80	Ba	0.04	0.92	7.05	0.06
Cl	0.51	11.11	89.28	9.91	Ca	4.44	100.05	16.51	16.52
K	0.12	2.51	90.89	2.29	Cd	0.01	0.28	2.71	0.01
La	0.01	0.12	3.64	0.00	Cl	0.06	1.26	88.79	1.12
Mo	0.02	0.47	79.08	0.37	Cr	0.52	11.79	87.02	10.26
Na	37.94	829.44	67.46	559.58	Cu	0.09	1.94	0.11	0.00
Pb	2.25	49.19	33.72	16.59	Fe	25.75	580.26	6.17	35.82
Px	0.18	3.94	88.98	3.50	Ga	0.01	0.18	49.20	0.09
Sx	0.63	13.82	65.09	8.99	K	0.08	1.75	87.02	1.52
V	0.01	0.12	100.00	0.12	Mn	3.38	76.17	0.91	0.69
Zn	8.54	186.70	47.83	89.29	Mo	0.02	0.49	80.01	0.39
Zr	0.01	0.19	3.57	0.01	Na	30.52	687.74	60.14	413.63
					Pb	0.49	11.06	25.25	2.79
					Px	0.07	1.54	68.12	1.05
					Si	0.45	10.10	30.29	3.06
					Sx	0.07	1.58	91.18	1.44
					Ti	0.02	0.53	3.54	0.02
					V	0.01	0.17	100.00	0.17
					Zn	6.51	146.70	54.04	79.28

Lixiviant Zinc ARL and extrapolated recovery from XRF (rest % oxygen)						Lixiviant Zinc BRL and extrapolated recovery from XRF (rest % oxygen)					
ICP	Zinc AR (wt%)	Zinc AR (tons)	Zinc ARL g/l	Recovery %	Zinc ARL (tons)	ICP	Zinc BR (wt%)	Zinc BR (tons)	Zinc BRL g/l	Recovery %	Zinc BRL (tons)
Al	0.59	12.92	0.76	44.22	5.71	Al	0.08	1.91	0.35	145.94	2.79
As	0.02	0.33	0.03	75.16	0.25	As	-	-	0.01	-	-
Ca	1.83	40.01	0.00	0.04	0.02	Cr	0.52	11.79	1.00	68.04	8.02
Cr	0.60	13.20	0.03	1.89	0.25	Cu	0.09	1.94	0.01	2.07	0.04
Cu	1.00	21.86	0.14	4.81	1.05	Fe	25.75	580.26	0.02	0.03	0.18
Fe	20.80	454.73	0.03	0.05	0.22	K	0.08	1.75	0.21	96.22	1.68
K	0.12	2.51	0.28	83.68	2.10	Mo	0.02	0.49	0.01	13.05	0.06
Mo	0.02	0.47	0.00	6.44	0.03	Pb	0.49	11.06	0.15	10.84	1.20
Pb	2.25	49.19	2.09	32.16	15.82	Si	0.45	10.10	0.35	27.83	2.81
Si	0.85	18.63	0.10	4.10	0.76	V	0.01	0.17	0.00	19.05	0.03
Sn	0.16	3.52	0.00	0.43	0.02	Zn	6.51	146.70	6.62	36.33	53.30
Zn	8.54	186.70	9.31	37.74	70.46						

XXII.

## Mass balance - Post-water washing step

Leaching product Zinc ARLWW, extrapolated from XRF (rest % oxygen)					Leaching product Zinc BRLWW, extrapolated from XRF (rest % oxygen)				
XRF	Zinc ARL (wt%)	Zinc ARL (tons)	Recovery (%)	Lixiviant Zinc ARLWW (tons)	XRF	Zinc BRL	Zinc BRL	Recovery	Lixiviant Zinc BRLWW
Ba	0.65	8.79	5.39	0.47	Cl	0.01	0.14	100.00	0.14
Bi	0.02	0.21	0.99	0.00	Cr	0.09	1.53	41.35	0.63
Ca	2.91	39.19	3.02	1.19	Cu	0.12	1.94	7.11	0.14
Cl	0.09	1.19	35.68	0.42	Fe	33.11	544.66	2.18	11.90
Cr	1.02	13.74	10.78	1.48	Ga	0.01	0.09	100.00	0.09
Cu	1.70	22.89	2.27	0.52	K	0.01	0.23	38.57	0.09
Fe	35.00	471.34	3.70	17.44	Mg	0.56	9.23	0.93	0.09
In	0.02	0.31	5.57	0.02	Mn	4.59	75.51	2.61	1.97
K	0.02	0.23	100.00	0.23	Na	16.67	274.22	60.91	167.02
La	0.01	0.12	27.19	0.03	Ni	0.06	1.05	4.21	0.04
Mg	0.24	3.22	3.23	0.10	Sx	0.01	0.14	100.00	0.14
Mn	0.63	8.54	2.81	0.24	Ti	0.03	0.51	2.41	0.01
Mo	0.01	0.10	100.00	0.10	Zn	4.10	67.44	6.85	4.62
Na	20.03	269.74	62.44	168.44					
Ni	0.42	5.68	3.06	0.17					
Pb	2.42	32.59	7.88	2.57					
Px	0.03	0.43	19.10	0.08					
Sb	0.04	0.49	0.64	0.00					
Sn	0.27	3.66	1.78	0.07					
Sr	0.04	0.50	1.25	0.01					
Sx	0.36	4.82	43.33	2.09					
Ti	0.28	3.74	4.50	0.17					
Zn	7.23	97.37	4.50	4.38					



Lixiviant Zinc ARLWW and extrapolated recovery						Lixiviant Zinc BRLWW and extrapolated recovery					
ICP	Zinc ARL wt%	Zinc ARL (tons)	Zinc ARLWW g/l	Recovery %	Lixiviant Zinc ARLWW (tons)	ICP	Zinc BRL wt%	Zinc BRL (tons)	Zinc BRLWW (g/L)	Recovery (%)	Lixiviant Zinc BRLWW (tons)
<b>Al</b>	1.56	21.01	0.16	5.26	1.10	<b>Al</b>	0.09	1.45	0.06	32.28	0.47
<b>As</b>	-	-	0.01	-	-	<b>Ca</b>	5.08	83.57	0.00	0.03	0.02
<b>Ca</b>	2.91	39.19	0.00	0.03	0.01	<b>Cr</b>	0.09	1.53	0.08	41.40	0.63
<b>Cr</b>	1.02	13.74	0.15	7.50	1.03	<b>Fe</b>	33.11	544.66	0.00	0.00	0.02
<b>Cu</b>	1.70	22.89	0.00	0.09	0.02	<b>K</b>	0.01	0.23	0.01	39.86	0.09
<b>Fe</b>	35.00	471.34	0.00	0.00	0.01	<b>Mo</b>	0.01	0.10	0.01	83.33	0.08
<b>K</b>	0.02	0.23	0.02	47.06	0.11	<b>Pb</b>	0.50	8.27	0.02	1.49	0.12
<b>Mo</b>	0.01	0.10	0.01	47.95	0.05	<b>Si</b>	0.43	7.04	0.16	18.34	1.29
<b>Pb</b>	2.42	32.59	0.17	3.45	1.12	<b>V</b>	-	-	0.00	-	-
<b>Si</b>	1.80	24.24	0.67	18.56	4.50	<b>Zn</b>	4.10	67.44	0.21	2.50	1.69
<b>Sn</b>	0.27	3.66	0.01	1.29	0.05						
<b>V</b>	-	-	0.00	-	-						
<b>Zn</b>	7.23	97.37	0.21	1.48	1.44						

### XXIII. Mass balance - Residue

Zinc ARLWW (rest % oxygen)			Zinc BRLWW (rest % oxygen)		
XRF	Zinc ARL-WW (wt%)	Zinc ARL-WW (Tons)	Wt%	Zinc BRL-WW (wt%)	Zinc ARL-WW (Tons)
Ag	0.01	0.16	Al	0.11	1.59
Al	1.93	21.70	As	-	-
As	-	-	Ba	0.06	0.89
Ba	0.74	8.32	Bi	-	-
Bi	0.02	0.21	Br	-	-
Br	-	-	Ca	5.98	84.21
Ca	3.38	38.01	Cd	0.02	0.28
Cd	0.03	0.29	Cl	-	-
Cl	0.07	0.77	Cr	0.06	0.90
Cr	1.09	12.26	Cs	-	-
Cs	-	-	Cu	0.13	1.80
Cu	1.99	22.38	Fe	37.82	532.55
Fe	40.37	453.96	Ga	-	-
Ga	0.01	0.09	Hf	-	-
Ge	0.01	0.06	I	-	-
In	0.03	0.29	K	0.01	0.14
K	-	-	La	-	-
La	0.01	0.08	Mg	0.65	9.14
Mg	0.28	3.11	Mn	5.22	73.50
Mn	0.74	8.30	Mo	0.01	0.10
Mo	-	-	Na	7.61	107.16
Na	9.01	101.32	Nb	-	-
Nd	-	-	Ni	0.07	1.01
Ni	0.49	5.51	Pb	0.60	8.39
Pb	2.67	30.02	Px	0.04	0.50
Px	0.03	0.35	Rb	-	-
Rb	-	-	S	-	-
Ru	-	-	Sb	-	-
Sb	0.04	0.49	Si	0.62	8.74
Si	2.26	25.41	Sn	0.02	0.27
Sn	0.32	3.60	Sr	-	-
Sr	0.04	0.49	Sx	-	-
Sx	0.24	2.73	Ti	0.04	0.49
Ti	0.32	3.58	V	-	-
V	-	-	Zn	4.46	62.80
Zn	8.27	93.00	Zr	0.06	0.77
Zr	0.02	0.19			

Zinc ARLWW chemical composition measured by acid digestion and ICP			Zinc BRLWW chemical composition measured by acid digestion and ICP		
ICP	ZincARL-WW (wt%)	ZincARL-WW (tons)	ICP	ZincBRL-WW (wt%)	ZincARL-WW (tons)
Al	2.66	29.91	Al	0.26	3.69
As	<0.001	-	As	<0.001	-
Ba	0.67	7.56	Ba	0.03	0.41
Ca	3.08	34.63	Ca	5.80	81.67
Cd	0.00	0.03	Cd	<0.001	-
Cr	0.52	5.81	Cr	0.04	0.51
Cu	1.61	18.10	Cu	0.14	2.01
Fe	35.30	396.94	Fe	35.60	501.29
K	0.16	1.80	K	0.16	2.22
Mg	0.86	9.63	Mg	1.97	27.74
Mn	0.64	7.15	Mn	4.56	64.21
Mo	<0.001	-	Mo	<0.001	-
Na	2.97	33.40	Na	4.72	66.46
Ni	0.38	4.23	Ni	<0.001	-
Pb	2.34	26.31	Pb	0.57	7.96
Si	2.77	31.15	Si	1.13	15.91
Sn	0.28	3.19	Sn	<0.001	-
Zn	7.24	81.41	Zn	3.98	56.04



#### XXIV. Mass balance - Cementation

ICP	Zinc C (kg/m3)	Zinc P (kg/m3)	Product (tons)
Al	0.698	0.681	0.460
As	0.026	0.026	-
B	0.014	0.013	0.020
Ca	0.008	0.006	0.050
Cd	4.69E-04	4.69E-04	-
Cr	0.306	0.278	0.782
Cu	0.108	0.000	2.967
Fe	0.018	0.017	0.027
K	1.001	1.042	-
Mn	1.99E-04	1.99E-04	-
Mo	0.006	0.006	-
Pb	1.786	0.699	29.998
Si	0.135	0.135	-
Sn	0.001	0.001	-
V	0.001	0.001	-
Zn	14.513	16.179	1.117

XXV. Mass balance - Electrowinning step

	Zinc D (kg/m3)	Tons	Product (ICP)	Product (XRF)
Al	0.68	18.79		
As	0.03	0.71		
B	0.01	0.35		
Ca	0.01	0.18		
Cd	0.00	0.01		
Cr	0.28	7.67	0.46	0.82
Fe	0.02	0.46		
K	1.04	28.74		
Mn	0.00	0.01		
Mo	0.01	0.18		
Pb	0.70	19.27		
Si	0.14	3.73		
Sn	0.00	0.04	19.96	35.94
V	0.00	0.03		
Zn	16.18	446.17	356.93	642.48

XXVI. Target and invention values for soil remediation and background concentrations for soil/sediment and groundwater for metals.

Tabel 1a: Streefwaarden en interventiewaarden bodemsanering en achtergrondconcentraties bodem/sediment en grondwater voor metalen. Waarden voor bodem/sediment zijn uitgedrukt als de concentratie in een standaardbodem (10% organisch stof en 25% lutum).

	GROND/SEDIMENT (mg/kg droge stof)			GRONDWATER (µg/l opgelost)			
	landelijke achtergrond concentratie	streef- waarde	interventie- waarde	streef- waarde ondiep	landelijke achtergrond concentratie diep	streef- waarde diep	interventie- waarde
	(AC)	(ind. AC)			(AC)	(ind. AC)	
I Metalen							
antimoon	3	3	15	-	0,09	0,15	20
arseen	29	29	55	10	7	7,2	60
barium	160	160	625	50	200	200	625
cadmium	0,8	0,8	12	0,4	0,06	0,06	6
chromium	100	100	380	1	2,4	2,5	30
cobalt	9	9	240	20	0,6	0,7	100
koper	36	36	190	15	1,3	1,3	75
kwik	0,3	0,3	10	0,05	-	0,01	0,3
lood	85	85	530	15	1,6	1,7	75
molybdeen	0,5	3	200	5	0,7	3,6	300
nikkel	35	35	210	15	2,1	2,1	75
zink	140	140	720	65	24	24	800